Pulling the strings on anti-cancer immunity

Kersten, K.

Pulling the strings on anti-cancer immunity

Kelly Kersten

About the cover:

Based on the research described in this thesis and inspired by the song 'Master of Puppets' by Metallica, I envision cancer as a puppet-master restraining the protective function of the immune system. Part of my PhD work has focused on how tumor cells manipulate the function of immune cells to favor their spread throughout the body. In other words, cancer is pulling the strings on anti-cancer immunity to prevent destruction by the immune system. With the recent advances of combinatorial anti-cancer therapies (including immunomodulatory drugs) we can gain back control over the strings on anti-cancer immunity.

Cover design:	Kelly Kersten & Tomasz Ahrends
Artwork:	Tomasz Ahrends
Lay-out:	Jasper Koning (koningjj@gmail.com)
Printing:	Gildeprint, Enschede
ISBN:	978-94-6233-496-0

The printing of the thesis was financially supported by the NKI-AVL.

The research described in this thesis was performed at the Divisions of Molecular Biology and Immunology of the Netherlands Cancer Institute – Antoni van Leeuwenhoek Hospital (NKI-AVL), Amsterdam, The Netherlands, and was supported by the Dutch Cancer Society (KWF2011-5004) and the European Research Council (InflaMet 615300).

Pulling the strings on anti-cancer immunity

Proefschrift

ter verkrijging van

de graad van Doctor aan de Universiteit Leiden

op gezag van Rector Magnificus Prof.Mr. C.J.J.M. Stolker,

volgens besluit van het College voor Promoties

te verdedigen op dinsdag 7 februari 2017

klokke 15.00 uur.

door

Kelly Kersten

geboren te Ede

in 1987

Promotores:
Prof.dr. Jos Jonkers, promotor
Dr. Karin E. de Visser, NKI-AVL, co-promotor

Promotiecommissie:
Prof.dr. Joke Bouwstra, voorzitter
Prof.dr. Meindert Danhof, secretaris
Prof.dr. Ferry Ossendorp
Prof.dr. Bob van de Water
Prof.dr. Jacco van Rheenen (Utrecht University)
Prof.dr. Jannie Borst (University of Amsterdam)

Table of contents

-1-

Scope of thesis

Breast cancer is the most common type of cancer in women; about 1 in 8 women will develop breast cancer during the course of her life [1]. Moreover, breast cancer is the main cause of cancer-related mortality among women. The majority of these deaths is caused by metastatic disease which is still largely unexplored, poorly understood, and incurable [2]. Most anti-cancer treatment strategies used to date are developed to target the primary tumor. However, we need to appreciate the fact that cancer is a systemic disease, and treatment of the primary tumor is often not sufficient to cure cancer patients.

Tumors do not merely consist of cancer cells, but together with a variety of stromal cell types like fibroblasts, vascular and lymphatic endothelial cells and infiltrating immune cells, form an entity collectively termed the tumor microenvironment (TME). In the past few decades it has become clear that the tumor microenvironment plays an important role in cancer development, progression and therapy responsiveness [3]. Immune cells are of particular interest because of their paradoxical role in cancer progression and metastasis.

Cancer metastasis is a step-by-step process

The complexity of metastasis lies in its multistep nature. During primary tumor growth genetic alterations accumulate in cancer cells that allow their dissemination from the primary tumor. During dissemination, these cells have to cross multiple barriers like the basement membrane and extracellular matrix before invading surrounding tissues. Via a process called intravasation, disseminated cancer cells enter the blood stream and lymphatics. Once in the circulation, many cancer cells are cleared due to the high sheer stress and attack by the immune system. However, a minor fraction of surviving cancer cells can get trapped in the small capillary structures at distant sites and extravasate into the tissue. Here cancer cells can form micrometastatic lesions that sometimes remain dormant for long periods of time [4]. However, when disseminated cancer cells reside in a permissive microenvironment, small lesions can progress to colonize distant organs forming macrometastatic disease.

During every step of the metastatic cascade there is a complex crosstalk between disseminated cancer cells and their surrounding microenvironment. As early as 1889 the English surgeon Stephen Paget proposed his ‘seed and soil’ hypothesis which states that metastasis depends on crosstalk between selected cancer cells (the ‘seeds’) and a specific organ microenvironment (the ‘soil’) [5]. Only if these cancer cells end up in a supportive environment or niche they are able to survive and give rise to metastatic lesions. Emerging evidence indicates that the immune system plays an important role in priming the ‘soil’ for metastasis [6,7].

The paradoxical role of the immune system in cancer progression

The mammalian immune system consists of two arms that together help to protect the body from disease-causing infectious agents. The innate immune system — composed of monocytes, macrophages, neutrophils, dendritic cells, natural killer cells and mast cells — acts as a first line of defense and can rapidly eradicate invading pathogens. T and B cells compose the adaptive immune system and provide antigen-specific responses upon

encounter with a pathogen. Moreover, adaptive immune cells can provide immunological memory. Many cancers are characterized by the influx of large numbers of immune cells. Recent studies show that the immune composition is predictive of prognosis in several cancer types [8,9]. However, the functional role of the immune system in cancer progression is paradoxical; some immune cell populations harbor pro-tumorigenic properties, while other populations counteract tumorigenesis [3,10,11].

To mount effective anti-tumor immunity, tumor-associated antigens need to be taken up and processed by antigen-presenting cells, like dendritic cells. After receiving maturation signals, these cells migrate to the tumor-draining lymph nodes where the antigen is presented to naïve T cells. Upon activation, these tumor antigen-specific T cells migrate to the tumor bed to exert their cytotoxic function and eliminate cancer cells. Unfortunately, tumors elicit a variety of mechanisms to evade anti-tumor immunity and prevent destruction by the immune system, such as antigen-loss and dysfunctional T cell priming [12]. In addition, many types of cancer are characterized by chronic inflammation which is one of the hallmarks of cancer [3,13]. During chronic inflammation, tumor cells and inflammatory cells produce a variety of cytokines, chemokines and growth factors that favor the recruitment and polarization of immune cells, and induce angiogenesis and tissue remodeling. Moreover, inflammation often results in immunosuppression which is unfavorable for anti-tumor T cell responses. The complex reciprocal interactions between neoplastic cells and adaptive and innate immune cells create a delicate balance between pro- and anti-tumor immunity.

Immunotherapy as a therapeutic strategy to combat cancer

In the past years, cancer immunotherapy – harnessing the patient's immune system to fight cancer – has proved to be a promising therapeutic strategy for several types of cancer [14]. A growing body of data reports beneficial responses in predominantly immunogenic cancer types like advanced melanoma and lung cancer [15–18]. However, a large proportion of patients does not show clinical benefit from cancer immunotherapy. Therefore the current focus in research is to better understand the underlying mechanisms of tumor-induced immune evasion to identify biomarkers that can predict whether a specific cancer patient will or will not respond to this type of therapy, and ultimately to develop strategies to overcome immune evasion.

It is now widely accepted that successful eradication of (metastasized) cancer requires a multi-disciplinary approach in which different anti-cancer treatment modalities are combined. While conventional therapies like chemotherapy, irradiation and targeted therapy usually show fast anti-tumor responses, the onset of acquired resistance often results in disease recurrence. In contrast, a proportion of patients treated with immunotherapy show slow but long-term durable anti-tumor immune responses, which makes immunotherapy an interesting modality to be combined with conventional anti-cancer therapies. To find the most optimal treatment combinations per cancer type, research in preclinical mouse cancer models is essential.

The research described in this thesis aims to gain a better understanding of the role of the immune system in cancer development and metastasis formation using preclinical

mouse models of metastatic breast cancer. With this knowledge, we aim to contribute to the development of immunomodulatory strategies to fight metastatic breast cancer and to increase the efficacy of conventional anti-cancer therapies.

Description of the chapters in this thesis

Despite the successful validation of novel anti-cancer drugs in preclinical models, the majority of phase III clinical trials fails to meet their primary endpoint [19]. The poor translation from preclinical mouse models to clinical practice illustrates the insufficient predictive power of the preclinical models that are currently used. To improve these disappointing statistics, it is desirable that preclinical models faithfully recapitulate human cancer. Genetically engineered mouse models (GEMMs) have proved indispensable for gaining biological insight into the many different aspects of human cancer, including genetic driver mutations, onset of metastasis, interaction with the surrounding microenvironment and responsiveness to anti-cancer therapies. Moreover, the presence of an intact immune system in these mice that co-evolves with *de novo* tumor development is very important in the context of studying the anti-cancer efficacy of immunomodulatory drugs. In **Chapter 2** we propose how the current technological advances in mouse cancer model engineering can contribute to improve the predictive power of preclinical studies. Ultimately this will result in more effective anti-cancer treatment strategies.

Our research described in the first part of this thesis is aimed at gaining a better understanding of the role of the immune system in breast cancer progression and metastasis formation. In this work we made use of a GEMM for *de novo* mammary tumorigenesis; *i.e. K14cre; Cdh1$^{F/F}$;Trp53$^{F/F}$* mice [20]. The mammary tumors that spontaneously develop in these animals closely resemble a subtype of human breast cancer known as invasive lobular carcinoma (ILC), which accounts for approximately 10% of all breast cancer cases [21]. We used this mouse model to study the tumor-induced mechanisms of immune evasion during breast cancer progression. In **Chapter 3**, we demonstrate that *de novo* mammary tumors that arise in the conditional *K14cre;Cdh1$^{F/F}$;Trp53$^{F/F}$* mouse model, induce a systemic pro-inflammatory cascade to facilitate breast cancer metastasis to distant organs. This pro-metastatic inflammation is characterized by interleukin (IL)-17 expressing γδ T cells and the subsequent expansion and polarization of immunosuppressive neutrophils. These neutrophils actively suppress the activity of $CD8^+$ T cells via iNOS. We found that IL-17 expression by γδ T cells is induced by mammary tumor-derived IL-1β. In **Chapter 4** we report an additional regulator of this tumor-induced systemic inflammatory cascade. We identified CCL2, a chemokine that is highly expressed in *K14cre; Cdh1$^{F/F}$;Trp53$^{F/F}$* mammary tumors, as a key driver of the γδ T cell – IL17 – neutrophil axis by inducing IL-1β expression in tumor-associated macrophages. In line with these findings, we show that expression of *CCL2* positively correlates with *IL1B* and macrophage markers in human breast tumors. Together our findings suggest that interfering with this pro-metastatic inflammatory cascade may provide therapeutic options for patients with metastasized breast cancer.

In the second part of this thesis I focused on the role of the immune system in therapy responsiveness. Studies suggest that the efficacy of anti-cancer therapy is (in part) dependent on immune-mediated mechanisms [22,23]. The success of cancer immunotherapy has reinvigorated the search for combinatorial treatment strategies that induce cancer cell death and boost anti-tumor immunity to optimize therapeutic response rates. One of the strategies proposed in this thesis is to combine the treatment of immunotherapy with conventional chemotherapy. Several chemotherapeutics have immunomodulatory properties and affect different populations of immunosuppressive immune cells. For example, cyclophosphamide (when administered in low doses) targets regulatory T cells [24], and gemcitabine specifically targets myeloid-derived suppressor cells (MDSC) that counteract T cell activity [25]. In **Chapter 5**, we summarize preclinical and clinical data that support the notion that combining T cell boosting immune checkpoint inhibitors with conventional chemotherapeutics that alleviate immunosuppression will enhance the efficacy of anti-cancer treatment strategies for patients.

Although the presence of tumor-infiltrating lymphocytes correlates with a good prognosis [26,27], breast cancer is not considered a highly immunogenic type of cancer. Clinical trials are currently ongoing to explore the efficacy of immunotherapy to enhance tumor-reactive T cells in breast cancer patients. Since objective response rates presented so far range from 5–20% [28–31], a substantial fraction of breast cancer patients requires optimized combinatorial treatment approaches. **Chapter 6** describes our research in which we utilized the *K14cre;Cdh1$^{F/F}$;Trp53$^{F/F}$* mouse model to explore the applicability of immunotherapy by immune checkpoint blockade in spontaneous breast cancer. We found that dual immune checkpoint blockade with anti-PD-1 and anti-CTLA-4 does not improve tumor-specific survival of mice. However, when combined with conventional chemotherapy we find synergistic responses in a drug-dependent manner. Improved anti-tumor responses were dependent on CD8$^+$ T cells. These results have important implications for treatment strategies in the clinic, because it shows the importance of the chemotherapy of choice. More importantly, our results demonstrate that – even in relatively poorly immunogenic cancer types – a combination of chemo- and immunotherapy is able to unleash anti-tumor immunity to combat cancer.

Chapter 7 summarizes the main results described in this thesis and puts these findings in context of the current literature. It also provides suggestions for clinical implications and future directions.

Taken together, the preclinical research described in this thesis demonstrates that anti-tumor immune responses occur, but are overruled by tumor-induced immune-evading mechanisms in a mouse model of breast cancer. By inducing a systemic inflammatory and immunosuppressive state the tumor manipulates the function of immune cells favoring its dissemination. In other words, the tumor is '**pulling the strings on anti-cancer immunity**' to prevent destruction by the immune system. With the recent advances in the field of immunomodulatory drugs we now have the proper tools to overrule this systemic immune evasive state and **gain back control over the strings on anti-cancer immunity**. Ultimately, this will improve therapeutic strategies and improve cancer patient care.

References

1. www.cijfersoverkanker.nl.
2. Weigelt, B., Peterse, J. L. & van't Veer, L. J. Breast cancer metastasis: markers and models. *Nat. Rev. Cancer* **5,** 591–602 (2005).
3. Hanahan, D. & Coussens, L. M. Accessories to the crime: functions of cells recruited to the tumor microenvironment. *Cancer Cell* **21,** 309–322 (2012).
4. Ghajar, C. M. Metastasis prevention by targeting the dormant niche. *Nat. Rev. Cancer* **15,** 238–247 (2015).
5. Paget, S. The distribution of secondary growths in cancer of the breast. *Lancet* **1,** 571–573 (1889).
6. McAllister, S. S. & Weinberg, R. A. The tumour-induced systemic environment as a critical regulator of cancer progression and metastasis. *Nat. Cell Biol.* **16,** 717–727 (2014).
7. Kitamura, T., Qian, B.-Z. & Pollard, J. W. Immune cell promotion of metastasis. *Nat. Rev. Immunol.* **15,** 73–86 (2015).
8. Gentles, A. J. *et al.* The prognostic landscape of genes and infiltrating immune cells across human cancers. *Nat. Med.* **21,** 938–945 (2015).
9. Mlecnik, B. *et al.* Integrative Analyses of Colorectal Cancer Show Immunoscore Is a Stronger Predictor of Patient Survival Than Microsatellite Instability. *Immunity* **44,** 698–711 (2016).
10. de Visser, K. E., Eichten, A. & Coussens, L. M. Paradoxical roles of the immune system during cancer development. *Nat. Rev. Cancer* **6,** 24–37 (2006).
11. DeNardo, D. G. & Coussens, L. M. Inflammation and breast cancer. Balancing immune response: crosstalk between adaptive and innate immune cells during breast cancer progression. *Breast Cancer Res.* **9,** 212 (2007).
12. Chen, D. S. & Mellman, I. Oncology meets immunology: the cancer-immunity cycle. *Immunity* **39,** 1–10 (2013).
13. Hanahan, D. & Weinberg, R. A. Hallmarks of cancer: the next generation. *Cell* **144,** 646–674 (2011).
14. Couzin-Frankel, J. Cancer Immunotherapy. *Science* **342,** 1432–1433 (2013).
15. Hodi, F. S. *et al.* Improved survival with ipilimumab in patients with metastatic melanoma. *N. Engl. J. Med.* **363,** 711–723 (2010).
16. Brahmer, J. R. *et al.* Safety and activity of anti-PD-L1 antibody in patients with advanced cancer. *N. Engl. J. Med.* **366,** 2455–2465 (2012).
17. Topalian, S. L. *et al.* Safety, activity, and immune correlates of anti-PD-1 antibody in cancer. *N. Engl. J. Med.* **366,** 2443–2454 (2012).
18. Wolchok, J. D. *et al.* Nivolumab plus ipilimumab in advanced melanoma. *N. Engl. J. Med.* **369,** 122–133 (2013).
19. Reichert, J. M. & Wenger, J. B. Development trends for new cancer therapeutics and vaccines. *Drug Discov. Today* **13,** 30–37 (2008).
20. Derksen, P. W. B. *et al.* Somatic inactivation of E-cadherin and p53 in mice leads to metastatic lobular mammary carcinoma through induction of anoikis resistance and angiogenesis. *Cancer Cell* **10,** 437–449 (2006).
21. Arpino, G., Bardou, V. J., Clark, G. M. & Elledge, R. M. Infiltrating lobular carcinoma of the breast: tumor characteristics and clinical outcome. *Breast Cancer Res.* **6,** R149-156 (2004).
22. Zitvogel, L., Galluzzi, L., Smyth, M. J. & Kroemer, G. Mechanism of action of conventional and targeted anticancer therapies: reinstating immunosurveillance. *Immunity* **39,** 74–88 (2013).
23. Coffelt, S. B. & de Visser, K. E. Immune-mediated mechanisms influencing the efficacy of anticancer therapies. *Trends Immunol.* **36,** 198–216 (2015).
24. Ghiringhelli, F. *et al.* Metronomic cyclophosphamide regimen selectively depletes CD4+CD25+ regulatory T cells and restores T and NK effector functions in end stage cancer patients. *Cancer Immunol. Immunother.* **56,** 641–648 (2007).
25. Suzuki, E., Kapoor, V., Jassar, A. S., Kaiser, L. R. & Albelda, S. M. Gemcitabine selectively eliminates splenic Gr-1+/CD11b+ myeloid suppressor cells in tumor-bearing animals and enhances antitumor immune activity. *Clin. Cancer Res.* **11,** 6713–6721 (2005).
26. Mahmoud, S. M. A. *et al.* Tumor-infiltrating CD8+ lymphocytes predict clinical outcome in breast cancer. *J. Clin. Oncol.* **29,** 1949–1955 (2011).
27. Ali, H. R. *et al.* Association between CD8+ T-cell infiltration and breast cancer survival in 12,439 patients. *Ann. Oncol.* **25,** 1536–1543 (2014).
28. Emens, L. A. *et al.* Abstract PD1-6: Inhibition of PD-L1 by MPDL3280A leads to clinical activity in patients

with metastatic triple-negative breast cancer [abstract]. In: Proceedings of the Thirty-Seventh Annual CTRC-AACR San Antonio Breast Cancer Symposium: 2014 Dec 9-13; San Antonio, TX. Philadelphia (PA): AACR; *Cancer Res.* **75,** Abstract nr PD1-6 (2015).

29. Dirix, L. Y. *et al.* Abstract S1-04: Avelumab (MSB0010718C), an anti-PD-L1 antibody, in patients with locally advanced or metastatic breast cancer: A phase Ib JAVELIN solid tumor trial [abstract]. In: Proceedings of the Thirty-Eighth Annual CTRC-AACR San Antonio Breast Cancer Symposium: 2015 Dec 8-12; San Antonio, TX. Philadelphia (PA): AACR; *Cancer Res.* **76,** Abstract nr S1-04 (2016).
30. Rugo, H. S. *et al.* Preliminary efficacy and safety of pembrolizumab (MK-3475) in patients with PD-L1–positive, estrogen receptor-positive (ER+)/HER2-negative advanced breast cancer enrolled in KEYNOTE-028. [abstract]. In: Proceedings of the Thirty-Eighth Annual CTRC-AACR San Antonio Breast Cancer Symposium: 2015 Dec 8-12; San Antonio, TX. Philadelphia (PA): AACR; *Cancer Res.* **76,** Abstract nr S5-07 (2016).
31. Nanda, R. *et al.* Pembrolizumab in Patients With Advanced Triple-Negative Breast Cancer: Phase Ib KEYNOTE-012 Study. *J. Clin. Oncol.* (2016). doi:10.1200/JCO.2015.64.8931

-2-

Genetically engineered mouse models in oncology and cancer medicine

Kelly Kersten[1], Karin E. de Visser[1], Martine H. van Miltenburg[2], Jos Jonkers[2]

[1]Division of Immunology and [2]Division of Molecular Pathology, Netherlands Cancer Institute, Plesmanlaan 121, 1066 CX Amsterdam, The Netherlands

EMBO Molecular Medicine, in revision.

Abstract

Genetically engineered mouse models (GEMMs) have made significant contributions to the field of cancer research. Tissue-specific induction of defined driver mutations in GEMMs triggers development of tumors in a natural immune-proficient microenvironment. These tumors closely mimic histopathological and molecular features of their human counterparts, and display genetic heterogeneity, thus faithfully recapitulating the natural course of human cancer. GEMMs capture both tumor cell-intrinsic and -extrinsic factors that drive *de novo* formation of tumors and progression toward metastatic disease, and are therefore indispensable for preclinical research. GEMMs have successfully been used to validate candidate cancer genes and drug targets, assess therapy efficacy, and evaluate mechanisms of drug resistance. Great efforts are made to further fine-tune engineering of GEMMs and to align *in vivo* preclinical testing in advanced mouse models with clinical studies in patients, which is anticipated to speed up the development of novel therapeutic strategies and their translation into the clinic.

Pending issues

- Understanding of tumor cell-intrinsic and -extrinsic mechanisms underlying cancer and metastasis development, and therapy resistance.
- Development of multidisciplinary therapeutic strategies including conventional anti-cancer drugs and immunotherapy to successfully fight disseminated cancer.
- Reduction of time and costs to generate next-generation genetically engineered mouse models that closely recapitulate human cancer.
- Close alignment of preclinical mouse studies and human clinical trials to improve cancer patient care.

Introduction

Despite the fact that survival rates of cancer patients have improved over the last decades, we are still facing numerous challenges in the clinic. One of the major problems is the development of drug resistance. Monotherapy with targeted anti-cancer agents or chemotherapeutics can result in drug resistance caused by *de novo* mutations or outgrowth of pre-existing therapy-resistant clones within heterogeneous tumors. Moreover, after seemingly successful treatment, small numbers of drug-tolerant tumor cells can survive treatment and remain dormant for extended periods of time and eventually relapse to form recurrent disease that can be phenotypically different from the original tumor [1,2]. Another major challenge is metastatic disease, which accounts for over ninety percent of cancer-related deaths [3]. These secondary tumors are often unresponsive to therapy and are at present mostly incurable. Encouraging advancements have been made with cancer immunotherapy, aimed at harnessing the patient's immune system to attack cancer. However, even though long term durable responses are observed in some cases, a large proportion of cancer patients does not show clinical benefit [4].

Successful treatment of cancer requires a multidisciplinary approach in which different strategies, such as surgery, irradiation, cytotoxic therapy and immunotherapy, are combined. In order to design such combinations, it is critical to improve our insights into the cancer cell-intrinsic and -extrinsic mechanisms underlying tumor development and metastasis, and therapy responsiveness. To find the most efficacious treatment for different cancer types, we heavily rely on preclinical research in animal models. Despite successful validation of novel anti-cancer therapies in conventional preclinical mouse models based on xenotransplantation of established human cancer cell lines or allotransplantation of mouse tumor cell lines, the majority of the phase 3 clinical trials fail [5]. The overall poor clinical predictability of these conventional *in vivo* tumor models emphasizes the need for more advanced preclinical *in vivo* models with a better predictive power. Until fairly recently, progress in the field was hampered by the poor availability of preclinical models that closely recapitulate the natural course of human cancer. However, recent technological developments have led to fast track generation of sophisticated mouse models that more closely mimic human cancer in terms of genetic composition, interactions of cancer cells with their tumor microenvironment, drug response and resistance. These next generation genetically engineered mouse models (GEMMs) are of great importance to improve our understanding of the complex mechanisms underlying cancer biology, and are anticipated to improve translation of new therapeutic strategies into the clinic — ultimately leading to increased survival of cancer patients. This review describes the evolution and recent technological advances of mouse model engineering, and the applications of the resulting models in basic and translational oncology research.

Evolution of mouse cancer modeling

Over the years, novel advances in the field of genome editing have led to the generation of various mouse models to study cancer biology. Here, we give a historic overview of the development of mouse models that are mostly used in cancer research.

Cancer cell line transplantation models

Allograft and xenograft cell line transplantation mouse models are the most commonly used mouse models, as they allow for rapid testing of potential cancer and metastasis-related genes and are often used for preclinical drug testing. Moreover, these cells – when tagged with biomarkers such as luciferase or fluorescent proteins to allow non-invasive imaging – have proven informative to identify metastasis-related genes. For example, orthotopic and intravenous administration of breast cancer cells has shed light on the mechanisms underlying organ tropism and metastatic dormancy [6–9]. Nevertheless, as cancer cell lines contain multiple mutations from the start and acquire additional aberrations when cultured in 2D for extended periods of time, these inoculation models do not reflect the morphology and genetic heterogeneity of human cancers, and are therefore commonly poor predictors of clinical response. While allografting of mouse cancer cell lines can be performed in immune proficient hosts, xenotransplantation of cell lines must be performed in immunocompromised mice to prevent rejection, which makes them less suitable to study the roles of the immune system in tumor development and therapy response.

Patient-derived tumor xenografts

Patient-derived tumor xenograft (PDTX) models are derived from fresh human tumor biopsies that are transplanted in immunodeficient mice. Unlike cell line transplantation models, PDTX tumors maintain the molecular, genetic and histological heterogeneity as observed in cancer patients, even after serial passaging in mice [10]. Therefore, PDTX models can be valuable tools to define personalized medicine as was demonstrated by preclinical drug screening in PDTX models of non-small cell lung cancer (NSCLC) [11–13], breast cancer [14], melanoma [15,16], prostate cancer [17,18] and colorectal cancer [19–24]. High-throughput efforts are now undertaken using PDTX models to predict responses of clinical drug candidates. Approximately 1000 PDTX models were established with a diverse panel of mutations, and subsequently used for *in vivo* compound screens, yielding correlations between drug response and tumor genotype that were both reproducible and clinically translatable [25]. In a recent study using PDTX models of triple-negative breast cancer, single-cell gene expression analysis revealed that early stage metastatic cells express distinct signatures enriched in stem-like genes, identifying novel potential drug targets to tackle metastatic breast cancer [26].

Unfortunately, a major obstacle of PDTX modeling is the disappointing take rate of various tumor types, such as estrogen receptor-positive breast cancer and prostate cancer [27,28]. In addition, PDTX modeling must be performed in immunocompromised mice, thereby circumventing the natural anti- and pro-tumor activity provided by the

adaptive immune system. Given the complex crosstalk between adaptive immune components, the innate immune system and cancer cells, it is important to realize that PDTX models can provide clinically valuable data, albeit in the absence of the influential adaptive immune system. Current efforts to generate humanized mice by engrafting immunodeficient mice with human $CD34^+$ hematopoietic stem cells or precursor cells have shown remarkable progress [29,30]. Although reconstitution of immune cells from specific lineages remains challenging, the introduction of transgenes encoding human cytokines, chemokines and growth factors can support the development of human myeloid cells in mice. To support development of HLA-restricted T cells, recipient immunodeficient mice can be further optimized by transgenic expression of human HLA molecules and deficiency of mouse MHC class I and II molecules. While the limited availability of hematopoietic donor stem cells (obtained from umbilical cord blood or fetal liver) and the relatively high costs of these models are potential disadvantages, humanized mouse models could provide a useful platform for preclinical evaluation of immunotherapeutics.

Modeling de novo cancer in genetically engineered mice

In the early 1980s, the first cloned cancer genes were introduced into the genome of transgenic mice, which were termed oncomice [31]. The first oncomouse was a GEMM with transgenic expression of a specific activated oncogene (*v-HRas*) under control of a mammary-specific promoter (*MMTV*), making the mouse prone to developing mammary tumors [32]. The first oncomice led to great excitement in the cancer research community as they provided unambiguous proof for the hypothesis that oncogene expression in normal cells could lead to tumor formation [32–36]. With the development of gene knockout technology in 1992, also cancer predisposition in tumor suppressor gene (TSG) knockout mice could be studied [37].

Though oncomice and TSG knockout mice have provided a wealth of knowledge, they also have their limitations. Given that transgenes are expressed in all cells of a particular tissue and TSGs in knockout mice are inactivated in all cells of the animal, these models fail to mimic sporadic cancers in which accumulation of genetic events in a single cell results in tumorigenesis in an otherwise healthy organ. To circumvent this, more sophisticated mouse models are currently available that allow somatic inactivation of tumor suppressors or activation of (mutant) oncogenes in conditional GEMMs [38]. One of the first examples is the generation of a mouse colorectal cancer model using Cre-*loxP* mediated somatic inactivation of *Apc*. With this technique any gene flanked by *loxP* recombination sites will be deleted after activation of the Cre-recombinase. APC loss in intestinal epithelial cells was sporadically induced through adenovirus-mediated delivery of Cre-recombinase, resulting in the rapid onset of colorectal adenomas that shared many features with adenomas in familial adenomatous polyposis coli (FAP) patients [39]. By introducing mutations associated with a specific type of cancer one can generate mouse models that closely mimic the histopathological, molecular and clinical features of tumors in patients [40,41].

Induction of somatic mutations at a chosen time and in a specific tissue can be achieved by using Cre-ERT fusion proteins, in which a mutated hormone-binding domain of the estrogen receptor (ERT) is fused to the Cre-recombinase. Cre-ERT is an inducible Cre-recombinase: administration of the estrogen analog tamoxifen leads to post-translational activation of Cre-recombinase activity and excision of the target gene flanked by *loxP* sites. Hence, mice with (tissue-specific) expression of Cre-ERT allow for spatiotemporally controlled Cre-mediated genomic recombination upon administration of tamoxifen [42].

Although the Cre-*loxP* system can be applied to alter the expression of more than one gene, it does so simultaneously, and therefore does not fully mimic the sequential accumulation of mutations during multistep carcinogenesis. Recently, an inducible dual-recombinase system was developed which combines Flp-*FRT* and Cre-*loxP* recombination systems, allowing sequential genetic manipulation of gene expression by two independent recombination systems [43]. This approach allows for (i) independent targeting of tumor cell autonomous and non-autonomous pathways/processes, (ii) sequential induction of mutations to faithfully model human multistep carcinogenesis, and (iii) genetic validation of therapeutic targets in autochthonous tumors.

Mouse models to study oncogene addiction

Some tumors are highly dependent on a single oncogene for their growth, a phenomenon called 'oncogene addiction'. Conditional GEMMs are unsuitable models to determine oncogene addiction, as the genetic lesion is irreversible, and thus requires another layer of regulation. Oncogene-ERT fusions can be employed to control oncogene expression; for example, $Trp53^{KI/KI}$ mice in which both *Trp53* alleles are replaced by the tamoxifen-inducible *Trp53-ERT* variant, have been used to determine the therapeutic efficacy of p53 restoration in established tumors [44].

Also systems for doxycycline-regulatable gene expression have been successfully used in GEMMs to turn oncogenes on, thereby allowing tumorigenesis; and off to investigate how established tumors respond to oncogene inactivation (43,44,45). To give an example, continuous expression of a doxycycline-inducible *Myc* transgene in hematopoietic cells resulted in the formation of malignant T cell lymphomas and acute myeloid leukemias that regressed upon de-induction of *Myc* expression [47]. The long-term effects of temporal MYC de-induction seem to differ between cancer types. For example, brief inactivation of MYC in osteogenic sarcomas resulted in sustained regression due to differentiation of sarcoma cells into mature osteocytes [48]. In contrast, invasive liver cancers regressed after MYC inactivation, but residual tumor cells remained dormant and immediately restored their neoplastic features upon MYC reactivation [49].

Speeding up and fine-tuning mouse cancer modeling

Although GEMMs have proven to be valuable tools for cancer research, there are still aspects that can be improved. A major limitation of germline GEMMs is that development and validation of these models is time-consuming, laborious and expensive. This is exemplified when a novel germline mutation has to be introduced in an existing multi-allelic mouse model, as this requires extensive breeding. The rapidly increasing number of mutations identified in cancer sequencing studies calls for novel mouse modeling strategies that enable accelerated *in vivo* evaluation of candidate cancer genes and patient-relevant allelic variants of known cancer genes.

Embryonic stem cell-based mouse cancer models

To speed up the generation of novel GEMMs of human cancer, embryonic stem cells (ESCs) can be genetically altered and used to produce cohorts of non-germline GEMMs [50]. An alternative approach is the recently developed GEMM-ESC strategy, which employs ESCs that are derived from existing (multi-allelic) GEMMs. These GEMM-derived ESCs can be used for rapid introduction of additional genetic modifications and subsequent production of chimeric mice that show the same characteristics as the established GEMM but now contain the additional genetic modification [51,52].

In vivo RNA interference

RNA interference (RNAi) by short hairpin RNAs (shRNAs) allows reversible silencing of gene expression without modifying the genome, and therefore it can be used as an alternative to homologous recombination-based gene inactivation approaches. RNAi-based genetic screens have proven powerful tools to rapidly identify and validate cancer genes. *In vivo* RNAi screens have been successfully used to identify novel TSGs in mouse models of hepatocellular carcinoma and lymphoma [53–55], and to identify genes involved in resistance to the tyrosine kinase inhibitor sorafenib in liver cancer [56]. Moreover, the development of systems for doxycycline-inducible shRNA expression in transgenic mice allows reversible expression of shRNAs in a time- and tissue-specific manner [57,58]. Using the latter approach, Dow *et al.* have shown that shRNA-mediated APC suppression in the presence of *Kras* and *Trp53* mutations induces intestinal carcinomas, which undergo sustained regression upon restoration of APC expression by turning off shRNA expression, highlighting the WNT pathway as a therapeutic target for treatment of colorectal cancer [59].

Genome editing using CRISPR/Cas9 technology

In the past decades, additional approaches for genome editing have been developed such as Zinc-finger nucleases (ZFNs) and transcription-activator-like effector nucleases (TALENs) [60,61]. These approaches have now been outperformed by the development of CRISPR/Cas9 systems for genome editing [62], which have revolutionized biological research over the past three years and are considered the biggest game changer since

PCR. The CRISPR (clustered regularly-interspaced short palindromic repeats) – Cas9 system was first discovered as a prokaryotic immune system that confers resistance to foreign genetic elements, but soon thereafter has been exploited to achieve gene editing [63–65]. By using appropriate single-guide RNAs (sgRNAs), the Cas9 nuclease can be directed to any genomic locus, where it induces double-stranded cleavage of matching target DNA sequences, leading to gene knockout [62]. The CRISPR/Cas9 system can also be used to introduce defined mutations or *loxP/FRT* recombination sites, by simply co-introducing oligonucleotides that can serve as a template for repair of the Cas9-induced break [66].

CRISPR/Cas technology seems the system of choice for rapid cancer modeling in mice, as it has proven to be an efficient gene-targeting strategy with the potential for multiplexed genome editing [67]. Virtually all (combinations of) genetic alterations found in human tumors can now be rapidly introduced in the mouse germline, including (conditional) gene deletions [68,69], point mutations [68] and translocations [70–72]. Other groups have successfully used CRISPR/Cas9 technology for somatic editing of oncogenes and TSGs in mice. These efforts have led to a new generation of non-germline models of hepatocellular carcinoma [73,74], lung cancer [75,76], brain cancer [77], pancreatic cancer [78,79] and breast cancer [80].

The CRISPR/Cas9 system has recently been modified to induce target gene repression (CRISPRi) or activation (CRISPRa) [81]. These modified systems may be used to generate mice with inducible and reversible activation of oncogenes and/or inactivation of TSGs. Though extremely powerful, CRISPR/Cas9 based systems for *in vivo* gene editing may also have certain drawbacks. For example, current CRISPR/Cas9 strategies are not suited to validate the oncogenic potential of putative oncogenes. To this end, CRISPRa-based systems may be used to activate transcription of target genes [82]. Moreover, somatic delivery of Cas9 may trigger Cas9-specific immune responses resulting in clearance of Cas9 expressing cells [80,83]. To circumvent this issue, experiments should be performed in immunodeficient animals or mice that are engineered to develop tolerance to Cas9. Finally, CRISPR/Cas9 mediated genome editing may create unwanted off-target mutations that may be circumvented by employing mice with inducible expression of a Cas9n 'nickase' variant [84].

Fine-tuning mouse cancer modeling with patient-relevant alleles

Many cancer-predisposing germline mutations and somatic mutations in human TSGs are missense or nonsense mutations that may result in the production of a mutant or truncated protein with residual activity. Such mutations are not adequately modeled in (conditional) knockout mice, in which deletion of one or more exons leads to complete loss of the protein. It is therefore essential to generate mouse models carrying patient-relevant mutations to study their contribution to tumorigenesis and therapy response. Several studies have shown that patient-relevant TSG mutations in mice induce different phenotypes compared to the null-alleles. Compared to *Trp53* knockouts, patient-relevant *Trp53* hotspot mutations in mice were shown to have enhanced oncogenic

activity [85,86]. Similarly, introduction of patient-relevant *Brca1* mutations in a conditional mouse model of BRCA1-associated breast cancer showed that, in contrast to *Brca1*-null tumors, mammary tumors with expression of *Brca1* alleles harboring mutations in the RING domain readily acquired resistance to DNA-damaging drugs due to residual activity of the RING-less BRCA1 protein [87,88]. Thus, by introducing specific somatic or germline mutations into GEMMs, the causal link between these mutations and therapy responsiveness can be determined.

Applications of GEMMs in basic cancer research

The generation of GEMMs has been detrimental for basic cancer research. Here, we discuss how GEMMs have contributed to understanding the basic intrinsic and extrinsic aspects of cancer biology.

Validation of candidate cancer genes

Given the growing number of candidate cancer genes that are identified in large-scale tumor sequencing studies, there is a clear need for rapid *in vivo* strategies to validate these genes. Considering their speed and relative simplicity, GEMM-ESC and CRISPR/Cas technologies are the methods of choice for fast-track validation of candidate cancer genes. Especially non-germline models based on somatic CRISPR/Cas9-mediated gene editing enable *in vivo* validation of (combinations of) candidate cancer genes in a truly high-throughput manner, as was demonstrated in a mouse model for pancreatic cancer [79]. Here, transfection-based multiplexed delivery of Cas9 and sgRNAs targeting 13 different cancer genes induced pancreatic cancer (PDAC) in the majority of mice. The PDACs displayed genome editing of over 60% of the target genes, indicating clonal expansion of CRISPR/Cas9-induced driver mutations that induce cancer [79]. Likewise, GEMMs with doxycycline-inducible Cas9 expression were employed to validate defined combinations of intestinal cancer genes, e.g. *Apc* and *Trp53* [84]. Besides modifying TSGs, CRISPR/Cas9 technology can be applied to validate the oncogenicity of chromosomal rearrangements, such as the *Eml4-Alk* gene fusion observed in lung cancer [89].

Determining cells-of-origin of cancers

Identifying the cancer cell-of-origin may provide important information for the development of improved therapeutic strategies. Studies in GEMMs have successfully identified the cell-of-origin for several different cancer types. For example, the cell-of-origin of small cell lung cancer (SCLC) was determined by intra-tracheal injection of cell-type-restricted Adeno-Cre viruses, to inactivate *Trp53* and *Rb1* in Clara, neuroendocrine (NE) and alveolar type 2 (SPC) cells, respectively. *Trp53* and *Rb1* inactivation in these specific cell types of the lung resulted in differences in tumor onset and tumor phenotype, and identified NE cells (and to a lesser extent SPC cells) as the cell-of-origin in SCLC [90]. Cell-of-origin studies can also deliver surprising results, as was the case for BRCA1-related basal-like breast cancer. While BRCA1-related basal-like breast cancer

was previously postulated to originate from basal epithelial stem cells, cell-of-origin studies in GEMMs revealed that in fact luminal progenitors are the source of basal-like tumors [91]. Genetic aberrations, such as *Pik3ca* mutations, can have a profound effect on the stem cell pool, as was demonstrated recently by two independent laboratories. Expression of *Pik3ca*^{H1047R} was shown to evoke dedifferentiation of lineage-committed mammary epithelial cells into a multipotent stem-like state [92,93]. Interestingly, the cell-of-origin of *Pik3ca*^{H1047R} mammary tumors dictates their malignancy, highlighting the importance of pinpointing the cancer cell-of-origin to improve specificity of anti-cancer drugs and therapeutic outcome.

Studying the contribution of the tumor microenvironment

GEMM models have been fundamental in deciphering the contribution of tumor cell-extrinsic factors such as cancer-associated fibroblasts (CAFs) and immune cells to tumorigenesis. CAFs are important cellular components of the tumor microenvironment as they regulate deposition of extracellular matrix (ECM) and formation of basement membrane by synthesizing ECM components such as collagen, fibronectin and laminin. Moreover, fibroblasts are a source of various soluble mediators including matrix metalloproteases (MMPs), which enable ECM turnover, reinforcing their crucial role in maintaining ECM homeostasis [94]. Studies in GEMMS have demonstrated dual roles of fibroblasts in cancer. During malignant transformation of epithelial cells, CAFs can stimulate tumor progression by enhancing inflammation, angiogenesis and ECM remodeling, as was demonstrated in the *K14-HPV16* squamous skin cancer model [95]. In contrast, a recent study demonstrated that genetic *in vivo* depletion of CAFs accelerates progression of pancreatic cancer [96], suggesting a tumor-restraining role for CAFs. The same controversy holds true for immune cells: originally it was hypothesized that immune cells suppress tumorigenesis by attacking transformed cells; however, work of recent years has revealed that these cells can also act as tumor-promoting entities. Early studies in the *K14-HPV16* model have shown that mast cells and bone marrow-derived cells promote squamous skin cancer by activating angiogenesis and by reorganizing stromal architecture via MMP9 [97,98]. Using the same skin cancer model, chronic inflammation was found to promote *de novo* carcinogenesis in a B lymphocyte-dependent manner [99]. Likewise, the tumor-promoting roles of tumor-associated macrophages (TAMs) [100,101] and neutrophils [102] have been described in several studies, emphasizing that immune cells can act as coconspirators in tumor development and progression.

Deciphering spontaneous metastasis formation

Despite the advancement of therapeutic options in the clinic, metastatic disease remains the primary cause of cancer-related death. The metastatic cascade is a complex multi-step process dictated by a constant crosstalk between cancer cells and their microenvironment [103,104]. Most preclinical metastasis research has been performed in cell line inoculation models, which do not recapitulate the subsequent steps of the metastatic process as it occurs in patients. Spontaneously

metastasizing GEMMs provide unique opportunities to study metastasis because the entire cascade occurs *de novo* in a natural setting (Figure 1). A complication of the use of GEMMs for metastasis research is that these mice generally need to be sacrificed due to their primary tumor burden, before macroscopic metastases have developed. This problem can be overcome by orthotopic transplantation of GEMM-derived tumor fragments – which maintain the intratumoral heterogeneity of donor tumors – followed by surgical resection, allowing the development of clinically overt metastatic disease [105]. GEMMs that closely recapitulate human cancer have proven indispensable for studying aspects of metastasis that have remained unclear until now. For example, metastasis was originally believed to be a late step in tumorigenesis. However, against all expectations, studies in *BALB-NeuT* and *MMTV-PyMT* mouse mammary tumor models revealed that transformed cells in early lesions are already capable of disseminating to bone marrow and lungs to form micro-metastasis [106].

	Intratumoral heterogeneity	Priming metastatic niche	Invasion	Circulation/ extravasation	Seeding/ colonization	Clinically overt multi-organ metastasis
	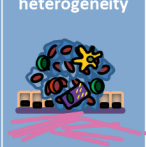				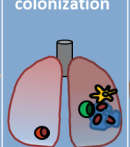	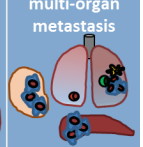
Cell line inoculation* - tail vein - orthotopic	✗ ✗	✗ ✓	✗ ✓	✓ ✓	✓ ✓	✓ ✓
PDTX *	✓	?	✓	Model-dependent	Model-dependent	Model-dependent
Conventional GEMM	✓	✓	✓	Model-dependent	Model-dependent	Model-dependent
Next generation GEMM	✓	✓	✓	?	?	?
GEMM-based orthotopic transplantation model for metastatic disease	✓	✓	✓	✓	✓	✓

Figure 1. The utility of mouse models in metastasis research

This overview summarizes the utility of different preclinical mouse models of experimental and spontaneous metastasis to study the different steps of the metastatic cascade. Conventional GEMMs represent oncomice and mice carrying germline mutations in TSGs. Next-generation GEMMs represent mouse models that are genetically engineered to accurately mimic sporadic human cancer. For some models, the utility for studying specific steps in the metastatic cascade has yet to be determined, as indicated by a question mark. Moreover, several studies have shown that components of the adaptive immune system contribute to the various steps of the metastatic cascade. These aspects cannot be studied in models based on xenografting of human cancer cells or tumor fragments in immunodeficient hosts (indicated by an asterisk). To circumvent this, humanized mice can be used as hosts.

Similarly, epithelial-to-mesenchymal transition (EMT) – a process in which cells lose their polarity and cell-cell adhesion, and gain migratory properties – is thought to play a key role in tumor cell dissemination and metastasis. Using a spontaneous squamous cell carcinoma mouse model it was found that reversible EMT, regulated by spatiotemporal expression of Twist1, is essential for metastasis formation [107]. However, recent studies in GEMMs of pancreatic and breast cancer show that cancer cells retain their epithelial characteristics whilst colonizing metastatic sites, suggesting that EMT is not essential for metastasis formation in these models [108,109]. Together these studies emphasize the complexity of spontaneous metastasis.

GEMMs have also revolutionized the metastasis field by revealing complex crosstalk between cancer cells and the immune system in metastasis formation. Several labs have shown that myeloid immune cells, such as macrophages and neutrophils, play key roles in promoting metastasis formation in different types of cancer [100,110–113]. Recently, we reported a mammary tumor-induced systemic inflammatory state characterized by IL17-producing γδ T cells and the subsequent expansion of immunosuppressive neutrophils that drives spontaneous metastasis formation in a GEMM of lobular breast cancer and a GEMM-based transplantation model for spontaneous metastatic disease [112]. Collectively, GEMMs have proven indispensable for understanding the complexity of metastasis and have challenged the current dogma that metastasis is a late-stage cancer cell-intrinsic process involving EMT. These findings may have important implications for treatment of metastatic cancer patients.

Applications of GEMMs in translational oncology

Besides providing essential insights into basic cancer research, GEMMs that harbor patient-relevant allelic variants of known cancer genes have proven detrimental for translation oncology. Close alignment of mouse and human studies can provide a platform that can aid in the development of novel treatment strategies for cancer patients (Figure 2). Below we discuss how GEMMs can provide clinically relevant information on the design of anti-cancer therapy.

Validation of novel drug targets

Considering that not all cancer genes are essential for maintenance of established tumors, it is important to test whether reactivation of a TSG or down-regulation of an oncogene results in durable regression of established tumors in a realistic preclinical setting, before drugs against these targets are developed. The relevance of oncogenes for tumor maintenance can be assessed in inducible mouse models in which oncogene expression can be de-induced once tumors have developed. For example, de-induction of oncogenic *Pik3ca*^{H1047R} expression in a mouse model of breast cancer caused (partial) tumor regression demonstrating that these tumors are 'addicted' to activated PI3K signaling. However, most tumors eventually recurred due to *Met* or *Myc* amplifications, indicating that these genetic lesions may induce resistance to PI3K inhibitors [114]. This

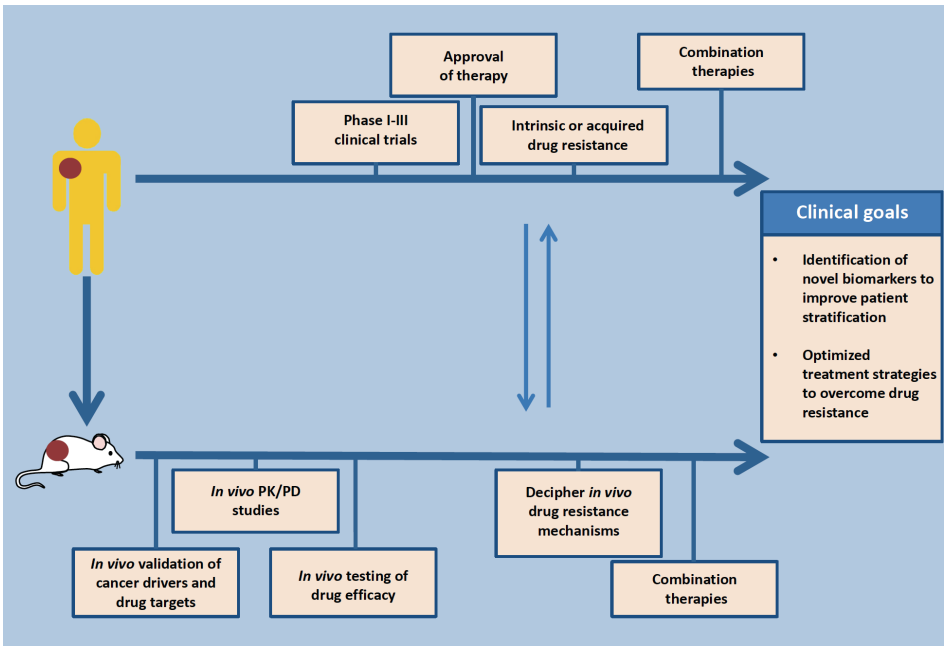

Figure 2. The utility of mouse models in cancer drug development

Development of novel treatment strategies in oncology requires preclinical studies in mouse cancer models to identify and validate novel cancer drivers and therapeutic targets, to determine *in vivo* drug pharmacokinetics and pharmacodynamics (PK/PD), and to evaluate *in vivo* anti-cancer efficacy of novel therapeutics. When promising preclinical results are obtained, the tolerability and anti-cancer efficacy of these drugs are evaluated in human patients in phase I-III clinical trials. A fraction of patients will show poor response due to intrinsic or acquired resistance, which may be studied mechanistically in preclinical mouse models to identify response biomarkers and combination therapies to prevent or overcome resistance. The close alignment of mouse studies and human clinical trials will lead to better patient stratification, identification of novel biomarkers and development of optimal combination therapies, culminating in improved cancer patient care.

example illustrates that preclinical studies in inducible GEMMs are not only useful for validating drug targets but also for identifying mechanisms underlying acquired drug resistance.

Also TSGs may in certain cases constitute valid drug targets. For example, p53 loss-of-function in cancer can result from dominant-negative or inactivating mutations in the *Trp53* gene or from amplification/overexpression of its specific inhibitors MDM2 and MDM4. Genetic studies in GEMMs with reversible inactivation of p53 have shown that restoration of p53 leads to rapid regression of established tumors [44,115,116], providing strong rationale for designing anticancer drugs that restore p53 function by inhibiting MDM2 [117] or by restoring wild-type function to mutant p53 [118]. Similarly, GEMMs of colorectal cancer with inducible knockdown of APC showed that APC restoration initiates rapid and extensive tumor cell differentiation and sustained regression without relapse, providing *in vivo* validation of the WNT pathway as a therapeutic target for treatment of APC-mutant colorectal cancers [59].

Unraveling therapy response and resistance

To minimize the risk of failure of novel anti-cancer therapeutics in clinical trials, preclinical evaluation of response and resistance in robust and predictive *in vivo* models is essential. Therapeutic responses of GEMMs to targeted therapy and conventional chemotherapy are very similar to those of human patients, as was assessed in GEMMs of *Kras*-mutant lung cancer and pancreatic cancer [119]. Hence, preclinical drug efficacy studies in GEMMs may advance the development of optimal (combinations of) anti-cancer drugs to target specific tumors, and the identification of determinants of therapy response that may be used as predictive biomarkers for patient stratification. In addition, GEMMs may be used to identify mechanisms by which therapy-sensitive tumors acquire drug resistance.

A clear example of a preclinical GEMM that has provided mechanistic insight into therapy response and resistance of *BRCA1*-mutated breast cancer is the *K14cre;Brca1$^{F/F}$;Trp53$^{F/F}$* (KB1P) mouse model. KB1P mice develop mammary tumors that mimic the histopathological features of human *BRCA1*-mutated breast cancers as well as their hypersensitivity to platinum drugs and PARP inhibitors [120,121]. Clinical trials evaluated the PARP inhibitor olaparib for the treatment of ovarian, breast and colorectal cancer [122]. While olaparib did not seem promising in this diverse group of cancer patients, it did show significant responses in *BRCA1*-mutation carriers, due to the synthetic lethal combination of PARP inhibition and BRCA1-deficiency [123,124]. *BRCA1*-mutant cells are more vulnerable to PARP inhibition because the single-strand DNA breaks induced by PARP inhibition, lead to double-strand breaks during replication, which cannot be repaired by BRCA1-deficient cells due to lack of homologous recombination. Based on promising results obtained in clinical trials [123,124], olaparib (trade name LynParza) was FDA approved in December 2014 for the treatment of patients with advanced *BRCA1/2*-mutated ovarian cancer. Despite the good response of *BRCA1/2*-mutated cancers to olaparib, acquired resistance is observed both in patients and GEMMs. Preclinical studies in KB1P mice revealed several mechanisms of resistance, such as elevated levels of drug efflux transporters and restoration of homologous recombination [121,125–127]. These studies could aid in understanding clinical resistance and in designing improved treatment strategies for olaparib-resistant patients in the clinic.

It is becoming clear that therapy response and resistance is not only influenced by tumor cell-intrinsic factors but also by stromal factors such as fibroblasts and immune cells [128–132]. The impact of these tumor cell-extrinsic factors can be more effectively studied in GEMMs than in xenograft models, as GEMMs closely recapitulate the constant crosstalk between cancer cells and their natural microenvironment. This is illustrated by tumor intervention studies in a GEMM of PDAC, which showed that therapeutic inhibition of paracrine Sonic Hedgehog (SHH) signaling reduced desmoplastic tumor stroma and increased tumor vasculature, resulting in enhanced delivery of gemcitabine to tumors [133]. However, the concept of targeting tumor stroma in PDAC has recently been challenged by two studies showing that stromal factors may suppress rather than promote PDAC growth, possibly by restraining tumor angiogenesis [96,134]. Together, these

studies demonstrate that the contribution of the tumor microenvironment to therapy resistance may be more profound but also more complex than previously anticipated.

Cancer immunotherapy

Over the past decades, increasing mechanistic insights into the principles of immune responses have culminated in therapeutic strategies that harness the patient's immune system to attack cancer. Recent clinical trials in patients with advanced melanoma and lung cancer confirm the remarkable potential of immune checkpoint blockade, including anti-CTLA-4 and anti-PD-1, to enhance effective anti-tumor immunity and to improve survival in a proportion of the patients [135,136]. The basis of these clinical trials comes from several decades of fundamental research in experimental mouse models that have revealed the importance of CTLA-4 and PD-1 in restraining immune responses, as most clearly illustrated by the severe spontaneous autoimmunity phenotype in CTLA-4-deficient [137] and to a milder extent in PD-1-deficient mice [138,139]. A seminal study from Allison and colleagues showed that CTLA-4 blockade in mice bearing inoculated tumors enhances anti-tumor T cell responses resulting in tumor rejection [140], illustrating that releasing the brake on T cells might be an interesting strategy to combat cancer. Nevertheless, a substantial proportion of patients do not respond to immunotherapy, and the current challenge is to understand why.

Although the majority of immunological studies are performed in transplantation models, we foresee a growing role for GEMMs that closely mimic human cancer patients in terms of genetic drivers, tumor histopathology and the crosstalk between cancer and immune cells that co-evolve with the developing cancer. Several studies in GEMMs show that during *de novo* carcinogenesis, tumor-specific T cell responses are dysfunctional due to tumor-induced tolerance mechanisms [141–143]. However, transplantation of GEMM-derived tumor cells in immunodeficient mice resulted in rapid tumor growth, while wild-type mice rejected these tumors [141–143], demonstrating that these tumor cells did not lose their immunogenicity and T cells are still able to recognize and attack them.

Why anti-tumor T cell responses fail to control *de novo* tumors remains largely unclear. Many tumors are characterized by chronic inflammation, which induces local and systemic immunosuppression that is unfavorable for T cells to perform their effector function [112,144,145]. Moreover, tumors often show dysfunctional dendritic cells, which results in impaired T cell priming. In the *MMTV-PyMT* mammary tumor model a rare population of dendritic cells can be found that are very potent activators of anti-tumor T cells [146]. However, these cells are outcompeted by the overabundant presence of macrophages preventing proper T cell activation [146,147]. Recent studies have demonstrated that boosting dendritic cell function [144,146,148,149] or blocking myeloid cell-induced immunosuppression [150,151] improves the anti-tumor efficacy of immune checkpoint blockade. Thus, patients that show acquired resistance to T cell boosting immunotherapy might show improved clinical benefit when treatment is combined with compounds that either target immunosuppression or enhance T cell priming.

Immunotherapy studies in GEMMs require a different approach compared to inoculation models. Since tumors in GEMMs develop *de novo,* individual mice – like patients – have their individual set of tumor-antigens. This will lead to heterogeneous responses, which may permit identification of molecular differences between responsive and non-responsive tumors to find biomarkers that can predict clinical benefit. A disadvantage is that in most GEMMs it is unclear whether the tumors express antigens that could potentially be recognized by T cells. To overcome this, clinically relevant tumor-antigens could be introduced by genetic engineering to allow tracking of tumor-specific T cell responses. The introduction of tumor-specific antigens in GEMMs that spontaneously develop poorly immunogenic sarcomas and lung cancer, increased the immunogenicity of tumors and resulted in a potent, but transient, anti-tumor T cell response [143,152]. The initial anti-tumor T cell response was quickly followed by regulatory T cell-mediated immunosuppression [153]. Thus, these models can aid ongoing and future research to unravel the complex mechanisms underlying immune evasion [154], and may ultimately lead to novel (combination) strategies to improve cancer immunotherapy.

Concluding remarks and future perspectives

Many anti-cancer drugs in clinical trials do not live up to the high expectations raised by preceding preclinical studies. How can we improve the predictive power of preclinical studies in the oncology arena? Most importantly, the preclinical tumor model of choice should reflect human disease as faithfully as possible. First, preclinical models should contain the patient-specific mutations that initiated the malignancy, and harbor the genetic variation as seen in patient populations. Second, the models should reflect the crosstalk with the tumor microenvironment (infiltrating immune cells, angiogenesis, fibroblasts) as observed in human cancer. Third, the mouse model should reflect the disease stage of the patients for which the therapy is intended. Patients that are enrolled in clinical trials, almost always present with advanced metastatic disease. We thus need to test compounds in preclinical models with advanced disease so that they mimic patient cohorts. Fourth, patients enrolled in clinical trials are frequently heavily pre-treated, which is likely to negatively affect therapy outcome. Preclinical studies performed in treatment-naïve animals may thus overestimate therapy efficacy. Next-generation GEMMs and GEMM-based orthotopic transplantation models for spontaneous advanced metastatic disease are currently the best available models to faithfully recapitulate human cancer. Besides providing good predictability for clinical trials, these models provide valuable tools to study the mechanisms underlying complex processes like cancer initiation, organ-specific metastasis formation, involvement of tumor microenvironment, (immune) therapy responsiveness and resistance, and disease recurrence. To enable rapid implementation of information obtained from mouse experiments, recent strategies have aimed to develop mouse trials in parallel with human clinical trials. By establishing a so called co-clinical trial paradigm, *in vivo* preclinical and early clinical studies are closely aligned [155]. This strategy may facilitate *in*

vivo testing of multiple drug combinations in a multitude of cancer subtypes using mouse models, whilst minimizing the cost and time required to study responses in thousands of human patients. These efforts will ultimately contribute to the design of novel anti-cancer strategies that will improve cancer patient care.

Conflict of interest

The authors declare that they have no conflict of interest.

Acknowledgements

Research in the lab of J.J. is supported by the Dutch Cancer Society (grants 6423, 6532, 7589 and 7877), the Netherlands Organization for Scientific Research (NWO; Cancer Genomics Netherlands [CGCNL], Cancer Systems Biology Center [CSBC], Zenith 93512009 and VICI 91814643), Worldwide Cancer Research (grant 14-0288 to J.J. and M.H.v.M.), the European Union Seventh Framework Program (EurocanPlatform project 260791 and Infrafrontier-I3 project 312325), the European Research Council (ERC Synergy project CombatCancer), and a National Roadmap grant for Large-Scale Research Facilities from the NWO. Research in the lab of K.E.d.V. is supported by a European Research Council Consolidator award (INFLAMET 615300), the European Union (FP7 MCA-ITN 317445 TIMCC) and the Beug Foundation for Metastasis Research. K.E.d.V. is an EMBO Young Investigator.

References

1. Blatter, S. & Rottenberg, S. Minimal residual disease in cancer therapy - Small things make all the difference. *Drug Resist Updat* (2015). doi:10.1016/j.drup.2015.08.003
2. Kottke, T. *et al.* Detecting and targeting tumor relapse by its resistance to innate effectors at early recurrence. *Nat. Med.* **19,** 1625–1631 (2013).
3. Weigelt, B., Peterse, J. L. & van't Veer, L. J. Breast cancer metastasis: markers and models. *Nat. Rev. Cancer* **5,** 591–602 (2005).
4. Sharma, P. & Allison, J. P. The future of immune checkpoint therapy. *Science* **348,** 56–61 (2015).
5. Reichert, J. M. & Wenger, J. B. Development trends for new cancer therapeutics and vaccines. *Drug Discov. Today* **13,** 30–37 (2008).
6. Bos, P. D. *et al.* Genes that mediate breast cancer metastasis to the brain. *Nature* **459,** 1005–1009 (2009).
7. Kang, Y. *et al.* A multigenic program mediating breast cancer metastasis to bone. *Cancer Cell* **3,** 537–549 (2003).
8. Minn, A. J. *et al.* Genes that mediate breast cancer metastasis to lung. *Nature* **436,** 518–524 (2005).
9. Ghajar, C. M. *et al.* The perivascular niche regulates breast tumour dormancy. *Nat. Cell Biol.* **15,** 807–817 (2013).
10. Hidalgo, M. *et al.* Patient-derived xenograft models: an emerging platform for translational cancer research. *Cancer Discov.* **4,** 998–1013 (2014).
11. Fichtner, I. *et al.* Establishment of patient-derived non-small cell lung cancer xenografts as models for the identification of predictive biomarkers. *Clin. Cancer Res.* **14,** 6456–6468 (2008).
12. Merk, J., Rolff, J., Becker, M., Leschber, G. & Fichtner, I. Patient-derived xenografts of non-small-cell lung cancer: a pre-clinical model to evaluate adjuvant chemotherapy? *Eur. J. Cardiothorac. Surg.* **36,** 454–459 (2009).
13. Merk, J., Rolff, J., Dorn, C., Leschber, G. & Fichtner, I. Chemoresistance in non-small-cell lung cancer: can multidrug resistance markers predict the response of xenograft lung cancer models to chemotherapy? *Eur. J. Cardiothorac. Surg.* **40,** e29-33 (2011).
14. Marangoni, E. *et al.* A new model of patient tumor-derived breast cancer xenografts for preclinical assays. *Clin. Cancer Res.* **13,** 3989–3998 (2007).
15. Girotti, M. R. *et al.* Application of Sequencing, Liquid Biopsies, and Patient-Derived Xenografts for Personalized Medicine in Melanoma. *Cancer Discov.* **6,** 286–299 (2016).
16. Kemper, K. *et al.* Intra- and inter-tumor heterogeneity in a vemurafenib-resistant melanoma patient and derived xenografts. *EMBO Mol. Med.* **7,** 1104–1118 (2015).
17. Qu, S. *et al.* Enhanced anticancer activity of a combination of docetaxel and Aneustat (OMN54) in a patient-derived, advanced prostate cancer tissue xenograft model. *Mol. Oncol.* **8,** 311–322 (2014).
18. Yoshida, T. *et al.* Antiandrogen bicalutamide promotes tumor growth in a novel androgen-dependent prostate cancer xenograft model derived from a bicalutamide-treated patient. *Cancer Res.* **65,** 9611–9616 (2005).
19. Bertotti, A. *et al.* The genomic landscape of response to EGFR blockade in colorectal cancer. *Nature* **526,** 263–267 (2015).
20. Misale, S. *et al.* Vertical suppression of the EGFR pathway prevents onset of resistance in colorectal cancers. *Nat. Commun.* **6,** 8305 (2015).
21. Kavuri, S. M. *et al.* HER2 activating mutations are targets for colorectal cancer treatment. *Cancer Discov.* **5,** 832–841 (2015).
22. Zanella, E. R. *et al.* IGF2 is an actionable target that identifies a distinct subpopulation of colorectal cancer patients with marginal response to anti-EGFR therapies. *Sci. Transl. Med.* **7,** 272ra12 (2015).
23. Bardelli, A. *et al.* Amplification of the MET receptor drives resistance to anti-EGFR therapies in colorectal cancer. *Cancer Discov.* **3,** 658–673 (2013).
24. Bertotti, A. *et al.* A molecularly annotated platform of patient-derived xenografts ('xenopatients') identifies HER2 as an effective therapeutic target in cetuximab-resistant colorectal cancer. *Cancer Discov.* **1,** 508–523 (2011).
25. Gao, H. *et al.* High-throughput screening using patient-derived tumor xenografts to predict clinical trial drug response. *Nat. Med.* **21,** 1318–1325 (2015).
26. Lawson, D. A. *et al.* Single-cell analysis reveals a stem-cell program in human metastatic breast cancer cells. *Nature* **526,** 131–135 (2015).
27. Landis, M. D., Lehmann, B. D., Pietenpol, J. A. & Chang, J. C. Patient-derived breast tumor xenografts facilitating personalized cancer therapy. *Breast Cancer Res.* **15,** 201 (2013).
28. Lawrence, M. G. *et al.* Establishment of primary patient-derived xenografts of palliative TURP specimens to study castrate-resistant prostate cancer. *The Prostate* **75,** 1475–1483 (2015).

29. Drake, A. C., Chen, Q. & Chen, J. Engineering humanized mice for improved hematopoietic reconstitution. *Cell. Mol. Immunol.* **9,** 215–224 (2012).
30. Holzapfel, B. M., Wagner, F., Thibaudeau, L., Levesque, J.-P. & Hutmacher, D. W. Concise review: humanized models of tumor immunology in the 21st century: convergence of cancer research and tissue engineering. *Stem Cells* **33,** 1696–1704 (2015).
31. Hanahan, D., Wagner, E. F. & Palmiter, R. D. The origins of oncomice: a history of the first transgenic mice genetically engineered to develop cancer. *Genes Dev.* **21,** 2258–2270 (2007).
32. Sinn, E. *et al.* Coexpression of MMTV/v-Ha-ras and MMTV/c-myc genes in transgenic mice: synergistic action of oncogenes in vivo. *Cell* **49,** 465–475 (1987).
33. Brinster, R. L. *et al.* Transgenic mice harboring SV40 T-antigen genes develop characteristic brain tumors. *Cell* **37,** 367–379 (1984).
34. Hanahan, D. Heritable formation of pancreatic beta-cell tumours in transgenic mice expressing recombinant insulin/simian virus 40 oncogenes. *Nature* **315,** 115–122 (1985).
35. Lacey, M., Alpert, S. & Hanahan, D. Bovine papillomavirus genome elicits skin tumours in transgenic mice. *Nature* **322,** 609–612 (1986).
36. Rüther, U., Komitowski, D., Schubert, F. R. & Wagner, E. F. c-fos expression induces bone tumors in transgenic mice. *Oncogene* **4,** 861–865 (1989).
37. Finlay, C. A. p53 loss of function: implications for the processes of immortalization and tumorigenesis. *BioEssays* **14,** 557–560 (1992).
38. Jonkers, J. & Berns, A. Conditional mouse models of sporadic cancer. *Nat. Rev. Cancer* **2,** 251–265 (2002).
39. Shibata, H. *et al.* Rapid colorectal adenoma formation initiated by conditional targeting of the Apc gene. *Science* **278,** 120–123 (1997).
40. Frese, K. K. & Tuveson, D. A. Maximizing mouse cancer models. *Nat. Rev. Cancer* **7,** 645–658 (2007).
41. Walrath, J. C., Hawes, J. J., Van Dyke, T. & Reilly, K. M. Genetically engineered mouse models in cancer research. *Adv. Cancer Res.* **106,** 113–164 (2010).
42. Bex, A., Vooijs, M., Horenblas, S. & Berns, A. Controlling gene expression in the urothelium using transgenic mice with inducible bladder specific Cre-lox recombination. *J. Urol.* **168,** 2641–2644 (2002).
43. Schönhuber, N. *et al.* A next-generation dual-recombinase system for time- and host-specific targeting of pancreatic cancer. *Nat. Med.* **20,** 1340–1347 (2014).
44. Martins, C. P., Brown-Swigart, L. & Evan, G. I. Modeling the therapeutic efficacy of p53 restoration in tumors. *Cell* **127,** 1323–1334 (2006).
45. Gossen, M. *et al.* Transcriptional activation by tetracyclines in mammalian cells. *Science* **268,** 1766–1769 (1995).
46. Lewandoski, M. Conditional control of gene expression in the mouse. *Nat. Rev. Genet.* **2,** 743–755 (2001).
47. Felsher, D. W. & Bishop, J. M. Reversible tumorigenesis by MYC in hematopoietic lineages. *Mol. Cell* **4,** 199–207 (1999).
48. Jain, M. *et al.* Sustained loss of a neoplastic phenotype by brief inactivation of MYC. *Science* **297,** 102–104 (2002).
49. Shachaf, C. M. *et al.* MYC inactivation uncovers pluripotent differentiation and tumour dormancy in hepatocellular cancer. *Nature* **431,** 1112–1117 (2004).
50. Heyer, J., Kwong, L. N., Lowe, S. W. & Chin, L. Non-germline genetically engineered mouse models for translational cancer research. *Nat. Rev. Cancer* **10,** 470–480 (2010).
51. Huijbers, I. J., Krimpenfort, P., Berns, A. & Jonkers, J. Rapid validation of cancer genes in chimeras derived from established genetically engineered mouse models. *BioEssays* **33,** 701–710 (2011).
52. Huijbers, I. J. *et al.* Rapid target gene validation in complex cancer mouse models using re-derived embryonic stem cells. *EMBO Mol. Med.* (2014). doi:10.1002/emmm.201303297
53. Hemann, M. T. *et al.* An epi-allelic series of p53 hypomorphs created by stable RNAi produces distinct tumor phenotypes in vivo. *Nat. Genet.* **33,** 396–400 (2003).
54. Zender, L. *et al.* An Oncogenomics-Based In Vivo RNAi Screen Identifies Tumor Suppressors in Liver Cancer. *Cell* **135,** 852–864 (2008).
55. Bric, A. *et al.* Functional Identification of Tumor Suppressor Genes Through an in vivo RNA Interference Screen in a Mouse Lymphoma Model. *Cancer Cell* **16,** 324–335 (2009).
56. Rudalska, R. *et al.* In vivo RNAi screening identifies a mechanism of sorafenib resistance in liver cancer. *Nat. Med.* **20,** 1138–1146 (2014).
57. Dickins, R. A. *et al.* Tissue-specific and reversible RNA interference in transgenic mice. *Nat. Genet.* **39,** 914–921 (2007).
58. Premsrirut, P. K. *et al.* A rapid and scalable system for studying gene function in mice using conditional RNA interference. *Cell* **145,** 145–158 (2011).

59. Dow, L. E. *et al.* Apc Restoration Promotes Cellular Differentiation and Reestablishes Crypt Homeostasis in Colorectal Cancer. *Cell* **161,** 1539–1552 (2015).
60. Li, H. *et al.* In vivo genome editing restores haemostasis in a mouse model of haemophilia. *Nature* **475,** 217–221 (2011).
61. Wefers, B. *et al.* Generation of targeted mouse mutants by embryo microinjection of TALEN mRNA. *Nat. Protoc.* **8,** 2355–2379 (2013).
62. Cong, L. *et al.* Multiplex genome engineering using CRISPR/Cas systems. *Science* **339,** 819–823 (2013).
63. Ishino, Y., Shinagawa, H., Makino, K., Amemura, M. & Nakata, A. Nucleotide sequence of the iap gene, responsible for alkaline phosphatase isozyme conversion in Escherichia coli, and identification of the gene product. *J. Bacteriol.* **169,** 5429–5433 (1987).
64. Jansen, R., Embden, J. D. A. van, Gaastra, W. & Schouls, L. M. Identification of genes that are associated with DNA repeats in prokaryotes. *Mol. Microbiol.* **43,** 1565–1575 (2002).
65. Mojica, F. J., Díez-Villaseñor, C., Soria, E. & Juez, G. Biological significance of a family of regularly spaced repeats in the genomes of Archaea, Bacteria and mitochondria. *Mol. Microbiol.* **36,** 244–246 (2000).
66. Yang, H., Wang, H. & Jaenisch, R. Generating genetically modified mice using CRISPR/Cas-mediated genome engineering. *Nat. Protoc.* **9,** 1956–1968 (2014).
67. Sánchez-Rivera, F. J. & Jacks, T. Applications of the CRISPR-Cas9 system in cancer biology. *Nat. Rev. Cancer* **15,** 387–395 (2015).
68. Wang, H. *et al.* One-step generation of mice carrying mutations in multiple genes by CRISPR/Cas-mediated genome engineering. *Cell* **153,** 910–918 (2013).
69. Yang, H. *et al.* One-step generation of mice carrying reporter and conditional alleles by CRISPR/Cas-mediated genome engineering. *Cell* **154,** 1370–1379 (2013).
70. Choi, P. S. & Meyerson, M. Targeted genomic rearrangements using CRISPR/Cas technology. *Nat. Commun.* **5,** 3728 (2014).
71. Torres, R. *et al.* Engineering human tumour-associated chromosomal translocations with the RNA-guided CRISPR-Cas9 system. *Nat. Commun.* **5,** 3964 (2014).
72. Blasco, R. B. *et al.* Simple and rapid in vivo generation of chromosomal rearrangements using CRISPR/Cas9 technology. *Cell Rep.* **9,** 1219–1227 (2014).
73. Xue, W. *et al.* CRISPR-mediated direct mutation of cancer genes in the mouse liver. *Nature* **514,** 380–384 (2014).
74. Weber, J. *et al.* CRISPR/Cas9 somatic multiplex-mutagenesis for high-throughput functional cancer genomics in mice. *Proc. Natl. Acad. Sci. U. S. A.* **112,** 13982–13987 (2015).
75. Platt, R. J. *et al.* CRISPR-Cas9 knockin mice for genome editing and cancer modeling. *Cell* **159,** 440–455 (2014).
76. Sánchez-Rivera, F. J. *et al.* Rapid modelling of cooperating genetic events in cancer through somatic genome editing. *Nature* **516,** 428–431 (2014).
77. Zuckermann, M. *et al.* Somatic CRISPR/Cas9-mediated tumour suppressor disruption enables versatile brain tumour modelling. *Nat. Commun.* **6,** 7391 (2015).
78. Chiou, S.-H. *et al.* Pancreatic cancer modeling using retrograde viral vector delivery and in vivo CRISPR/Cas9-mediated somatic genome editing. *Genes Dev.* **29,** 1576–1585 (2015).
79. Maresch, R. *et al.* Multiplexed pancreatic genome engineering and cancer induction by transfection-based CRISPR/Cas9 delivery in mice. *Nat. Commun.* **7,** 10770 (2016).
80. Annunziato, S. *et al.* Modeling invasive lobular breast carcinoma by CRISPR/Cas9-mediated somatic genome editing of the mammary gland. *Genes Dev.* **30,** 1470–1480 (2016).
81. Gilbert, L. A. *et al.* CRISPR-mediated modular RNA-guided regulation of transcription in eukaryotes. *Cell* **154,** 442–451 (2013).
82. Braun, C. J. *et al.* Versatile in vivo regulation of tumor phenotypes by dCas9-mediated transcriptional perturbation. *Proc. Natl. Acad. Sci. U. S. A.* (2016). doi:10.1073/pnas.1600582113
83. Wang, D. *et al.* Adenovirus-Mediated Somatic Genome Editing of Pten by CRISPR/Cas9 in Mouse Liver in Spite of Cas9-Specific Immune Responses. *Hum. Gene Ther.* **26,** 432–442 (2015).
84. Dow, L. E. *et al.* Inducible in vivo genome editing with CRISPR-Cas9. *Nat. Biotechnol.* (2015). doi:10.1038/nbt.3155
85. Olive, K. P. *et al.* Mutant p53 gain of function in two mouse models of Li-Fraumeni syndrome. *Cell* **119,** 847–860 (2004).
86. Lang, G. A. *et al.* Gain of function of a p53 hot spot mutation in a mouse model of Li-Fraumeni syndrome. *Cell* **119,** 861–872 (2004).
87. Drost, R. *et al.* BRCA1 RING Function Is Essential for Tumor Suppression but Dispensable for Therapy

Resistance. *Cancer Cell* **20,** 797–809 (2011).
88. Drost R *et al.* BRCA1-185delAG tumors may acquire therapy resistance through expression of RING-less BRCA1. *J. Clin. Invest.* (In press).
89. Maddalo, D. *et al.* In vivo engineering of oncogenic chromosomal rearrangements with the CRISPR/Cas9 system. *Nature* **516,** 423–427 (2014).
90. Sutherland, K. D. *et al.* Cell of origin of small cell lung cancer: inactivation of Trp53 and Rb1 in distinct cell types of adult mouse lung. *Cancer Cell* **19,** 754–764 (2011).
91. Molyneux, G. *et al.* BRCA1 basal-like breast cancers originate from luminal epithelial progenitors and not from basal stem cells. *Cell Stem Cell* **7,** 403–417 (2010).
92. Koren, S. *et al.* PIK3CA(H1047R) induces multipotency and multi-lineage mammary tumours. *Nature* **525,** 114–118 (2015).
93. Van Keymeulen, A. *et al.* Reactivation of multipotency by oncogenic PIK3CA induces breast tumour heterogeneity. *Nature* **525,** 119–123 (2015).
94. Kalluri, R. & Zeisberg, M. Fibroblasts in cancer. *Nat. Rev. Cancer* **6,** 392–401 (2006).
95. Erez, N., Truitt, M., Olson, P., Arron, S. T. & Hanahan, D. Cancer-Associated Fibroblasts Are Activated in Incipient Neoplasia to Orchestrate Tumor-Promoting Inflammation in an NF-kappaB-Dependent Manner. *Cancer Cell* **17,** 135–147 (2010).
96. Özdemir, B. C. *et al.* Depletion of carcinoma-associated fibroblasts and fibrosis induces immunosuppression and accelerates pancreas cancer with reduced survival. *Cancer Cell* **25,** 719–734 (2014).
97. Coussens, L. M. *et al.* Inflammatory mast cells up-regulate angiogenesis during squamous epithelial carcinogenesis. *Genes Dev.* **13,** 1382–1397 (1999).
98. Coussens, L. M., Tinkle, C. L., Hanahan, D. & Werb, Z. MMP-9 supplied by bone marrow-derived cells contributes to skin carcinogenesis. *Cell* **103,** 481–490 (2000).
99. de Visser, K. E., Korets, L. V. & Coussens, L. M. De novo carcinogenesis promoted by chronic inflammation is B lymphocyte dependent. *Cancer Cell* **7,** 411–423 (2005).
100. Lin, E. Y., Nguyen, A. V., Russell, R. G. & Pollard, J. W. Colony-stimulating factor 1 promotes progression of mammary tumors to malignancy. *J. Exp. Med.* **193,** 727–740 (2001).
101. Noy, R. & Pollard, J. W. Tumor-Associated Macrophages: From Mechanisms to Therapy. *Immunity* **41,** 49–61 (2014).
102. Coffelt, S. B., Wellenstein, M. D. & de Visser, K. E. Neutrophils in cancer: neutral no more. *Nat. Rev. Cancer* **16,** 431–446 (2016).
103. McAllister, S. S. & Weinberg, R. A. The tumour-induced systemic environment as a critical regulator of cancer progression and metastasis. *Nat. Cell Biol.* **16,** 717–727 (2014).
104. Quail, D. F. & Joyce, J. A. Microenvironmental regulation of tumor progression and metastasis. *Nat. Med.* **19,** 1423–1437 (2013).
105. Doornebal, C. W. *et al.* A preclinical mouse model of invasive lobular breast cancer metastasis. *Cancer Res.* **73,** 353–363 (2013).
106. Hüsemann, Y. *et al.* Systemic spread is an early step in breast cancer. *Cancer Cell* **13,** 58–68 (2008).
107. Tsai, J. H., Donaher, J. L., Murphy, D. A., Chau, S. & Yang, J. Spatiotemporal Regulation of Epithelial-Mesenchymal Transition Is Essential for Squamous Cell Carcinoma Metastasis. *Cancer Cell* **22,** 725–736 (2012).
108. Zheng, X. *et al.* Epithelial-to-mesenchymal transition is dispensable for metastasis but induces chemoresistance in pancreatic cancer. *Nature* **527,** 525–530 (2015).
109. Fischer, K. R. *et al.* Epithelial-to-mesenchymal transition is not required for lung metastasis but contributes to chemoresistance. *Nature* **527,** 472–476 (2015).
110. DeNardo, D. G. *et al.* CD4(+) T cells regulate pulmonary metastasis of mammary carcinomas by enhancing protumor properties of macrophages. *Cancer Cell* **16,** 91–102 (2009).
111. Bald, T. *et al.* Ultraviolet-radiation-induced inflammation promotes angiotropism and metastasis in melanoma. *Nature* **507,** 109–113 (2014).
112. Coffelt, S. B. *et al.* IL-17-producing γδ T cells and neutrophils conspire to promote breast cancer metastasis. *Nature* **522,** 345–348 (2015).
113. Wculek, S. K. & Malanchi, I. Neutrophils support lung colonization of metastasis-initiating breast cancer cells. *Nature* **528,** 413–417 (2015).
114. Liu, P. *et al.* Oncogenic PIK3CA-driven mammary tumors frequently recur via PI3K pathway-dependent and PI3K pathway-independent mechanisms. *Nat. Med.* **17,** 1116–1120 (2011).
115. Ventura, A. *et al.* Restoration of p53 function leads to tumour regression in vivo. *Nature* **445,** 661–665 (2007).

116. Xue, W. *et al.* Senescence and tumour clearance is triggered by p53 restoration in murine liver carcinomas. *Nature* **445,** 656–660 (2007).
117. Vassilev, L. T. *et al.* In vivo activation of the p53 pathway by small-molecule antagonists of MDM2. *Science* **303,** 844–848 (2004).
118. Bykov, V. J. N. *et al.* Restoration of the tumor suppressor function to mutant p53 by a low-molecular-weight compound. *Nat. Med.* **8,** 282–288 (2002).
119. Singh, M. *et al.* Assessing therapeutic responses in Kras mutant cancers using genetically engineered mouse models. *Nat. Biotechnol.* **28,** 585–593 (2010).
120. Rottenberg, S. *et al.* Selective induction of chemotherapy resistance of mammary tumors in a conditional mouse model for hereditary breast cancer. *Proc. Natl. Acad. Sci.* **104,** 12117–12122 (2007).
121. Rottenberg, S. *et al.* High sensitivity of BRCA1-deficient mammary tumors to the PARP inhibitor AZD2281 alone and in combination with platinum drugs. *Proc. Natl. Acad. Sci. U. S. A.* **105,** 17079–17084 (2008).
122. Lee, J.-M., Ledermann, J. A. & Kohn, E. C. PARP Inhibitors for BRCA1/2 mutation-associated and BRCA-like malignancies. *Ann. Oncol.* **25,** 32–40 (2014).
123. Ledermann, J. *et al.* Olaparib maintenance therapy in platinum-sensitive relapsed ovarian cancer. *N. Engl. J. Med.* **366,** 1382–1392 (2012).
124. Ledermann, J. *et al.* Olaparib maintenance therapy in patients with platinum-sensitive relapsed serous ovarian cancer: a preplanned retrospective analysis of outcomes by BRCA status in a randomised phase 2 trial. *Lancet Oncol.* **15,** 852–861 (2014).
125. Jaspers, J. E. *et al.* Loss of 53BP1 causes PARP inhibitor resistance in Brca1-mutated mouse mammary tumors. *Cancer Discov.* **3,** 68–81 (2013).
126. Henneman, L. *et al.* Selective resistance to the PARP inhibitor olaparib in a mouse model for BRCA1-deficient metaplastic breast cancer. *Proc. Natl. Acad. Sci. U. S. A.* **112,** 8409–8414 (2015).
127. Xu, G. *et al.* REV7 counteracts DNA double-strand break resection and affects PARP inhibition. *Nature* **521,** 541–544 (2015).
128. Acharyya, S. *et al.* A CXCL1 paracrine network links cancer chemoresistance and metastasis. *Cell* **150,** 165–178 (2012).
129. Boelens, M. C. *et al.* Exosome transfer from stromal to breast cancer cells regulates therapy resistance pathways. *Cell* **159,** 499–513 (2014).
130. DeNardo, D. G. *et al.* Leukocyte complexity predicts breast cancer survival and functionally regulates response to chemotherapy. *Cancer Discov.* **1,** 54–67 (2011).
131. Farmer, P. *et al.* A stroma-related gene signature predicts resistance to neoadjuvant chemotherapy in breast cancer. *Nat. Med.* **15,** 68–74 (2009).
132. Nakasone, E. S. *et al.* Imaging tumor-stroma interactions during chemotherapy reveals contributions of the microenvironment to resistance. *Cancer Cell* **21,** 488–503 (2012).
133. Olive, K. P. *et al.* Inhibition of Hedgehog signaling enhances delivery of chemotherapy in a mouse model of pancreatic cancer. *Science* **324,** 1457–1461 (2009).
134. Rhim, A. D. *et al.* Stromal Elements Act to Restrain, Rather Than Support, Pancreatic Ductal Adenocarcinoma. *Cancer Cell* **25,** 735–747 (2014).
135. Hodi, F. S. *et al.* Improved survival with ipilimumab in patients with metastatic melanoma. *N. Engl. J. Med.* **363,** 711–723 (2010).
136. Topalian, S. L. *et al.* Safety, activity, and immune correlates of anti-PD-1 antibody in cancer. *N. Engl. J. Med.* **366,** 2443–2454 (2012).
137. Waterhouse, P. *et al.* Lymphoproliferative disorders with early lethality in mice deficient in Ctla-4. *Science* **270,** 985–988 (1995).
138. Nishimura, H., Nose, M., Hiai, H., Minato, N. & Honjo, T. Development of lupus-like autoimmune diseases by disruption of the PD-1 gene encoding an ITIM motif-carrying immunoreceptor. *Immunity* **11,** 141–151 (1999).
139. Nishimura, H. *et al.* Autoimmune dilated cardiomyopathy in PD-1 receptor-deficient mice. *Science* **291,** 319–322 (2001).
140. Leach, D. R., Krummel, M. F. & Allison, J. P. Enhancement of antitumor immunity by CTLA-4 blockade. *Science* **271,** 1734–1736 (1996).
141. Willimsky, G. & Blankenstein, T. Sporadic immunogenic tumours avoid destruction by inducing T-cell tolerance. *Nature* **437,** 141–146 (2005).
142. Garbe, A. I. *et al.* Genetically induced pancreatic adenocarcinoma is highly immunogenic and causes spontaneous tumor-specific immune responses. *Cancer Res.* **66,** 508–516 (2006).

143. DuPage, M. *et al.* Endogenous T cell responses to antigens expressed in lung adenocarcinomas delay malignant tumor progression. *Cancer Cell* **19,** 72–85 (2011).
144. Ruffell, B. *et al.* Macrophage IL-10 blocks CD8+ T cell-dependent responses to chemotherapy by suppressing IL-12 expression in intratumoral dendritic cells. *Cancer Cell* **26,** 623–637 (2014).
145. Mitchem, J. B. *et al.* Targeting Tumor-Infiltrating Macrophages Decreases Tumor-Initiating Cells, Relieves Immunosuppression, and Improves Chemotherapeutic Responses. *Cancer Res.* **73,** 1128–1141 (2013).
146. Broz, M. L. *et al.* Dissecting the Tumor Myeloid Compartment Reveals Rare Activating Antigen-Presenting Cells Critical for T Cell Immunity. *Cancer Cell* **26,** 638–652 (2014).
147. Engelhardt, J. J. *et al.* Marginating dendritic cells of the tumor microenvironment cross-present tumor antigens and stably engage tumor-specific T cells. *Cancer Cell* **21,** 402–417 (2012).
148. Salmon, H. *et al.* Expansion and Activation of CD103+ Dendritic Cell Progenitors at the Tumor Site Enhances Tumor Responses to Therapeutic PD-L1 and BRAF Inhibition. *Immunity* **44,** 924–938 (2016).
149. Sánchez-Paulete, A. R. *et al.* Cancer Immunotherapy with Immunomodulatory Anti-CD137 and Anti-PD-1 Monoclonal Antibodies Requires BATF3-Dependent Dendritic Cells. *Cancer Discov.* **6,** 71–79 (2016).
150. Zhu, Y. *et al.* CSF1/CSF1R Blockade Reprograms Tumor-Infiltrating Macrophages and Improves Response to T-cell Checkpoint Immunotherapy in Pancreatic Cancer Models. *Cancer Res.* **74,** 5057–5069 (2014).
151. Highfill, S. L. *et al.* Disruption of CXCR2-mediated MDSC tumor trafficking enhances anti-PD1 efficacy. *Sci. Transl. Med.* **6,** 237ra67 (2014).
152. DuPage, M., Mazumdar, C., Schmidt, L. M., Cheung, A. F. & Jacks, T. Expression of tumour-specific antigens underlies cancer immunoediting. *Nature* **482,** 405–409 (2012).
153. Joshi, N. S. *et al.* Regulatory T Cells in Tumor-Associated Tertiary Lymphoid Structures Suppress Anti-tumor T Cell Responses. *Immunity* **43,** 579–590 (2015).
154. DuPage, M. & Jacks, T. Genetically engineered mouse models of cancer reveal new insights about the antitumor immune response. *Curr. Opin. Immunol.* **25,** 192–199 (2013).
155. Clohessy, J. G. & Pandolfi, P. P. Mouse hospital and co-clinical trial project-from bench to bedside. *Nat. Rev. Clin. Oncol.* **12,** 491–498 (2015).

-3-

IL-17-producing γδ T cells and neutrophils conspire to promote breast cancer metastasis

Seth B. Coffelt[1], Kelly Kersten[1]*, Chris W. Doornebal[1]*, Jorieke Weiden[1], Kim Vrijland[1], Cheei-Sing Hau[1], Niels J. M. Verstegen[1], Metamia Ciampricotti[1], Lukas J. A. C. Hawinkels[2,3], Jos Jonkers[4] & Karin E. de Visser[1]

[1]Division of Immunology, Netherlands Cancer Institute, Amsterdam, The Netherlands
[2]Department of Molecular Cell Biology, Leiden University Medical Center, Leiden, The Netherlands
[3]Centre for Biomedical Genetics, Leiden University Medical Center, Leiden, The Netherlands
[4]Division of Molecular Pathology, Netherlands Cancer Institute, Amsterdam, The Netherlands

*These authors contributed equally to this work.

Nature 522:345-348 (2015)

Abstract

Metastatic disease remains the primary cause of death for patients with breast cancer. The different steps of the metastatic cascade rely on reciprocal interactions between cancer cells and their microenvironment. Within this local microenvironment and in distant organs, immune cells and their mediators are known to facilitate metastasis formation [1,2]. However, the precise contribution of tumor-induced systemic inflammation to metastasis and the mechanisms regulating systemic inflammation are poorly understood. Here we show that tumors maximize their chance of metastasizing by evoking a systemic inflammatory cascade in mouse models of spontaneous breast cancer metastasis. We mechanistically demonstrate that interleukin (IL)-1β elicits IL-17 expression from gamma delta (γδ) T cells, resulting in systemic, granulocyte colony-stimulating factor (G-CSF)-dependent expansion and polarization of neutrophils in mice bearing mammary tumors. Tumor-induced neutrophils acquire the ability to suppress cytotoxic T lymphocytes carrying the CD8 antigen, which limit the establishment of metastases. Neutralization of IL-17 or G-CSF and absence of γδ T cells prevents neutrophil accumulation and downregulates the T-cell-suppressive phenotype of neutrophils. Moreover, the absence of γδ T cells or neutrophils profoundly reduces pulmonary and lymph node metastases without influencing primary tumor progression. Our data indicate that targeting this novel cancer cell-initiated domino effect within the immune system — the γδ T cell/IL-17/neutrophil axis — represents a new strategy to inhibit metastatic disease.

In patients with breast cancer, increased neutrophil abundance predicts worsened metastasis-specific survival [3,4]. Currently, the role of neutrophils in metastasis is controversial, since both pro- and anti-metastatic functions have been described [5–7]. We found a profound systemic expansion of neutrophils in mammary tumor-bearing *K14cre;Cdh1$^{F/F}$;Trp53$^{F/F}$* (KEP) mice [8], compared with wild-type (WT) littermates (Extended Data Fig. 1a, b). Neutrophils, defined as CD45$^+$CD11b$^+$Ly6G$^+$Ly6C$^+$F4/80$^-$ cells, accumulated throughout every organ examined (Extended Data Fig. 1c, d). We also investigated our recently described KEP-based model of spontaneous breast cancer metastasis [9] (Fig. 1a), where systemic neutrophil expansion was observed as well (Fig. 1b and Extended Data Fig. 1e, f). Neutrophil expansion was tumor-induced, because surgical removal of the primary tumor resulted in their immediate reduction (Extended Data Fig. 1g).

To determine the functional significance of neutrophils in metastasis, neutrophils were depleted using anti-Ly6G antibodies (Extended Data Fig. 2a–c). Treatment was initiated when tumors were palpable and continued until mice developed overt metastatic disease. Neutrophil depletion did not influence tumor growth (Extended Data Fig. 2d), tumor histopathology (Extended Data Fig. 2e) or microvessel density (Extended Data Fig. 2e, f). In contrast, neutrophil depletion resulted in significant reduction in both pulmonary and lymph node metastasis (Fig. 1c). These data indicate that neutrophils assist the spread of cancer cells to multiple locations.

Next, we evaluated the role of neutrophils in different phases of the metastatic cascade. Neutrophils were depleted during primary tumor growth (early phase) or after removal of the primary tumor (late phase) (Fig. 1a). Interestingly, neutrophil depletion decreased multi-organ metastasis in the early phase, but not the late phase (Fig. 1d). Metastatic nodule size was not affected (Extended Data Fig. 2g), suggesting that neutrophils facilitate multi-organ metastasis during the early steps of the metastatic cascade.

To understand the mechanism by which neutrophils facilitate metastasis, their phenotype was investigated. Previous reports identified the hematopoietic stem cell marker cKIT on pro-metastatic myeloid cells [6,10–12], and CD11b$^+$VEGFR1$^+$ cells have been implicated in the pre-metastatic niche [10,13,14]. A greater proportion of neutrophils from tumor-bearing KEP mice expressed cKIT, while both neutrophils and monocytes from WT and KEP mice expressed VEGFR1 (Extended Data Fig. 3a, b). In the metastasis model, cKIT$^+$ neutrophils also expanded systemically, as tumors grew larger (Extended Data Fig. 3c) and reduced to baseline levels after tumor resection (Extended Data Fig. 3d). Nuclear morphological analysis revealed characteristics of immature cells [15], including banded, circular and non-segmented nuclei, whereas most WT neutrophils appeared hyper-segmented (Extended Data Fig. 3e), suggesting that KEP mammary tumors promote the release of immature neutrophils into circulation.

Next-generation RNA sequencing (RNA-seq) was performed on circulating neutrophils from WT and tumor-bearing KEP mice, revealing 100 differentially expressed genes (Extended Data Fig. 4a and Extended Data Table 1). Several genes upregulated in neutrophils from KEP mice, including *Prok2* (also known as *Bv8*), *S100a8* and *S100a9*

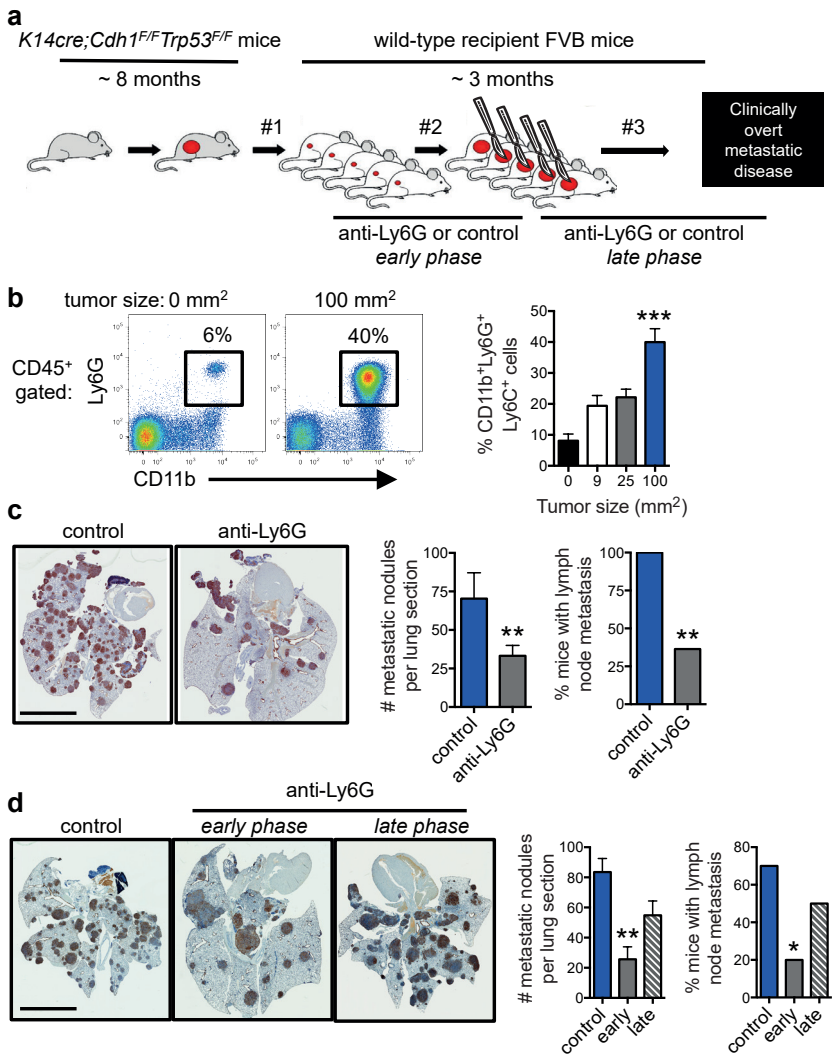

Figure 1. Neutrophils promote breast cancer metastasis. a) Spontaneous metastasis model. Tumor fragments from KEP mice are orthotopically transplanted into WT female FVB/N recipient mice (designated by #1), allowed to proliferate (#2), then surgically resected (#3) [9]. Metastases develop in 100% of recipient mice. Antibody-mediated depletion experiments were performed in three ways: from palpable tumors to metastasis-related death (continuous treatment), during primary tumor growth (early phase) or after surgery until metastasis-related death (late phase). b) Neutrophil proportions in lungs at the indicated tumor size (n=6, 5, 6 and 8 mice for 0, 9, 25 and 100mm^2, respectively; Kruskal-Wallis test followed by post-hoc Dunn's test). c, d) Images of cytokeratin 8-stained lung sections, quantification of lung metastases and incidence of metastasis in lymph nodes. Neutrophils were depleted continuously until metastasis-related death in c (n=11 mice per group; Mann-Whitney U-test and Fisher's exact test) or depleted during the early or late phases in d (n=9 control, 11 early phase, 14 late phase; Kruskal-Wallis test followed by post-hoc Dunn's test and Fisher's exact test). Data in d are representative of two independent experiments. All data are mean + s.e.m. *P<0.05, **P<0.01, ***P<0.001. Scale bars, 6mm.

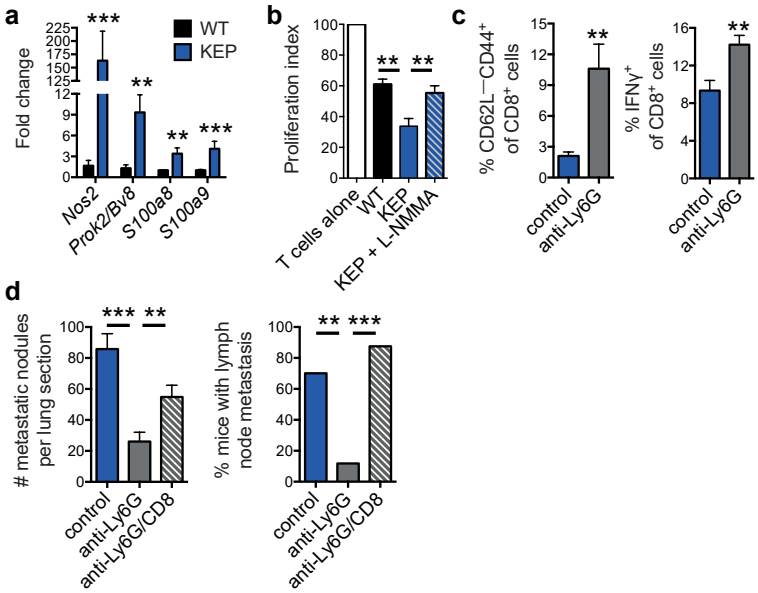

Figure 2. Neutrophils suppress CD8⁺ T cell activation to facilitate metastasis. a) Gene expression in circulating neutrophils (n=5 WT, 10 KEP mice). b) Circulating neutrophils from either WT (n=7) or tumor-bearing KEP mice (n=8) were incubated with CFSE-labelled splenic CD8⁺ T cells from WT mice and CD3/CD28 stimulation beads. The iNOS inhibitor L-NMMA was added where indicated (n=8). After 48 h, CD8⁺ T cell proliferation was measured. c) CD8⁺ T cell activation status in lungs of transplanted tumor-bearing control and neutrophil-depleted mice (n=6 per group). d) Quantification of lung metastases and incidence of lymph node metastasis following neutrophil and CD8⁺ T cell depletion (n=11 control, 16 anti-Ly6G, 8 anti-Ly6G/CD8; Kruskal-Wallis test followed by post-hoc Dunn's test and Fisher's exact test). All data are mean + s.e.m. *P<0.05, **P<0.01, ***P<0.001.

(Fig. 2a), have previously been linked to metastasis [6,14]. *Nos2*, the gene encoding inducible nitric oxide synthase (iNOS), was the most strongly upregulated gene, by more than 150-fold (Fig. 2a). Because iNOS suppresses T cells [16–18], we hypothesized that neutrophils promote metastasis via immunosuppression. Indeed, neutrophils from KEP mice inhibited the CD3/CD28-induced proliferation of naive splenic CD8⁺ T cells *ex vivo* compared with WT neutrophils, and an iNOS inhibitor reversed this effect (Fig. 2b and Extended Data Fig. 4b). In lungs of control and neutrophil-depleted tumor-bearing mice, the proportions of CD8⁺ T cells did not differ (Extended Data Fig. 4c). However, the effector phenotype of CD8⁺ T cells was markedly enhanced upon neutrophil depletion, as evidenced by a significantly greater proportion of CD62L⁻CD44⁺ and interferon-γ⁺ (IFN-γ⁺) cells (Fig. 2c and Extended Data Fig. 4d, e). To establish further a mechanistic link between neutrophils and CD8⁺ T cell activity, we depleted both cell populations in the metastasis model. Combined depletion of neutrophils and CD8⁺ T cells reversed the metastasis phenotype of neutrophil depletion alone (Fig. 2d), without affecting primary tumor growth (Extended Data Fig. 4f). Depletion of CD8⁺ T cells alone did not alter tumor growth or multi-organ metastasis (data not shown). These data suggest that neutrophils

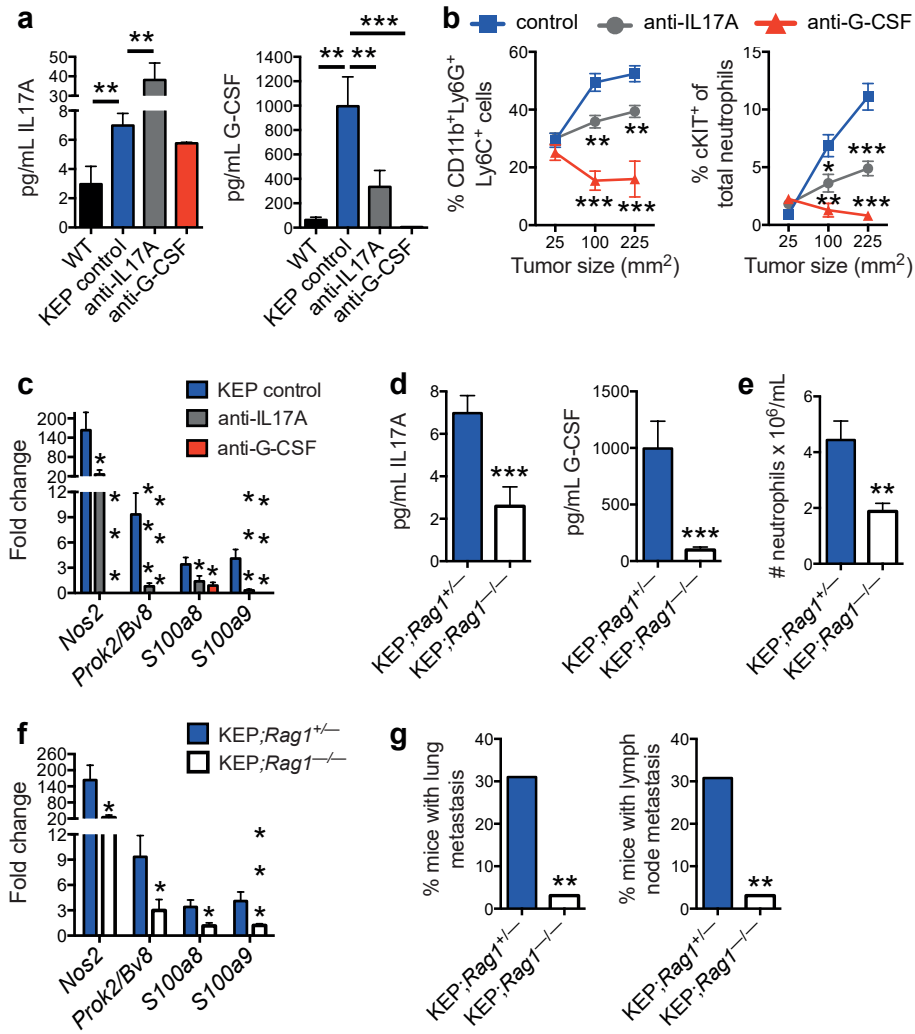

Figure 3. Lymphocyte-derived IL-17 is required for G-CSF-induced neutrophil expansion and phenotype. a) Cytokine levels in serum of WT (n=5), tumor-bearing KEP mice (n=9) and anti-IL-17- (n=7) or anti-GCSF- treated KEP mice (n=6). b) Proportions of circulating neutrophils and cKIT-expressing neutrophils in KEP mice during primary tumor growth (n=9 control, 8 anti-IL-17, 6 anti-G-CSF). c) Gene expression in circulating neutrophils from tumor-bearing KEP control mice (n=9), anti-IL-17- (n=6) or anti-G-CSF-treated KEP mice (n=6). d) Cytokine levels in serum of tumor-bearing KEP;*Rag1*$^{+/-}$ (n=9) and KEP;*Rag1*$^{-/-}$ mice (n=7). e) Absolute blood neutrophil counts in tumor-bearing KEP;*Rag1*$^{+/-}$ mice (n=8) or KEP;*Rag1*$^{-/-}$ mice (n=5). f) Gene expression in circulating neutrophils from KEP;*Rag1*$^{+/-}$ (n=10) and KEP;*Rag1*$^{-/-}$ mice (n=8). g) Percentage of tumor-bearing mice with lung or lymph node metastasis (n=50 KEP;*Rag1*$^{+/-}$, 32 KEP;*Rag1*$^{-/-}$ mice). All data are mean + s.e.m. *P<0.05, **P<0.01, ***P<0.001 as determined by Mann-Whitney U-test or Fisher's exact test.

facilitate cancer cell spread by suppressing $CD8^+$ T cells. As such, neutrophils in the KEP model can be categorized as a subpopulation of myeloid-derived suppressor cells [15].

We then asked how mammary tumors induce systemic neutrophil expansion. Cytokine profile comparison of WT mammary glands and KEP mammary tumors showed that granulocyte-macrophage colony stimulating factor (GM-CSF) and G-CSF levels — two key regulators of neutrophil biology [19]— were not significantly increased in KEP tumors (Extended Data Fig. 5a, b). However, expression of IL-1β, IL-6 and IL- 12p40, a subunit of IL-23, was increased (Extended Data Fig. 5a, b). These cytokines are known to stimulate IL-17 from lymphocytes [20–23]. In inflammatory diseases such as psoriasis, lymphocyte-derived IL-17 regulates neutrophil expansion via systemic induction of G-CSF [21,22,24].

We hypothesized that the same inflammatory cascade is important in breast cancer metastasis. Indeed, serum levels of IL-17A and G-CSF were higher in tumor-bearing KEP mice than in WT mice (Fig. 3a). Neutralization of IL-17A in tumor-bearing KEP mice decreased G-CSF serum levels, while G-CSF blockade did not affect IL-17A levels (Fig. 3a), indicating that IL-17 is upstream of G-CSF. Inhibition of either cytokine reduced circulating neutrophils, lowered $cKIT^+$ neutrophil proportions (Fig. 3b) and reversed neutrophil phenotype (Fig. 3c). Injection of recombinant G-CSF to anti-IL-17-treated tumor-bearing KEP mice overcame the effects of anti-IL-17 treatment (Extended Data Fig. 5c–e). Additionally, treatment of WT mice with recombinant G-CSF resulted in neutrophil expansion, increased presence of $cKIT^+$ neutrophil proportions and changed neutrophil phenotype (Extended Data Fig. 5c–e). These data demonstrate a requirement for the IL-17/G-CSF signaling cascade in both neutrophil expansion and phenotype.

Next, we determined the source of IL-17. As T cells are known to produce IL-17 [20,21,23], splenic $CD3^+$ T cells were analyzed using a T cell-specific gene expression array. This analysis validated upregulation of IL-17-related cytokines in T cells from tumor-bearing KEP mice (Extended Data Fig. 5f). We then asked whether lymphocytes are the only source of IL-17 and whether they drive metastasis. KEP mice were crossed with *Rag1*$^{-/-}$ mice, which lack T and B cells. Tumor initiation, proliferation and histology were the same between KEP;*Rag1*$^{+/-}$ and KEP;*Rag1*$^{-/-}$ mice (Extended Data Fig. 6a and data not shown). However, KEP;*Rag1*$^{-/-}$ mice exhibited lower levels of IL-17A and G-CSF in serum (Fig. 3d), decreased neutrophil counts (Fig. 3e) and altered neutrophil phenotype (Fig. 3f). Transforming growth factor β1 (TGF-β1) levels were unchanged between KEP;*Rag1*$^{+/-}$ and KEP;*Rag1*$^{-/-}$ mice (Extended Data Fig. 6b), suggesting that, unlike other models [25], TGF-β plays a lesser role in modulating neutrophil phenotype than IL-17-induced G-CSF. Importantly, KEP;*Rag1*$^{-/-}$ mice displayed less pulmonary and lymph node metastases (Fig. 3g). The metastasis phenotype in KEP;*Rag1*$^{-/-}$ mice was validated in the metastasis model where *Rag1*$^{-/-}$ mice were recipients of transplanted KEP tumor fragments, resulting in reduced pulmonary metastasis (Extended Data Fig. 6c). Thus, IL-17-producing lymphocytes drive neutrophil accumulation, phenotype and metastasis.

Direct *ex vivo* intracellular cytokine staining was performed to determine which T lymphocyte subset produces IL-17. Both $CD4^+$ T cells and γδ T cells expressed IL-17A (Fig. 4a), and both IL-17-producing subpopulations were increased in various organs of

tumor-bearing KEP mice compared with WT mice (Fig. 4b and Extended Data Fig. 7a). In primary tumors, the abundance of γδ and $CD4^+$ T cells was too low (<0.2% and <2% of all live cells, respectively) to assess IL-17 expression reliably. γδ T cells exhibited higher IL-17A levels than $CD4^+$ T cells (Fig. 4a and Extended Data Fig. 7b). Both cell populations were depleted to determine their functional importance. $CD4^+$ T cell depletion lowered $cKIT^+$ neutrophils, but failed to influence total neutrophil expansion, IL-17A or G-CSF levels (Extended Data Fig. 7c–e). Conversely, depletion of γδ T cells decreased IL-17A and G-CSF serum levels (Fig. 4c), reduced circulating neutrophils, lowered $cKIT^+$ neutrophil proportions (Fig. 4d and Extended Data Fig. 7c) and reversed neutrophil phenotype (Fig. 4e). These data indicate that IL-17-producing γδ T cells promote neutrophil expansion and phenotypic alterations. IL-17-producing γδ T cells in tumor-bearing KEP mice were $CD27^-$, mostly $Vγ4^+$, and a proportion expressed CCR6, IL-1R1 and ROR-γt (Extended Data Fig. 8a, b) similar to other inflammatory diseases [21]. We then asked how KEP mammary tumors activate IL-17-producing γδ T cells. On the basis of literature [20–23] and cytokine analysis (Extended Data Fig. 5a, b), we focused on IL-23 and IL-1β. IL-17A expression by γδ T cells, G-CSF serum levels and neutrophil expansion was decreased by neutralization of IL-1β, but unaffected by inhibition of IL-23 (Fig. 4f–h). Macrophages were the most abundant IL-1β-expressing cell type in KEP tumors (Extended Data Fig. 8c, d). These data provide a mechanistic link between mammary tumors and γδ T cells.

Depletion of γδ T cells in the early phase of the metastasis model did not affect tumor histopathology, microvessel density or primary tumor growth (Extended Data Fig. 8e and data not shown). Importantly, however, pulmonary and lymph node metastases were significantly decreased in γδ T cell-depleted mice (Fig. 4i). These data were validated with *Tcrd*$^{-/-}$ mice, which lack γδ T cells. KEP tumor fragments were orthotopically transplanted into *Tcrd*$^{+/-}$ and *Tcrd*$^{-/-}$ mice and resected after outgrowth. Genetic elimination of γδ T cells also resulted in a significant reduction in pulmonary metastasis (Fig. 4j) without affecting primary tumor growth (Extended Data Fig. 8f). These data confirm a pro-metastatic role for γδ T cells.

In summary, we show that mammary tumor-induced, IL-17-producing γδ T cells drive systemic expansion and polarization of neutrophils towards a $CD8^+$ T cell-suppressive phenotype and subsequent metastasis formation in distant organs (Extended Data

Figure 4. ► IL-1β-activated, IL-17-producing γδ T cells regulate neutrophil expansion, neutrophil phenotype and metastasis. a) Intracellular staining within circulating T cells of tumor-bearing KEP mice. b) Proportion of IL-17A-producing γδ T cells (WT, n=5; KEP, n=6). c) Cytokine levels in serum of control (n=10) and anti-γδTCR-treated (n=7) KEP mice. d) Proportions of circulating neutrophils and cKIT-expressing neutrophils in KEP mice during primary tumor growth (n=8 per group). e) Gene expression in circulating neutrophils from tumor-bearing KEP control mice (n=10) and anti-γδTCR-treated KEP mice (n=6). f) Proportion of IL-17A-producing γδ T cells in tumor-bearing mice (n=6 KEP control, 5 anti-IL-23p19, 5 anti- IL-1β). g) Cytokine levels in serum (n=9 KEP control, 5 anti-IL-23p19, 6 anti-IL 1β). h) Proportions of circulating neutrophils and cKIT-expressing neutrophils in KEP mice during primary tumor growth (n=9 control, 5 anti- IL-23p19, 5 anti-IL-1β). i, j) Quantification of lung metastases and incidence of lymph node metastasis in the metastasis model (n=10 control, 9 anti-γδTCR-treated mice; n=9 per group *Tcrd*$^{+/-}$ and *Tcrd*$^{-/-}$ mice). All data are mean + s.e.m. *P<0.05, **P<0.01, ***P<0.001 as determined by Mann-Whitney U-test or Fisher's exact test.

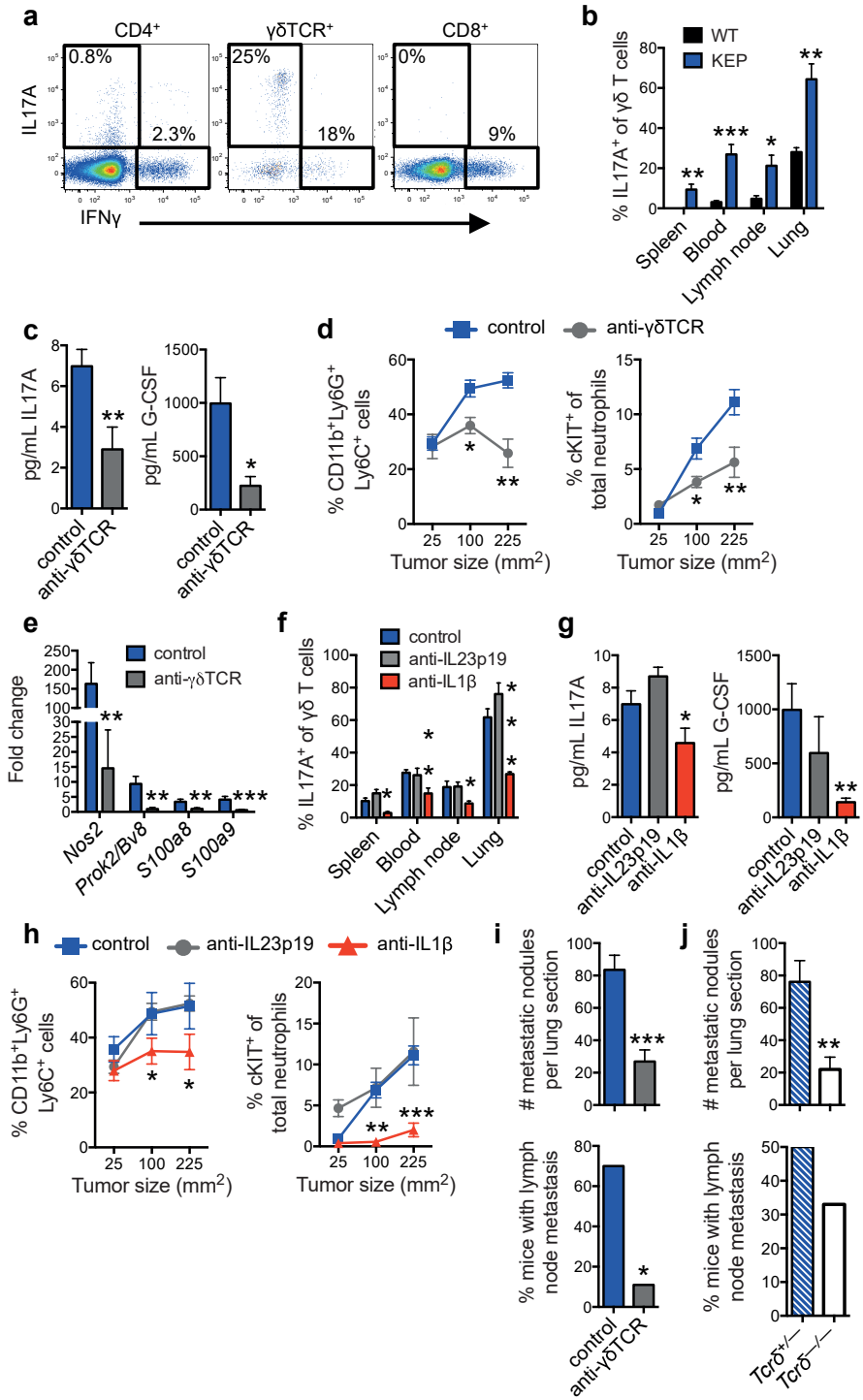
a
CD4+
γδTCR+
CD8+
0.8%
2.3%
25%
18%
0%
9%
IL17A
IFNγ
b
WT
KEP
% IL17A+ of γδ T cells
Spleen
Blood
Lymph node
Lung
c
pg/mL IL17A
pg/mL G-CSF
control
anti-γδTCR
d
control
anti-γδTCR
% CD11b+Ly6G+ Ly6C+ cells
% cKIT+ of total neutrophils
Tumor size (mm2)
e
control
anti-γδTCR
Fold change
Nos2
Prok2/Bv8
S100a8
S100a9
f
control
anti-IL23p19
anti-IL1β
% IL17A+ of γδ T cells
Spleen
Blood
Lymph node
Lung
g
pg/mL IL17A
pg/mL G-CSF
control
anti-IL23p19
anti-IL1β
h
control
anti-IL23p19
anti-IL1β
% CD11b+Ly6G+ Ly6C+ cells
% cKIT+ of total neutrophils
Tumor size (mm2)
i
metastatic nodules per lung section
% mice with lymph node metastasis
control
anti-γδTCR
j
metastatic nodules per lung section
% mice with lymph node metastasis
Tcrδ+/−
Tcrδ−/−

Fig. 9). The importance of neutrophils during the early steps of the metastatic cascade and the upregulation of *Prok2*, *S100a8* and *S100a9* in neutrophils suggest that neutrophils may help to establish the pre-metastatic niche [6,10,14]; however, the role of these neutrophil-derived factors and others remains to be established in the KEP model. In patients with breast cancer, independent clinical studies consistently point towards a pro-metastatic role for neutrophils, γδ T cells and IL-17 [3,4,26–29]. Here, we establish a mechanistic connection between these independent clinical observations. In infection and inflammatory disorders, the γδ T cell/IL-17/neutrophil axis drives disease pathogenesis [21,23,30]. We now demonstrate that this targetable pathway also perpetuates breast cancer metastasis.

Methods

Mice

The generation and characterization of *K14cre;Cdh1$^{F/F}$;Trp53$^{F/F}$* (KEP) mice—a conditional model of invasive lobular breast cancer—has been described [8]. KEP mice were backcrossed onto the FVB/N background. KEP mice were crossed with Rag1$^{-/-}$ mice (FVB/N; a gift from L. Coussens)[31] to generate KEP;*Rag1*$^{+/-}$ and KEP;*Rag1*$^{-/-}$ *mice* [32]. The onset of mammary tumor formation was monitored twice weekly by palpation and caliper measurements starting at 4 months of age. *Tcrd*$^{-/-}$ mice on the FVB/N background were a gift from A. Hayday [33]. The spontaneous metastasis model has also been described [9]. Briefly, this model is based on the orthotopic transplantation of KEP tumor pieces into 10- to 12-week-old female recipient FVB/N mice, *Rag1*$^{-/-}$ mice, *Tcrd*$^{+/-}$ or *Tcrd*$^{-/-}$ mice. These tumor pieces are allowed to grow out, then surgically removed at 100 mm^2, after which 100% of mice develop overt metastatic disease. To deplete immune cells or neutralize cytokines, mice were injected intraperitoneally with an initial 400 mg followed by 100 mg thrice weekly for anti-Ly6G (clone 1A8; BioXCell), 200 mg twice weekly for anti-CD8 (clone 2.43; BioXCell) or 100 mg twice weekly for anti-γδTCR (clone GL3; purified by the NKI protein facility). For cytokine neutralization experiments, KEP mice were injected intraperitoneally with 50 mg twice weekly for anti-IL-17A (clone 17F3; BioXCell), 50 mg thrice weekly for anti-G-CSF (clone 67604; R&DSystems), 50 mg twice weekly anti-IL-23p19 (clone G23-8; eBioscience) or 50 mg twice weekly anti-IL-1b (clone B122; BioXCell). Control mice received equal amounts of isotope control antibodies or equal volumes of PBS. Where indicated, WT and KEP mice were injected intraperitoneally with 5 mg rG-CSF (Peprotech) for four consecutive days and were killed on the fifth day. Tumor-bearing KEP mice injected with rG-CSF received anti-IL-17 at the same schedule as above. Antibody injections began when KEP mammary tumors reached 25 mm^2 until death at 225 mm^2, or transplanted tumors reached 9 mm^2 where indicated until surgery at 100 mm^2. Three independent KEP donor tumors were tested in neutrophil depletion experiments resulting in the same outcome. One of these donor tumors was used throughout the remainder of the study. Blood samples were taken before and during antibody injections for flow cytometry analyses.

Animals were randomized before beginning the treatment schedule. Mice were kept in individually ventilated and open cages, and food and water were provided *ad libitum*. Animal experiments were approved by the Animal Ethics Committee of the Netherlands Cancer Institute and performed in accordance with institutional, national and European guidelines for Animal Care and Use.

Immunohistochemistry

Formalin-fixed tissues were processed by routine procedures. Hematoxylin and eosin staining was performed as described [9]. Citrate antigen retrieval was used for all staining procedures. Neutrophils were detected using either anti-Ly6B (clone 7/4; Cedarlane) or anti-Ly6G (clone 1A8; BD Biosciences), when primary tumors reached 100 mm^2. Quantitative analysis of neutrophil abundance was performed by counting cells in five high-power (X40) fields of view (FOV) per tissue. Metastases were detected using anti-cytokeratin 8 (clone Troma1; Developmental Studies Hybridoma Bank, University of Iowa). In the metastasis model, the total number of cytokeratin 8^+ nodules was scored in one lung section of each animal. The size of each nodule was measured using ImageJ, then represented as arbitrary units. Lymph node metastases were scored as positive or negative on the basis of the presence of cytokeratin 8^+ metastases. Mice that developed overt metastatic disease (that is, respiratory distress or 225 mm^2 axillary lymph node metastasis) were included in the analysis; mice that were killed as a result of local recurrence were excluded. Vimentin, E-cadherin and CD34 staining was performed as previously described [9] and scored independently by two blinded researchers. Microvessel density was scored by averaging the total number of blood vessels from five fields of view for each tumor section. For metastasis quantification in *K14cre;Cdh1$^{F/F}$;Trp53$^{F/F}$;Rag1$^{+/-}$* and *K14cre;Cdh1$^{F/F}$;Trp53$^{F/F}$;Rag1$^{-/-}$* mice, single lung or lymph node sections were scored as positive or negative on the basis of the presence of cytokeratin 8^+ metastases. Stained slides were digitally processed using the Aperio ScanScope and captured using ImageScope software version 11.0.2. Brightness and contrast for representative images were adjusted equally among groups.

Flow cytometry and intracellular staining

Tissues were collected in ice-cold PBS. Blood samples were collected in tubes containing heparin. Tumors and lungs were mechanically chopped using a McIlwain tissue chopper (Mickle Laboratory Engineering). Tumors were digested for 1 h at 37°C in 3 mg/ml collagenase type A (Roche) and 25 mg/ml DNase (Sigma) in serum-free DMEM medium. Lungs were digested for 30 min at 37°C in 100 mg/ml Liberase TM (Roche). Enzyme activity was neutralized by addition of cold DMEM/ 8%FCS and suspension was dispersed through a 70 µm cell strainer. Spleen, lymph nodes and liver were mashed through a 70 µm cell strainer. All single-cell suspensions were treated with NH4Cl erythrocyte lysis buffer. Cells were stained with directly conjugated antibodies (listed below) for 30 min at 4°C in the dark in PBS/1% BSA. 7AAD (1:20; eBioscience) or Fixable Viability Dye eFluor 780 (1:1,000; eBioscience) was added to exclude dead cells. For intracellular staining,

single-cell suspensions were stimulated in IMDM containing 8% FCS, 100 IU/ml penicillin, 100 mg/ml streptomycin, 0.5% β-mercaptoethanol, 50 ng/ml PMA, 1 mM ionomycin and (1:1,000) Golgi-Plug (BD Biosciences) for 3 h at 37°C. Surface antigens were stained first, followed by fixation and permeabilization using the Cytofix/Cytoperm kit (BD Biosciences), then staining of intracellular proteins. All experiments were performed using a BD LSRII flow cytometer using Diva software. Data analyses used FlowJo Software version 9.7.1. Median fluorescence intensity of IL-17A expression was calculated after gating on IL-17$^+$ cells within individual T cell subsets. All antibodies were purchased from eBioscience, except Ly6G-AlexaFluor 700, CCR6 and Vc1 from BioLegend, and VEGFR1, CCR2, IL-23R and IL-1R1 from R&D Systems.

The following antibodies were used in these experiments:

Myeloid panel: CD45-eFluor 605NC (1:50; clone 30-F11), CD11b-eFluor 650NC (1:400; clone M1/70), Ly6G-AlexaFluor 700 (1:400; clone 1A8), Ly6C-eFluor 450 (1:400; clone HK1.4), F4/80-APC-eFluor 780 (1:200; clone BM8), VEGFR1-APC (1:50; clone 141522), cKIT-PE-Cy7 (1:400; clone 2B8), CCR2-PE (1:50; clone 475301), CXCR4-PerCP-eFluor 710 (1:400; clone 2B11), CD49d-FITC (1:400; clone R1-2) or Gr1-FITC (1:400; clone RB6-8C5), 7AAD.

Lymphoid panel I: CD45-eFluor 605NC (1:50; clone 30-F11), CD11b-eFluor650NC (1:400; clone M1/70), CD3-PE-Cy7 (1:200; clone 145-2C11), CD4-APCeFluor 780 (1:200; clone GK1.5), CD8-PerCP-eFluor 710 (1:400; clone 53-6.7), γδTCR-FITC (1:400; clone GL3), CD49b-APC (1:400; clone DX5), IL-17A-PE (1:200; clone eBio17B7), IFNγ-eFluor 450 (1:200; clone XMG1.2), 7AAD.

Lymphoid panel II: CD45-eFluor 605NC (1:50; clone 30-F11), CD11b-APCeFluor780 (1:200; cloneM1/70),CD3-PE-Cy7 (1:200; clone 145-2C11),CD4-APCeFluor 780 (1:200; clone GK1.5), CD8-PerCP-eFluor 710 (1:400; clone 53-6.7), γδTCR-PE (1:400; clone GL3), CD49b-APC (1:400; cloneDX5), CD62L-AlexaFluor 700 (1:400; clone MEL-14), CD44-FITC (1:400; clone IM7), IFNγ-eFluor 450 (1:200; clone XMG1.2), CD19-APC-eFluor 780 (1:200; clone eBio1D3), Fixable Viability Dye eFluor 780.

γδ T cell phenotyping panel I: CD45-eFluor 605NC(1:50; clone 30-F11),CD11b-APC-eFluor 780 (1:200; clone M1/70), CD3-PerCP-eFluor 710 (1:200; clone 145-2C11),CD4-APC-eFluor 780 (1:200; cloneGK1.5), γδTCR-PE (1:400; clone GL3), CD19-APC-eFluor 780 (1:200; clone eBio1D3), CD27-PE-Cy7 (1:200; clone LG.7F9), IL-1R1-FITC (1:25; clone 129304), CCR6-Brillant Violet 421 (1:200: clone 29-2L17), IL-23R-AlexaFluor 700 (1:25; clone 753317), RORγt-APC (1:100; clone B2D), Fixable Viability Dye eFluor 780.

γδT cell phenotyping panel II: CD45-eFluor 605NC (1:50; clone 30-F11),CD11b- APC-eFluor 780 (1:200; cloneM1/70), CD4-APC-eFluor 780 (1:200; clone GK1.5), γδTCR-PE (1:400; clone GL3), CD19-APC-eFluor 780 (1:200; clone eBio1D3), CD27-PE-Cy7 (1:200; clone LG.7F9), Vγ1-

FITC (1:100; clone 2.11), Vγ4-PerCPeFluor 710 (1:100; clone UC3-10A6), IFNγ-eFluor 450 (1:200; clone XMG1.2), IL-17A-APC (1:200; clone eBio17B7), Fixable Viability Dye eFluor 780.

White blood cell counts

Total white blood cell numbers were measured on a hematology analyzer (Becton Dickinson). Neutrophil numbers were then calculated on the basis of the percentage of $CD11b^+Ly6G^+Ly6C^+$ cells.

Giemsa staining

Blood was collected by tail vein puncture in heparin-coated tubes. Red blood cells were lysed with NH4Cl lysis buffer. White blood cells were smeared onto glass slides then stained with decreasing concentrations of Wright– Giemsa solution.

RNA-seq

$Ly6G^+$ neutrophils were isolated by magnetic column (Miltenyi) from blood of mice. KEP mice with mammary tumors around 225 mm^2 in size and age-matched WT mice were used. Purity of isolated neutrophils was validated by flow cytometry and only samples greater than 90% purity were used. RNA was isolated using Trizol and then treated with DNase I (Invitrogen). Samples were put over a Qiagen RNeasy column for cleanup. RNA quality was confirmed with a 2100 Bioanalyzer from Agilent. RNA-Seq libraries were prepared using the reagents provided in the Illumina TruSeq RNA Sample Preparation Kit, following the manufacturer's protocol. Libraries were PCR amplified for 12 cycles and sequenced on an Illumina HiSeq 2000 System with TruSeq reagent kits and software, generating paired-end 51 base-pair reads. Sequence reads were aligned to the mouse reference genome (National Center for Biotechnology Information build 37) using TopHat. HTSeq-count was then used to generate a list of the total number of uniquely mapped reads for each gene and sample. Sequence reads were normalized to 10 million reads per sample and $\log_2$ transformed with the formula, $\log_2(((\text{expression gene X : library size})10^6)+1)$, where the library size was the sum of all expression values per sample. To determine which genes were differentially expressed between samples, the R package Limma was used. Absolute gene expressions were used as input and genes with no expression in any sample were removed from the data set. Voom was used to transform the count data to $\log_2$ counts per million and estimation of the variance. The P value was set to a cut-off of 0.05, resulting in 100 significant, differentially expressed genes. Unsupervised clustering was performed on these 100 genes and the data were transformed into a heat-map.

Real-time PCR

Neutrophil RNA was extracted as above then converted to complementary DNA (cDNA) with an AMV reverse transcriptase using Oligo(dT) primers (Invitrogen). cDNA (20 ng per well) was analyzed by SYBR green real time PCR with 500 nM primers using a LightCycler 480 thermocycler (Roche). β-actin was used as a reference gene. The following primer sequences

were used for each gene: *Nos2* forward 5'-GTTCTCAGCCCAACAATACAAGA-3', reverse 5'- GTGGACGGGTCGATGTCAC-3'; *Prok2* forward 5'-CTTCGCCCTTCTTCTTTCCT-3', reverse 5'-GCATGTGCTGTGCTGTCAGT-3'; *S100a8* forward 5'-TGAGCAACCTCATTGATGTCTACC-3', reverse 5'-ATGCCACACCCACTTTTATCACC-3'; *S100a9* forward 5'-GAAGAAAGAGAA GAGAAATGAAGCC-3'; reverse 5'-CTTTGCCATCAGCATCATACACTCC-3'; *Il1b* forward 5'-CAACCAACAAGTGATATTCTCCATG-3', reverse 5'-GATCCACACTCTCCAGCTGCA-3'; *Actb* forward 5'-CCTCATGAAGATCCTGACCGA-3', reverse 5'-TTTGATGTCACGCACGATTTC-3'. Fold change was calculated using the formula: 2^-(ΔCt -[ΔCt_{WT}]).

T cell proliferation assay

Blood neutrophils from WT mice and splenic $CD8^+$ T cells from WT mice were isolated by magnetic column (Miltenyi). Blood neutrophils from KEP mice with mammary tumors around 225 mm^2 in size were also used. $CD8^+$ T cells were labelled with Cell Trace CFSE following the manufacturer's instructions (Invitrogen). Equal numbers of cells (2 x 10^5) were co-cultured in a 96-well flat bottom plate. CD3/CD28 Dynabeads (Invitrogen) were added according to manufacturer's instruction, and the iNOS inhibitor, L-NMMA (Sigma), was added at 0.5 mM where indicated. After 48 h, T cell proliferation was evaluated on a BD LSRII flow cytometer using Diva software using the following antibodies: CD8a-PE (1:600; clone 53-6.7), CD11b-APC (1:400; clone M1/70), Ly6C-eFluor 450 (1:400; clone HK1.4), Ly6G-AlexaFluor 700 (1:400; clone 1A8) and 7AAD viability marker. Data analyses used FlowJo Software version 9.7.1. Proliferation index was calculated using the formula (percentage of proliferated, co-cultured $CD8^+$ T cells) / (percentage of proliferated $CD8^+$ T cells without co-culture) x 100, for each replicate experiment.

Cytokine analysis

Multiplex quantification of cytokines and chemokines in mammary glands and tumors was performed using the premixed 24-plex Bio-Plex Pro Mouse Cytokine Assay (Bio-Rad) according to the manufacturer's recommendations. Protein lysates were prepared as previously described [34]. Unsupervised clustering was performed on normalized, median-centered data then converted to a heat-map using Genesis software. For IL-17A and G-CSF serum levels, BD Cytometric Bead Arrays were used as directed and analyzed on a Cyan flow cytometer with Summit software (Beckman Coulter). Data analyses used FlowJo Software version 9.7.1. For TGF-β1, a DuoSet ELISA kit was purchased from R&D Systems and performed according to the manufacturer's instructions.

PCR array

The spleens of three WT or KEP mammary tumor-bearing mice were pooled and labelled with anti-CD3 antibodies. $CD3^+$ T cells were sorted using a BD FACSAria II. RNA was isolated with Trizol as above. Gene expression differences were analyzed using a mouse T cell-specific PCR array from Qiagen according to their instructions and software. Genes exhibiting a threefold change were considered biologically relevant.

Statistical analysis

Data analyses used GraphPad Prism version 7. Applied analyses are indicated in corresponding legends. No statistical methods were used to predetermine sample sizes. Sample sizes were based on previous experience with the models [9,32,34]. Differences with $P < 0.05$ were considered statistically significant.

Author contributions

S.B.C, J.J., and K.E.dV conceived the ideas and designed the experiments. S.B.C, C.W.D., K.K., J.W., C.H., K.V., N.J.V., M.C., L.J.A.C.H. and K.E.dV performed the experiments. S.B.C, C.W.D., K.K., J.W., C.H., K.V., N.J.V., L.J.A.C.H. and K.E.dV analyzed the data. S.B.C, K.K. and K.E.dV wrote the paper.

Acknowledgements

This work was supported by a Marie Curie Intra-European Fellowship to S.B.C. (BMDCMET 275610); an European Research Council Consolidator award (INFLAMET 615300) to K.E.dV; grants from the Dutch Cancer Society to K.E.dV and J.J. (2011-5004); the Association for International Cancer Research (AICR 11-0677) to K.E.dV; the Netherlands Organization for Scientific Research NWO VIDI (917.96.307) to K.E.dV; and a Dutch Cancer Society/Bas Mulder Award to L.J.A.C.H. (UL2011-5051). We thank J. Borst and J. Coquet for discussions. We thank the core facilities at the Netherlands Cancer Institute, and the genomics facility for performing and analyzing the RNA-Seq experiment. We thank L. Coussens for *Rag1*$^{-/-}$ mice and A. Hayday for *Tcr*$\delta^{-/-}$ mice. We also thank C. Ries and K. Wartha for assistance with Luminex-based cytokine analysis.

Author information

RNA-seq data are deposited in the Gene Expression Omnibus (GEO) under the accession number GSE55633. The authors declare no competing financial interests. Correspondence and request for materials should be addressed to K.E.dV (k.d.visser@nki.nl).

References

1. Quail, D. F. & Joyce, J. A. Microenvironmental regulation of tumor progression and metastasis. *Nat. Med.* **19,** 1423–1437 (2013).
2. McAllister, S. S. & Weinberg, R. A. The tumour-induced systemic environment as a critical regulator of cancer progression and metastasis. *Nat. Cell Biol.* **16,** 717–727 (2014).
3. Noh, H., Eomm, M. & Han, A. Usefulness of pretreatment neutrophil to lymphocyte ratio in predicting disease-specific survival in breast cancer patients. *J. Breast Cancer* **16,** 55–59 (2013).
4. Azab, B. *et al.* Usefulness of the neutrophil-to-lymphocyte ratio in predicting short- and long-term mortality in breast cancer patients. *Ann. Surg. Oncol.* **19,** 217–224 (2012).
5. Granot, Z. *et al.* Tumor entrained neutrophils inhibit seeding in the premetastatic lung. *Cancer Cell* **20,** 300–314 (2011).
6. Kowanetz, M. *et al.* Granulocyte-colony stimulating factor promotes lung metastasis through mobilization of Ly6G+Ly6C+ granulocytes. *Proc. Natl. Acad. Sci. U. S. A.* **107,** 21248–21255 (2010).
7. Bald, T. *et al.* Ultraviolet-radiation-induced inflammation promotes angiotropism and metastasis in melanoma. *Nature* **507,** 109–113 (2014).
8. Derksen, P. W. B. *et al.* Somatic inactivation of E-cadherin and p53 in mice leads to metastatic lobular mammary carcinoma through induction of anoikis resistance and angiogenesis. *Cancer Cell* **10,** 437–449 (2006).
9. Doornebal, C. W. *et al.* A preclinical mouse model of invasive lobular breast cancer metastasis. *Cancer Res.* **73,** 353–363 (2013).
10. Kaplan, R. N. *et al.* VEGFR1-positive haematopoietic bone marrow progenitors initiate the pre-metastatic niche. *Nature* **438,** 820–827 (2005).
11. Erler, J. T. *et al.* Hypoxia-induced lysyl oxidase is a critical mediator of bone marrow cell recruitment to form the premetastatic niche. *Cancer Cell* **15,** 35–44 (2009).
12. Kuonen, F. *et al.* Inhibition of the Kit ligand/c-Kit axis attenuates metastasis in a mouse model mimicking local breast cancer relapse after radiotherapy. *Clin. Cancer Res.* **18,** 4365–4374 (2012).
13. Hiratsuka, S. *et al.* MMP9 induction by vascular endothelial growth factor receptor-1 is involved in lung-specific metastasis. *Cancer Cell* **2,** 289–300 (2002).
14. Hiratsuka, S., Watanabe, A., Aburatani, H. & Maru, Y. Tumour-mediated upregulation of chemoattractants and recruitment of myeloid cells predetermines lung metastasis. *Nat. Cell Biol.* **8,** 1369–1375 (2006).
15. Pillay, J., Tak, T., Kamp, V. M. & Koenderman, L. Immune suppression by neutrophils and granulocytic myeloid-derived suppressor cells: similarities and differences. *Cell. Mol. Life Sci.* **70,** 3813–3827 (2013).
16. Mazzoni, A. *et al.* Myeloid suppressor lines inhibit T cell responses by an NO-dependent mechanism. *J. Immunol.* **168,** 689–695 (2002).
17. Young, M. R., Wright, M. A., Matthews, J. P., Malik, I. & Prechel, M. Suppression of T cell proliferation by tumor-induced granulocyte-macrophage progenitor cells producing transforming growth factor-beta and nitric oxide. *J. Immunol.* **156,** 1916–1922 (1996).
18. Lejeune, P. *et al.* Nitric oxide involvement in tumor-induced immunosuppression. *J. Immunol.* **152,** 5077–5083 (1994).
19. Hamilton, J. A. & Achuthan, A. Colony stimulating factors and myeloid cell biology in health and disease. *Trends Immunol.* **34,** 81–89 (2013).
20. Chung, Y. *et al.* Critical regulation of early Th17 cell differentiation by interleukin-1 signaling. *Immunity* **30,** 576–587 (2009).
21. Cai, Y. *et al.* Pivotal role of dermal IL-17-producing γδ T cells in skin inflammation. *Immunity* **35,** 596–610 (2011).
22. Mei, J. *et al.* Cxcr2 and Cxcl5 regulate the IL-17/G-CSF axis and neutrophil homeostasis in mice. *J. Clin. Invest.* **122,** 974–986 (2012).
23. Sutton, C. E. *et al.* Interleukin-1 and IL-23 induce innate IL-17 production from gammadelta T cells, amplifying Th17 responses and autoimmunity. *Immunity* **31,** 331–341 (2009).
24. Schwarzenberger, P. *et al.* Requirement of endogenous stem cell factor and granulocyte-colony-stimulating factor for IL-17-mediated granulopoiesis. *J. Immunol.* **164,** 4783–4789 (2000).
25. Fridlender, Z. G. *et al.* Polarization of tumor-associated neutrophil phenotype by TGF-beta: 'N1' versus 'N2' TAN. *Cancer Cell* **16,** 183–194 (2009).
26. Han, Y. *et al.* Prognostic value of chemotherapy-induced neutropenia in early-stage breast cancer. *Breast Cancer Res. Treat.* **131,** 483–490 (2012).
27. Ma, C. *et al.* Tumor-infiltrating γδ T lymphocytes predict clinical outcome in human breast cancer. *J.*

Immunol. **189,** 5029–5036 (2012).
28. Novitskiy, S. V. *et al.* TGF-β receptor II loss promotes mammary carcinoma progression by Th17 dependent mechanisms. *Cancer Discov.* **1,** 430–441 (2011).
29. Chen, W.-C. *et al.* Interleukin-17-producing cell infiltration in the breast cancer tumour microenvironment is a poor prognostic factor. *Histopathology* **63,** 225–233 (2013).
30. Sutherland, T. E. *et al.* Chitinase-like proteins promote IL-17-mediated neutrophilia in a tradeoff between nematode killing and host damage. *Nat. Immunol.* **15,** 1116–1125 (2014).
31. de Visser, K. E., Korets, L. V. & Coussens, L. M. De novo carcinogenesis promoted by chronic inflammation is B lymphocyte dependent. *Cancer Cell* **7,** 411–423 (2005).
32. Ciampricotti, M., Hau, C.-S., Doornebal, C. W., Jonkers, J. & de Visser, K. E. Chemotherapy response of spontaneous mammary tumors is independent of the adaptive immune system. *Nat. Med.* **18,** 344–346 (2012).
33. Girardi, M. *et al.* Regulation of cutaneous malignancy by gammadelta T cells. *Science* **294,** 605–609 (2001).
34. Ciampricotti, M. *et al.* Development of metastatic HER2(+) breast cancer is independent of the adaptive immune system. *J. Pathol.* **224,** 56–66 (2011).

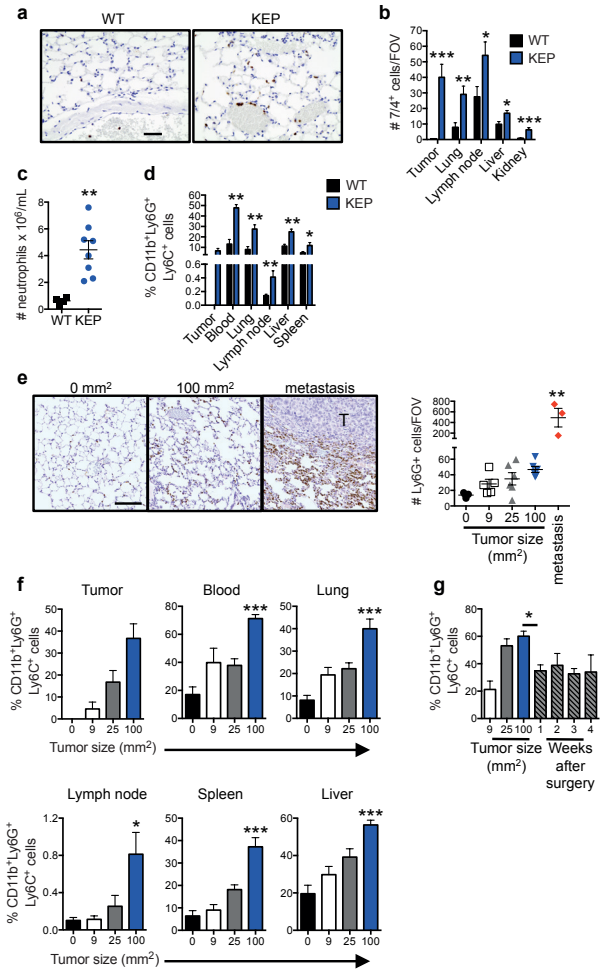

Extended Data Figure 1. Systemic neutrophil expansion and accumulation in mammary tumor-bearing KEP mice and the metastasis model. a) Representative images of neutrophils identified by the 7/4 antibody in lung sections in WT or KEP mice. Scale bar = 50 μm. b) Quantification of neutrophil accumulation per field of view (FOV) in various organs by immunohistochemistry using the 7/4 antibody (n = 6-22/group). c) Absolute neutrophil counts in blood of WT and tumor-bearing KEP mice (n = 4-8/group). d) Quantification of neutrophil accumulation in various organs determined by flow cytometry and gated on $CD45^+$ cells. Neutrophils were not detectable in WT mammary glands (n = 5-14/group). e) Representative images of Ly6G-stained lung sections and quantification of neutrophil accumulation in the metastasis model. Data were generated from mock-transplanted, non-tumor-bearing mice (0 mm^2), or tumor-transplanted recipient mice sacrificed when tumors reached the tumor size shown or when mice exhibited signs of respiratory distress due to pulmonary metastasis. For quantification in lungs with metastases, neutrophils residing inside metastases were excluded. T = pulmonary metastatic lesion. Scale bar = 100 μm (n = 3-6/group). f) Kinetics of neutrophil accumulation in various organs of the metastasis model by flow cytometry after gating on $CD45^+$ cells. Recipient mice transplanted with KEP tumor pieces were sacrificed at the tumor size shown (n = 5-8/group). g) Kinetics of neutrophil proportions in blood (gated on $CD45^+$ cells), before and after surgical removal of their primary tumor (n = 4-5/group). All data are mean + s.e.m. *p<0.05, **p<0.01, ***p<0.001 as determined by Mann-Whitney U test or Kruskal–Wallis test followed by Dunn's post test.

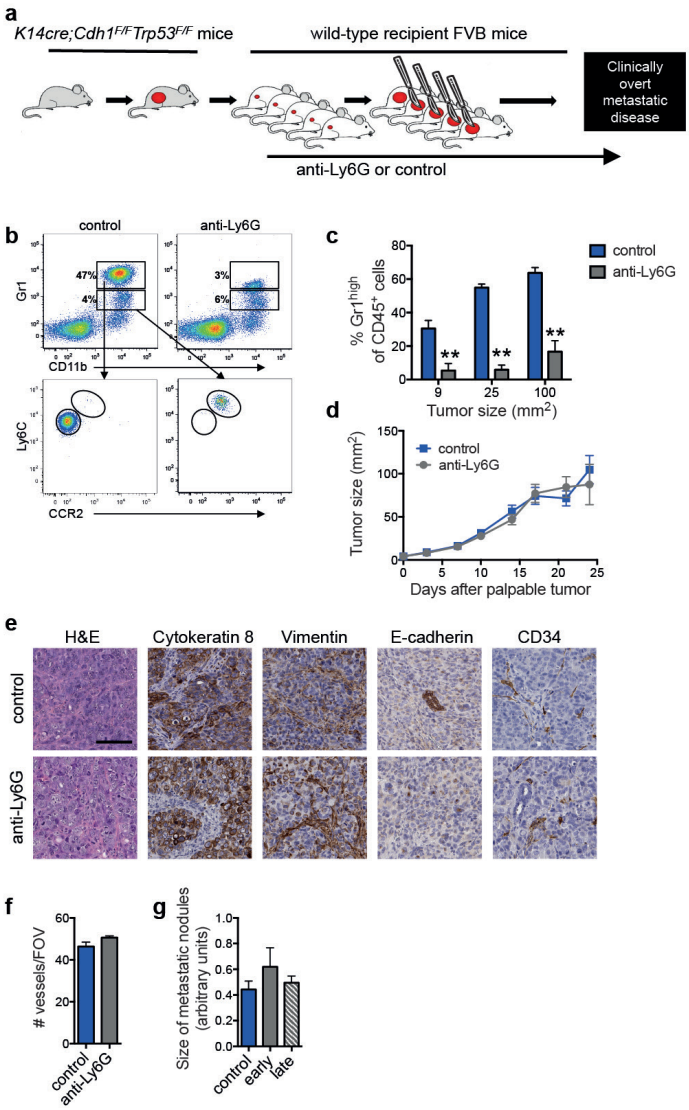

Extended Data Figure 2. Neutrophil depletion does not affect primary tumor or metastatic nodule growth. a) Schematic illustration of the neutrophil depletion experiment in the spontaneous metastasis model. b) Representative dot plots of neutrophils gated on $CD45^+$ cells in blood of control and anti-Ly6G-treated recipient mice. The Gr1 antibody was used here to avoid false negative results since the anti-Ly6G depleting antibody may mask the Ly6G epitope. $CD11b^+Gr1^{high}$ cells were $Ly6C^+CCR2^-$, indicating that these cells were neutrophils. $CD11b^+Gr1^{low}$ cells that were $Ly6C^+$ and $CCR2^+$ represented the monocytic fraction. c) Quantification of neutrophil depletion in blood of control and anti-Ly6G-treated recipient mice at the tumor size indicated. d) Primary tumor growth kinetics of mice treated as indicated (n = 12-14/group). e) Representative images of primary tumors in the metastasis model treated as shown and stained with H&E, cytokeratin 8, vimentin, E-cadherin and CD34. Scale bar = 100 μm. f) Quantification of blood vessels per field of view (FOV) in control and anti-Ly6G-treated mice by anti-CD34 immunohistochemistry (n = 10/group). g) Quantification of pulmonary metastatic nodule size following treatment with anti-Ly6G or control (n = 10-14/group). All data are mean + s.e.m.

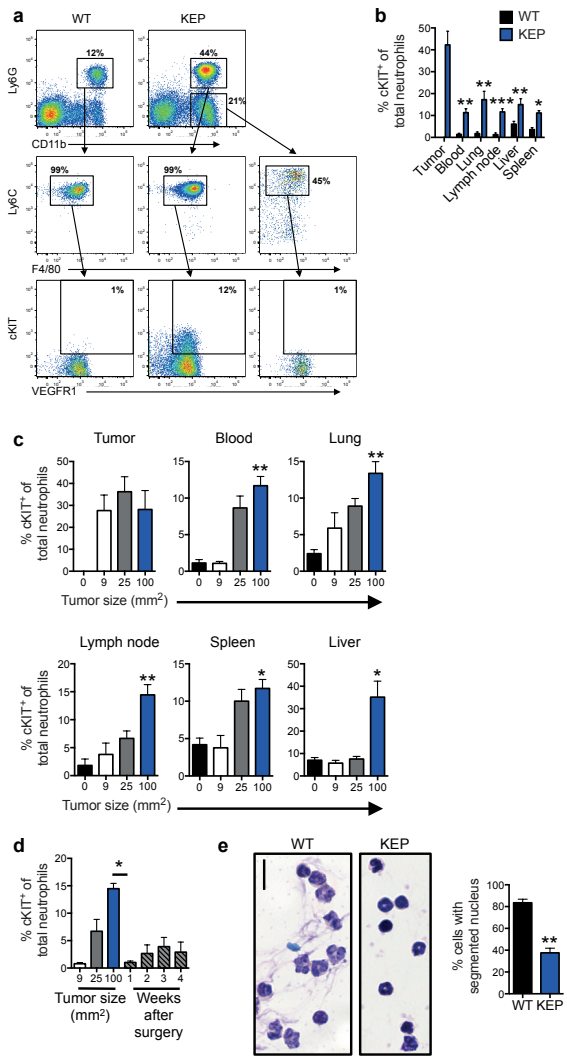

Extended Data Figure 3. Subpopulations of neutrophils in mammary tumor-bearing mice are immature. a) Gating strategy for identification of neutrophils ($CD45^+CD11b^+Ly6G^+Ly6C^+F4/80^-$ cells), $cKIT^+$ neutrophils and monocytes ($CD45^+CD11b^+Ly6G^-Ly6C^+F4/80^-$ cells) by flow cytometry. Blood cells from WT and tumor-bearing KEP mice are shown here. b) Quantification of $cKIT^+$ neutrophil accumulation in various organs determined by flow cytometry after gating on $CD45^+CD11b^+Ly6G^+Ly6C^+F4/80^-$ cells. $cKIT^+$ neutrophils were not detectable in WT mammary glands (n = 5-14/group; Mann-Whitney U test). c) $cKIT^+$ neutrophil proportions in various organs of the metastasis model as determined by flow cytometry after gating on $CD45^+CD11b^+Ly6G^+Ly6C^+F4/80^-$ cells. Mice were sacrificed at the tumor size shown (n = 5-8/group; Kruskal–Wallis test followed by Dunn's post test). d) Kinetics of $cKIT^+$ neutrophil proportions in blood (gated on $CD45^+CD11b^+Ly6G^+Ly6C^+F4/80^-$ cells), before and after surgical removal of their primary tumor (n = 4-5/group; Mann-Whitney U test). e) Representative images and quantification of neutrophil nuclear morphology. $Ly6G^+$ cells were isolated from blood of WT and tumor-bearing KEP mice then assessed by Giemsa stain. Hyper-segmented cells were considered mature, whereas all other cells were considered immature. Scale bar = 10 mm. (n = 5-6/group; Mann-Whitney U test). All data are mean + s.e.m. *p<0.05, **p<0.01, ***p<0.001.

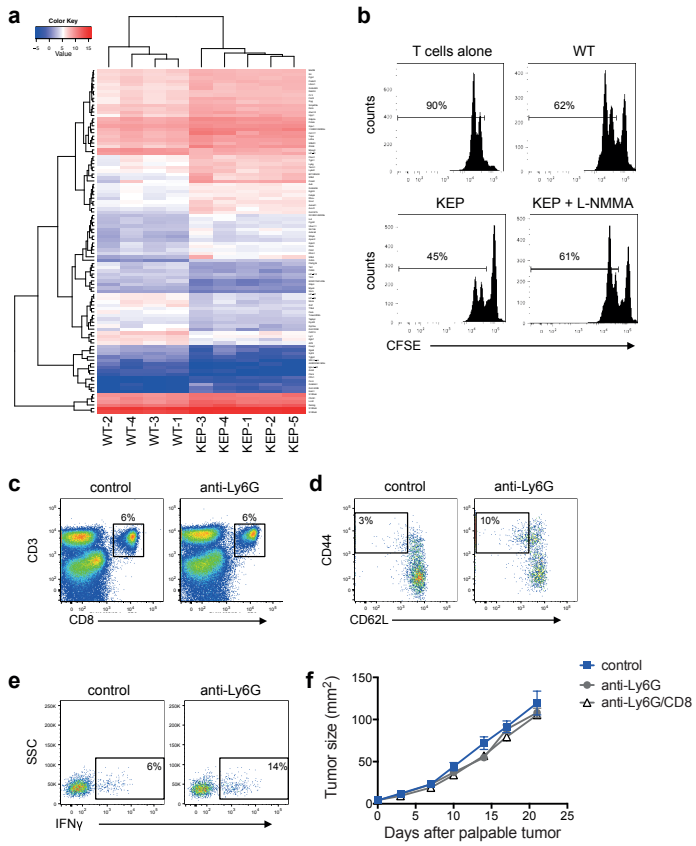

Extended Data Figure 4. Neutrophils influence the function and phenotype of CD8⁺ T cells. a) Unsupervised hierarchical clustering of RNA-Seq analysis depicting 100 differentially expressed genes between circulating neutrophils from WT and tumor-bearing KEP mice. *P* value (0.05) was used as a cutoff (n = 4 WT, 5 KEP mice). See also Extended Data Table 1 for top 50 genes ranked by fold change. b) Circulating neutrophils from either WT or tumor-bearing KEP mice were incubated with CFSE-labeled splenic $CD8^+$ T cells from WT mice and CD3/CD28 stimulation beads. The iNOS inhibitor, L-NMMA, was added where indicated. After 48 hours, $CD8^+$ T cell proliferation was measured by flow cytometry. Representative histograms are depicted of $CD8^+$ T cell-gated CFSE fluorescence. c) Dot plots depicting live cell-gated $CD8^+$ T cell proportions in lungs of mice in control and neutrophil-depleted mice , killed when transplanted tumors reached 100 mm^2. d) Dot plots of effector $CD8^+$ T cell ($CD62L^-CD44^+$) proportions in lungs of transplanted mammary tumor-bearing mice that were killed when tumors reached 100 mm^2. e) IFNγ expression by $CD8^+$ T cells in lungs of transplanted mammary tumor-bearing mice that were killed when tumors reached 100 mm^2. f) Tumor growth kinetics in neutrophil-depleted or combined neutrophil- and $CD8^+$ T cell-depleted, mammary tumor-transplanted recipient mice, as compared with control (n = 13-21/group). Data are mean + s.e.m.

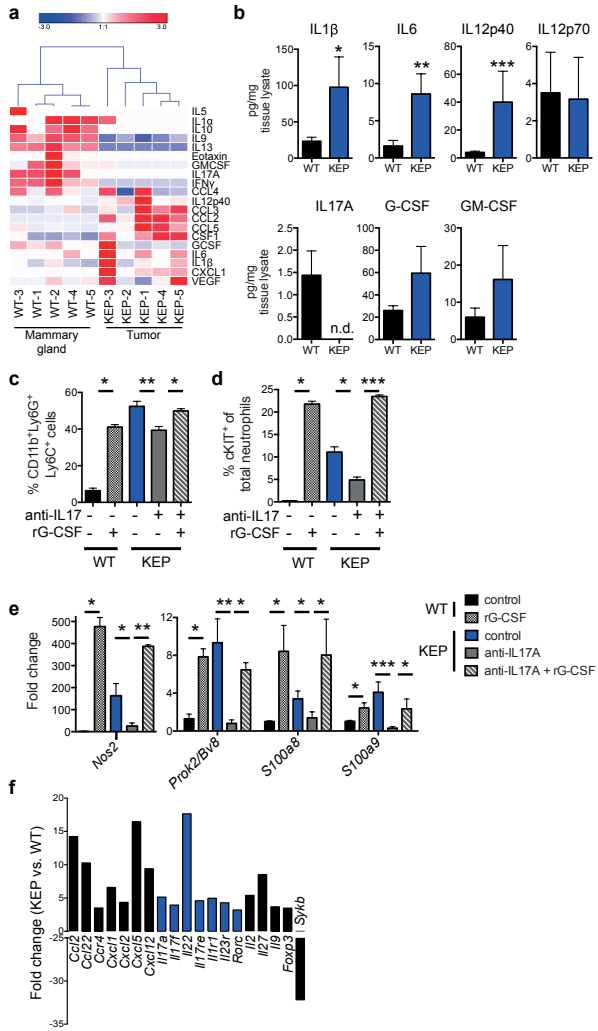

Extended Data Figure 5. Cytokine expression levels in tumors and T cells, and their effects on neutrophils. a) Unsupervised clustering of cytokine expression analysis in WT mammary glands and KEP tumors. Protein lysates were prepared as previously described from whole tissue[31] and analyzed for expression of various cytokines by Luminex-based assay (n = 5 per group). b) Protein levels of indicated cytokines in WT mammary glands and KEP tumors, determined by Luminex-based cytokine profiling; n.d., not detectable (n = 10 per group; Mann–Whitney U-test). c, d) Quantification of neutrophil and cKIT-expressing neutrophil accumulation in blood as determined by flow cytometry and gated on CD45+ cells. WT (n = 4) or tumor-bearing KEP mice (n = 9) were treated with anti-IL17 (n = 8) and/or recombinant G-CSF (rG-CSF; n = 4) where indicated (Mann-Whitney U test or Kruskal–Wallis test followed by Dunn's post test). e, Gene expression in circulating neutrophils from WT control (n = 5), rG-CSF-treated WT mice (n = 4), KEP control (n = 10), anti-IL-17-treated (n = 6), anti-IL-17+G-CSF-treated KEP mice (n = 4; Mann–Whitney U-test or Kruskal–Wallis test followed by post-hoc Dunn's test). e) Spleens of three WT mice and three KEP mice were pooled and CD3+ T cells were isolated. These cells were analyzed by a real-time PCR array containing 86 different genes. Gene expression changes of greater than three-fold are shown. Members of the IL17 signaling pathway are depicted in blue. *p<0.05, **p<0.01, ***p<0.001. All data are mean + s.e.m.

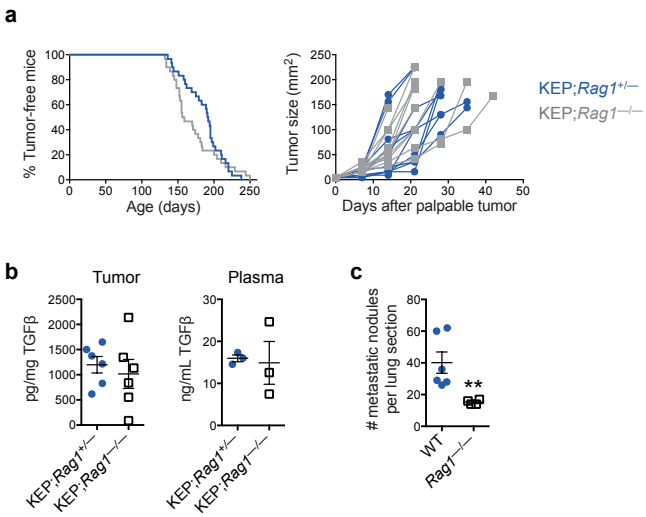

Extended Data Figure 6. Absence of the adaptive immune system reduces metastasis. a) Graphic representation of mammary tumor latency (left) and tumor growth (right) in lymphocyte-proficient KEP;*Rag1*$^{+/-}$ and lymphocyte-deficient KEP;*Rag1*$^{-/-}$ mice (n = 30 per group left panel, 10 mice per group right panel). b) Levels of TGFβ1 in mammary tumors and the plasma of tumor-bearing mice (n = 6 tumors, 3 plasma). c) Quantification of metastatic burden in lungs of recipient WT or *Rag1*$^{-/-}$ mice that were transplanted with KEP mammary tumor fragments and underwent surgical removal of the primary tumor (n = 6 WT, 4 *Rag1*$^{-/-}$ mice; $^{**}p<0.01$, Mann-Whitney U test). Data are mean + s.e.m.

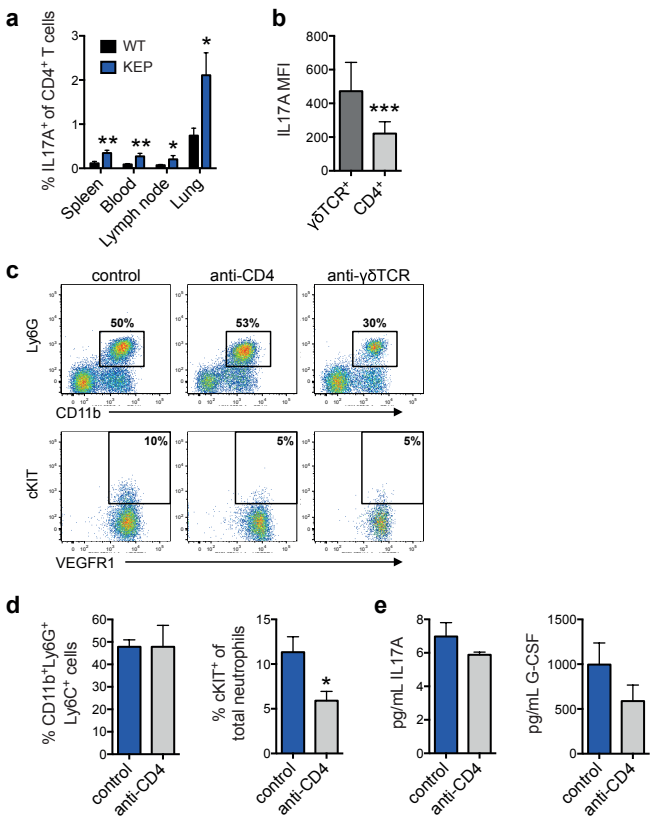

Extended Data Figure 7. Depletion of CD4⁺ T cells does not affect systemic cytokine levels or neutrophil expansion. a) The proportion of IL17A⁺ cells among CD4⁺ T cells in organs of wild-type (WT) and tumor-bearing *K14cre;Cdh1$^{F/F}$;Trp53$^{F/F}$* (KEP) mice (n = 6 per group; Mann-Whitney U test). b) Median fluorescence intensity (MFI) of IL17A expression in circulating γδ and CD4⁺ T cells from tumor-bearing KEP mice, as determined by flow cytometry (n = 11 per group; Wilcoxon matched-pairs test). c) Representative dot plots depicting total neutrophil and cKIT⁺ proportions in blood of control, anti-CD4- and anti-γδTCR-treated tumor-bearing KEP mice. d) Quantification of total neutrophil and cKIT⁺ neutrophil proportions in blood of control and anti-CD4-treated KEP mice (n = 7 per group; Mann-Whitney U test). e) Serum levels of IL-17A and G-CSF in control and anti-CD4-treated tumor-bearing KEP mice (n = 10 control, 6 anti-CD4; Mann-Whitney U test). **p*<0.05, ***p*<0.01. All data are mean + s.e.m.

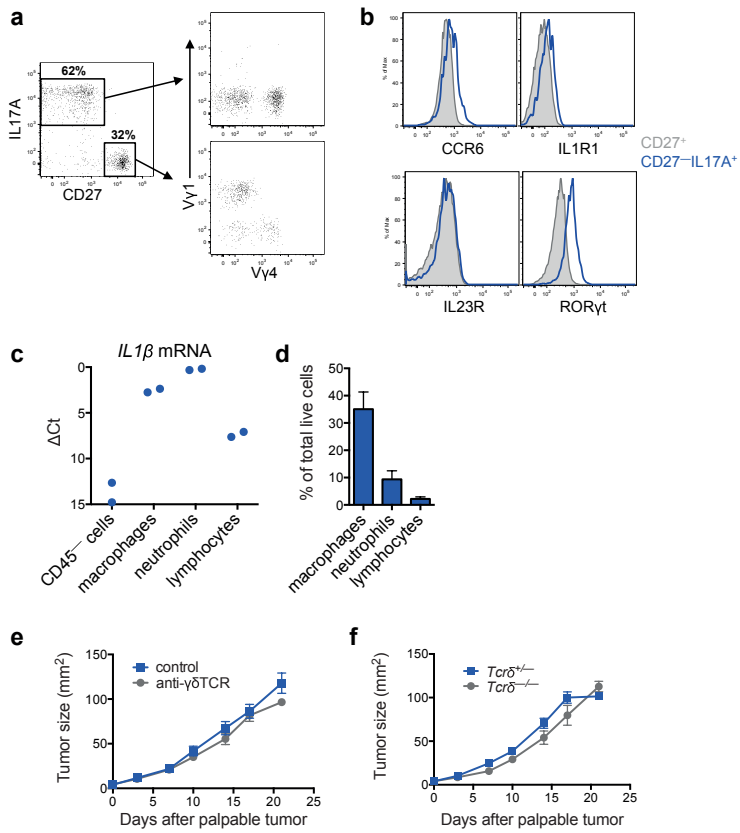

Extended Data Figure 8. γδ T cell phenotype in KEP mice and their lack of influence on tumor growth in the metastasis model. a) γδ T cells from lungs of tumor-bearing KEP mice were analyzed by flow cytometry for IL17, CD27, Vγ1, and Vγ4 expression. Two major populations of γδ T cells were observed including IL17$^+$CD27$^-$ and IL17$^-$CD27$^+$ cells. b) Representative histograms of CCR6, IL1R1, IL23R and RORγt expression in IL17$^+$CD27$^-$ and IL17$^-$CD27$^+$ γδ T cell populations shown in a. c) *Il1*β gene expression in various cells populations from KEP tumors. Tumors from three mice were pooled to form one group. CD45$^-$ cells (which includes cancer cells, endothelial cells and fibroblasts), CD45$^+$CD11b$^+$F4/80$^+$ macrophages, CD45$^+$CD11b$^+$Ly6G$^+$ neutrophils and CD45$^+$CD11b$^-$ lymphocytes were sorted from these two groups. Real time-PCR was performed on individual cell populations for *Il1*β expression. Relative expression among different cells is shown. d) Graphic representation of immune cell proportions in KEP tumors (n = 4). e) Primary tumor growth kinetics of control and γδ T cell-depleted tumor transplant recipient mice (n = 13 per group). f) Growth kinetics of primary tumors transplanted into *Tcrd*$^{+/-}$ (n = 10) and *Tcrd*$^{-/-}$ mice (n = 6). All data are mean + s.e.m.

Extended Data Table 1. The top 100 most differentially expressed genes between neutrophils from wild-type and *K14cre;Cdh1$^{F/F}$;Trp53$^{F/F}$* mice.

Gene ID	Gene name	Ensembl gene ID	fold change	p value
Nos2	nitric oxide synthase 2, inducible	ENSMUSG00000020826	31.5	0.345
Car4	carbonic anhydrase 4	ENSMUSG00000000805	25.5	0.111
Lipg	lipase, endothelial	ENSMUSG00000053846	24.6	0.128
Gm11430	predicted gene 11430	ENSMUSG00000080927	16.7	0.292
Gm6551	predicted gene 6551	ENSMUSG00000078100	14.2	0.039
Stfa3	stefin A3	ENSMUSG00000054905	14.1	0.047
Pvrl2	poliovirus receptor-related 2	ENSMUSG00000062300	13.8	0.143
Gm16748	predicted gene, 16748	ENSMUSG00000085308	13.5	0.087
Prok2	prokineticin 2	ENSMUSG00000030069	12.3	0.024
Esm1	endothelial cell-specific molecule 1	ENSMUSG00000042379	12.1	0.010
Ano2	anoctamin 2	ENSMUSG00000038115	10.6	0.138
Saa1	serum amyloid A 1	ENSMUSG00000074115	10.1	0.192
Nov	nephroblastoma overexpressed gene	ENSMUSG00000037362	9.6	0.295
Gpr15	G protein-coupled receptor 15	ENSMUSG00000047293	9.5	0.204
Ggt1	gamma-glutamyltransferase 1	ENSMUSG00000006345	9.3	0.076
Cish	cytokine inducible SH2-containing protein	ENSMUSG00000032578	9.1	0.217
Stfa2	stefin A2	ENSMUSG00000022902	8.9	0.020
Gm14028	predicted gene 14028	ENSMUSG00000082339	8.4	0.036
Stfa1	stefin A1	ENSMUSG00000071562	7.5	0.087
Cfhr1	complement factor H-related 1	ENSMUSG00000057037	7.1	0.029
Ms4a3	membrane-spanning 4-domains, subfamily A, member 3	ENSMUSG00000024681	6.8	0.177
Kit	kit oncogene	ENSMUSG00000005672	6.8	0.085
Jph3	junctophilin 3	ENSMUSG00000025318	6.8	0.076
Cnnm2	cyclin M2	ENSMUSG00000064105	6.6	0.128
Gnb5	guanine nucleotide binding protein (G protein), beta 5	ENSMUSG00000032192	6.4	0.004
Alox12	arachidonate 12-lipoxygenase	ENSMUSG00000000320	-11.2	0.103
Slfn14-ps	schlafen family member 14, pseudogene	ENSMUSG00000082101	-11.2	0.049
Gm6634	predicted gene 6634	ENSMUSG00000086538	-11.3	0.139
Syt13	synaptotagmin XIII	ENSMUSG00000027220	-11.4	0.213
Tsc22d1	TSC22 domain family, member 1	ENSMUSG00000022010	-11.4	0.107
Gm10419	predicted gene 10419	ENSMUSG00000072769	-11.5	0.231
Sh3bgrl2	SH3 domain binding glutamic acid-rich protein like 2	ENSMUSG00000032261	-11.6	0.117
Fhl1	four and a half LIM domains 1	ENSMUSG00000023092	-11.9	0.131
Trpc6	transient receptor potential cation channel, subfamily C, member 6	ENSMUSG00000031997	-11.9	0.076
Ctla2a	cytotoxic T lymphocyte-associated protein 2 alpha	ENSMUSG00000044258	-12.0	0.107
Csgalnact1	chondroitin sulfate N-acetylgalactosaminyltransferase 1	ENSMUSG00000036356	-12.2	0.156
Gng11	guanine nucleotide binding protein (G protein), gamma 11	ENSMUSG00000032766	-12.2	0.123
2610109H07Rik	RIKEN cDNA 2610109H07 gene	ENSMUSG00000029005	-12.3	0.195
Nrgn	neurogranin	ENSMUSG00000053310	-12.5	0.087
Gm11274	predicted gene 11274	ENSMUSG00000085331	-12.6	0.101
Peg10	paternally expressed 10	ENSMUSG00000092035	-13.1	0.177
Angpt1	angiopoietin 1	ENSMUSG00000022309	-13.6	0.168
Plp1	proteolipid protein (myelin) 1	ENSMUSG00000031425	-13.6	0.132
Dlg2	discs, large homolog 2 (Drosophila)	ENSMUSG00000052572	-14.6	0.080
Sytl4	synaptotagmin-like 4	ENSMUSG00000031255	-14.6	0.138
Mpl	myeloproliferative leukemia virus oncogene	ENSMUSG00000006389	-15.6	0.197
Mras	muscle and microspikes RAS	ENSMUSG00000032470	-15.7	0.053
Gp6	glycoprotein 6 (platelet)	ENSMUSG00000078810	-15.9	0.215
Cd226	CD226 antigen	ENSMUSG00000034028	-18.4	0.134
Bean1	brain expressed, associated with Nedd4, 1	ENSMUSG00000031872	-19.2	0.053

-4-

Mammary tumor-derived CCL2 enhances pro-metastatic systemic inflammation through upregulation of macrophage-derived IL1β

Kelly Kersten[1], Seth B. Coffelt[1], Marlous Hoogstraat[2], Niels J.M. Verstegen[1], Kim Vrijland[1], Metamia Ciampricotti[1], Chris W. Doornebal[1,3], Cheei-Sing Hau[1], Parul Doshi[4], Esther H. Lips[5], Lodewyk F.A. Wessels[2,6], & Karin E. de Visser[1]

[1]Division of Immunology, Netherlands Cancer Institute, Amsterdam, The Netherlands
[2]Division of Molecular Carcinogenesis, Netherlands Cancer Institute, Amsterdam, The Netherlands
[3]Department of Anesthesiology, Academic Medical Center, Amsterdam, The Netherlands
[4]Janssen Research and Development, LLC, Spring House, USA.
[5]Division of Molecular Pathology, Netherlands Cancer Institute, Amsterdam, The Netherlands
[6]Department of EEMCS, Delft University of Technology, Delft, The Netherlands

In revision.

Abstract

Metastasis is regulated by extensive crosstalk between cancer cells and immune cells. Compelling evidence in clinical and experimental studies shows the accumulation of neutrophils in tumor-bearing hosts. Moreover, elevated proportions of circulating neutrophils correlate with increased risk of metastasis. Recently, we demonstrated a mechanistic link between mammary tumor-induced IL17-producing γδ T cells, systemic expansion of immunosuppressive neutrophils and metastasis formation in a genetically engineered mouse model for invasive breast cancer. How tumors orchestrate this systemic inflammatory cascade to facilitate dissemination remains unclear. Here we show that activation of this cascade relies on CCL2-mediated induction of IL1β in tumor-associated macrophages. In line with these findings, expression of *CCL2* positively correlates with *IL1B* and macrophage markers in human breast tumors. We demonstrate that blockade of CCL2 in mammary tumor-bearing mice results in reduced IL17 production by γδ T cells, decreased neutrophil expansion and enhanced $CD8^+$ T cell activity. These results suggest that CCL2 acts as a key driver of the inflammatory γδ T cell – IL17 – neutrophil axis to support breast cancer metastasis.

Introduction

Over 90% of breast cancer deaths are due to complications as a consequence of metastasis [1]. Thus there is an urge for the identification of new therapeutic targets through a better understanding of the molecular mechanisms underlying breast cancer metastasis formation. Emerging evidence indicates that metastasis is regulated to a great extent by reciprocal interactions between cancer cells and immune cells in the tumor microenvironment [2,3]. In addition to a local inflammatory microenvironment, tumors frequently induce a systemic inflammatory state in distant organs through the release of various mediators that mobilize and activate immune cells to support metastasis [2]. As such, systemic inflammation represents an interesting target for patients with metastatic breast cancer.

Previously, we reported that neutrophils exert pro-metastatic functions by suppressing anti-tumor $CD8^+$ T cells in the *K14cre;Cdh1$^{F/F}$;Trp53$^{F/F}$* (KEP) conditional mouse model of invasive breast cancer [4]. The systemic expansion and polarization of these neutrophils is elicited by tumor-associated macrophage (TAM)-derived interleukin (IL)1β that activates IL17-producing γδ T cells leading to increased systemic levels of G-CSF, a cytokine known for its role in granulopoiesis [5]. However, the mediators that initiate this systemic inflammatory cascade from the primary tumor are unknown.

In the current study, we identify the pro-inflammatory chemokine (C-C motif) ligand 2 (CCL2) as an important mammary tumor-derived factor that stimulates the γδ T cell – IL17 – neutrophil axis to promote breast cancer metastasis. CCL2 is a cytokine largely known for its involvement in the recruitment of $CCR2^+$ monocytes from the bone marrow to other sites in the body where they differentiate into macrophages [6]. In breast cancer patients, high CCL2 expression is linked to macrophage infiltration and poor prognosis [7,8].

Here, we show that *in vivo* blockade of CCL2 in mammary tumor-bearing KEP mice results in reduced IL17-producing γδ T cells and impaired G-CSF-dependent expansion of immunosuppressive neutrophils. We found that CCL2 initiates the γδ T cell – IL17 – neutrophil axis by promoting the expression of TAM-derived IL1β. In human breast cancers, *CCL2* expression is enriched in basal-like tumors and is positively correlated with *IL1B* and macrophage marker *CD68* across all breast cancer subtypes, supporting our findings that these two cytokines are co-dependent. These data identify CCL2 as a key regulator of the mammary tumor-induced systemic inflammatory γδ T cell – IL17 – neutrophil axis promoting metastasis.

Results

Mammary tumor-bearing K14cre;Cdh1$^{F/F}$;Trp53$^{F/F}$ (KEP) mice show elevated intratumoral and systemic CCL2 levels

Previously, we analyzed the expression profile of a panel of cytokines and chemokines in KEP mammary tumors and mammary glands from wild-type mice [4]. Among these molecules, CCL2 was the most upregulated cytokine in KEP tumor tissue (Fig. 1a). We also found increased CCL2 serum levels in mammary tumor-bearing KEP mice compared to wild-type littermates (Fig. 1b). RNA *in situ* hybridization analysis showed that *Ccl2* mRNA in KEP mammary tumors is highly expressed in stromal cells and tumor cells (Fig. 1c). *Ccl2* expression in wild-type mammary glands was almost undetectable (Fig. 1c). Gene expression analysis on sorted cell populations from KEP tumors revealed that many cell types express *Ccl2* (Fig. 1d), but due to their high abundance in KEP tumors, macrophages and tumor cells comprise the main cellular source (Fig. 1e).

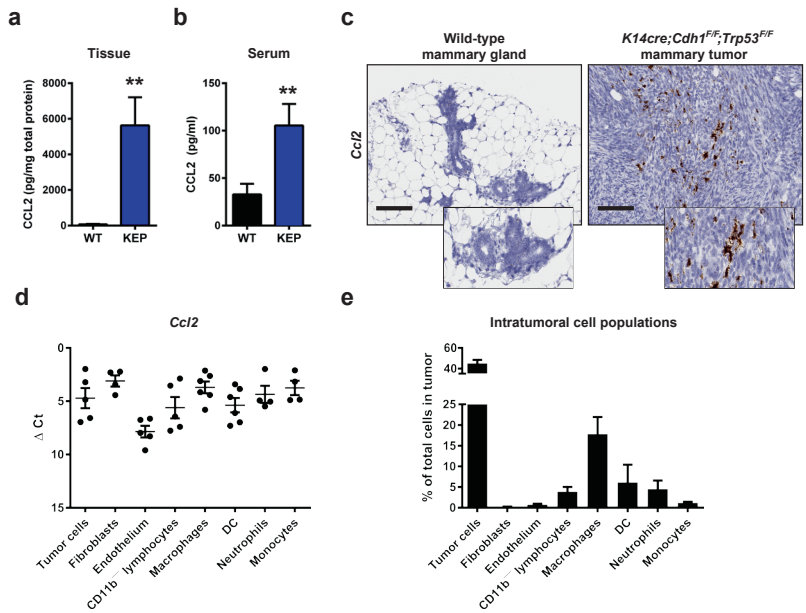

Figure 1. CCL2 expression in mammary tumor-bearing *K14cre;Cdh1$^{F/F}$;Trp53$^{F/F}$* (KEP) mice. a) Protein expression of CCL2 in KEP mammary tumors compared to wild-type mammary glands, (n = 5 per group; Mann-Whitney U test). b) Serum levels of CCL2 in wild-type mice and mammary tumor-bearing KEP mice, (n = 6 per group; Mann-Whitney U test). a-b are determined by a Luminex-based cytokine array. c) RNA *in situ* hybridization of *Ccl2* mRNA in wild-type mammary gland (left) and KEP mammary tumors (right). Representative images are shown. Scale bar 100 µm. d, e) Tumor cells (CD31$^-$CD45$^-$CD11b$^-$), lymphocytes (CD45$^+$CD11b$^-$), fibroblasts (PDGFRβ$^+$CD31$^-$CD45$^-$CD11b$^-$), endothelium (CD31$^+$CD45$^-$CD11b$^-$), macrophages (CD11b$^+$F4/80$^+$), dendritic cells (DC) (CD11b$^+$F4/80$^-$CD11c$^+$), neutrophils (CD11b$^+$F4/80$^-$Ly6G$^+$Ly6C^{lo}) and monocytes (CD11b$^+$F4/80$^-$Ly6G$^-$Ly6C^{hi}) were isolated from mammary tumor-bearing KEP mice using FACS (n = 6 per group). d) *Ccl2* gene expression was determined by quantitative RT-PCR and corrected for *β-actin*. e) Quantification of intratumoral cell populations by flow cytometry. (** p<0.01). All data are mean ± s.e.m.

CCL2 influences breast cancer metastasis

Several studies report a pro-metastatic role for CCL2 in breast cancer by recruiting monocytes and macrophages to primary tumors and metastatic sites [9–11]. To study the role of CCL2 in metastasis, we utilized our previously described KEP-based model of spontaneous breast cancer metastasis [4,12]. KEP mammary tumor-bearing mice were treated with anti-CCL2 in a neo-adjuvant and adjuvant setting (Fig. 2a). Neo-adjuvant CCL2 blockade did not affect primary tumor growth (Fig. 1b), but increased the metastatic burden in the lungs (Fig. 1c) without affecting overall survival (Fig. 1d). These data corroborate previous results showing that cessation of CCL2 blockade can enhance metastasis due to a cytokine rebound effect [13]. Conversely, adjuvant CCL2 blockade reduced metastatic burden in the lung (Fig. 2e), albeit not statistically significant, and resulted in a modest survival benefit (Fig. 2f). Likewise, CCL2 blockade in KEP mice bearing spontaneously arising mammary tumors also resulted in decreased pulmonary metastases (Fig. 2h), without affecting primary tumor growth (Fig. 2g). Together, the data generated in both the metastasis model and genetically engineered KEP model suggest that CCL2 functions as a pro-metastatic cytokine. However, these data also emphasize the complexity of targeting CCL2 in breast cancer metastasis, as described by others [13,14].

CCL2 drives the pro-metastatic γδ T cell – IL17 – neutrophil axis

To further understand the underlying mechanisms of CCL2 action during breast cancer metastasis, we analyzed the expression of the CCL2 receptor, CCR2, on different immune cell populations in the circulation of mammary tumor-bearing KEP mice. Flow cytometric analysis revealed that monocytes and γδ T cells express high levels of CCR2 (Fig. 3a, b). Unlike other reports [9,10], we found no effect of CCL2 blockade on the proportion of circulating monocytes in KEP mice (data not shown). Therefore we focused our attention on γδ T cells. Based on the expression of co-stimulatory factor CD27, γδ T cells can be phenotypically subdivided into IFNγ-producing $CD27^+$ γδ T cells and IL17-producing $CD27^-$ γδ T cells [15]. In mammary tumor-bearing KEP mice we could find these distinct subpopulations of γδ T cells and we discovered that CCR2 expression is restricted to the IL17-producing $CD27^-$ γδ T cell population (Fig. 3c, d). Moreover, the proportion of $CD27^-CCR2^+$ γδ T cells was significantly increased throughout all organs analyzed in mammary tumor-bearing KEP animals compared to wild-type littermates (Fig. 3e).

Because metastasis in the KEP model is driven by IL17-producing γδ T cells and subsequent expansion of immunosuppressive neutrophils [4], we assessed whether CCL2 affects the functionality of IL17-producing γδ T cells by treating mammary tumor-bearing KEP mice with neutralizing antibodies against CCL2. CCL2 blockade resulted in a significant reduction of the percentage of IL17-producing γδ T cells in blood, lymph nodes and lungs (Fig. 4a), without affecting total γδ T cell proportions (data not shown). A two-fold reduction in IL17 serum levels was also observed in mammary tumor-bearing KEP mice treated with anti-CCL2 (Fig. 4b), concomitant with decreased G-CSF levels (Fig. 4c). Flow cytometric analysis revealed that the total proportion of $CD11b^+Ly6G^+Ly6C^+$ neutrophils was reduced in various organs after CCL2 blockade (Fig. 4d). As observed in metastatic

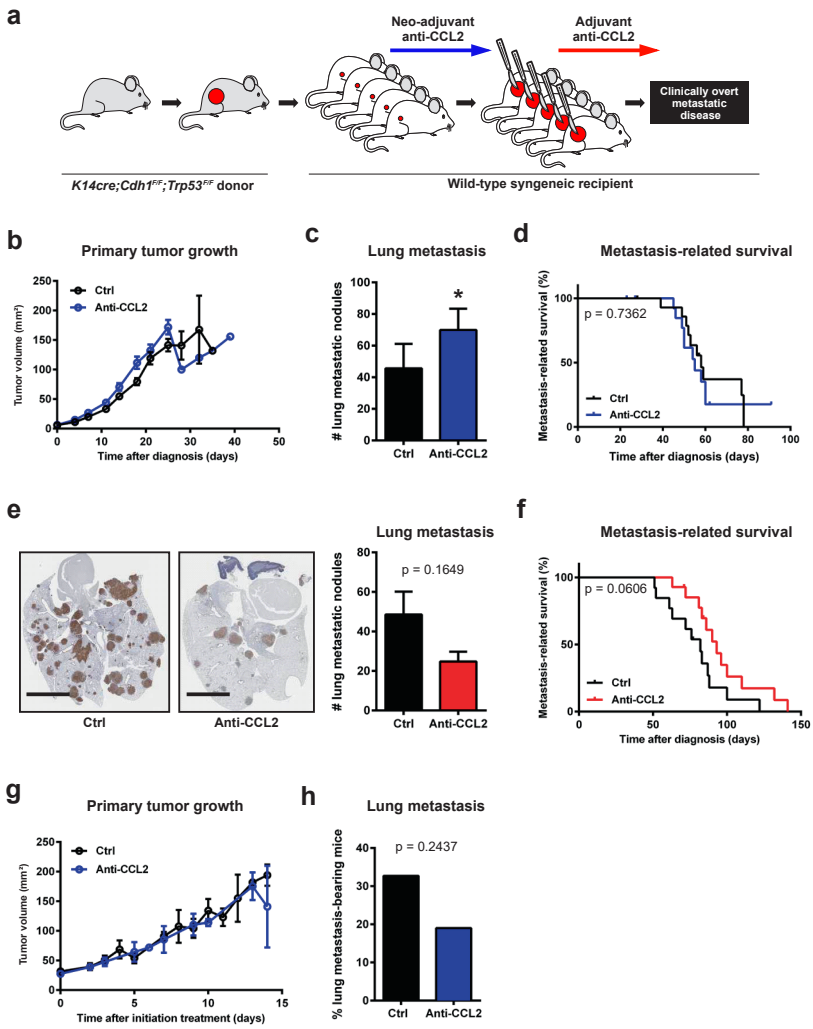

Figure 2. CCL2 blockade during spontaneous breast cancer metastasis. a) Schematic representation of the KEP-based mouse model for spontaneous breast cancer metastasis treated with neo-adjuvant or adjuvant anti-CCL2. b) Primary tumor growth kinetics upon neo-adjuvant CCL2 blockade (n = 15 per group). c) Quantification of lung metastatic nodules in mice treated with neo-adjuvant anti-CCL2 (n = 8) versus controls (n = 11) that succumb due to respiratory distress. (*p<0.05, Mann-Whitney U test). d) Metastasis-related survival of mice treated with neo-adjuvant anti-CCL2 versus controls (n = 15 per group). Animals that succumb due to local relapse of the primary tumor are censored. Statistical analysis was conducted using Log-rank test. e) Representative images of cytokeratin-8-stained lung sections, and quantification of lung metastatic nodules in mice treated with adjuvant anti-CCL2 (n = 8) or controls (n = 10) that succumb due to respiratory distress. Scale bar 5 mm. Statistical analysis was conducted using Mann-Whitney U test. f) Metastasis-related survival of mice treated with adjuvant anti-CCL2 (n = 14) compared to controls (n = 13). Statistical analysis was conducted using the Log-rank test. g) Primary tumor growth kinetics of KEP mice bearing spontaneous mammary tumors treated with anti-CCL2 (n = 6) compared to controls (n = 15). h) Proportion of KEP mice bearing pulmonary metastasis after CCL2 blockade (n = 21) or controls (n = 52). Statistical analysis was conducted using Chi-square test. All data are mean ± s.e.m.

breast cancer patients [16], one hallmark of KEP tumor-induced neutrophils is the expression of hematopoietic stem cell marker cKIT on a proportion of these cells [4]. In anti-CCL2 treated mice the proportion of cKIT$^+$ neutrophils was significantly reduced in all organs (Fig. 4e), indicating that CCL2 blockade reverts the immature phenotype of neutrophils. In the KEP model, neutrophils exert their pro-metastatic function through suppression of CD8$^+$ T cells [4]. To assess whether CCL2 blockade affects CD8$^+$ T cell activity, we analyzed the presence and activation status of T cells upon anti-CCL2 treatment in animals bearing orthotopically transplanted KEP tumors. The proportion of interferon (IFN)-γ producing (Fig. 4f) and activated CD8$^+$ T cells (Fig. 4g) in the lungs was significantly increased while total CD8$^+$ T cell proportions remained unaffected (data not shown). Together these data demonstrate that CCL2 contributes to mammary tumor-induced immunosuppression at distant sites in KEP mice through the activation of IL17-expressing γδ T cells and G-CSF-dependent expansion of immunosuppressive neutrophils.

CCL2 is not sufficient to induce IL17 expression from γδ T cells

To understand how CCL2 is involved in the γδ T cell – IL17 – neutrophil axis, we asked whether CCL2 is sufficient to induce IL17 expression from γδ T cells *in vivo*, since these cells express the CCR2 receptor (Fig. 3a-e). We treated wild-type mice with recombinant murine CCL2 (rCCL2) and analyzed the proportion of IL17$^+$ γδ T cells in the circulation. Administration of rCCL2 did not induce IL17 expression from γδ T cells (Fig. 5a) and did not expand the neutrophil population (Fig. 5b). rCCL2 increased circulating CD11b$^+$Ly6C^{hi} monocytes confirming that rCCR2 was functional *in vivo* (Fig. 5c). Similar results were obtained in γδ T cell-deficient *Tcrd*$^{-/-}$ mice where rCCL2 induced an increase in blood monocytes but did not elicit neutrophil expansion (Fig. 5d).

We took another approach by sorting CD27$^-$ and CD27$^+$ γδ T cells from mammary tumor-bearing KEP mice. These cells were cultured *ex vivo* in the presence or absence of rCCL2. While the positive control rIL23 [17] induced IL17 expression from CD27$^-$ γδ T cells, rCCL2 did not (Fig. 5e). As expected, CD27$^+$ γδ T cells did not produce IL17 (Fig. 5e). Together, these results indicate that CCL2 is not sufficient to induce IL17 expression from γδ T cells or to induce the expansion of neutrophils, and thus might require a cancer-associated intermediate cell type or mediator.

CCL2 induces IL1β expression from CCR2$^+$ TAMs to drive the γδ T cell – IL17 – neutrophil axis

Hypothesizing that CCL2 exerts its effect via an intratumoral component, we next examined the presence of potential CCL2-responsive cells at the primary tumor site. Flow cytometric analysis of primary KEP tumors revealed that KEP cancer cells do not express CCR2 (Supplementary Fig. 1b). Instead, CCR2 is abundantly expressed on CD11b$^+$F4/80$^+$CD206$^+$ TAMs, but can also be found on the surface of CD11b$^+$F4/80$^-$ Ly6G$^-$Ly6C^{hi} monocytes and to a lesser extent on CD11b$^+$F4/80$^-$Ly6G$^+$Ly6C^{lo} neutrophils (Fig. 6a,b and Supplementary Fig. 1a, b). Nevertheless, inhibition of CCL2 did not alter the intratumoral accumulation of these myeloid cells (Fig. 6c).

Because neutralization of CCL2 failed to affect immune cell recruitment, we hypothesized that CCL2 influences the phenotype and polarization state of macrophages. Therefore, we sorted TAMs from anti-CCL2-treated and control KEP tumors and examined the expression of several genes that have been associated with the polarization of TAMs [18]. We found no significant changes in gene expression of *Arg1*, *Cd206*, *Decoy Il1r2* and *Nos2* in TAMs upon CCL2 blockade (Fig. 6d).

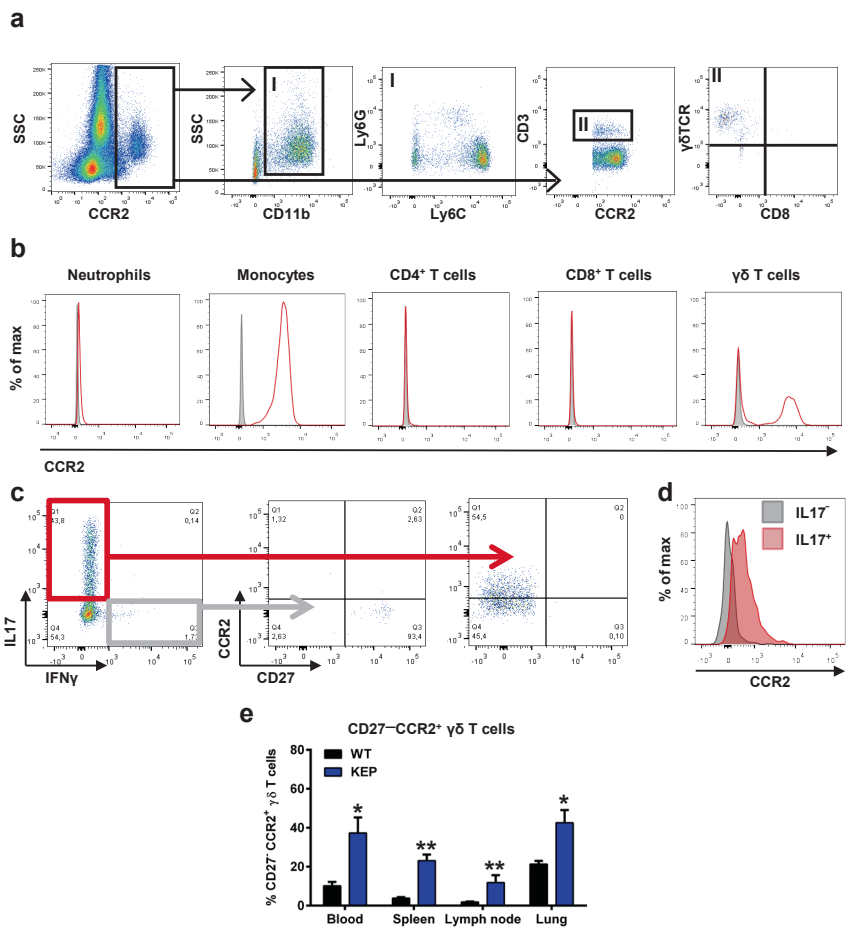

Figure 3. CCR2 is expressed on IL17-producing CD27⁻ γδ T cells. a) Representative dot plots of CCR2⁺ cells gated on total CD45⁺ cells in blood of mammary tumor-bearing KEP mice. A proportion of the CCR2⁺ cells was CD11b⁺Ly6C^{hi} (I) representing monocytes and a proportion was CD3⁺γδTCR⁺ (II) representing γδ T cells. b) Representative flow cytometry histograms showing CCR2 expression (red) compared to fluorescence minus one (FMO) controls (grey) on circulating immune cell populations in mammary tumor-bearing KEP mice. c) Representative dot plots of CCR2 and CD27 expression on IL17- and IFNγ-producing γδ T cells in lungs of KEP mice (~225 mm²) measured by flow cytometry. d) Representative histogram of CCR2 expression on IL17⁺ (red) and IL17⁻ γδ T cells (grey). e) Quantification of the proportion of CD27⁻CCR2⁺ cells gated on total γδ T cells in different organs of wild-type (n = 5) versus KEP mice (tumor ~225 mm²) (n = 7). (*p<0.05, **p<0.01, Mann-Whitney U test). All data are mean ± s.e.m.

Previously, we showed that IL1β induces IL17 expression in γδ T cells and TAMs are the main source of IL1β in the tumor microenvironment [4]. Therefore, we examined whether CCL2 regulates IL1β and other known inducers of IL17 – such as TGFβ , IL6 and IL23 [17] – in TAMs. Interestingly, we observed a significant decrease in TAM-derived *Il1β* mRNA, while expression of *Tgfβ, Il6* and *Il23p19* was unaffected in TAMs upon CCL2 blockade (Fig. 6e).

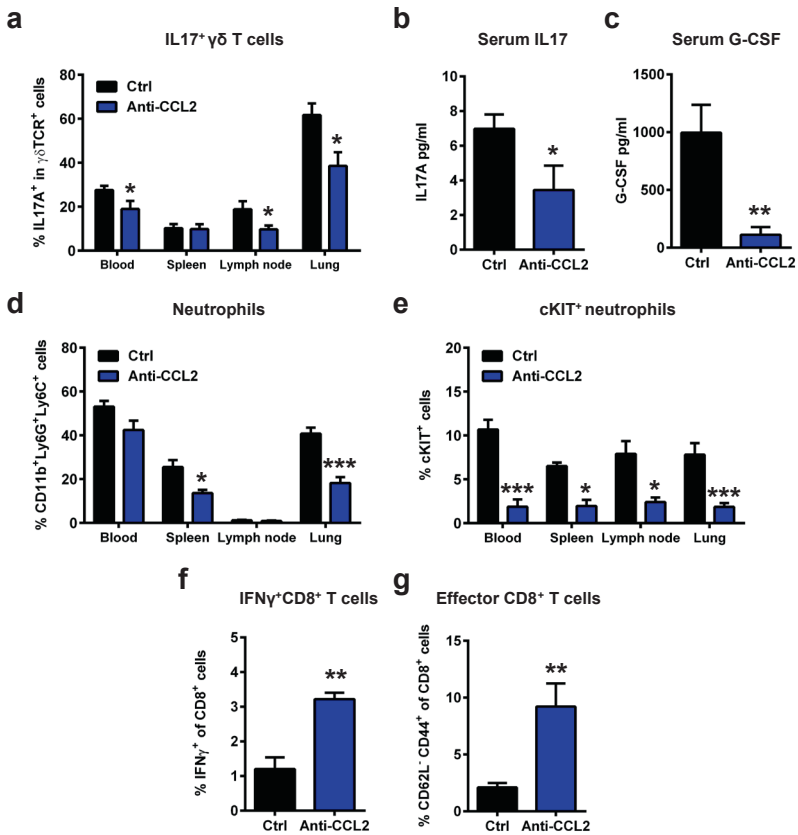

Figure 4. Mammary tumor-derived CCL2 promotes systemic inflammation characterized by IL17-producing γδ T cells, neutrophil expansion and suppression of T cells. KEP mice were treated with anti-CCL2 or PBS (Ctrl) during primary tumor growth starting at 25 mm^2. Animals were sacrificed when tumors reached 225 mm^2 and organs were collected for flow cytometric analysis. Proportions of IL17$^+$ cells gated on total γδ T cells in blood, spleen, lymph nodes and lungs of KEP mice treated with anti-CCL2 (n = 8) and controls (n = 10) (a). Serum levels of IL17A (b) and G-CSF (c) in KEP mice determined by cytometric bead array (n = 6 per group). Flow cytometric analysis of the proportions of total CD11b$^+$Ly6G$^+$Ly6C$^+$ neutrophils (gated on total CD45$^+$ cells) (d) and cKIT$^+$ neutrophils (gated on total neutrophils) (e) in blood, spleen, lymph nodes and lungs of KEP mice treated with anti-CCL2 (n = 6) and controls (n = 10). Flow cytometric analysis of intracellular IFNγ staining in CD8$^+$ T cells (f) and the proportion of CD62L$^-$CD44$^+$ effector CD8$^+$ T cells of total CD8$^+$ T cells (g) in lungs of KEP-derived tumor-bearing animals (~100 mm^2) treated with anti-CCL2 (n = 6) or controls (n = 5). (*p<0.05, **p<0.01, ***p<0.001, Mann-Whitney U test). All data are mean ± s.e.m.

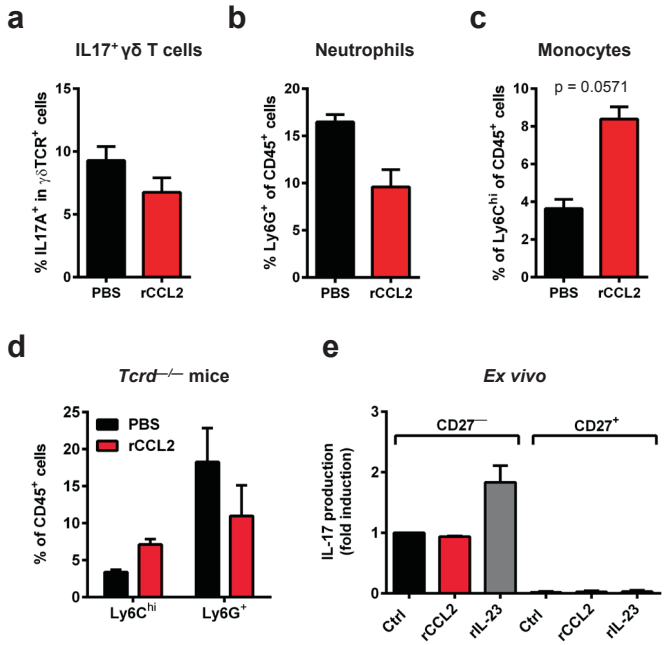

Figure 5. CCL2 is not sufficient to induce IL17 expression from γδ T cells. a-d) Wild-type (a-c) or *Tcrd*$^{-/-}$ mice (d) were treated with recombinant murine CCL2 (n = 4) or PBS (n = 2) for 5 consecutive days. One hour after the last treatment animals were sacrificed for flow cytometric analysis. The fraction of IL17-producing γδ T cells gated of total γδ T cells (a), CD11b^{+}Ly6G^{+} neutrophils (b) and CD11b^{+}Ly6C^{hi} monocytes (c) of total CD45^{+} cells in the blood determined by flow cytometry. d) The fraction of CD11b^{+}Ly6C^{hi} monocytes and CD11b^{+}Ly6G^{+} neutrophils gated of total CD45^{+} cells in the blood of *Tcrd*$^{-/-}$ mice after CCL2 (n = 3) or PBS (n = 3) treatment determined by flow cytometry. Statistical analysis was conducted by Mann-Whitney U test. e) γδ T cells from KEP mice were sorted based on CD27 expression and cultured *ex vivo* for 48 hours in the presence of rCCL2 (50ng/ml), rIL23 (10ng/ml) or DMSO. IL17A concentrations in supernatants were determined by cytometric bead array. Data of two independent experiments are normalized to corresponding CD27^{-} control situation and pooled. All data are mean ± s.e.m.

To further confirm that CCL2 activates the γδ T cell – IL17 – neutrophil axis via TAM-derived IL1β, we performed *in vivo* rescue experiments in which tumor-bearing KEP animals treated with anti-CCL2 or PBS were reconstituted with recombinant murine IL1β (rIL1β) (Fig. 6f). Intracellular flow cytometry analyses revealed that reconstitution with rIL1β reversed the anti-CCL2-induced reduction of IL17-producing γδ T cells (Fig. 6g) and restored neutrophil accumulation in KEP lungs (Fig. 6h). Together these results demonstrate that tumor-derived CCL2 locally orchestrates — via the induction of IL1β expression by TAMs — a systemic cascade of inflammatory events (Fig. 8).

Correlation between CCL2 and IL1B gene expression levels in human breast cancer

To determine whether there is support for the causal link between CCL2 and IL1β as observed in the KEP mice in human breast cancer patients, we took advantage of gene expression data from tumors obtained from treatment naïve breast cancer patients. *CCL2*

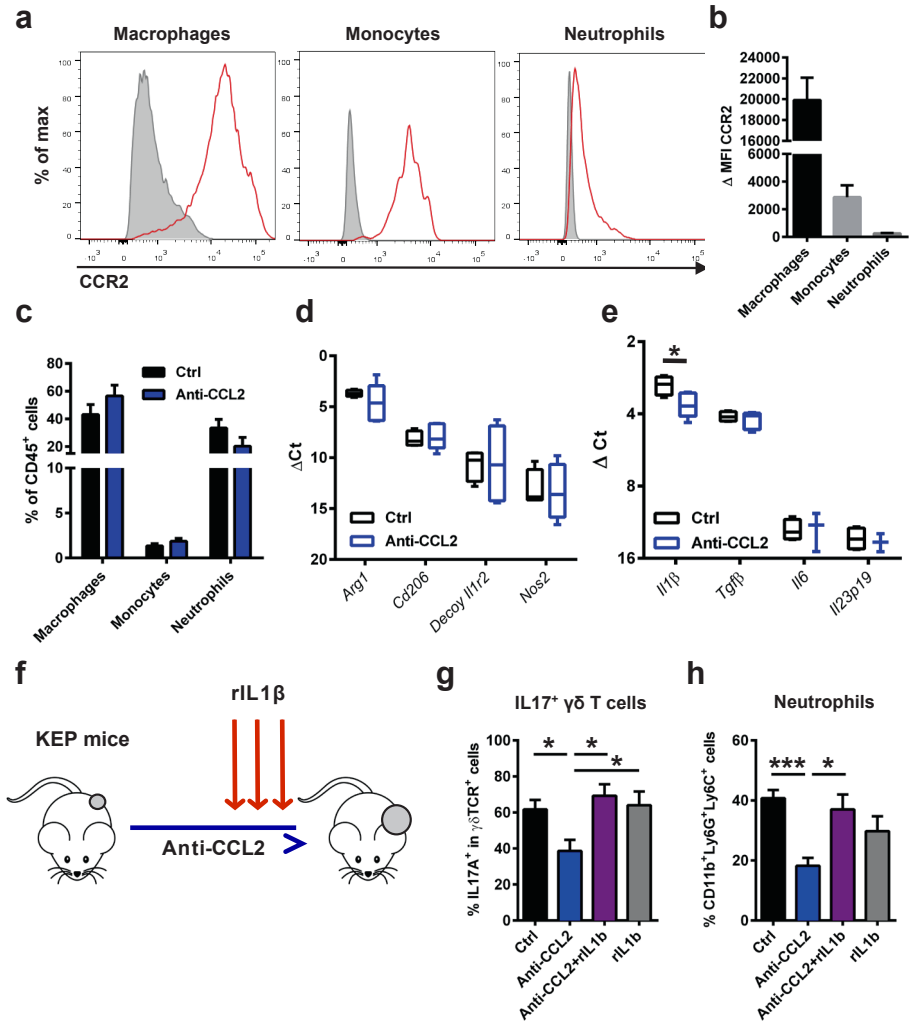

Figure 6. CCL2-induced IL1β expression by CCR2⁺ tumor-associated macrophages activates the γδ T cell – IL17 – neutrophil axis. a) Representative histograms of CCR2 expression (red) compared to FMO (grey) on intratumoral CD11b⁺F4/80⁺CD206⁺ TAMs, CD11b⁺F4/80⁻Ly6G⁻Ly6C^{hi} monocytes and CD11b⁺F4/80⁻Ly6G⁺Ly6C^{lo} neutrophils. b) Quantification of delta median fluorescence intensity (MFI) (MFI stained sample – MFI of FMO) of CCR2 on different populations of tumor-infiltrating myeloid cells. c) Quantification of tumor-infiltrating immune populations in tumors (~225 mm²) of KEP mice treated with anti-CCL2 (n= 7) or controls (n = 3). d, e) TAMs were sorted from orthotopically transplanted KEP mammary tumors (~225 mm²) treated with anti-CCL2 (n = 5) or controls (n = 4). Transcripts of *Arg1*, *Cd206*, *decoy Il1r2* and *Nos2* (d) and *Il1ß, Tgfß, Il6* and *Il23p19* (e) were determined by quantitative RT-PCR and normalized to *ß-actin* .f).Experimental set up of rescue of anti-CCL2 induced phenotypes with recombinant IL1β. KEP mice were treated with anti-CCL2 or PBS and for 3 consecutive days with recombinant IL1β (rIL1β). 24 hours after the last injection with rIL1β and anti-CCL2 animals were sacrificed and lungs were collected for flow cytometric analysis. The proportion of IL17⁺ cells gated on total γδ T cells (g) and CD11b⁺Ly6G⁺Ly6C⁺ neutrophils gated on CD45⁺ cells (h) in lungs of KEP mice treated with control (n = 9), anti-CCL2 (n = 8), anti-CCL2 + rIL1β (n = 7) and rIL1β (n = 6). (*p<0.05, **p<0.01, ***p<0.001, Mann-Whitney U test). All data are mean ± s.e.m.

and *IL1B* gene expression are enriched in basal-like tumors when compared to other subtypes of human breast cancer (Fig. 7a, b). Gene expression analysis of two independent datasets (METABRIC [19] and 295 NKI [20]) confirmed these results (Supplementary Fig. 2a-f). Consistent with our data obtained in the KEP model, the expression of *CCL2* and *IL1B* transcripts in treatment naïve human breast cancers is positively correlated across all breast cancer subtypes, with the strongest correlation in basal breast cancer (Fig. 7c). Consistent with our observations in the KEP mouse model, expression of *G-CSF* and *IL17A* in human breast tumors was very low, and was only detectable in basal tumors (data not shown).

CCL2 and *IL1B* expression correlated with macrophage marker *CD68* (Fig. 7d, e), suggesting that macrophage-rich tumors express higher levels of CCL2 and IL1β. In line with this, analysis of intratumoral immune composition by Cibersort [21,22] revealed that basal-like breast tumors contain significantly higher proportions of macrophages compared to luminal A/B and HER2^{+} subtypes (Fig. 7f). Together these results support the link between CCL2 and IL1β in macrophage-rich human tumors.

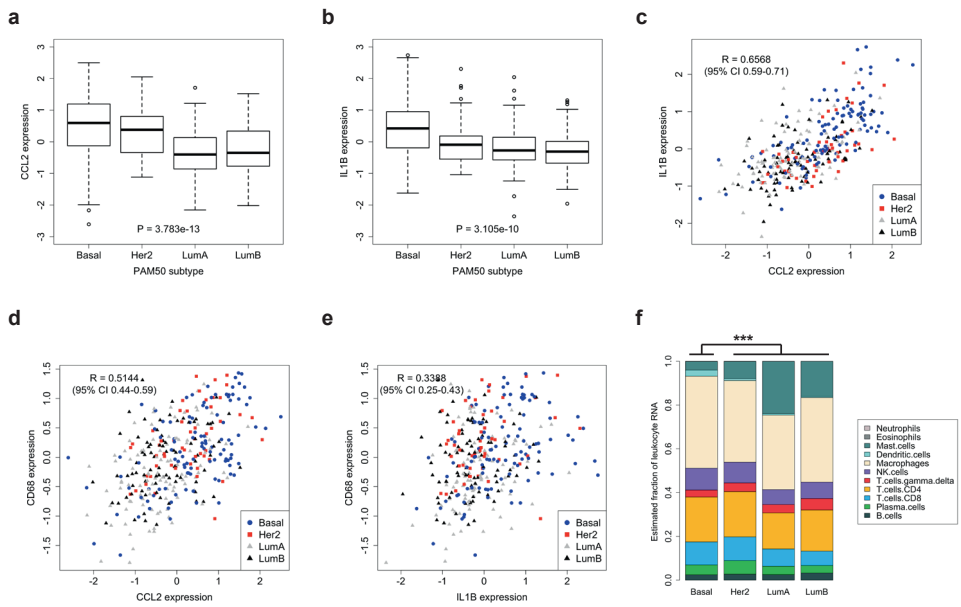

Figure 7. Gene expression of *CCL2* and *IL1B* is positively correlated in human breast cancer. a-b) Gene expression of *CCL2* (a) and *IL1B* (b) in different subtypes of treatment naïve human breast cancer (Basal n = 106; Her2 n = 52; LumA n = 107; LumB n = 86 patients). Statistical significance was determined by Kruskal-Wallis test. c) *CCL2* and *IL1B* gene expression are highly correlated across all subtypes of human breast cancer. *CCL2* (d) and *IL1B* (e) gene expression in human breast cancer correlates with macrophage marker *CD68*. f) The intratumoral immune composition in different subtypes of human breast cancer as determined by Cibersort ([21,22]). The immune composition of basal breast tumors is enriched for macrophages compared to Her2, LumA and LumB combined (***p<0.001, Two-sided t-test was conducted to compare the fraction of macrophages between breast cancer subtypes).

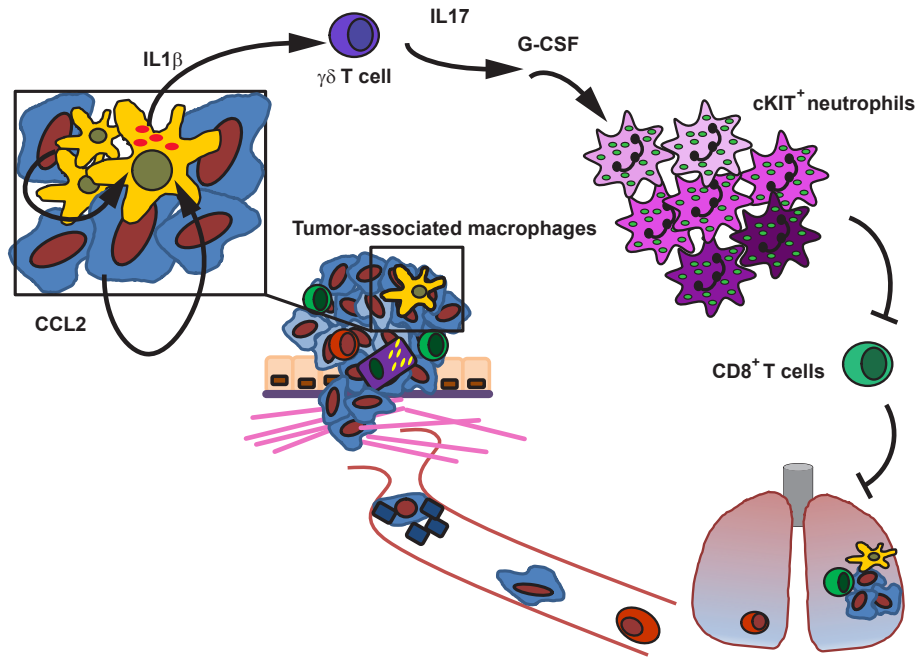

Figure 8. CCL2 promotes breast cancer metastasis through activation of systemic inflammation via TAM-derived IL1β. Mammary tumors elicit a systemic inflammatory cascade via the expression of CCL2. This cascade is initiated at the primary tumor where CCL2 induces the expression of IL1β in TAMs leading to the systemic induction of IL17 production by γδ T cells, G-CSF-dependent expansion and polarization of neutrophils and suppression of $CD8^+$ T cell activity. By inducing this cascade of events tumors elicit an immunosuppressive state in distant organs to facilitate the formation of metastatic disease.

Discussion

Compelling evidence demonstrates that cancer progression and metastasis are tightly regulated by tumor-induced systemic inflammation [2]. Cancer patients frequently present with elevated neutrophil counts in blood, which is associated with increased risk for metastasis [23]. In line with these clinical observations, a causal link between neutrophils and metastasis formation has recently been demonstrated in various independent transgenic mouse models that mimic human cancer [4,24–26]. Using the KEP transgenic mouse model for invasive breast cancer [27], we have recently identified a mammary tumor-induced inflammatory cascade characterized by the systemic expansion of immunosuppressive neutrophils that protect disseminated cancer cells from destruction by anti-tumor T cells [4]. We reported that IL1β from the tumor microenvironment induces IL17 production in γδ T cells, which is required for the subsequent expansion and polarization of pro-metastatic neutrophils in a G-CSF-dependent manner [4]. However, how other mammary tumor-derived factors contribute to driving this systemic inflammatory state remains largely unknown.

Here we identified CCL2 as a driver of this systemic immunosuppressive cascade by inducing IL1β expression in TAMs. Previous experimental studies have reported that CCL2 exerts a pro-metastatic role through recruitment and/or polarization of inflammatory monocytes and macrophages [11,10,28–30]. Therapeutic targeting of macrophages by interfering with CCL2/CCR2 signaling in experimental models has resulted in increased anti-tumor T cell responses [31–33]. While some studies report direct T cell suppression by macrophages [32,33], it remains elusive whether neutrophils contribute to CCL2-mediated immunosuppression. Here, we report that CCL2 induces immune evasion by promoting mammary tumor-induced systemic neutrophil expansion and polarization which subsequently suppresses T cell activity. In line with our finding, it was reported recently that CCL2 promotes the accumulation and immunosuppressive properties of polymorphonuclear-myeloid-derived suppressor cells (PMN-MDSCs), which share many features with neutrophils, in a mouse model for colorectal carcinogenesis [34]. Together, our findings and previous studies provide evidence that targeting CCL2/CCR2 signaling could relieve immunosuppression and unleash anti-tumor immune responses.

Our experiments shed light on the multi-step mechanism underlying the interaction between CCL2 and immunosuppressive neutrophils, by showing that CCL2 promotes IL1β expression in TAMs, which triggers a cascade of downstream systemic events involving IL17 expression by γδ T cells leading to G-CSF-induced expansion of pro-metastatic neutrophils. Interestingly, the connection between CCL2/CCR2 signaling and IL1β is also important in non-tumor settings. In a model for microbiota-induced intestinal inflammation, CCR2 signaling mediates the release of IL1β from monocytes which triggers inflammation upon epithelial injury [35]. Also, CCL2 has been described to activate and mobilize γδ T cells in various inflammatory conditions including allergy and sepsis [36,37]. Furthermore, inflammation-induced CCL2 expression has been shown to recruit IL17-producing $CCR2^{+}$ γδ T cells that are activated by IL1β and IL23 in a mouse model for rheumatoid arthritis [38]. These striking similarities between non-tumor and tumor-induced inflammation hint towards a more general causal link between CCL2, IL1β and γδ T cell signaling in various inflammatory conditions.

Intriguingly, some studies report tumor-protective properties of CCL2 [39,40]. For example, anti-tumor γδ T cells have been shown to infiltrate tumors in a CCL2-mediated manner in the B16 melanoma inoculation model [40]. In this model, CCL2 directly affected the migration and recruitment of γδ T cells, and the role of IL1β was not assessed. Whether and how these opposite functions of CCL2 on tumor biology are dictated by the genetic make-up of tumors, tumor type, tumor stage and/or other cancer cell-intrinsic or -extrinsic properties remains to be established.

Several independent clinical studies show that expression of CCL2, IL17, the intratumoral presence of macrophages, γδ T cells, and systemic neutrophil accumulation each correlate with poor prognosis in breast cancer patients [41,7,42–44]. Moreover, expression of IL1β is elevated in human invasive breast cancers compared to healthy tissue [45]. In line with these reports, we show in human treatment naïve breast cancers that *CCL2* and *IL1B* gene expression are highly correlated in macrophage-rich tumors. The findings in

our previous [4] and current studies suggest that these inflammatory cells and mediators are causally linked, and that interruption of this systemic inflammatory cascade can be a potential therapeutic target to relieve tumor-induced systemic immunosuppression. A recent phase 1b clinical trial in patients with pancreatic cancer revealed that therapeutic targeting of CCL2/CCR2 signaling in combination with a chemotherapy regimen has clinical activity and resulted in reduced immunosuppression and an increase in the number of tumor-infiltrating lymphocytes [46]. Whether this treatment strategy also unleashes anti-tumor immune responses to attack metastatic disease remains to be seen. Together these results advocate for the exploration of CCL2/CCR2 targeting drugs for the treatment of metastasized breast cancer. However, the risk of enhancing metastatic spread upon discontinuation of therapeutic blockade of CCL2 should be taken into careful consideration.

Materials and Methods

Patient material and Cibersort

Biopsies of primary breast tumors were collected prior to treatment from women who received neoadjuvant chemotherapy at the Netherlands Cancer Institute between 2000 and 2013 as part of ongoing clinical trials, or were treated off protocol according to the standard arms of one of these studies (NCT00448266, NCT01057069). The studies have been approved by the ethical committee and informed consent was obtained from all patients. Biopsies were taken using a core needle and were snap-frozen in liquid nitrogen. RNA was isolated from samples with a tumor percentage > 50% and analyzed on a microarray or using RNAseq (details are available in Supplementary Materials and methods). The microarray data was generated and analyzed as described previously [47] and made available through the GEO database, accession GSE34138. To determine the relative abundance of immune cells in our samples, we analyzed the microarray data using CIBERSORT ([21] and https://cibersort.stanford.edu/).

Animal studies

The generation of *K14cre;Cdh1$^{F/F}$;Trp53$^{F/F}$* (KEP) mice has been described in detail [27]. KEP mice were backcrossed to the FVB/N background. Mammary tumor formation was monitored twice weekly by palpation and caliper measurements. For transplantation studies female FBV/N mice (10-12 weeks) were purchased from Charles River Laboratories (Sulzfeld, Germany). Orthotopic transplantation and surgical removal of KEP tumors was performed as described earlier [12]. Female *Tcrd$^{-/-}$* mice on the FVB/N background were kindly provided by A. Hayday [48]. Animals were kept in open cages and food and water were provided *ad libitum*. Animal experimental procedures were approved by the Animal Ethics Committee of the Netherlands Cancer Institute and performed in accordance with national and institutional guidelines for Animal Care and Use.

In vivo CCL2 neutralization

Mammary tumor-bearing KEP animals were treated twice weekly with anti-CCL2 (C1142 Janssen Pharmaceuticals) by intraperitoneal injection dosed at 10mg/kg starting from a tumor size of 25 mm^2 and continued until animals were sacrificed once their primary tumor reached 225 mm^2. For metastasis studies, FVB/N animals bearing orthotopically transplanted KEP tumors were treated with neo-adjuvant anti-CCL2 starting from a tumor size of 6 mm^2 until the primary tumor was surgically removed (225 mm^2). For adjuvant CCL2 blockade, treatment with anti-CCL2 was initiated 3 days after surgical removal of the primary tumor and continued until animals had to be sacrificed due to clinical signs of metastatic disease. Animals were randomized before beginning the treatment schedule.

Surface and intracellular staining for flow cytometry

Tissues were collected in ice-cold PBS. Blood samples were collected in tubes containing heparin (Leo Pharma, USA) and treated with NH_4 lysis buffer. Tumors and lungs were mechanically chopped using a McIlwain Tissue Chopper (Mickle Laboratory Engineering Co. Ltd, Guildford, UK) and digested for 1 hour at 37°C in a digestion mix of 3 mg/ml collagenase type A (Roche, Mannheim, Germany) and 25 µg/ml DNAse (Sigma), or 30 min at 37°C in 100 µg/ml Liberase (Roche, Mannheim, Germany) respectively, in serum-free DMEM (Invitrogen). Reactions were terminated by addition of DMEM containing 8% FCS. Cell suspensions were dispersed through a 70 µm cell strainer (BD Falcon). All single cell suspensions were treated with NH_4 lysis buffer to remove red blood cells.

For *ex vivo* cytokine stimulation, single cells were collected at 1500 rpm for 5 min in a round bottom 96-wells tissue culture plate (Thermo Scientific) in IMDM containing 8% FCS, 100 IU/ml penicillin, 100 µg/ml streptomycin (Invitrogen) and 0.5% β-mercaptoethanol. Cells were stimulated with phorbol 12-myristate 13-acetate (PMA; 50 ng/ml) and ionomycin (1 µM) in the presence of Golgi-Plug™(BD) for 3 h at 37°C.

For flow cytometric staining, either stimulated or unstimulated single cells were collected at 1500 rpm for 5 min and resuspended in PBS containing 1% BSA (Sigma-Aldrich, USA). Single cell suspensions were plated in round bottom 96-wells plates (Thermo Scientific) and incubated for 30 min in the dark at 4°C with different combinations of fluorescently labelled monoclonal antibodies (see Supplementary information). For intracellular staining cells were washed twice with PBS containing 1% BSA and fixed and permeabilised using the Cytofix/Cytoperm™ kit (BD) according to manufacturer's instructions. Cells were subsequently incubated for 30 min in the dark at 4°C with antibodies against IFNγ and IL17A. Fixable Viability Dye APC eFluor780 (eBioscience) or 7AAD viability staining solution (eBioscience) was added in order to exclude dead cells. Flow cytometric analysis was performed on a BD LSRII using Diva Software (BD Biosciences, USA). Data analyses were performed using FlowJo Software version 10.0 (Tree Star, Ashland, OR, USA).

The following antibody panels were used:
Myeloid – CD45-eFluor605NC (1:50; clone 30-F11), CD11b-eFluor650NC (1:400; clone M1/70), Ly6G-AlexaFluor700 (1:400; clone 1A8; BD Pharmingen), Ly6C-eFluor450 (1:400; clone HK1.4), F4/80-APC-eFluor780 (1:200; clone BM8), VEGFR1-APC (1:50; clone 141522; R&D Systems), cKIT-PE-Cy7 (1:400; clone 2B8), CCR2-PE (1:50; clone 475301; R&D Systems), CXCR4-PerCP-eFluor 710 (1:400; clone 2B11), CD49d-FITC (1:400; clone R1-2) or Gr1-FITC (1:400; clone RB6-8C5), 7AAD.

Lymphoid I – CD45-eFluor605NC (1:50; clone 30-F11), CD11b-eFluor650NC (1:400; clone M1/70), CD3-PE-Cy7 (1:200; clone 145-2C11), CD4-APC-eFluor780 (1:200; clone GK1.5), CD8-PerCP-eFluor710 (1:400; clone 53-6.7), γδTCR-FITC (1:400; clone GL3; BD Biosciences), CD49b-APC (1:400; clone DX5), IL17A-PE (1:200; clone eBio17B7), IFNγ-eFluor450 (1:200; clone XMG1.2), 7AAD.

Lymphoid II – CD45-eFluor605NC (1:50; clone 30-F11), CD11b-APC-eFluor780 (1:200; clone M1/70), CD3-PE-Cy7 (1:200; clone 145-2C11), CD4-APC-eFluor780 (1:200; clone GK1.5), CD8-PerCP-eFluor710 (1:400; clone 53-6.7), γδTCR-PE (1:400; clone GL3), CD49b-APC (1:400; clone DX5), CD62L-AlexaFluor700 (1:400; clone MEL-14), CD44-FITC (1:400; clone IM7; BD Pharmingen), IFNγ-eFluor450 (1:200; clone XMG1.2), CD19-APC-eFluor780 (1:200; clone eBio1D3), Fixable Viability Dye eFluor® 780.

Phenotyping γδ T cells I – CD27-PE-Cy7 (1:200; clone LG.7F9), γδTCR-FITC (1:400; clone GL3; BD Biosciences), CD45-eFluor605NC (1:50; clone 30-F11), CD3-eFluor450 (1:200; clone 145-2C11), CCR2-PE (1:50; clone 475301; R&D Systems), CD8-PerCP-eFluor710 (1:400; clone 53-6.7), CD4-APC-eFluor780 (1:200; clone GK1.5), CD19-APC-eFluor780 (1:200; clone eBio1D3), CD11b-APC-eFluor780 (1:200; clone M1/70), Fixable Viability Dye eFluor® 780.

Phenotyping γδ T cells II – CD27-PE-Cy7 (1:200; clone LG.7F9), γδTCR-FITC (1:400; clone GL3; BD Biosciences), CD45-eFluor605NC (1:50; clone 30-F11), CD3-eFluor450 (1:200; clone 145-2C11), CCR2-PE (1:50; clone 475301; R&D Systems), IL17A-APC (1:50, clone TC11-18H10; BD Pharmingen), IFNγ-eFluor450 (1:200; clone XMG1.2). Fixable Viability Dye eFluor® 780. All antibodies were obtained from eBiosciences, unless indicated otherwise.

In vivo rescue with recombinant proteins
For CCL2 rescue experiments, female wild-type or *Tcrd*$^{-/-}$ mice (10-12 weeks of age) were injected intraveneously (i.v.) with 1 µg/day recombinant murine CCL2 (Peprotech) in 100 µl sterile PBS or vehicle for 5 consecutive days. On the last day animals were sacrificed 1 hr after rCCL2 or vehicle administration and blood and lungs were collected and processed for flow cytometric analysis. For the IL17^{+} γδ T cell read out, lung and blood cells were pooled to gain sufficient cells. For neutrophil and monocytes read-out, only blood was used.

For IL1β rescue experiments, mammary tumor-bearing KEP animals were treated twice weekly with anti-CCL2 (C1142 Janssen Pharmaceuticals) by intraperitoneal injection dosed at 10 mg/kg starting from a tumor size of 25 mm^2 until animals were sacrificed. When tumors reached a size of ~130 mm^2 animals were injected intraperitoneally (i.p.) with 0,5 µg/day recombinant murine IL1β (Peprotech) for 3 consecutive days. Animals were sacrificed 24 hrs after the last injection and organs were collected and processed for flow cytometry.

Cytokine analysis

Multiplex quantification of inflammatory cytokines and chemokines was performed using the premixed 32-plex Mouse Immunology Multiplex assay (Milliplex-Map, MCYTMAG-70K-PX32, Millipore). Assays and tissue preparations were performed according to manufacturer's recommendations. 100 µg of total protein from lysed tissues was used for measurements. Fluorescence was measured on a Luminex FlexMap3D System using xPonent 4.0 software (Luminex Corporation). IL-17A and G-CSF levels in serum or culture supernatant were measured by BD Cytometric Bead Array (CBA) Flex Set (mouse IL-17A, cat. no. 560283; mouse G-CSF, cat. no. 560152, BD Biosciences). Assays were performed according to manufacturer's recommendations. Flow cytometric analysis was performed on a Cyan flow cytometer using Summit Software (Beckman Coulter, Inc.). Data analyses were performed using FlowJo Software version 10.0 (Tree Star, Ashland, OR, USA). Spatiotemporal expression of CCL2 was determined by DuoSet ELISA (R&D Systems, DY479) in 10 µg of total protein from lysed tissues according to manufacturer's recommendations.

Fluorescence activated cell sorting

Single cell suspensions from KEP mammary tumors were prepared as described above. CD11b-APC (clone M1/70; eBioscience) myeloid cells were isolated by anti-APC beads over a magnetic column (Milteny). The $CD11b^+$ fraction was stained with F4/80-PE (clone BM8; eBioscience), Ly6C-eFluor450 (clone HK1.4; eBioscience), CD11c-PE-Cy7 (clone HL3; BD Bioscience) and Ly6G-FITC (clone 1A8; BD Pharmingen).The $CD11b^-$ fraction was stained with CD45-PerCp-Cy5.5 (clone 30-F11; eBioscience), CD31-FITC (clone 390; eBioscience), PDGFRβ-PE (clone APB5; eBioscience) and sorted using a BD FACS Aria II, and collected in Trizol for further analysis.

The following populations were identified based on the expression of the following surface markers: tumor cells ($CD31^-CD45^-CD11b^-$), lymphocytes ($CD45^+CD11b^-$), fibroblasts ($PDGFR\beta^+CD31^-CD45^-CD11b^-$), endothelium ($CD31^+CD45^-CD11b^-$), macrophages ($CD11b^+F4/80^+$), dendritic cells (DC) ($CD11b^+F4/80^-CD11c^+$), neutrophils ($CD11b^+F4/80^-Ly6G^+Ly6C^{lo}$), and monocytes ($CD11b^+F4/80^-Ly6G^-Ly6C^{hi}$). All cells were collected in Trizol for further analysis.

For γδ T cell sorts, single cells from KEP spleen and lymph nodes were pooled, collected at 1500 rpm for 5 min and stained for 30 min in the dark at 4°C with CD3-FITC (eBioscience; clone 145-2C11) in PBS containing 1% BSA. After staining, cells were

collected at 1500 rpm for 5 min and suspended in IMDM containing 2% FCS, 100 IU/mL penicillin, 100 µg/mL streptomycin (Invitrogen) and 0.5% β-mercaptoethanol. Subsequently, cells were pre-sorted for $CD3^+$ T cells using a BD FACS Aria II and collected in 100% FCS. Next, cells were collected at 1500 rpm for 5 min and stained for 30 min in the dark at 4°C with γδ TCR-PE (clone GL3; eBioscience) in PBS containing 1% BSA. After staining, cells were sorted for total γδ T cells and collected in 100% FCS for further use.

Ex vivo culture of γδ T cells
Sorted γδ T cells were cultured 1:1 with irradiated splenocytes (40 Gy) in flat bottom 96-wells tissue culture plate (Thermo Scientific) in IMDM containing 8% FCS, 100 IU/mL penicillin, 100 µg/mL streptomycin (Invitrogen) and 0.5% β-mercaptoethanol. T cells were activated by addition of Dynabeads Mouse T-activation CD3/CD28 beads. Culture medium was supplemented with recombinant murine IL-23 (10 ng/mL; purified by the NKI protein facility) or 50 ng/mL recombinant murine CCL2 (Peprotech). After 48 hours of culture, supernatant was collected and stored in -20°C until further use.

Real-time polymerase chain reaction (RT-PCR)
RNA was extracted from FACS-sorted immune cell populations using Trizol-chloroform method. RNA was cleaned with DNAse (Invitrogen) and the yield was measured by using Nanodrop. cDNA first-strand synthesis was performed using Cloned AMV First-Strand cDNA Synthesis Kit (Invitrogen) using Oligo(dT) primers. qRT-PCR analysis was performed using LightCycler 480 SYBR Green I Master (Roche Applied Sciences) according to the manufacturer's instructions. Briefly, 20 ng cDNA was dissolved in 1x LightCycler 480 SYBR Green Master mix containing 500 nM of forward and reverse primers (see Supplementary Table 1). For quantification the delta Ct method was used. All transcripts were normalized to *β-actin*.

RNA in situ hybridization
Tissues were fixed in 10% neutral buffered formalin for 24 hrs, embedded in paraffin (FFPE), and sectioned at 5µm. Localization of *Ccl2* mRNA in KEP mammary tumors was examined by performing RNA *in situ* hybridization on fresh FFPE slides using RNAscope 2.0 FFPE assay (Advanced Cell Diagnostics, Hayward, CA). As controls, probes against DapB (negative control) and PPIB (positive control) were used. Assay was performed as described in [49]. Stained slides were digitally processed using the Aperio ScanScope (Aperio, Vista, CA, USA) and captured using ImageScope software version 11.0.2 (Aperio, Vista, CA, USA).

Immunohistochemistry
Formalin-fixed tissues were processed by routine procedures. Lung metastases were detected as described previously [4,12]. Briefly, one lung section for each animal was used for detection of metastatic nodules using anti-cytokeratin 8 (clone Troma1; Developmental Studies HybridomaBank, University of Iowa) with citrate antigen retrieval. Only mice

that were sacrificed due to respiratory distress were included in this analysis. The number of cytokeratin 8^+ metastatic nodules in the lung was blindly scored by at least two researchers. Stained slides were digitally processed using the Aperio ScanScope (Aperio, Vista, CA, USA) and captured using ImageScope software version 11.0.2 (Aperio, Vista, CA, USA). Brightness and contrast for representative images were adjusted equally among groups.

Statistical analysis

Data analyses were performed using GraphPad Prism version 6.01 (GraphPad Software Inc, La Jolla, CA, USA). Applied analyses are indicated in the corresponding legends. No statistical methods were used to determine sample sizes. Sample sizes were based on previous experience with the models [12,4,50]. Differences with a $p<0.05$ were considered statistically significant.

Author contributions

K.K., S.B.C., and K.E.dV. conceived the ideas and designed the experiments. K.K., S.B.C., N.J.M.V., K.V., M.C., C.W.D., C.H. performed the experiments. K.K., S.B.C., N.J.M.V., K.V., M.C., C.W.D., C.H. and K.E.dV. analyzed the data. Computational analysis and collection of patient data was performed by M.H., E.H.L. and L.F.A.W. P.D. provided the CCL2 neutralizing antibody. K.K., S.B.C. and K.E.dV. wrote the paper.

Acknowledgements

This work was supported by a European Research Council Consolidator award (INFLAMET 615300) and grants from the Dutch Cancer Society (2011-5004 to K.E.dV. and 2013-6007 to L.F.A.W.); Worldwide Cancer Research (AICR 11-0677); the Netherlands Organization for Scientific Research NWO VIDI (917.96.307); the European Union (FP7 MCA-ITN 317445 TIMCC) to K.E.dV. We thank L. Mulder for the preparation of the patient samples, and C. Salvagno, M. Wellenstein, J. Borst, T. Schumacher and J. Jonkers for discussions. We thank the core facilities at the Netherlands Cancer Institute. We thank A. Hayday for *Tcrd*$^{-/-}$ mice. P.D. is an employee of Janssen Research and Development, USA. The authors declare no additional competing financial interests.

References

1. Weigelt, B., Peterse, J. L. & van't Veer, L. J. Breast cancer metastasis: markers and models. *Nat Rev Cancer* **5,** 591–602 (2005).
2. McAllister, S. S. & Weinberg, R. A. The tumour-induced systemic environment as a critical regulator of cancer progression and metastasis. *Nat. Cell Biol.* **16,** 717–727 (2014).
3. Kitamura, T., Qian, B.-Z. & Pollard, J. W. Immune cell promotion of metastasis. *Nat. Rev. Immunol.* **15,** 73–86 (2015).
4. Coffelt, S. B. *et al.* IL-17-producing γδ T cells and neutrophils conspire to promote breast cancer metastasis. *Nature* **522,** 345–348 (2015).
5. Hamilton, J. A. & Achuthan, A. Colony stimulating factors and myeloid cell biology in health and disease. *Trends Immunol.* **34,** 81–89 (2013).
6. Fuentes, M. E. *et al.* Controlled recruitment of monocytes and macrophages to specific organs through transgenic expression of monocyte chemoattractant protein-1. *J. Immunol.* **155,** 5769–5776 (1995).
7. Ueno, T. *et al.* Significance of macrophage chemoattractant protein-1 in macrophage recruitment, angiogenesis, and survival in human breast cancer. *Clin. Cancer Res.* **6,** 3282–3289 (2000).
8. Saji, H. *et al.* Significant correlation of monocyte chemoattractant protein-1 expression with neovascularization and progression of breast carcinoma. *Cancer* **92,** 1085–1091 (2001).
9. Qian, B.-Z. *et al.* CCL2 recruits inflammatory monocytes to facilitate breast-tumour metastasis. *Nature* **475,** 222–225 (2011).
10. Yoshimura, T. *et al.* Monocyte Chemoattractant Protein-1/CCL2 produced by stromal cells promotes lung metastasis of 4T1 murine breast cancer cells. *PLoS ONE* **8,** e58791 (2013).
11. Kitamura, T. *et al.* CCL2-induced chemokine cascade promotes breast cancer metastasis by enhancing retention of metastasis-associated macrophages. *J. Exp. Med.* **212,** 1043–1059 (2015).
12. Doornebal, C. W. *et al.* A preclinical mouse model of invasive lobular breast cancer metastasis. *Cancer Res.* **73,** 353–363 (2013).
13. Bonapace, L. *et al.* Cessation of CCL2 inhibition accelerates breast cancer metastasis by promoting angiogenesis. *Nature* **515,** 130–133 (2014).
14. Li, M., Knight, D. A., A Snyder, L., Smyth, M. J. & Stewart, T. J. A role for CCL2 in both tumor progression and immunosurveillance. *Oncoimmunology* **2,** e25474 (2013).
15. Ribot, J. C. *et al.* CD27 is a thymic determinant of the balance between interferon-gamma- and interleukin 17-producing gammadelta T cell subsets. *Nat. Immunol.* **10,** 427–436 (2009).
16. Cattin, S. *et al.* Bevacizumab specifically decreases elevated levels of circulating KIT+CD11b+ cells and IL-10 in metastatic breast cancer patients. *Oncotarget* **7,** 11137–11150 (2016).
17. Zhu, S. & Qian, Y. IL-17/IL-17 receptor system in autoimmune disease: mechanisms and therapeutic potential. *Clinical Science* **122,** 487–511 (2012).
18. Mantovani, A. *et al.* The chemokine system in diverse forms of macrophage activation and polarization. *Trends Immunol.* **25,** 677–686 (2004).
19. Curtis, C. *et al.* The genomic and transcriptomic architecture of 2,000 breast tumours reveals novel subgroups. *Nature* **486,** 346–352 (2012).
20. van de Vijver, M. J. *et al.* A gene-expression signature as a predictor of survival in breast cancer. *N. Engl. J. Med.* **347,** 1999–2009 (2002).
21. Newman, A. M. *et al.* Robust enumeration of cell subsets from tissue expression profiles. *Nat. Methods* **12,** 453–457 (2015).
22. Gentles, A. J. *et al.* The prognostic landscape of genes and infiltrating immune cells across human cancers. *Nat. Med.* **21,** 938–945 (2015).
23. Templeton, A. J. *et al.* Prognostic role of neutrophil-to-lymphocyte ratio in solid tumors: a systematic review and meta-analysis. *J. Natl. Cancer Inst.* **106,** dju124 (2014).
24. Bald, T. *et al.* Ultraviolet-radiation-induced inflammation promotes angiotropism and metastasis in melanoma. *Nature* **507,** 109–113 (2014).
25. Wculek, S. K. & Malanchi, I. Neutrophils support lung colonization of metastasis-initiating breast cancer cells. *Nature* **528,** 413–417 (2015).
26. Tüting, T. & Visser, K. E. de. How neutrophils promote metastasis. *Science* **352,** 145–146 (2016).
27. Derksen, P. W. B. *et al.* Somatic inactivation of E-cadherin and p53 in mice leads to metastatic lobular mammary carcinoma through induction of anoikis resistance and angiogenesis. *Cancer Cell* **10,** 437–449 (2006).
28. Lu, X. & Kang, Y. Chemokine (C-C Motif) Ligand 2 engages CCR2+ stromal cells of monocytic origin to

promote breast cancer metastasis to lung and bone. *J. Biol. Chem.* **284,** 29087–29096 (2009).
29. Fridlender, Z. G. *et al.* Monocyte chemoattractant protein-1 blockade inhibits lung cancer tumor growth by altering macrophage phenotype and activating CD8+ cells. *Am. J. Respir. Cell Mol. Biol.* **44,** 230–237 (2011).
30. Qian, B.-Z. *et al.* CCL2 recruits inflammatory monocytes to facilitate breast-tumour metastasis. *Nature* **475,** 222–225 (2011).
31. Kudo-Saito, C., Shirako, H., Ohike, M., Tsukamoto, N. & Kawakami, Y. CCL2 is critical for immunosuppression to promote cancer metastasis. *Clin. Exp. Metastasis* **30,** 393–405 (2013).
32. Mitchem, J. B. *et al.* Targeting Tumor-Infiltrating Macrophages Decreases Tumor-Initiating Cells, Relieves Immunosuppression, and Improves Chemotherapeutic Responses. *Cancer Res.* **73,** 1128–1141 (2013).
33. Li, X. *et al.* Targeting of tumour-infiltrating macrophages via CCL2/CCR2 signalling as a therapeutic strategy against hepatocellular carcinoma. *Gut* (2015). doi:10.1136/gutjnl-2015-310514
34. Chun, E. *et al.* CCL2 promotes colorectal carcinogenesis by enhancing polymorphonuclear myeloid-derived suppressor cell population and function. *Cell Reports* **12,** 244–257 (2015).
35. Seo, S.-U. *et al.* Distinct commensals induce interleukin-1β via NLRP3 inflammasome in inflammatory monocytes to promote intestinal inflammation in response to injury. *Immunity* **42,** 744–755 (2015).
36. Penido, C. *et al.* Involvement of CC chemokines in gammadelta T lymphocyte trafficking during allergic inflammation: the role of CCL2/CCR2 pathway. *Int. Immunol.* **20,** 129–139 (2008).
37. Costa, M. F. de S. *et al.* Murine IL-17+ Vγ4 T lymphocytes accumulate in the lungs and play a protective role during severe sepsis. *BMC Immunol.* **16,** 36 (2015).
38. Akitsu, A. *et al.* IL-1 receptor antagonist-deficient mice develop autoimmune arthritis due to intrinsic activation of IL-17-producing CCR2(+)Vγ6(+)γδ T cells. *Nat Commun* **6,** 7464 (2015).
39. Granot, Z. *et al.* Tumor entrained neutrophils inhibit seeding in the premetastatic lung. *Cancer Cell* **20,** 300–314 (2011).
40. Lança, T. *et al.* Protective role of the inflammatory CCR2/CCL2 chemokine pathway through recruitment of type 1 cytotoxic γδ T lymphocytes to tumor beds. *J. Immunol.* **190,** 6673–6680 (2013).
41. Leek, R. D. *et al.* Association of macrophage infiltration with angiogenesis and prognosis in invasive breast carcinoma. *Cancer Res.* **56,** 4625–4629 (1996).
42. Ma, C. *et al.* Tumor-infiltrating γδ T lymphocytes predict clinical outcome in human breast cancer. *J. Immunol.* **189,** 5029–5036 (2012).
43. Noh, H., Eomm, M. & Han, A. Usefulness of pretreatment neutrophil to lymphocyte ratio in predicting disease-specific survival in breast cancer patients. *J Breast Cancer* **16,** 55–59 (2013).
44. Chen, W.-C. *et al.* Interleukin-17-producing cell infiltration in the breast cancer tumour microenvironment is a poor prognostic factor. *Histopathology* **63,** 225–233 (2013).
45. Jin, L. *et al.* Expression of interleukin-1beta in human breast carcinoma. *Cancer* **80,** 421–434 (1997).
46. Nywening, T. M. *et al.* Targeting tumour-associated macrophages with CCR2 inhibition in combination with FOLFIRINOX in patients with borderline resectable and locally advanced pancreatic cancer: a single-centre, open-label, dose-finding, non-randomised, phase 1b trial. *The Lancet Oncology* **17,** 651–662 (2016).
47. de Ronde, J. J. *et al.* SERPINA6, BEX1, AGTR1, SLC26A3, and LAPTM4B are markers of resistance to neoadjuvant chemotherapy in HER2-negative breast cancer. *Breast Cancer Res. Treat.* **137,** 213–223 (2013).
48. Girardi, M. *et al.* Regulation of cutaneous malignancy by gammadelta T cells. *Science* **294,** 605–609 (2001).
49. Wang, F. *et al.* RNAscope: a novel in situ RNA analysis platform for formalin-fixed, paraffin-embedded tissues. *J Mol Diagn* **14,** 22–29 (2012).
50. Ciampricotti, M., Hau, C.-S., Doornebal, C. W., Jonkers, J. & de Visser, K. E. Chemotherapy response of spontaneous mammary tumors is independent of the adaptive immune system. *Nat. Med.* **18,** 344–346 (2012).
51. Trapnell, C., Pachter, L. & Salzberg, S. L. TopHat: discovering splice junctions with RNA-Seq. *Bioinformatics* **25,** 1105–1111 (2009).
52. Anders, S., Pyl, P. T. & Huber, W. HTSeq--a Python framework to work with high-throughput sequencing data. *Bioinformatics* **31,** 166–169 (2015).
53. Love, M. I., Huber, W. & Anders, S. Moderated estimation of fold change and dispersion for RNA-seq data with DESeq2. *Genome Biol.* **15,** 550 (2014).
54. Leek, J. T., Johnson, W. E., Parker, H. S., Jaffe, A. E. & Storey, J. D. The sva package for removing batch effects and other unwanted variation in high-throughput experiments. *Bioinformatics* **28,** 882–883 (2012).

Supplementary Materials and methods

Patient material (continued)

For the RNAseq data, RNA was isolated from approximately thirty 30 µm cryosections. A 5 µm section halfway through the biopsy was stained for hematoxylin and eosin and analyzed by a pathologist for tumor percentage. Total RNA was isolated with RNA-Bee (Bio-Connect, cat no. CS-100B). Isolated total RNA was subsequently DNase-treated by using the Qiagen RNase-free DNase Set (Qiagen, cat no. 79254) and RNeasy spin columns (Qiagen, cat no. 74104) and dissolved in RNase-free H_2O.

Quality and quantity of the total RNA was assessed by the 2100 Bioanalyzer using a Nano chip (Agilent, Santa Clara, CA). Total RNA samples having RIN>6.4 were subjected to library generation. Illumina TruSeq mRNA libraries were generated using the TruSeq RNA Library Preparation Kit v2 sample preparation kit (Illumina Inc., San Diego, cat. no RS-122-2001/2) according to the manufacturer's instruction (Part # 15026495 Rev. B) Briefly, polyadenylated RNA from 1000 ng intact total RNA was purified using oligodT beads. Following purification the RNA was fragmented, random primed and reverse transcribed using SuperScript II Reverse Transcriptase (Invitrogen, part # 18064-014). Second strand synthesis was accomplished by using Polymerase I and RNaseH. The generated cDNA fragments were 3' end adenylated and ligated to Illumina single-end sequencing adapters and subsequently amplified by 15 cycles of PCR. The libraries were analyzed on a 2100 Bioanalyzer using a 7500 chip (Agilent, Santa Clara, CA), diluted and pooled equimolar into a 10 nM sequencing pool containing 9 libraries each. The libraries were then sequenced with 50 base single reads on a HiSeq2000 using V3 chemistry (Illumina Inc., San Diego).

After sequencing, reads were aligned to the human transcriptome (Homo_sapiens. GRCh37.75.gtf) using Tophat version 2.1 [51]. Read counts per gene were calculated using lcount which is based on HTSeq-count [52]. These countdata were normalized based on relative library size using DESeq2 version 1.8.2 [53]. RNAseq and microarray data were mean centred and subsequently combined using the sva R package [54]. All following analyses were done using R version 3.2.1.

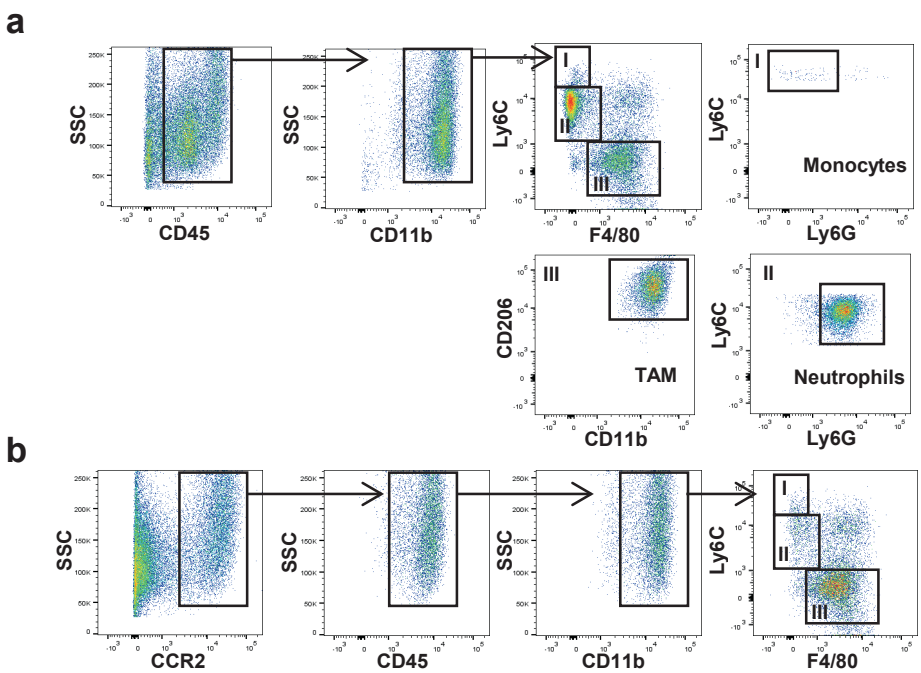

Supplementary Figure 1. Gating strategy to determine intratumoral CCR2$^+$ immune populations by flow cytometry. a) Gating strategy for the identification of tumor-infiltrating monocytes (I) (CD11b$^+$F4/80$^-$Ly6G$^-$Ly6C^{hi}), tumor-infiltrating neutrophils (II) (CD11b$^+$F4/80$^-$Ly6G$^+$Ly6C^{lo}) and TAMs (III) (CD11b$^+$F4/80$^+$CD206$^+$). b) Representative dot plots of CCR2$^+$ cells gated on total live cells in mammary tumors of KEP mice. All CCR2$^+$ cells were CD45$^+$CD11b$^+$ representing myeloid immune cells. The majority of these CCR2$^+$CD45$^+$CD11b$^+$ cells are macrophages (III) and a minority represent monocytes (I) and neutrophils (II) based on the markers used in a.

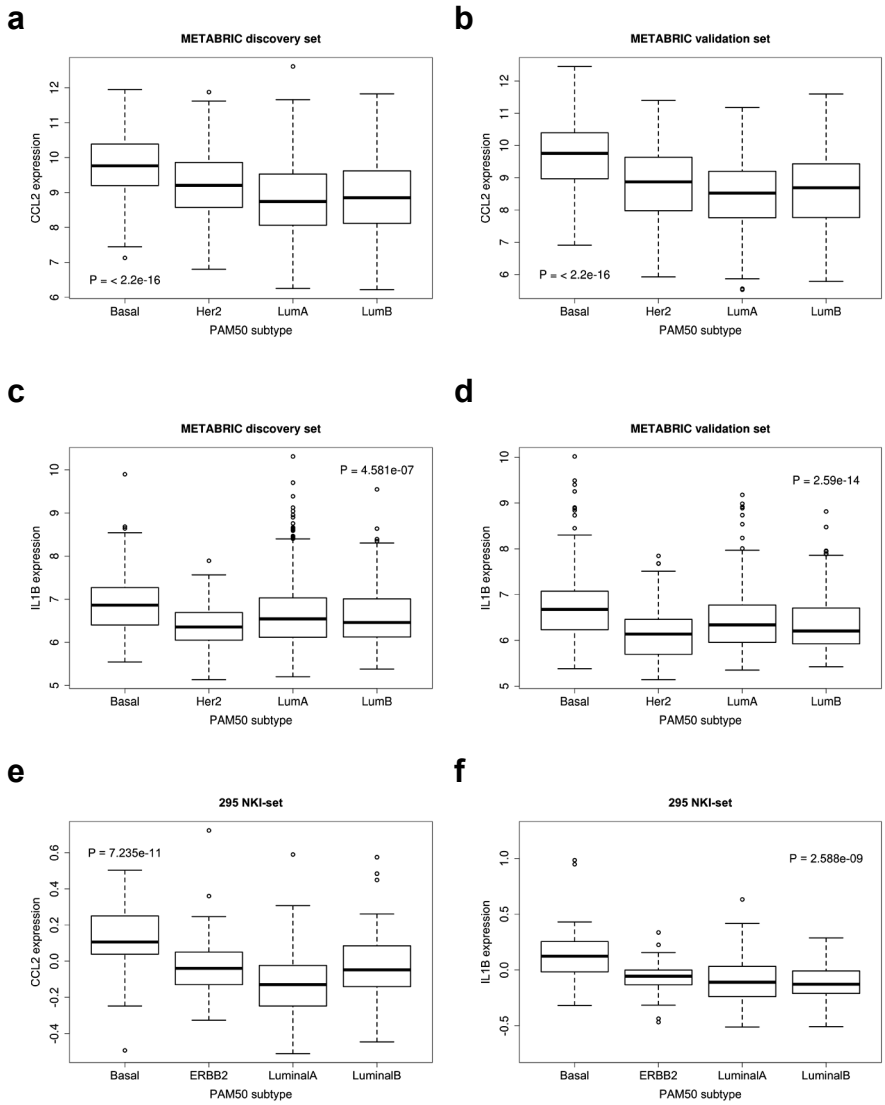

Supplementary Figure 2. *CCL2* and *IL1B* gene expression in human breast cancer subtypes and its correlation with intratumoral immune composition. a-d) Gene expression analysis of the METABRIC dataset. a-b) Discovery set (Basal n = 118; Her2 n = 87; LumA n = 466; LumB n = 268 patients): expression of *CCL2* is enriched in basal-like human breast cancer. c-d) Validation set (Basal n = 213; Her2 n = 153; LumA n = 255; LumB n = 224 patients): expression of *IL1B* is enriched in basal-like human breast cancer. e-f) Gene expression analysis of the 295 NKI dataset (Basal n = 46; ERBB2 n = 49; LumA n = 88; LumB n = 81 patients). Expression of *CCL2* (e) and *IL1B* (f) is enriched in basal-like human cancer. Statistical significance was determined by Kruskal-Wallis test.

-5-

Exploiting the immunomodulatory properties of chemotherapeutic drugs to improve the success of cancer immunotherapy

Kelly Kersten[1]*, Camilla Salvagno[1]*, Karin E. de Visser[1]

[1]Division of Immunology, Netherlands Cancer Institute, Amsterdam, The Netherlands

*These authors contributed equally to this work.

Frontiers in Immunology 6:516 (2015)

Abstract

Cancer immunotherapy is gaining momentum in the clinic. The current challenge is to understand why a proportion of cancer patients do not respond to cancer immunotherapy, and how this can be translated into the rational design of combinatorial cancer immunotherapy strategies aimed at maximizing success of immunotherapy. Here, we discuss how tumors orchestrate an immunosuppressive microenvironment, which contributes to their escape from immune attack. Relieving the immunosuppressive networks in cancer patients is an attractive strategy to extend the clinical success of cancer immunotherapy. Since the clinical availability of drugs specifically targeting immunosuppressive cells or mediators is still limited, an alternative strategy is to use conventional chemotherapy drugs with immunomodulatory properties to improve cancer immunotherapy. We summarize the preclinical and clinical studies that illustrate how the anti-tumor T cell response can be enhanced by chemotherapy-induced relief of immunosuppressive networks. Treatment strategies aimed at combining chemotherapy-induced relief of immunosuppression and T cell-boosting checkpoint inhibitors provide an attractive and clinically feasible approach to overcome intrinsic and acquired resistance to cancer immunotherapy, and to extend the clinical success of cancer immunotherapy.

Introduction

Cancer immunotherapy – harnessing the patient's immune system against cancer – is currently gaining momentum in the clinic. Clinical trials with immune checkpoint inhibitors show remarkable success in patients with advanced metastatic melanoma, non-small cell lung cancer, renal cancer, bladder cancer and Hodgkin's lymphoma [1–6]. As a result, the journal *Science* proclaimed cancer immunotherapy as the breakthrough of 2013 [7]. Furthermore, these encouraging results led to FDA approval of the immune checkpoint inhibitors ipilimumab (anti-CTLA-4), nivolumab and pembrolizumab (anti-PD-1) in the past few years. Although cancer immunotherapy was proclaimed a breakthrough, a significant proportion of cancer patients do not show clinical benefit. There are various cancer cell-intrinsic and cancer cell-extrinsic processes that regulate intrinsic or acquired resistance to cancer immunotherapy. Cancer cell-intrinsic characteristics like the mutational load have been reported to affect responsiveness to immunotherapy [8,9]. In terms of cancer cell-extrinsic processes, tumors exploit different strategies to induce immune escape by hampering the recruitment and activation of effector T cells, and by creating a local immunosuppressive environment through recruitment of suppressive myeloid and regulatory T cells that dampen T cell effector functions. Which of these immune escape mechanisms are active in a certain tumor depends on the tumor type, tumor stage and therapy history. A deeper understanding of the molecular mechanisms underlying these processes will contribute to the identification of biomarkers that can predict therapeutic efficacy of immunotherapy and to the design of combinatorial strategies aimed at maximizing the success of immunotherapy.

In this review, we discuss how tumor-induced immunosuppressive networks counteract efficacious anti-tumor immune responses, and how disruption of these networks can increase the anti-cancer efficacy of cancer immunotherapy with immune checkpoint inhibitors. Development and clinical testing of novel drugs specifically targeting immunosuppressive networks are ongoing and preliminary results are promising [10]. An alternative strategy to relieve tumor-induced immunosuppressive states is to use conventional, and more easily accessible, anti-cancer treatment strategies with known immunomodulatory properties, such as chemotherapy, radiotherapy and targeted therapy [11–15]. Here, we focus on the immunomodulatory properties of conventional chemotherapy, and how these properties can be exploited to improve the anti-cancer efficacy of immune checkpoint inhibitors.

Cancer immunotherapy: opportunities and challenges

Tumor-induced mechanisms of immune escape

Cancers do not merely consist of tumor cells, but comprise a variety of cell types that together form the tumor microenvironment (TME) (Fig. 1&2). Infiltrating immune cells are of special interest because of their paradoxical role in cancer progression. While some immune cell populations have pro-tumorigenic properties, others counteract

tumorigenesis [16–18]. Many tumors are characterized by an immunosuppressive TME, which makes it unfavorable for anti-tumor immunity. To mount effective anti-tumor immunity, tumor-associated antigens need to be sampled and processed by antigen-presenting cells (APCs). After receiving specific maturation signals, these APCs migrate to tumor-draining lymphoid organs where antigens are presented to T cells. Upon activation and proliferation, tumor antigen-specific T cells migrate to the tumor bed where they exert their cytotoxic function. At every step of this T cell priming and effector process, tumors employ strategies to hamper anti-cancer immunity.

Tumors often show dysfunctional recruitment and activation of dendritic cells (DCs), which are the most potent APCs for initiating immune responses. Several studies show that tumor-infiltrating DCs display an immature phenotype [19,20]. Tumor-derived factors like IL10, IL6, CSF1 and VEGF interfere with DC maturation, causing failure to migrate to the tumor-draining lymphoid organs, and to provide the appropriate co-stimulatory signals required to stimulate T cells [20]. Although a thorough analysis of the antigen-presenting myeloid immune cell compartment in the *MMTV-PyMT* mammary tumor model showed that intratumoral DCs are able to ingest and present tumor-antigens to T cells, they fail to activate them [21]. Nevertheless, even in these immunoevasive tumors, a rare population of IL12-expressing CD103$^+$ DCs exists that is able to prime tumor antigen-specific T cells [22]. Besides hampered T cell priming, the recruitment of activated T cells and their access into the tumor bed is often disrupted by the disorganized tumor vasculature and impaired expression of adhesion molecules on endothelial cells [23,24].

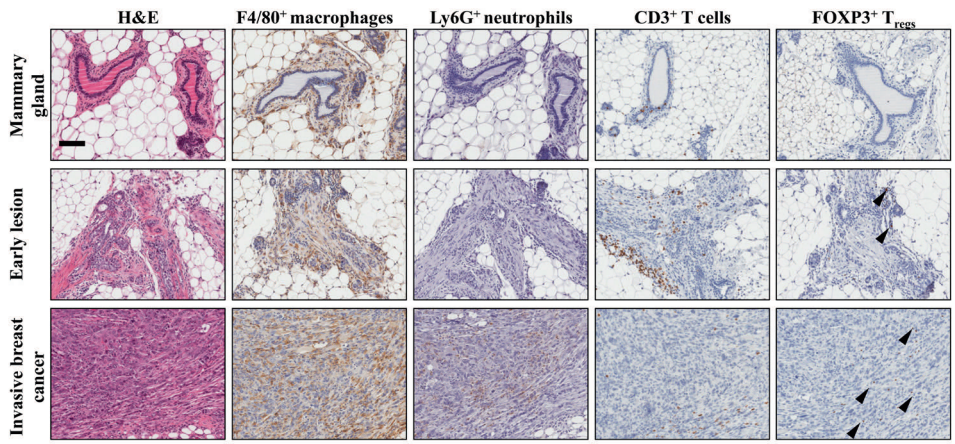

Figure 1. Establishment of the immune microenvironment during breast cancer progression in a conditional mouse model for mammary tumorigenesis. Female *K14Cre;Cdh1$^{F/F}$;Trp53$^{F/F}$* mice develop *de novo* invasive mammary tumors that closely resemble human invasive lobular carcinoma [183]. Immunohistochemical staining on mammary tissue from *K14Cre;Cdh1$^{F/F}$;Trp53$^{F/F}$* mice obtained during different stages of mammary tumor progression. From top to bottom are represented wild-type mammary gland (top), early lesion (middle), established mammary tumor (bottom). From left to right, identification of different immune cell populations by H&E, F4/80 (macrophages), Ly6G (neutrophils), CD3 (total T cells) and FOXP3 (regulatory T cells) staining showing the dynamics of the tumor microenvironment. Arrowheads indicate FOXP3$^+$ nuclei. Scale bar 100 µm.

Some studies suggest that tumor-derived chemokines may cause selective trapping of T cells in the tumor stroma preventing access into the tumor bed [25]. When tumor-specific T cells do succeed to reach the tumor, downregulation of MHC class I expression on tumor cells renders them invisible to T cell attack [26]. Additionally, T cells face systemic and local tumor-induced immunosuppression which limits their activation and function [27]. Tumor-associated immunosuppression can be caused by tumor-infiltrating or systemically expanded myeloid cells or regulatory T cells (T_{regs}) that – directly or indirectly via secretion of soluble mediators – hamper T cell priming and effector function or even induce T cell death [27]. These mechanisms will be discussed in more detail later.

Enhancing anti-tumor immunity by immune checkpoint inhibitors

To improve anti-tumor T cell immunity, different types of cancer immunotherapy approaches exist. While passive immunotherapy is based on adoptive transfer of (genetically engineered) autologous T cells, active immunotherapy boosts the endogenous immune response via cancer vaccines or inhibitors of immune checkpoints. The therapeutic effect of the latter is aimed at inhibition of negative immune regulatory pathways including cytotoxic T-lymphocyte-associated protein-4 (CTLA-4) and the programmed cell death protein-1 (PD-1) receptor and one of its ligands, PD-L1 (B7-H1; CD274) [28]. CTLA-4 is a member of the CD28 immunoglobulin superfamily and is expressed mainly on the surface of activated $CD4^+$ T cells and T_{regs}, while absent on naïve T cells[29]. CTLA-4 plays a central role in maintaining immune tolerance by competing with CD28 to bind the ligands CD80 and CD86 present on activated APCs to inhibit T cell co-stimulation. The PD-1/PD-L1 axis shows similarities to that of CTLA-4. PD-1 is mainly expressed on activated T cells upon TCR engagement and on T_{regs}, while naïve and memory T cells do not usually express this surface marker. Recent studies suggest that PD-1, rather than being a marker of activated T cells, identifies exhausted T cells [30].

PD-L1 is expressed on multiple cell types whereas expression of PD-L2 (B7-DC; CD273) seems to be restricted to APCs [31,32]. Like CTLA-4, binding of PD-L1/PD-L2 to its receptor results in an inhibitory signal that prevents T cell activation. While CTLA-4 blockade is hypothesized to act mainly in secondary lymphoid organs during the T cell priming phase, it is believed that blockade of PD-1 or PD-L1 targets the TME during the T cell effector phase [33]. However, PD-1 can also play a role in the early T cell response as a regulator of $CD8^+$ T cell expansion upon antigen recognition [34]. In addition to its role in T cell priming, CTLA-4 also regulates the suppressive function of tumor-infiltrating T_{regs} [35,36]. In line with this, blockade of CTLA-4 in the B16 melanoma model acts locally in the TME by inactivating T_{regs} in a Fc-dependent manner resulting in a favorable shift in the effector T cell/T_{reg} ratio [37]. The exact mechanisms of action of anti-CTLA-4 and anti-PD-1/PD-L1 are not completely clear. Just recently, the combination of anti-CTLA-4 and anti-PD-1 was reported to significantly increase the fraction of melanoma patients responding to immunotherapy compared to anti-CTLA-4 monotherapy-treated patients [38], emphasizing the different modes of action of CTLA-4 and PD-1.

The rational of using CTLA-4 blockade in cancer therapy is to release the brake on pre-existing tumor-reactive T cells and to generate new T cell responses. Ipilimumab (anti-CTLA-4) was the first immune checkpoint inhibitor that yielded a significant increase in survival of patients with metastatic melanoma, for which all conventional therapeutic options had failed [1]. Interestingly, a broadening of the tumor-reactive T cell repertoire was reported upon ipilimumab treatment [39]. In a second clinical study, ipilimumab was combined with dacarbazine in metastatic melanoma patients resulting in prolonged survival compared to dacarbazine alone [40]. In both studies a fraction of patients showed long term durable responses [41]. Similarly, clinical trials with anti-PD-1 have shown tumor regression in a substantial fraction of cancer patients [3]. These initial results lead to an immense increase in clinical trials with drugs targeting the PD-1/PD-L1 axis in different cancer types, and many report anti-tumor efficacy [3–6,42]. Recent clinical observations show that the combination of anti-CTLA-4 and anti-PD-1 is more effective than either monotherapy [38]. Although very successful and promising, a significant proportion of cancer patients do not show long-term benefit of immune checkpoint inhibitors. Therefore, it is of utmost importance to mechanistically understand intrinsic and acquired resistance to cancer immune checkpoint inhibitors, in order to identify biomarkers that can be used to pre-select those patients that will or will not benefit from cancer immunotherapy and to develop therapeutic strategies to overcome or bypass resistance mechanisms.

What are the requirements for therapeutic response to checkpoint inhibitors?

To predict the response to immunotherapy per patient and tumor type, several variables should be taken into account. For successful activation of a T cell-mediated anti-tumor immune response, T cells need to 'see' the cancer cells with their T cell receptor (TCR). In general, there are three classes of tumor-antigens that can potentially be recognized by T cells: viral antigens, self-antigens and neo-antigens. Our T cell repertoire is basically built to recognize and respond to viral antigens, because these antigens are perceived as foreign or non-self. However, only a subset of established human cancers expresses viral antigens. During the T cell maturation process, thymic selection eliminates maturing lymphocytes that display a high avidity for self-antigens. As a consequence, only low-avidity self-specific T cells can be found in the peripheral T cell repertoire, which may not be ideal for cancer immunotherapy. Non-synonymous somatic mutations can give rise to neo-antigens towards which no central T cell tolerance is present. Recently, neo-antigen specific T cell responses have been reported in melanoma patients [43–45], indicating that these mutations can be recognized by T cells and induce tumor-specific T cell responses. In line with this, the number of predicted neo-antigens is linked with a metric for immune cytolytic activity based on gene expression in a large panel of cancer types [46]. Thus, the extent of the mutational load of a certain tumor would serve – albeit at a low resolution – as a predictor of response to cancer immunotherapy. Indeed, a growing body of data supports this hypothesis [47]. Whole-exome sequencing analyses revealed that melanoma and lung cancer – the two cancer types that show promising

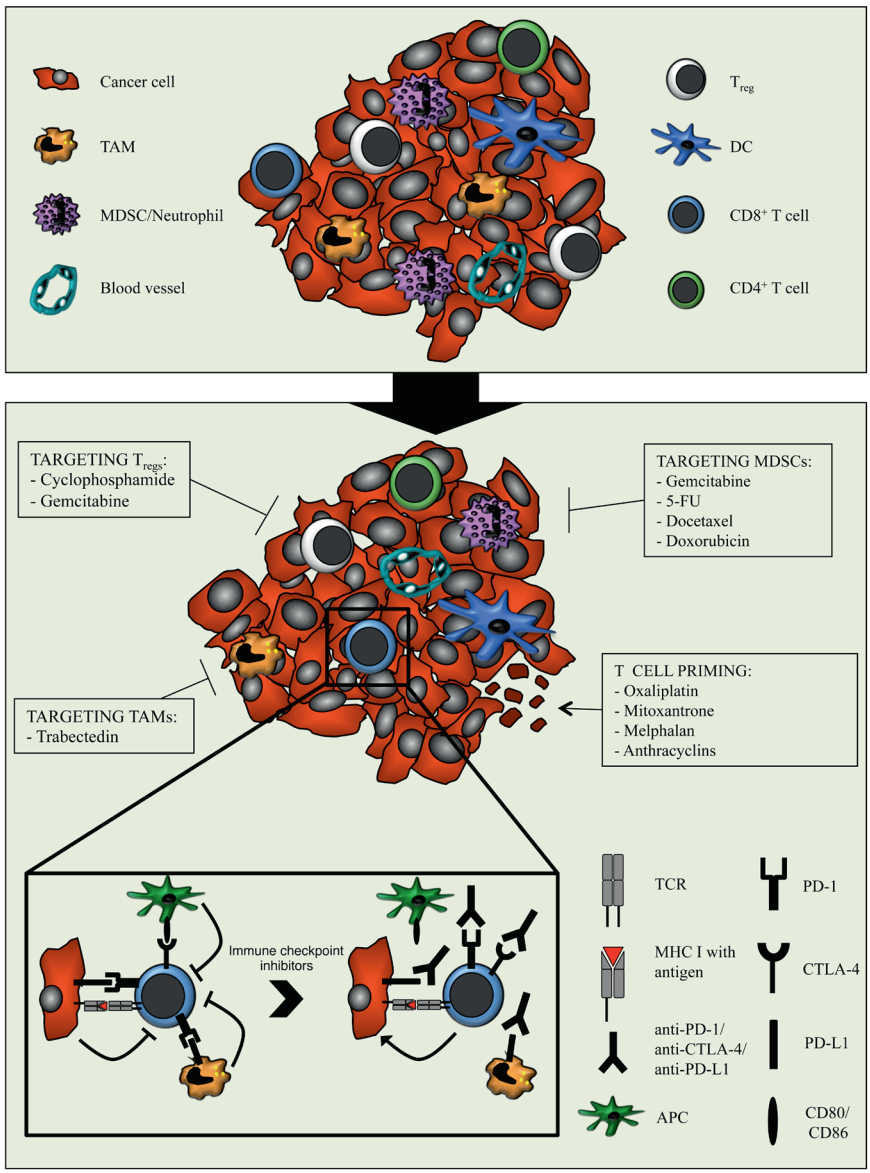

Figure 2. Combination strategies aimed at relieving the immunosuppressive tumor microenvironment with chemotherapy and potentiating cytotoxic T cells with immune checkpoint inhibitors. The tumor microenvironment is characterized by the presence of various immune cell types, including different subsets of adaptive immune cells and TAMs, MDSCs and T_{regs}. The latter dampen the anti-cancer activity of T cells through several mechanisms. Moreover, cancer cells and myeloid cells express PD-L1/PD-L2 and APCs express CD80/CD86. Binding of these molecules to PD-1 and CTLA-4 respectively, expressed on T cells, results in inhibitory signals that counteract T cell activation and function. The immunomodulatory properties of different types of chemotherapeutic drugs can be exploited to enhance anti-tumor immunity. By optimally matching the immunomodulatory features of specific chemotherapeutic drugs with the T cell-boosting effect of immune checkpoint inhibitors, the efficacy of immunotherapy might be improved.

responses to immunotherapy – bear relatively high mutational loads compared to other types of cancer, due to their exposure to DNA damaging insults like UV radiation and tobacco smoke, respectively [48]. Recent studies uncovered that a high mutational load is associated with long-term clinical benefit to checkpoint inhibitors [8,9]. However, not all cancer patients with tumors bearing a high mutational load respond to checkpoint inhibitors, and some patients bearing tumors with low mutational load do [8,9]. Together, these results suggest that the mutational load of tumors is correlated with response to immune checkpoint inhibitors, but it cannot solely be used to predict response.

A growing body of clinical observations suggests that the intratumoral presence of pre-existing T cells is required for clinical benefit of immunotherapy [49]. PD-1 expression on tumor-infiltrating $CD8^+$ T cells has been suggested to identify the repertoire of clonally expanded tumor-reactive T cells [50]. In addition, T cell infiltration correlates with PD-L1 expression in tumors and is associated with increased responsiveness to drugs targeting the PD-1/PD-L1 axis in melanoma patients [49,51,52]. Expression of PD-L1 in tumors is one of the main characteristics pursued as a potential biomarker for response to PD-1/PD-L1 blockade. However, there are examples of tumors with high expression of PD-L1 that do not respond to PD-1 blockade, and PD-L1 negative tumors that do respond [52]. Why certain tumors express PD-L1 and others do not remains to be elucidated.

Interestingly, expression of PD-L1 and responsiveness to immune checkpoint blockade is associated with genomic instability in different tumor types [53]. Patients bearing mismatch-repair deficient colorectal cancer (CRC) respond better to anti-PD-1 therapy than mismatch-repair proficient CRC patients [53]. In line with this, a microsatellite instable (MSI) subset of CRC patients shows high T cell influx [54]. However, this is counterbalanced by simultaneous upregulation of checkpoint molecules including PD-1, PD-L1 and CTLA-4 leaving T cells dysfunctional [54]. Moreover, in breast cancer, the expression of PD-L1 is correlated with TIL infiltration, and is mostly prevalent in basal-like, hormone-receptor-negative and triple-negative tumors [55,56]. Furthermore, in glioma patients increased expression of PD-L1 in tumors was correlated with PTEN loss [57], suggesting that patients bearing genetically unstable cancer types might benefit from treatment with checkpoint inhibitors. Intriguingly, not only cancer cells, but also tumor-infiltrating myeloid cells express PD-L1, and counteract anti-tumor immunity in ovarian carcinoma and MSI-CRC [54,58]. Actually, PD-L1 expression on tumor-infiltrating immune cells has been suggested to be a better predictor of clinical response to anti-PD-L1 therapy than PD-L1 expression on cancer cells [51]. It will be interesting to explore which other cancer types are characterized by the influx of PD-L1-expressing myeloid cells.

In conclusion, to increase the efficacy of immunotherapy in different types of cancer, we could consider manipulating the many variables that determine intrinsic and acquired resistance. While altering cancer cell-intrinsic characteristics, such as mutational load or genomic instability, might be challenging, cancer cell-extrinsic characteristics, like an immunosuppressive TME, are easier to manipulate.

Evasion from cancer immunotherapy: relieving immunosuppression as an attractive strategy to improve the efficacy of immune checkpoint blockade

Established tumors are characterized by an abundant influx of a variety of immune cells with immunosuppressive activity, including T_{regs}, myeloid-derived suppressor cells (MDSCs) and tumor-associated macrophages (TAMs) (Fig. 1&2). There is accumulating evidence that interference with these immunosuppressive networks can improve anti-tumor immunity. Here, we discuss the different types of immunosuppressive immune cells present in the TME, and how blockade or reprogramming of these cells or their downstream effects can enhance anti-tumor immunity and the efficacy of immune checkpoint blockade.

Regulatory T cells

T_{regs} play an important role in maintaining homeostasis during infections and in preventing the development of autoimmune diseases by blocking proliferation and cytotoxic activity of effector T cells. The history of T_{regs} goes back to the 1970s, when it was discovered that a subpopulation of thymocytes induced tolerance to certain antigens in mice [59]. A turning point in the research of these 'suppressor cells' came in 1995. T_{regs}, phenotyped as $CD4^+CD25^+$ cells, were shown to be important for self-tolerance in mice, as inoculation of $CD4^+$ cells depleted of $CD4^+CD25^+$ cells resulted in autoimmunity in nude mice [60]. Another big step forward in the characterization of T_{regs} was the identification of FOXP3, a member of the fork-head/winged-helix family of transcription factors and a key regulator of T_{reg} development and function [61]. In the following years the knowledge of T_{regs} expanded enormously. Two subpopulations of T_{regs} were identified: natural T_{regs} and induced T_{regs} (or adaptive T_{regs}), which are formed in the thymus and in the periphery, respectively. Regardless of their origin, both natural and induced T_{regs} inhibit effector T cells [62].

In 1980, it was hypothesized that a T cell population in tumors suppresses anti-tumor immune responses [63]. Indeed, many experimental studies support the notion that tumor-associated T_{regs} contribute to immune escape via suppression of anti-tumor $CD8^+$ T cells. For example, elimination of T_{regs} in MO4 melanoma cell line-bearing mice results in T cell-dependent tumor rejection [64]. Moreover, in a xenotransplant model for $HER2^+$ ovarian cancer, adoptive transfer of autologous $CD3^+CD25^-$ T cells and dendritic cells loaded with $HER2^+$ antigen results in T cell-mediated tumor regression, whereas concomitant transfer of T_{regs} blocks this antigen-specific immune response [65]. T_{regs} not only suppress $CD8^+$ T cells, but also $CD4^+$ T cells, NK, NKT and B cells [66]. T_{regs} exert their immunosuppressive function either by direct suppression of effector cells, or indirectly by affecting the activation state of APCs. Importantly, in order to exert their functions, T_{regs} need to be activated via their TCR, but once activated their suppressive function is non-specific [67,68]. The direct T cell-suppressive functions are mediated by release of cytokines, serine proteases and the expression of enzymes that catabolize ATP. For

example, T_{regs} inhibit T cells via secretion of cytokines like TGFβ, IL10 and IL35 [69–71] or even induce T cell apoptosis by the release of granzyme B (GRZMB) or perforin [72–74]. In addition, T_{regs} express CD39 and CD73, two ectoenzymes that generate the immunosuppressive molecule adenosine from extracellular ATP [75]. It has been shown that T_{regs} from CD39 knock out mice fail to inhibit $CD4^+CD25^-$ cell proliferation [75]. Finally, CTLA-4^+ T_{regs} can indirectly impair T cells by reducing the CD80/CD86 levels on APCs [35].

Supporting these data, increased numbers of intratumoral T_{regs} correlate with worse overall survival in patients with ovarian cancer, breast cancer, gastric cancer and hepatocellular carcinoma [65,76–80]. Interestingly, this is not true for CRC in which a high number of $CD8^+$ cells and $FOXP3^+$ cells correlates with a good prognosis [81]. This may be explained by the fact that T_{regs} in CRC attenuate inflammation against gut microbiota that would otherwise enhance tumor growth [81]. These findings illustrate that the tumor context dictates the function of associated immune cells. Although strategies targeting CD25 (like the neutralizing monoclonal antibody daclizumab and the recombinant interleukin 2/diphtheria toxin conjugate Ontak) showed transient depletion of peripheral T_{regs} and increased activity of $CD8^+$ T cells, these approaches only result in a modest clinical benefit in cancer patients [82,83]. This might be explained by the fact that CD25 is also expressed on active effector T cells, so the lack of specificity for T_{regs} might complicate their clinical applicability. Therefore, a mechanistic understanding of the role of T_{regs} in different tumor contexts will be important for the design of therapeutic strategies aimed at suppressing the downstream effects of T_{regs}.

Myeloid-derived suppressor cells

The first report describing the existence of MDSCs showed that bone marrow-derived cells were able to suppress the killing activity of splenocytes *in vitro* [84]. These cells were called 'natural suppressor cells' or 'null cells' because they did not express markers of B, T or NK cells or macrophages [85]. Subsequently, these cells were found to expand in inflammatory conditions and in tumor-bearing hosts [84,86]. In tumor-bearing mice, tumor-derived growth factors trigger the accumulation of T cell suppressive myeloid cells in the bone marrow and spleen [86,87]. The identification of these cells was hampered by the lack of clear markers, which caused variation in terminology and ambiguity among researchers. In order to bring some clarity into the field, Gabrilovich and colleagues published a consensus paper in 2007 in which they coined the term 'MDSC' to refer to a heterogeneous population of myeloid cells with the ability to suppress T cell activity [88]. MDSCs consist of a group of immature and mature myeloid cells that are defined by their immunosuppressive function. Within the MDSC population, two subpopulations can be distinguished based on the expression of Ly6G and Ly6C: $Ly6C^{high}Ly6G^-$ monocytic-MDSC and $Ly6C^{low}Ly6G^+$ granulocytic-MDSC. In humans, MDSCs are defined as $CD11b^+CD33^+HLA\text{-}DR^-Lin^-$ cells with the addition of CD14 or CD15 to discriminate between monocytic- or granulocytic-MDSCs, respectively [89].

In patients with various cancer types, including melanoma, gastric, breast and CRC, increased numbers of MDSCs in the circulation correlate with poor survival [90–92].

Numerous cytokines have been implicated in the expansion of MDSCs during cancer progression, including G-CSF, GM-CSF and stem-cell factor (SCF or KIT ligand) [93–95].

MDSCs exert their immunosuppressive function by different mechanisms, one of which is the consumption of essential amino acids from the environment. MDSCs frequently express high levels of arginase I which catabolizes arginine, thereby depriving T cells from arginine which is essential for their metabolism and function [96,97]. L-arginine is also the substrate of another enzyme highly expressed in MDSCs, called iNOS. The release of reactive oxygen species (ROS) and nitric oxide (NO) by iNOS can lead to the inhibition of MHC class II expression on APCs causing impaired antigen presentation to $CD4^+$ T cells [98]. Moreover, NO can cause apoptosis of $CD8^+$ T cells [99]. Another amino acid is tryptophan, whose breakdown by the enzyme IDO suppresses T cell proliferation. MDSCs isolated from human breast cancer tissues inhibit T cell proliferation and induce T cell apoptosis in an IDO-dependent manner [100]. Moreover, IDO inhibitors enhance the therapeutic efficacy of anti-CTLA-4 treatment leading to intratumoral accumulation of T cells and improved survival in the B16 melanoma model [101]. Additionally, the amino acid cysteine is also important for T cell activation and function. T cells depend on other cells (macrophages and DCs) for cysteine metabolism. MDSCs internalize cystine (formed of two cysteines linked via a disulfide bond), catabolize it to cysteine and, unlike macrophages and DCs, do not release it into the environment. Therefore, MDSCs limit the amount of cystine that macrophages and DCs can metabolize to activate T cells [102]. Finally, MDSCs contribute to an immunosuppressive TME by inducing the development of T_{regs} in tumor-bearing mice, as adoptive transfer of MDSCs and $CD4^+$ T cells in MCA26 colon carcinoma cell line-bearing irradiated mice, induces expression of FOXP3 in transferred T cells [103]. Thus, these data suggest that MDSCs play an important role in creating an immunosuppressive network in tumors, supporting the idea that reprogramming or depletion of MDSCs could benefit immunotherapy strategies. Strategies to inhibit MDSCs include blocking their development or recruitment, targeting their immunosuppressive molecules or depleting them.

Tumor-induced neutrophils

In various cancer patients, a high neutrophil to T lymphocyte ratio in blood is associated with poor disease outcome [104,105]. Recent studies have reported that neutrophils also expand in experimental mouse tumor models, and that they exert immunosuppressive activity. A distinguishing feature of murine neutrophils is the expression of Ly6G, a surface marker shared with granulocytic-MDSC. When the T cell suppressive ability of neutrophils is confirmed, they can be categorized into the granulocytic-MDSC population [106]. We recently showed in a mouse model for *de novo* breast cancer metastasis that neutrophils have a pro-metastatic phenotype and exert their function through suppression of $CD8^+$ T cells. While depletion of $Ly6G^+$ neutrophils results in decreased multi-organ metastasis, double depletion of neutrophils and $CD8^+$ T cells reverses this phenotype [107]. In line with this, chemotherapy-induced neutropenia correlates with improved overall survival in breast cancer patients [108]. The metastasis-promoting role of neutrophils has also been

demonstrated in UV-induced melanoma and in tumor inoculation models [109,110]. It would be interesting to study whether – as in the experimental tumor models – T cells in neutropenic cancer patients are more active. Interestingly, in 4T1-tumor-bearing mice, neutrophils inhibit the seeding of metastatic cells in the lung by the release of hydrogen peroxide [111]. These data indicate a controversial role of neutrophils in metastasis that might be explained by the differences in tumor subtype or tumor model.

We and others have shown that T cell-suppressive neutrophils accumulate systemically during cancer progression in a G-CSF-dependent fashion [107,112]. In the transgenic *MMTV-PyMT* mammary tumor mouse model, tumor-derived G-CSF skews hematopoietic cell differentiation towards the granulocytic lineage in the bone marrow, resulting in increased numbers of immunosuppressive neutrophils in the circulation [112]. In 4T1 mammary tumor-bearing mice, TGFβ polarizes mature neutrophils from cytotoxic anti-tumor activity towards pro-tumor immature immunosuppressive neutrophils [113]. This is in line with previous findings identifying TGFβ as one of the drivers of pro-tumor polarized neutrophils [114]. As such, it is tempting to speculate that for those tumors characterized by pro-metastatic neutrophils, inhibition of these cells – either by targeting upstream or downstream molecules – may be an interesting strategy for therapeutic intervention, in particular when combined with cancer immunotherapy.

Tumor-associated macrophages

Macrophages are frequently the most predominant immune cell type in tumors. In the past, macrophages were subdivided into classically activated macrophages (M1) exerting microbicidal and anti-tumor activity, or alternatively activated macrophages (M2) exerting pro-tumoral, immunosuppressive and tissue repair functions [115,116]. TAMs are frequently classified as M2 macrophages. However, there is a growing realization that this black and white distinction of macrophage subsets is too simplistic and does not accurately reflect the heterogeneity, plasticity and versatility of macrophages [117]. Transcriptome and bioinformatic analyses of cultured macrophages exposed to different stimuli revealed a spectrum of activation programs for each stimulus that goes beyond the M1 and M2 model [118]. Based on these data, it is to be expected that TAMs will also change their phenotype and function according to the cytokine milieu present in a specific tumor type. In the vast majority of cancers, high intratumoral macrophage density correlates with poor prognosis [119,120]. However, macrophages in CRC are associated with good prognosis, and in other types of cancers, like prostate and lung cancer, their role is still controversial [121]. Depletion of macrophages by genetic ablation of CSF-1 in the *MMTV-PyMT* mammary tumor model reduces metastasis formation without affecting primary tumor growth [122]. Likewise, several other experimental studies have reported a pro-metastatic role of macrophages [123,124]. TAMs produce a variety of factors that foster tumor growth and invasiveness, angiogenesis and immunosuppression [119,123,125].

TAMs exert their immunosuppressive activity in a similar fashion as MDSCs. TAMs can express various enzymes like arginase 1, IDO [126–128], and cytokines like IL10 [129]. Another mechanism by which TAMs suppress T cells is the upregulation of PD-L1. In hepatocellular

carcinoma, high density of peritumoral macrophages that express PD-L1$^+$ correlates with worse overall survival [130]. Co-culture experiments showed that PD-L1$^+$ macrophages suppress T cell activity unless anti-PD-L1 antibody is added in the culture [130]. Based on these immunosuppressive properties, it is tempting to speculate that interference with TAMs will unleash anti-tumor immunity. Indeed, this idea has recently been supported by experimental studies in mouse models for glioblastoma and pancreatic cancer showing that CSF-1/CSF-1R pathway blockade can shift TAM polarization towards an anti-tumor phenotype, resulting in enhanced CD8$^+$ T cell-mediated anti-tumor immunity [131,132]. Similarly, targeting the CCL2/CCR2 chemokine pathway – involved in recruitment of monocytes and macrophages – relieves the immunosuppressive phenotype of TAMs and enhances anti-tumor CD8$^+$ T cell responses [133,134]. Based on these encouraging results, clinical trials are ongoing in which compounds targeting TAMs are being tested in cancer patients. Preliminary results of a clinical trial with anti-CSF-1R in patients with various types of solid malignancies showed a decrease in TAMs and an increase in intratumoral CD8/CD4 ratio [10].

Blocking the suppressors to release anti-tumor T cells

As discussed above many immunosuppressive cells and mediators can be identified in the TME that dampen anti-tumor T cell responses and may contribute to immune escape upon cancer immunotherapy. The combination of compounds that relieve immunosuppression with T cell-boosting therapy seems attractive to overcome immune tolerance towards the tumor.

T_{regs} seem to be interesting targets, since, as discussed earlier in this review, these cells suppress the functionality of CD4$^+$ and CD8$^+$ effector cells. In line with this, in the transgenic TRAMP prostate cancer model – engineered to express prostate specific antigen (PSA) – T_{reg}-depletion enhances IFNγ production by PSA-specific CD8$^+$ T cells [135]. This augmented effect of anti-tumor immunity is further enhanced by CTLA-4 blockade, and results in delayed tumor growth. Interestingly, the same experiments performed in the parental TRAMP model show only a modest activation of PSA-specific T cells upon anti-CD25 and anti-CTLA-4, and no survival benefit, suggesting the requirement of a tumor-specific antigen for this anti-tumor response [135]. In the ID8 ovarian cancer model, tumor-infiltrating T_{regs} – which express both CTLA-4 and PD-1 – are reduced upon CTLA-4 and PD-1 dual blockade coinciding with increased tumor-infiltrating CD8$^+$ T cells [136]. However, additional depletion of T_{regs} does not further enhance this effect. In the same model, blockade of PD-L1, expressed on tumor cells and tumor-infiltrating immune cells, reduces the number of MDSCs and T_{regs} and enhances the frequency of effector T cells, resulting in prolonged survival [137]. Furthermore, in a mouse model for rhabdomyosarcoma, PD-1 blockade increases the numbers of tumor-infiltrating CD8$^+$ T cells, but does not change their activation status. Upon interference with the chemokine receptor CXCR2, which prevents MDSC trafficking into the tumor, enhanced activation of CD8$^+$ T cells is observed [138]. Blockade of CXCR2 improves the therapeutic efficacy of anti-PD-1 treatment resulting in a significant survival benefit [138]. Moreover, in a mouse

model of pancreatic ductal adenocarcinoma, blockade of CSF-1/CSF-1R signaling results in macrophage reprogramming to support anti-tumor immune function and modestly delays tumor growth [132]. TAMs obtained from anti-CSF1 treated mice are impaired in suppressing $CD8^+$ T cell proliferation compared to control TAMs. The induction of CTLA-4 expression on $CD8^+$ T cells and PD-L1 expression on tumor cells suggests the onset of acquired resistance to effective anti-tumor immune responses. Combining anti-CTLA-4 and anti-PD-1 with a CSF-1R inhibitor shows profound synergy with a significant reduction in tumor burden [132]. Thus, together these results indicate that alleviation of immunosuppression reactivates anti-tumor immunity, which can be further enhanced by checkpoint inhibition.

Immunomodulatory properties of chemotherapeutic drugs

Although various novel compounds targeting tumor-associated myeloid cells and their immunosuppressive mediators are being developed and tested, their clinical availability is still limited. An alternative and clinically available strategy is to relieve immunosuppression by exploiting the immunomodulatory effects of conventional anti-cancer strategies like chemotherapy (Fig. 2). The impact of chemotherapeutic drugs on the proportion and phenotypic and functional characteristics of immune cells is to a great extend dictated by the type of drug and the dosing scheme: while high dose chemotherapy usually results in lympho- or myelodepletion, low dose (metronomic) treatment has more subtle anti-angiogenic and immunomodulatory effects depending [139,140]. In this section we discuss the effects of chemotherapy on the immunosuppressive TME.

The impact of chemotherapy on T cell priming

Optimal T cell priming is dependent on antigen processing, presentation and co-stimulation by properly matured and activated DCs. As discussed, impaired DC function and T cell priming are important mechanisms of immune escape by tumors. Certain chemotherapeutics induce anti-cancer immune responses by improving the recruitment and functionality of intratumoral DCs [141,142]. For example, low dose cyclophosphamide promotes DC maturation [143]. Besides the enhanced release of tumor-antigens through induction of cancer cell death, chemotherapeutics, including oxaliplatin, doxorubicin, mitoxantrone and melphalan, induce HMGB1 release and calreticulin translocation in cancer cells, facilitating antigen uptake by DCs and subsequent T cell stimulation [144–146]. In addition, in the MCA205 fibrosarcoma model, anthracyclins induce the differentiation of myeloid cells in the tumor bed towards a DC-like phenotype in an ATP-dependent manner [141]. In these relatively high immunogenic tumor models, the activated T cells subsequently enhance the anti-cancer efficacy of chemotherapy [141,142,144].

In less immunogenic models, such as *de novo* tumorigenesis models, an important role for T cells in chemotherapy efficacy is lacking [119,147,148]. One possible explanation is that spontaneously arising tumors are characterized by local and systemic immunosuppression, which may overrule any chemotherapy-induced T cell responses.

Indeed, in the *MMTV-PyMT* mammary tumor model, TAM-derived IL10 indirectly blocks anti-tumor $CD8^+$ T cell activity by suppressing IL12 expression by intratumoral DCs upon paclitaxel treatment [148]. These results apply to human breast cancer patients, since low $CD68^+$ macrophage over $CD8^+$ T cell ratio prior to neo-adjuvant chemotherapy correlates with a better pathologic response [119]. Moreover, high levels of *IL12A* mRNA in human breast cancer samples correlates with expression of DC-related transcription factors and *GRZMB*, *CD8A* and *IFNγ* expression, suggesting an active anti-tumor T cell response [148]. However, the role of TAMs and their potential suppressive function in cancer patients was not evaluated. Together, these results suggest that therapeutic targeting of TAMs could enhance the functionality of intratumoral DCs and anti-tumor T cell responses in chemotherapy treatment.

Impact of chemotherapy on T_{regs}

With the knowledge that T_{regs} play an important role in suppressing effector T cell responses, a lot of effort has been put into the identification of chemotherapeutic drugs that target these cells. The best studied is cyclophosphamide, an alkylating agent which crosslinks DNA, thus interfering with replication. Cyclophosphamide is known for its dose-dependent effect on the immune system. High doses of cyclophosphamide result in immunosuppression by reducing T cell proliferation and inducing apoptosis, thus making it useful for the prevention of graft-versus host disease or rejection of transplanted organs [149,150]. In contrast, low doses selectively ablate T_{regs} and dampen their T cell suppressive ability [151]. While the anti-tumor effect of high dose cyclophosphamide is mainly due to its cytotoxic activity against cancer cells, the anti-tumor effect of low dose cyclophosphamide depends on its immune-modulatory effects [152]. Indeed, studies in T cell-deficient mice bearing inoculated tumors show loss of the anti-cancer activity of low dose cyclophosphamide [152,153]. Moreover, reinfusion of $CD4^+CD25^+$ T cells in tumor-bearing mice, pre-treated with low dose cyclophosphamide, abrogated the anti-tumor effect of the drug, emphasizing that T_{regs} counteract the therapeutic efficacy of the drug [152]. In line with this, patients with different types of metastasized solid tumors receiving low dose metronomic cyclophosphamide show a specific decrease of T_{regs} in the periphery with concomitant enhancement of NK lytic activity and T cell proliferation [154]. In cancer patients receiving higher doses of metronomic cyclophosphamide, all lymphocyte populations were depleted, emphasizing the importance of accurate drug dosing to achieve selective T_{reg} depletion [154]. It has been proposed that the increased sensitivity of T_{regs} for cyclophosphamide is linked to their low ATP levels. Low levels of ATP result in decreased synthesis of glutathione, which is important for cyclophosphamide detoxification [155] .

Another chemotherapeutic drug affecting T_{regs} is gemcitabine, a nucleoside analog interfering with DNA replication. In an orthotopic pancreatic cancer model, gemcitabine reduces the percentage of T_{regs} in the tumor resulting in a small but significant survival benefit [156]. Whether this also results in improved $CD8^+$ and $CD4^+$ T cell activity remains unknown. A study performed in cancer patients showed that the percentage of T_{regs} in

blood was decreased after gemcitabine treatment [157]. Among the $CD4^+$ cells, T_{regs} were identified as the most proliferative cells, which may explain the selectivity of gemcitabine for these cells. However, the effect of gemcitabine on other T cell populations was not assessed in this study [157]. Also other (combinations of) chemotherapy drugs have been reported to influence the presence or function of T_{regs} [158,159].

Chemotherapeutics with inhibitory activity towards tumor-associated myeloid cells
Several chemotherapy drugs have been implicated in the selective reduction of MDSCs in the tumor and spleen of tumor-bearing mice [160,161]. In an EL4 inoculation tumor model, a set of chemotherapy drugs was tested for their influence on the number of splenic and intratumoral MDSCs [160]. This study showed that high dose gemcitabine and 5-Fluorouracil (5-FU), two anti-metabolite drugs that interfere with DNA replication, reduce MDSC accumulation [160]. Consequently, 5-FU-mediated MDSC depletion results in increased IFNγ-producing intratumoral $CD8^+$ T cells. This effect is reverted by adoptive transfer of MDSCs, suggesting that the effect of 5-FU is exerted through MDSCs [160]. Similar results were obtained in the MCA203 cell line-inoculation sarcoma model combined with cytotoxic T cell transfer [162], highlighting the critical role of MDSCs in dampening T cell activity upon 5-FU treatment. While the exact mechanisms underlying the selectivity of 5-FU for MDSCs are unknown, it has been proposed that 5-FU inhibits the enzyme thymidylate synthase and that the resistance to 5-FU is due to insufficient inhibition of this enzyme [163]. Indeed, low levels of thymidylate synthase are found in MDSCs compared to splenocytes and EL4 tumor cells, suggesting that 5-FU selectivity for MDSCs could be due to this low enzymatic expression [160].

High dose gemcitabine induces similar effects on MDSCs as 5-FU [161]. *In vitro* analyses of splenocytes from TC-1 lung cancer-bearing mice showed the cytotoxic specificity of gemcitabine for MDSCs, while $CD4^+$, $CD8^+$ T cells and B cells are unaffected [161]. Although the exact mechanism underlying this specificity has not been identified, it has been hypothesized that gemcitabine induces apoptosis in MDSCs [161]. Yet, a thorough mechanistic analysis of gemcitabine-induced apoptotic cell death in various immune cell populations has not been performed. In the 4T1 breast cancer mouse model, gemcitabine treatment also reduces splenic MDSC accumulation, which results in increased proliferation and IFNγ production by splenic lymphocytes upon antigen stimulation compared to untreated mice [164]. However, no difference in anti-cancer efficacy of gemcitabine was observed between immunocompetent and nude mice, indicating a T cell-independent mechanism of 4T1 tumor control by gemcitabine [164]. Perhaps, this observation might be explained by the presence of other immunosuppressive cells in the TME, like T_{regs} or macrophages.

The beneficial effect of chemotherapeutic drugs on the immunosuppressive TME is not only a direct result of reduced MDSC numbers, but also a result of a more favorable phenotype of the remaining MDSCs. For example, in the 4T1-Neu mammary tumor model, docetaxel reduces splenic granulocytic-MDSCs and enhances $CD8^+$ and $CD4^+$ cytotoxic activity [165]. The remaining MDSCs exhibit a different phenotypic profile compared to MDSCs from untreated mice. In line with these *in vivo* findings, MDSCs pre-treated

with docetaxel induce the proliferation of OVA-exposed OT-II $CD4^+$ T cells compared to untreated MDSCs *in vitro*, suggesting that docetaxel treatment induces a phenotypical switch to a more favorable state [165]. Likewise, doxorubicin selectively decreases the proportion of MDSCs in the 4T1 breast tumor model via apoptosis and subdues the immunosuppressive phenotype of the remaining MDSCs. The remaining MDSCs have a lower expression of immunosuppressive molecules like ROS, ARG-1 and IDO [166]. This less suppressive environment caused by doxorubicin enhanced the activity of adoptively transferred T helper cells [166]. Interestingly, some subpopulations of MDSCs may be more susceptible to chemotherapy than others. Whether chemotherapy selectively depletes pro-tumorigenic MDSCs or skews them towards an anti-tumor phenotype is unknown. Future studies using lineage tracing methodologies would provide more insight into this topic.

Besides the favorable immunomodulatory 'off-target' effects of various chemotherapeutic drugs, these drugs can at the same time exert less desirable functions. For instance, in addition to its inhibitory effect on T_{regs}, cyclophosphamide increases the number of $CD11b^+Gr1^+$ MDSCs. In a transgenic mouse model for melanoma, a single injection of low dose cyclophosphamide increases the accumulation of MDSCs in the tumor and spleen, stimulates their immunosuppressive ability by inducing NO and ROS production, and reduces splenocyte proliferation [167]. In line with these findings, MDSCs accumulate in the blood of breast cancer patients after treatment with doxorubicin or cyclophosphamide [168]. This may be due to IFNγ release by $CD4^+$ and $CD8^+$ T cells that promotes survival of MDSCs [169]. Based on these data, a combination of cyclophosphamide and cancer immunotherapy might not work; however, additional studies in other tumor models should be performed to test this.

Another study underscoring the complex impact of chemotherapy on myeloid cells shows that in EL4-tumor-bearing mice 5-FU induces IL1β secretion in MDSCs in a Nlrp3 inflammasome-dependent manner [170]. Using depletion experiments and knock-out mice, it was shown that the MDSC-derived IL1β triggers IL17 production by $CD4^+$ T cells which limits the anti-cancer efficacy of 5-FU [170]. These data highlight that the effect of certain chemotherapy drugs is not simply limited to depletion of immunosuppressive cells but these drugs also change the functionality of cells that may impair their efficacy. These results suggest that the combination of chemotherapeutic and immunomodulatory compounds must be chosen carefully to increase their anti-cancer efficacy [171].

While several chemotherapy drugs have been reported to target MDSCs, thus far only one drug seems to strongly affect TAMs. Trabectedin, a drug that binds DNA and affects transcription and DNA repair pathways, depletes macrophages and suppresses the differentiation of monocytes in the tumor bed in the transplantable MN/MCA1 fibrosarcoma tumor model through a TRAIL-dependent mechanism [172]. Importantly, this macrophage selectivity is also observed in sarcoma patients after trabectedin neo-adjuvant treatment [172]. It would be interesting to assess whether the anti-cancer activity of trabectedin is $CD8^+$ T cell-mediated. The macrophage-depleting effect of trabectedin makes it an interesting candidate for combination strategies with immunotherapy.

As discussed before, many studies illustrate the complexity of immunomodulation by conventional chemotherapeutics which is highly context-dependent. The differential effect on specific immune cells of different types of chemotherapeutics is to a large extent dependent on the timing and dosing schedule. While high dose chemotherapy often depletes immune cell subsets, low dose metronomic chemotherapy exerts a more subtle anti-angiogenic and immunomodulatory mode of action [139,140]. It will be interesting to perform a side-by-side comparison of various types of chemotherapies administered at high versus low (metronomic) dose and evaluate their immunomodulatory effects, followed by more mechanistic studies. Ideally, these types of experiments would be performed in clinically relevant mouse models that faithfully recapitulate human cancer (Box 1) to facilitate clinical translation.

Future perspectives: exploiting the immunomodulatory properties of chemotherapeutic drugs to improve cancer immunotherapy

Given their immunomodulatory properties, conventional chemotherapy drugs are interesting candidates to combine with T cell-boosting immunotherapy – a concept termed chemo-immunotherapy [173]. Clinical trials report enhanced anti-tumor T cell responses in cancer patients treated with chemotherapy in combination with cancer vaccines [13]. Moreover, clinical testing of chemotherapy combined with other immunotherapy approaches like adoptive transfer of (genetically engineered) autologous T cells or toll-like receptor (TLR) agonists are likely to be explored in the near future. Indeed, various experimental studies support the concept that chemotherapy-induced relieve of immunosuppression could improve cancer immunotherapy. In a passive immunotherapy setting, in the MC203 fibrosarcoma and TC-1 lung cancer cell line inoculation models, low dose gemcitabine and 5-FU reduced the splenic population of $CD11b^{+}Gr1^{+}$ MDSCs, resulting in enhanced anti-tumor activity of adoptively transferred tumor-specific CTL [162]. The results obtained in preclinical models combining chemotherapeutics with immune checkpoint inhibitors are promising. The immunomodulatory effects of melphalan – administered in a subtherapeutic dose – synergizes with CTLA-4 blockade in a plasmacytoma model [174]. *In vitro* assays revealed that splenocytes obtained from melphalan-treated mice co-cultured with anti-CTLA-4 induced tumor cell cytotoxicity, while splenocytes from non-treated mice – irrespective of CTLA-4 blockade – did not [174]. Furthermore, in the poorly immunogenic AB-1 malignant mesothelioma and Lewis lung cancer (LLC) inoculation tumor models, a combination therapy of gemcitabine and CTLA-4 blockade synergizes, inducing potent anti-tumor immune responses and subsequent regression of tumors in a CD4- and CD8-dependent manner [175]. In addition, in a subcutaneous murine mesothelioma model, synergy is observed between cisplatin and CTLA-4 blockade, resulting in a profound anti-tumor effect that is characterized by increased influx and activation of $CD4^{+}$ and $CD8^{+}$ T cells in the tumor [176]. Moreover, preclinical studies in mice show that doxorubicin, cisplatin and paclitaxel in addition to

their immunomodulatory role, can sensitize tumor cells for CTL attack in a direct manner [177]. Here, chemotherapy causes increased permeability of tumor cell membranes to GRZMB, which sensitizes cancer cells to the cytotoxic effects of T cells and improved different cancer immunotherapy strategies [177]. Together, these preclinical studies – albeit limited numbers – show the potential to exploit immunomodulatory chemotherapeutic drugs to improve the efficacy of checkpoint blockade.

Clinical trials that evaluate the combination of chemotherapeutic drugs and checkpoint inhibitors in cancer patients are still limited. Some studies in melanoma and lung cancer have used chemotherapeutics in combination with checkpoint blockade resulting in improved survival compared to chemotherapy alone [40,178]. However, the rational of these studies was not to evaluate the effect of treatment on the immunosuppressive microenvironment. Moreover, the design of clinical trials makes it impossible to perform a structural comparison in patients to study the effect of the immunosuppressive microenvironment on immunotherapy efficacy and whether this efficacy can be enhanced by adding chemotherapeutics to the treatment regimen. Therefore, we need to rely on preclinical research in mouse tumor models that faithfully recapitulate human cancer in terms of the genetic composition, anti-tumor immunity and the immunosuppressive tumor microenvironment (Box 1). Results obtained in mouse models that mimic human cancer might shape the design of clinical trials and guide towards interesting treatment strategies. There are still various important

Box 1 | Experimental mouse models to study the anti-tumor immune response

Understanding the complex crosstalk between innate and adaptive immune cells and (disseminated) cancer cells requires the use of preclinical mouse models that faithfully recapitulate human cancer. The most widely used experimental mouse models are carcinogen-induced cancer models and cell line inoculation models. The latter is based on inoculation of large numbers of (genetically modified) homogenous cancer cells grown in 2D conditions. Implantation of these cells often results in massive cell death thereby priming an effective anti-tumor immune response. Shaping of the tumor immune microenvironment during cancer progression in these models can hardly take place in the short amount of time that it takes for transplanted tumors to grow to their maximum tolerated size. Of notice, when implanting human cancer cells, either patient-derived tumor material (PDX) or established human cancer cell lines, immunocompromised mice are used, thereby excluding the important role of the adaptive immune system.

While cell line inoculation models proved useful to decipher some aspects of the anti-tumor immune response, we should keep in mind that these models do not reflect physiological processes as they occur in human patients. Genetically engineered mouse (GEM) models, which develop *de novo* cancers, generally mimic human cancer genetically — because of the introduction of specific driver mutations — and histopathologically [179]. In addition, tumor progression occurs in a multi-step nature in their natural microenvironment shaping the local immune responses (Fig 1), therefore mimicking the human setting. In contrast to inoculation models expressing known tumor antigens, the anti-tumor immune response in GEM models can be considered a black box. Due to their cellular and genetic heterogeneity, GEM models induce a variety of T cell responses directed against multiple unknown tumor neo-antigens which faithfully reflects human cancer. Interestingly, comparative studies have shown that inoculation models greatly differ from GEM models in terms of response to anticancer therapies and endogenous T cell responses [180,181]. The advantages and disadvantages of different experimental mouse models in studying responsiveness to anti-cancer therapy have been recently discussed [14,182].

questions that need to be addressed to maximally exploit the therapeutic efficacy of chemotherapy and immunotherapy combinations, like the determination of the most optimal combinations. Based on preclinical findings, different cancer types will likely require different combinations of therapy. In addition, despite the devastating effects of metastatic disease, mechanistic insights into the site-specific therapeutic response profiles and resistance mechanisms of cancer immunotherapy are completely lacking. Moreover, it is critical to gain insights into the mechanisms underlying intrinsic and acquired resistance to cancer immunotherapy. To answer these questions within the next decade, it is critical that basic researchers and clinicians intensify their efforts to join forces, so that results from preclinical research can guide the design of clinical trials, and the results from clinical trials, in turn, can guide mechanistic studies in mouse models. Together, these efforts will improve treatment strategies using chemotherapeutics to alleviate immunosuppression and enhance cancer immunotherapy.

Author contributions

KK, CS and KV reviewed relevant literature and drafted the manuscript. KV revised the manuscript and supervised KK and CS. All authors read and approved the final manuscript.

Conflict of Interest Statement

The authors declare that the research was conducted in the absence of any commercial or financial relationships that could be construed as a potential conflict of interest.

Acknowledgements

We thank Seth Coffelt for insightful comments on the manuscript. Work in the lab is supported by grants from the European Union (FP7 MCA-ITN 317445 TIMCC), the European Research Council (ERC consolidator award INFLAMET 615300), the Beug Foundation for Metastasis Research, the Dutch Cancer Society (2011-5004), and the Netherlands Organization for Scientific Research (NWO VIDI 917.96.307).

References

1. Hodi, F. S. *et al.* Improved survival with ipilimumab in patients with metastatic melanoma. *N. Engl. J. Med.* **363,** 711–723 (2010).
2. Powles, T. *et al.* MPDL3280A (anti-PD-L1) treatment leads to clinical activity in metastatic bladder cancer. *Nature* **515,** 558–562 (2014).
3. Topalian, S. L. *et al.* Safety, activity, and immune correlates of anti-PD-1 antibody in cancer. *N. Engl. J. Med.* **366,** 2443–2454 (2012).
4. Wolchok, J. D. *et al.* Nivolumab plus ipilimumab in advanced melanoma. *N. Engl. J. Med.* **369,** 122–133 (2013).
5. Ansell, S. M. *et al.* PD-1 blockade with nivolumab in relapsed or refractory Hodgkin's lymphoma. *N. Engl. J. Med.* **372,** 311–319 (2015).
6. Motzer, R. J. *et al.* Nivolumab for Metastatic Renal Cell Carcinoma: Results of a Randomized Phase II Trial. *J. Clin. Oncol.* **33,** 1430–1437 (2015).
7. Couzin-Frankel, J. Cancer Immunotherapy. *Science* **342,** 1432–1433 (2013).
8. Snyder, A. *et al.* Genetic basis for clinical response to CTLA-4 blockade in melanoma. *N. Engl. J. Med.* **371,** 2189–2199 (2014).
9. Rizvi, N. A. *et al.* Cancer immunology. Mutational landscape determines sensitivity to PD-1 blockade in non-small cell lung cancer. *Science* **348,** 124–128 (2015).
10. Ries, C. H. *et al.* Targeting tumor-associated macrophages with anti-CSF-1R antibody reveals a strategy for cancer therapy. *Cancer Cell* **25,** 846–859 (2014).
11. Vanneman, M. & Dranoff, G. Combining immunotherapy and targeted therapies in cancer treatment. *Nat. Rev. Cancer* **12,** 237–251 (2012).
12. Verbrugge, I. *et al.* Radiotherapy increases the permissiveness of established mammary tumors to rejection by immunomodulatory antibodies. *Cancer Res.* **72,** 3163–3174 (2012).
13. Chen, G. & Emens, L. A. Chemoimmunotherapy: reengineering tumor immunity. *Cancer Immunol. Immunother.* **62,** 203–216 (2013).
14. Coffelt, S. B. & de Visser, K. E. Immune-mediated mechanisms influencing the efficacy of anticancer therapies. *Trends Immunol.* **36,** 198–216 (2015).
15. Wargo, J. A., Reuben, A., Cooper, Z. A., Oh, K. S. & Sullivan, R. J. Immune Effects of Chemotherapy, Radiation, and Targeted Therapy and Opportunities for Combination With Immunotherapy. *Semin. Oncol.* **42,** 601–616 (2015).
16. DeNardo, D. G. & Coussens, L. M. Inflammation and breast cancer. Balancing immune response: crosstalk between adaptive and innate immune cells during breast cancer progression. *Breast Cancer Res.* **9,** 212 (2007).
17. Hanahan, D. & Coussens, L. M. Accessories to the crime: functions of cells recruited to the tumor microenvironment. *Cancer Cell* **21,** 309–322 (2012).
18. de Visser, K. E., Eichten, A. & Coussens, L. M. Paradoxical roles of the immune system during cancer development. *Nat. Rev. Cancer* **6,** 24–37 (2006).
19. Bell, D. *et al.* In breast carcinoma tissue, immature dendritic cells reside within the tumor, whereas mature dendritic cells are located in peritumoral areas. *J. Exp. Med.* **190,** 1417–1426 (1999).
20. Pinzon-Charry, A., Maxwell, T. & López, J. A. Dendritic cell dysfunction in cancer: a mechanism for immunosuppression. *Immunol. Cell Biol.* **83,** 451–461 (2005).
21. Engelhardt, J. J. *et al.* Marginating dendritic cells of the tumor microenvironment cross-present tumor antigens and stably engage tumor-specific T cells. *Cancer Cell* **21,** 402–417 (2012).
22. Broz, M. L. *et al.* Dissecting the Tumor Myeloid Compartment Reveals Rare Activating Antigen-Presenting Cells Critical for T Cell Immunity. *Cancer Cell* **26,** 638–652 (2014).
23. Shrimali, R. K. *et al.* Antiangiogenic agents can increase lymphocyte infiltration into tumor and enhance the effectiveness of adoptive immunotherapy of cancer. *Cancer Res.* **70,** 6171–6180 (2010).
24. Buckanovich, R. J. *et al.* Endothelin B receptor mediates the endothelial barrier to T cell homing to tumors and disables immune therapy. *Nat. Med.* **14,** 28–36 (2008).
25. Molon, B. *et al.* Chemokine nitration prevents intratumoral infiltration of antigen-specific T cells. *J. Exp. Med.* **208,** 1949–1962 (2011).
26. Pardoll, D. M. The blockade of immune checkpoints in cancer immunotherapy. *Nat. Rev. Cancer* **12,** 252–264 (2012).
27. Joyce, J. A. & Fearon, D. T. T cell exclusion, immune privilege, and the tumor microenvironment. *Science* **348,** 74–80 (2015).

28. Sharma, P. & Allison, J. P. The future of immune checkpoint therapy. *Science* **348,** 56–61 (2015).
29. Walunas, T. L. *et al.* CTLA-4 can function as a negative regulator of T cell activation. *Immunity* **1,** 405–413 (1994).
30. Barber, D. L. *et al.* Restoring function in exhausted CD8 T cells during chronic viral infection. *Nature* **439,** 682–687 (2006).
31. Okazaki, T. & Honjo, T. PD-1 and PD-1 ligands: from discovery to clinical application. *Int. Immunol.* **19,** 813–824 (2007).
32. Shin, D. S. & Ribas, A. The evolution of checkpoint blockade as a cancer therapy: what's here, what's next? *Curr. Opin. Immunol.* **33,** 23–35 (2015).
33. Topalian, S. L., Drake, C. G. & Pardoll, D. M. Immune Checkpoint Blockade: A Common Denominator Approach to Cancer Therapy. *Cancer Cell* **27,** 450–461 (2015).
34. Goldberg, M. V. *et al.* Role of PD-1 and its ligand, B7-H1, in early fate decisions of CD8 T cells. *Blood* **110,** 186–192 (2007).
35. Wing, K. *et al.* CTLA-4 control over Foxp3+ regulatory T cell function. *Science* **322,** 271–275 (2008).
36. Peggs, K. S., Quezada, S. A., Chambers, C. A., Korman, A. J. & Allison, J. P. Blockade of CTLA-4 on both effector and regulatory T cell compartments contributes to the antitumor activity of anti-CTLA-4 antibodies. *J. Exp. Med.* **206,** 1717–1725 (2009).
37. Simpson, T. R. *et al.* Fc-dependent depletion of tumor-infiltrating regulatory T cells co-defines the efficacy of anti–CTLA-4 therapy against melanoma. *J. Exp. Med.* **210,** 1695–1710 (2013).
38. Postow, M. A. *et al.* Nivolumab and ipilimumab versus ipilimumab in untreated melanoma. *N. Engl. J. Med.* **372,** 2006–2017 (2015).
39. Kvistborg, P. *et al.* Anti-CTLA-4 therapy broadens the melanoma-reactive CD8+ T cell response. *Sci. Transl. Med.* **6,** 254ra128 (2014).
40. Robert, C. *et al.* Ipilimumab plus dacarbazine for previously untreated metastatic melanoma. *N. Engl. J. Med.* **364,** 2517–2526 (2011).
41. Schadendorf, D. *et al.* Pooled Analysis of Long-Term Survival Data From Phase II and Phase III Trials of Ipilimumab in Unresectable or Metastatic Melanoma. *J. Clin. Oncol.* JCO.2014.56.2736 (2015). doi:10.1200/JCO.2014.56.2736
42. Brahmer, J. R. *et al.* Safety and activity of anti-PD-L1 antibody in patients with advanced cancer. *N. Engl. J. Med.* **366,** 2455–2465 (2012).
43. Gubin, M. M. *et al.* Checkpoint blockade cancer immunotherapy targets tumour-specific mutant antigens. *Nature* **515,** 577–581 (2014).
44. Linnemann, C. *et al.* High-throughput epitope discovery reveals frequent recognition of neo-antigens by CD4+ T cells in human melanoma. *Nat. Med.* **21,** 81–85 (2015).
45. van Rooij, N. *et al.* Tumor exome analysis reveals neoantigen-specific T-cell reactivity in an ipilimumab-responsive melanoma. *J. Clin. Oncol.* **31,** e439-442 (2013).
46. Rooney, M. S., Shukla, S. A., Wu, C. J., Getz, G. & Hacohen, N. Molecular and genetic properties of tumors associated with local immune cytolytic activity. *Cell* **160,** 48–61 (2015).
47. Schumacher, T. N. & Schreiber, R. D. Neoantigens in cancer immunotherapy. *Science* **348,** 69–74 (2015).
48. Alexandrov, L. B. *et al.* Signatures of mutational processes in human cancer. *Nature* **500,** 415–421 (2013).
49. Tumeh, P. C. *et al.* PD-1 blockade induces responses by inhibiting adaptive immune resistance. *Nature* **515,** 568–571 (2014).
50. Gros, A. *et al.* PD-1 identifies the patient-specific $CD8^+$ tumor-reactive repertoire infiltrating human tumors. *J. Clin. Invest.* **124,** 2246–2259 (2014).
51. Herbst, R. S. *et al.* Predictive correlates of response to the anti-PD-L1 antibody MPDL3280A in cancer patients. *Nature* **515,** 563–567 (2014).
52. Taube, J. M. *et al.* Association of PD-1, PD-1 ligands, and other features of the tumor immune microenvironment with response to anti-PD-1 therapy. *Clin. Cancer Res.* **20,** 5064–5074 (2014).
53. Le, D. T. *et al.* PD-1 Blockade in Tumors with Mismatch-Repair Deficiency. *N. Engl. J. Med.* (2015). doi:10.1056/NEJMoa1500596
54. Llosa, N. J. *et al.* The vigorous immune microenvironment of microsatellite instable colon cancer is balanced by multiple counter-inhibitory checkpoints. *Cancer Discov.* **5,** 43–51 (2015).
55. Wimberly, H. *et al.* PD-L1 Expression Correlates with Tumor-Infiltrating Lymphocytes and Response to Neoadjuvant Chemotherapy in Breast Cancer. *Cancer Immunol. Res.* **3,** 326–332 (2015).
56. Ali, H. R. *et al.* PD-L1 protein expression in breast cancer is rare, enriched in basal-like tumours and associated with infiltrating lymphocytes. *Ann. Oncol.* (2015). doi:10.1093/annonc/mdv192
57. Parsa, A. T. *et al.* Loss of tumor suppressor PTEN function increases B7-H1 expression and

immunoresistance in glioma. *Nat. Med.* **13,** 84–88 (2007).
58. Curiel, T. J. *et al.* Blockade of B7-H1 improves myeloid dendritic cell-mediated antitumor immunity. *Nat. Med.* **9,** 562–567 (2003).
59. Gershon, R. K. & Kondo, K. Cell interactions in the induction of tolerance: the role of thymic lymphocytes. *Immunology* **18,** 723–737 (1970).
60. Sakaguchi, S., Sakaguchi, N., Asano, M., Itoh, M. & Toda, M. Immunologic self-tolerance maintained by activated T cells expressing IL-2 receptor alpha-chains (CD25). Breakdown of a single mechanism of self-tolerance causes various autoimmune diseases. *J. Immunol.* **155,** 1151–1164 (1995).
61. Fontenot, J. D., Gavin, M. A. & Rudensky, A. Y. Foxp3 programs the development and function of CD4+CD25+ regulatory T cells. *Nat. Immunol.* **4,** 330–336 (2003).
62. Adeegbe, D. O. & Nishikawa, H. Natural and induced T regulatory cells in cancer. *Front. Immunol.* **4,** 190 (2013).
63. Berendt, M. J. & North, R. J. T-cell-mediated suppression of anti-tumor immunity. An explanation for progressive growth of an immunogenic tumor. *J. Exp. Med.* **151,** 69–80 (1980).
64. Li, X., Kostareli, E., Suffner, J., Garbi, N. & Hämmerling, G. J. Efficient Treg depletion induces T-cell infiltration and rejection of large tumors. *Eur. J. Immunol.* **40,** 3325–3335 (2010).
65. Curiel, T. J. *et al.* Specific recruitment of regulatory T cells in ovarian carcinoma fosters immune privilege and predicts reduced survival. *Nat. Med.* **10,** 942–949 (2004).
66. Shevach, E. M. Mechanisms of foxp3+ T regulatory cell-mediated suppression. *Immunity* **30,** 636–645 (2009).
67. Thornton, A. M. & Shevach, E. M. Suppressor effector function of CD4+CD25+ immunoregulatory T cells is antigen nonspecific. *J. Immunol.* **164,** 183–190 (2000).
68. Thornton, A. M. & Shevach, E. M. CD4+CD25+ immunoregulatory T cells suppress polyclonal T cell activation in vitro by inhibiting interleukin 2 production. *J. Exp. Med.* **188,** 287–296 (1998).
69. Chen, W. *et al.* Conversion of peripheral CD4+CD25- naive T cells to CD4+CD25+ regulatory T cells by TGF-beta induction of transcription factor Foxp3. *J. Exp. Med.* **198,** 1875–1886 (2003).
70. Groux, H. *et al.* A CD4+ T-cell subset inhibits antigen-specific T-cell responses and prevents colitis. *Nature* **389,** 737–742 (1997).
71. Collison, L. W. *et al.* The inhibitory cytokine IL-35 contributes to regulatory T-cell function. *Nature* **450,** 566–569 (2007).
72. Cao, X. *et al.* Granzyme B and perforin are important for regulatory T cell-mediated suppression of tumor clearance. *Immunity* **27,** 635–646 (2007).
73. Grossman, W. J. *et al.* Human T regulatory cells can use the perforin pathway to cause autologous target cell death. *Immunity* **21,** 589–601 (2004).
74. Gondek, D. C., Lu, L.-F., Quezada, S. A., Sakaguchi, S. & Noelle, R. J. Cutting edge: contact-mediated suppression by CD4+CD25+ regulatory cells involves a granzyme B-dependent, perforin-independent mechanism. *J. Immunol.* **174,** 1783–1786 (2005).
75. Deaglio, S. *et al.* Adenosine generation catalyzed by CD39 and CD73 expressed on regulatory T cells mediates immune suppression. *J. Exp. Med.* **204,** 1257–1265 (2007).
76. Bates, G. J. *et al.* Quantification of regulatory T cells enables the identification of high-risk breast cancer patients and those at risk of late relapse. *J. Clin. Oncol.* **24,** 5373–5380 (2006).
77. Sasada, T., Kimura, M., Yoshida, Y., Kanai, M. & Takabayashi, A. CD4+CD25+ regulatory T cells in patients with gastrointestinal malignancies: possible involvement of regulatory T cells in disease progression. *Cancer* **98,** 1089–1099 (2003).
78. Gao, Q. *et al.* Intratumoral balance of regulatory and cytotoxic T cells is associated with prognosis of hepatocellular carcinoma after resection. *J. Clin. Oncol.* **25,** 2586–2593 (2007).
79. Li, Y.-Q. *et al.* Tumor secretion of CCL22 activates intratumoral Treg infiltration and is independent prognostic predictor of breast cancer. *PloS One* **8,** e76379 (2013).
80. Huang, Y. *et al.* Prognostic value of tumor-infiltrating FoxP3+ T cells in gastrointestinal cancers: a meta analysis. *PloS One* **9,** e94376 (2014).
81. Ladoire, S., Martin, F. & Ghiringhelli, F. Prognostic role of FOXP3+ regulatory T cells infiltrating human carcinomas: the paradox of colorectal cancer. *Cancer Immunol. Immunother.* **60,** 909–918 (2011).
82. Rasku, M. A. *et al.* Transient T cell depletion causes regression of melanoma metastases. *J. Transl. Med.* **6,** 12 (2008).
83. Rech, A. J. *et al.* CD25 blockade depletes and selectively reprograms regulatory T cells in concert with immunotherapy in cancer patients. *Sci. Transl. Med.* **4,** 134ra62 (2012).
84. Bennett, J. A., Rao, V. S. & Mitchell, M. S. Systemic bacillus Calmette-Guérin (BCG) activates natural

suppressor cells. *Proc. Natl. Acad. Sci. U. S. A.* **75,** 5142–5144 (1978).
85. Oseroff, A., Okada, S. & Strober, S. Natural suppressor (NS) cells found in the spleen of neonatal mice and adult mice given total lymphoid irradiation (TLI) express the null surface phenotype. *J. Immunol.* **132,** 101–110 (1984).
86. Tsuchiya, Y., Igarashi, M., Suzuki, R. & Kumagai, K. Production of colony-stimulating factor by tumor cells and the factor-mediated induction of suppressor cells. *J. Immunol.* **141,** 699–708 (1988).
87. Lee, M. Y. & Rosse, C. Depletion of lymphocyte subpopulations in primary and secondary lymphoid organs of mice by a transplanted granulocytosis-inducing mammary carcinoma. *Cancer Res.* **42,** 1255–1260 (1982).
88. Gabrilovich, D. I. *et al.* The terminology issue for myeloid-derived suppressor cells. *Cancer Res.* **67,** 425; author reply 426 (2007).
89. Dumitru, C. A., Moses, K., Trellakis, S., Lang, S. & Brandau, S. Neutrophils and granulocytic myeloid-derived suppressor cells: immunophenotyping, cell biology and clinical relevance in human oncology. *Cancer Immunol. Immunother.* **61,** 1155–1167 (2012).
90. Chevolet, I. *et al.* Clinical significance of plasmacytoid dendritic cells and myeloid-derived suppressor cells in melanoma. *J. Transl. Med.* **13,** 9 (2015).
91. Wang, L. *et al.* Increased myeloid-derived suppressor cells in gastric cancer correlate with cancer stage and plasma S100A8/A9 proinflammatory proteins. *J. Immunol.* **190,** 794–804 (2013).
92. Solito, S. *et al.* A human promyelocytic-like population is responsible for the immune suppression mediated by myeloid-derived suppressor cells. *Blood* **118,** 2254–2265 (2011).
93. Waight, J. D., Hu, Q., Miller, A., Liu, S. & Abrams, S. I. Tumor-derived G-CSF facilitates neoplastic growth through a granulocytic myeloid-derived suppressor cell-dependent mechanism. *PloS One* **6,** e27690 (2011).
94. Serafini, P. *et al.* High-dose granulocyte-macrophage colony-stimulating factor-producing vaccines impair the immune response through the recruitment of myeloid suppressor cells. *Cancer Res.* **64,** 6337–6343 (2004).
95. Pan, P.-Y. *et al.* Reversion of immune tolerance in advanced malignancy: modulation of myeloid-derived suppressor cell development by blockade of stem-cell factor function. *Blood* **111,** 219–228 (2008).
96. Rodriguez, P. C. *et al.* Arginase I in myeloid suppressor cells is induced by COX-2 in lung carcinoma. *J. Exp. Med.* **202,** 931–939 (2005).
97. Rodriguez, P. C. *et al.* Arginase I-producing myeloid-derived suppressor cells in renal cell carcinoma are a subpopulation of activated granulocytes. *Cancer Res.* **69,** 1553–1560 (2009).
98. Harari, O. & Liao, J. K. Inhibition of MHC II gene transcription by nitric oxide and antioxidants. *Curr. Pharm. Des.* **10,** 893–898 (2004).
99. Saio, M., Radoja, S., Marino, M. & Frey, A. B. Tumor-infiltrating macrophages induce apoptosis in activated CD8(+) T cells by a mechanism requiring cell contact and mediated by both the cell-associated form of TNF and nitric oxide. *J. Immunol.* **167,** 5583–5593 (2001).
100. Yu, J. *et al.* Myeloid-derived suppressor cells suppress antitumor immune responses through IDO expression and correlate with lymph node metastasis in patients with breast cancer. *J. Immunol. Baltim. Md 1950* **190,** 3783–3797 (2013).
101. Holmgaard, R. B., Zamarin, D., Munn, D. H., Wolchok, J. D. & Allison, J. P. Indoleamine 2,3-dioxygenase is a critical resistance mechanism in antitumor T cell immunotherapy targeting CTLA-4. *J. Exp. Med.* **210,** 1389–1402 (2013).
102. Srivastava, M. K., Sinha, P., Clements, V. K., Rodriguez, P. & Ostrand-Rosenberg, S. Myeloid-derived suppressor cells inhibit T-cell activation by depleting cystine and cysteine. *Cancer Res.* **70,** 68–77 (2010).
103. Huang, B. *et al.* Gr-1+CD115+ immature myeloid suppressor cells mediate the development of tumor-induced T regulatory cells and T-cell anergy in tumor-bearing host. *Cancer Res.* **66,** 1123–1131 (2006).
104. Noh, H., Eomm, M. & Han, A. Usefulness of pretreatment neutrophil to lymphocyte ratio in predicting disease-specific survival in breast cancer patients. *J. Breast Cancer* **16,** 55–59 (2013).
105. Tomita, M., Shimizu, T., Ayabe, T., Yonei, A. & Onitsuka, T. Preoperative neutrophil to lymphocyte ratio as a prognostic predictor after curative resection for non-small cell lung cancer. *Anticancer Res.* **31,** 2995–2998 (2011).
106. Pillay, J., Tak, T., Kamp, V. M. & Koenderman, L. Immune suppression by neutrophils and granulocytic myeloid-derived suppressor cells: similarities and differences. *Cell. Mol. Life Sci.* **70,** 3813–3827 (2013).
107. Coffelt, S. B. *et al.* IL-17-producing γδ T cells and neutrophils conspire to promote breast cancer metastasis. *Nature* **522,** 345–348 (2015).
108. Han, Y. *et al.* Prognostic value of chemotherapy-induced neutropenia in early-stage breast cancer. *Breast*

Cancer Res. Treat. **131,** 483–490 (2012).
109. Bald, T. *et al.* Ultraviolet-radiation-induced inflammation promotes angiotropism and metastasis in melanoma. *Nature* **507,** 109–113 (2014).
110. Kowanetz, M. *et al.* Granulocyte-colony stimulating factor promotes lung metastasis through mobilization of Ly6G+Ly6C+ granulocytes. *Proc. Natl. Acad. Sci. U. S. A.* **107,** 21248–21255 (2010).
111. Granot, Z. *et al.* Tumor entrained neutrophils inhibit seeding in the premetastatic lung. *Cancer Cell* **20,** 300–314 (2011).
112. Casbon, A.-J. *et al.* Invasive breast cancer reprograms early myeloid differentiation in the bone marrow to generate immunosuppressive neutrophils. *Proc. Natl. Acad. Sci. U. S. A.* (2015). doi:10.1073/pnas.1424927112
113. Sagiv, J. Y. *et al.* Phenotypic Diversity and Plasticity in Circulating Neutrophil Subpopulations in Cancer. *Cell Rep.* (2015). doi:10.1016/j.celrep.2014.12.039
114. Fridlender, Z. G. *et al.* Polarization of tumor-associated neutrophil phenotype by TGF-beta: 'N1' versus 'N2' TAN. *Cancer Cell* **16,** 183–194 (2009).
115. Mantovani, A. *et al.* The chemokine system in diverse forms of macrophage activation and polarization. *Trends Immunol.* **25,** 677–686 (2004).
116. Murray, P. J. *et al.* Macrophage Activation and Polarization: Nomenclature and Experimental Guidelines. *Immunity* **41,** 14–20 (2014).
117. Schultze, J. L. Transcriptional programming of human macrophages: on the way to systems immunology. *J. Mol. Med.* (2015). doi:10.1007/s00109-015-1286-y
118. Xue, J. *et al.* Transcriptome-based network analysis reveals a spectrum model of human macrophage activation. *Immunity* **40,** 274–288 (2014).
119. DeNardo, D. G. *et al.* Leukocyte Complexity Predicts Breast Cancer Survival and Functionally Regulates Response to Chemotherapy. *Cancer Discov.* **1,** 54–67 (2011).
120. Leek, R. D. *et al.* Association of macrophage infiltration with angiogenesis and prognosis in invasive breast carcinoma. *Cancer Res.* **56,** 4625–4629 (1996).
121. Ruffell, B. & Coussens, L. M. Macrophages and Therapeutic Resistance in Cancer. *Cancer Cell* **27,** 462–472 (2015).
122. Lin, E. Y., Nguyen, A. V., Russell, R. G. & Pollard, J. W. Colony-stimulating factor 1 promotes progression of mammary tumors to malignancy. *J. Exp. Med.* **193,** 727–740 (2001).
123. DeNardo, D. G. *et al.* CD4(+) T cells regulate pulmonary metastasis of mammary carcinomas by enhancing protumor properties of macrophages. *Cancer Cell* **16,** 91–102 (2009).
124. Qian, B.-Z. *et al.* CCL2 recruits inflammatory monocytes to facilitate breast-tumour metastasis. *Nature* **475,** 222–225 (2011).
125. Lin, E. Y. *et al.* Macrophages regulate the angiogenic switch in a mouse model of breast cancer. *Cancer Res.* **66,** 11238–11246 (2006).
126. Sharda, D. R. *et al.* Regulation of macrophage arginase expression and tumor growth by the Ron receptor tyrosine kinase. *J. Immunol.* **187,** 2181–2192 (2011).
127. Rodriguez, P. C. *et al.* L-arginine consumption by macrophages modulates the expression of CD3 zeta chain in T lymphocytes. *J. Immunol.* **171,** 1232–1239 (2003).
128. Munn, D. H. *et al.* Inhibition of T cell proliferation by macrophage tryptophan catabolism. *J. Exp. Med.* **189,** 1363–1372 (1999).
129. Sica, A. *et al.* Autocrine production of IL-10 mediates defective IL-12 production and NF-kappa B activation in tumor-associated macrophages. *J. Immunol.* **164,** 762–767 (2000).
130. Kuang, D.-M. *et al.* Activated monocytes in peritumoral stroma of hepatocellular carcinoma foster immune privilege and disease progression through PD-L1. *J. Exp. Med.* **206,** 1327–1337 (2009).
131. Pyonteck, S. M. *et al.* CSF-1R inhibition alters macrophage polarization and blocks glioma progression. *Nat. Med.* **19,** 1264–1272 (2013).
132. Zhu, Y. *et al.* CSF1/CSF1R Blockade Reprograms Tumor-Infiltrating Macrophages and Improves Response to T-cell Checkpoint Immunotherapy in Pancreatic Cancer Models. *Cancer Res.* **74,** 5057–5069 (2014).
133. Fridlender, Z. G. *et al.* CCL2 blockade augments cancer immunotherapy. *Cancer Res.* **70,** 109–118 (2010).
134. Fridlender, Z. G. *et al.* Monocyte chemoattractant protein-1 blockade inhibits lung cancer tumor growth by altering macrophage phenotype and activating CD8+ cells. *Am. J. Respir. Cell Mol. Biol.* **44,** 230–237 (2011).
135. Klyushnenkova, E. N. *et al.* Breaking immune tolerance by targeting CD25+ regulatory T cells is essential for the anti-tumor effect of the CTLA-4 blockade in an HLA-DR transgenic mouse model of prostate cancer. *The Prostate* **74,** 1423–1432 (2014).

136. Duraiswamy, J., Kaluza, K. M., Freeman, G. J. & Coukos, G. Dual blockade of PD-1 and CTLA-4 combined with tumor vaccine effectively restores T-cell rejection function in tumors. *Cancer Res.* **73,** 3591–3603 (2013).
137. Duraiswamy, J., Freeman, G. J. & Coukos, G. Therapeutic PD-1 Pathway Blockade Augments with Other Modalities of Immunotherapy T-Cell Function to Prevent Immune Decline in Ovarian Cancer. *Cancer Res.* **73,** 6900–6912 (2013).
138. Highfill, S. L. *et al.* Disruption of CXCR2-Mediated MDSC Tumor Trafficking Enhances Anti-PD1 Efficacy. *Sci. Transl. Med.* **6,** 237ra67-237ra67 (2014).
139. Nars, M. S. & Kaneno, R. Immunomodulatory effects of low dose chemotherapy and perspectives of its combination with immunotherapy. *Int. J. Cancer* **132,** 2471–2478 (2013).
140. Kerbel, R. S. & Kamen, B. A. The anti-angiogenic basis of metronomic chemotherapy. *Nat. Rev. Cancer* **4,** 423–436 (2004).
141. Ma, Y. *et al.* Anticancer chemotherapy-induced intratumoral recruitment and differentiation of antigen-presenting cells. *Immunity* **38,** 729–741 (2013).
142. Ghiringhelli, F. *et al.* Activation of the NLRP3 inflammasome in dendritic cells induces IL-1beta-dependent adaptive immunity against tumors. *Nat. Med.* **15,** 1170–1178 (2009).
143. Wada, S. *et al.* Cyclophosphamide augments antitumor immunity: studies in an autochthonous prostate cancer model. *Cancer Res.* **69,** 4309–4318 (2009).
144. Apetoh, L. *et al.* Toll-like receptor 4-dependent contribution of the immune system to anticancer chemotherapy and radiotherapy. *Nat. Med.* **13,** 1050–1059 (2007).
145. Obeid, M. *et al.* Calreticulin exposure dictates the immunogenicity of cancer cell death. *Nat. Med.* **13,** 54–61 (2007).
146. Bezu, L. *et al.* Combinatorial strategies for the induction of immunogenic cell death. *Front. Immunol.* 187 (2015). doi:10.3389/fimmu.2015.00187
147. Ciampricotti, M., Hau, C.-S., Doornebal, C. W., Jonkers, J. & de Visser, K. E. Chemotherapy response of spontaneous mammary tumors is independent of the adaptive immune system. *Nat. Med.* **18,** 344–346 (2012).
148. Ruffell, B. *et al.* Macrophage IL-10 blocks CD8+ T cell-dependent responses to chemotherapy by suppressing IL-12 expression in intratumoral dendritic cells. *Cancer Cell* **26,** 623–637 (2014).
149. Luznik, L., Jones, R. J. & Fuchs, E. J. High-dose cyclophosphamide for graft-versus-host disease prevention. *Curr. Opin. Hematol.* **17,** 493–499 (2010).
150. Luznik, L. *et al.* HLA-haploidentical bone marrow transplantation for hematologic malignancies using nonmyeloablative conditioning and high-dose, posttransplantation cyclophosphamide. *Biol. Blood Marrow Transplant.* **14,** 641–650 (2008).
151. Lutsiak, M. E. C. *et al.* Inhibition of CD4(+)25+ T regulatory cell function implicated in enhanced immune response by low-dose cyclophosphamide. *Blood* **105,** 2862–2868 (2005).
152. Motoyoshi, Y. *et al.* Different mechanisms for anti-tumor effects of low- and high-dose cyclophosphamide. *Oncol. Rep.* **16,** 141–146 (2006).
153. Ghiringhelli, F. *et al.* CD4+CD25+ regulatory T cells suppress tumor immunity but are sensitive to cyclophosphamide which allows immunotherapy of established tumors to be curative. *Eur. J. Immunol.* **34,** 336–344 (2004).
154. Ghiringhelli, F. *et al.* Metronomic cyclophosphamide regimen selectively depletes CD4+CD25+ regulatory T cells and restores T and NK effector functions in end stage cancer patients. *Cancer Immunol. Immunother.* **56,** 641–648 (2007).
155. Zhao, J. *et al.* Selective depletion of CD4+CD25+Foxp3+ regulatory T cells by low-dose cyclophosphamide is explained by reduced intracellular ATP levels. *Cancer Res.* **70,** 4850–4858 (2010).
156. Shevchenko, I. *et al.* Low-dose gemcitabine depletes regulatory T cells and improves survival in the orthotopic Panc02 model of pancreatic cancer. *Int. J. Cancer J. Int. Cancer* **133,** 98–107 (2013).
157. Rettig, L. *et al.* Gemcitabine depletes regulatory T-cells in human and mice and enhances triggering of vaccine-specific cytotoxic T-cells. *Int. J. Cancer J. Int. Cancer* **129,** 832–838 (2011).
158. Beyer, M. *et al.* Reduced frequencies and suppressive function of CD4+CD25hi regulatory T cells in patients with chronic lymphocytic leukemia after therapy with fludarabine. *Blood* **106,** 2018–2025 (2005).
159. Chen, C. *et al.* Suppressive effects of gemcitabine plus cisplatin chemotherapy on regulatory T cells in nonsmall-cell lung cancer. *J. Int. Med. Res.* **43,** 180–187 (2015).
160. Vincent, J. *et al.* 5-Fluorouracil selectively kills tumor-associated myeloid-derived suppressor cells resulting in enhanced T cell-dependent antitumor immunity. *Cancer Res.* **70,** 3052–3061 (2010).

161. Suzuki, E., Kapoor, V., Jassar, A. S., Kaiser, L. R. & Albelda, S. M. Gemcitabine selectively eliminates splenic Gr-1+/CD11b+ myeloid suppressor cells in tumor-bearing animals and enhances antitumor immune activity. *Clin. Cancer Res.* **11,** 6713–6721 (2005).
162. Ugel, S. *et al.* Immune Tolerance to Tumor Antigens Occurs in a Specialized Environment of the Spleen. *Cell Rep.* **2,** 628–639 (2012).
163. Peters, G. J. *et al.* Thymidylate synthase and drug resistance. *Eur. J. Cancer* **31A,** 1299–1305 (1995).
164. Le, H. K. *et al.* Gemcitabine directly inhibits myeloid derived suppressor cells in BALB/c mice bearing 4T1 mammary carcinoma and augments expansion of T cells from tumor-bearing mice. *Int. Immunopharmacol.* **9,** 900–909 (2009).
165. Kodumudi, K. N. *et al.* A novel chemoimmunomodulating property of docetaxel: suppression of myeloid-derived suppressor cells in tumor bearers. *Clin. Cancer Res.* **16,** 4583–4594 (2010).
166. Alizadeh, D. *et al.* Doxorubicin eliminates myeloid-derived suppressor cells and enhances the efficacy of adoptive T-cell transfer in breast cancer. *Cancer Res.* **74,** 104–118 (2014).
167. Sevko, A. *et al.* Cyclophosphamide promotes chronic inflammation-dependent immunosuppression and prevents antitumor response in melanoma. *J. Invest. Dermatol.* **133,** 1610–1619 (2013).
168. Diaz-Montero, C. M. *et al.* Increased circulating myeloid-derived suppressor cells correlate with clinical cancer stage, metastatic tumor burden, and doxorubicin–cyclophosphamide chemotherapy. *Cancer Immunol. Immunother.* **58,** 49–59 (2009).
169. Guo, Q. *et al.* IFN-γ producing T cells contribute to the increase of myeloid derived suppressor cells in tumor-bearing mice after cyclophosphamide treatment. *Int. Immunopharmacol.* **12,** 425–432 (2012).
170. Bruchard, M. *et al.* Chemotherapy-triggered cathepsin B release in myeloid-derived suppressor cells activates the Nlrp3 inflammasome and promotes tumor growth. *Nat. Med.* **19,** 57–64 (2013).
171. Shurin, M. R. Dual role of immunomodulation by anticancer chemotherapy. *Nat. Med.* **19,** 20–22 (2013).
172. Germano, G. *et al.* Role of Macrophage Targeting in the Antitumor Activity of Trabectedin. *Cancer Cell* **23,** 249–262 (2013).
173. Lake, R. A. & Robinson, B. W. S. Immunotherapy and chemotherapy--a practical partnership. *Nat. Rev. Cancer* **5,** 397–405 (2005).
174. Mokyr, M. B., Kalinichenko, T., Gorelik, L. & Bluestone, J. A. Realization of the therapeutic potential of CTLA-4 blockade in low-dose chemotherapy-treated tumor-bearing mice. *Cancer Res.* **58,** 5301–5304 (1998).
175. Lesterhuis, W. J. *et al.* Synergistic effect of CTLA-4 blockade and cancer chemotherapy in the induction of anti-tumor immunity. *PloS One* **8,** e61895 (2013).
176. Wu, L., Yun, Z., Tagawa, T., Rey-McIntyre, K. & de Perrot, M. CTLA-4 blockade expands infiltrating T cells and inhibits cancer cell repopulation during the intervals of chemotherapy in murine mesothelioma. *Mol. Cancer Ther.* **11,** 1809–1819 (2012).
177. Ramakrishnan, R. *et al.* Chemotherapy enhances tumor cell susceptibility to CTL-mediated killing during cancer immunotherapy in mice. *J. Clin. Invest.* **120,** 1111–1124 (2010).
178. Lynch, T. J. *et al.* Ipilimumab in combination with paclitaxel and carboplatin as first-line treatment in stage IIIB/IV non-small-cell lung cancer: results from a randomized, double-blind, multicenter phase II study. *J. Clin. Oncol.* **30,** 2046–2054 (2012).

-6-

Dual immune checkpoint blockade synergizes with chemotherapy in a drug-dependent manner in a mouse model for *de novo* mammary tumorigenesis

Kelly Kersten[1], Kim Vrijland[1], Camilla Salvagno[1], Max D. Wellenstein[1], Seth B. Coffelt[1,2], Cheei-Sing Hau[1] and Karin E. de Visser[1]

[1]Division of Immunology, Netherlands Cancer Institute, Amsterdam, The Netherlands

[2]current address: Cancer Research UK Beatson Institute, Institute of Cancer Sciences, University of Glasgow, United Kingdom

In preparation

Abstract

Recent clinical successes with cancer immunotherapy have reinvigorated the field of tumor immunology. Although successful for some patients, the majority does not show clinical benefit, urging the need for novel combinatorial treatment strategies that unleash anti-tumor immune responses. Several studies in genetically engineered mouse models illustrate that *de novo* cancers fail to induce effective anti-tumor T cell responses, but the mechanisms of immune evasion remain largely unclear. In this study we report that tumor-infiltrating T lymphocytes in the *K14Cre;Cdh1$^{F/F}$;Trp53$^{F/F}$* (KEP) conditional mouse model for spontaneous breast cancer are functionally impaired and display an exhausted phenotype. We hypothesized that treatment with immune checkpoint blockade would enhance anti-tumor T cell responses. While dual immune checkpoint blockade with anti-CTLA-4 and anti-PD-1 failed to unleash effective anti-tumor immunity, we observed a synergistic anti-tumor effect when immunotherapy was combined with chemotherapy, albeit in a drug-dependent manner. The synergistic effect of cisplatin and immunotherapy was characterized by increased numbers of intratumoral T cells and more IFNγ production by CD8$^+$ T cells. *In vivo* depletion experiments revealed that the beneficial effect of immunotherapy with cisplatin was CD8$^+$ T cell-dependent. Our results raise the question why cisplatin, and not docetaxel, synergizes with immunotherapy. Preliminary data suggest that cisplatin reprograms the pro-inflammatory tumor microenvironment and enhances the proportion CD103$^+$ dendritic cells, which could improve T cell priming in the tumor-draining lymph nodes. Taken together, our data show that therapeutic regimens including a combination of immune checkpoint blockade and chemotherapy can unleash anti-tumor immunity in breast cancer. Our data also emphasize that the beneficial effect of immune checkpoint blockade is drug-dependent, thus the clinical application of combination strategies for immunotherapy should be subject to careful selection of conventional chemotherapeutic agents.

Introduction

A growing body of literature demonstrate the prognostic value of specific immune cell populations in different cancer types [1,2]. The presence of tumor-infiltrating lymphocytes almost invariably correlates with improved prognosis [3,4]. Moreover, boosting patient's T cells with immunotherapy — including immune checkpoint inhibitors like anti-CTLA-4 and anti-PD-1/PD-L1 — can unleash anti-tumor immune responses resulting in successful attack of immunogenic cancer types like melanoma and lung cancer [5–8]. Breast cancer, on the other hand, is generally not considered an immunogenic type of cancer, illustrated by the observation that the incidence is not increased in patients with a dysfunctional adaptive immune system [9,10], and that most breast tumors have a limited number of mutations [11]. Nevertheless, the presence of tumor-infiltrating lymphocytes correlates with improved clinical outcome, mostly in triple-negative breast cancers [12–15]. Clinical trials that assess the efficacy of immune checkpoint blockade in breast cancer patients are currently ongoing, and objective response rates presented so far range from 5–20% [16–19]. Thus, although effective in some breast cancer patients, the majority does not respond to single-agent immunotherapy. The current challenge is to understand how breast cancers evade anti-tumor immunity, and how we can improve current immunotherapy strategies to improve response rates.

To generate an effective immune response against cancer, several steps have to be set into motion. Tumor-antigens need to be released from cancer cells, and taken up and processed by antigen-presenting cells (APC) to prime T cells in the tumor-draining lymph nodes. Subsequently, these activated tumor-reactive T cells have to traffic to the tumor where they recognize and kill cancer cells [20]. However, tumors can employ a variety of mechanisms — ranging from suboptimal T cell priming, loss of antigen and immunosuppression — to prevent effector T cells to perform their cytolytic function [21]. Several studies in genetically engineered mouse models illustrate that *de novo* cancers frequently fail to spontaneously induce effective anti-cancer immune responses and escape destruction by the adaptive immune system [22–27]. Some studies demonstrate that failure of tumor control by T cells cannot solely be explained by selection of antigen-loss, because cell lines derived from spontaneous tumors are rapidly rejected in immunocompetent mice [22,23,25], suggesting that tumors use alternative pathways to escape from attack by the adaptive immune system.

Despite the successful responses observed in patients with immunogenic cancer types, a growing body of data suggests that the majority of cancer patients cannot be cured merely by inhibiting negative regulators present on T cells, but require more elaborate therapy approaches. Currently, there is an growing interest in exploring combinatorial treatment strategies that include immunotherapy and conventional anti-cancer drugs like chemotherapy to improve response rates. Chemotherapy treatment has both cancer cell-intrinsic and cancer cell-extrinsic effects, some of which are beneficial for anti-tumor immunity [28]. Several experimental studies suggest that certain types of chemotherapy induce cell death that elicits potent anti-tumor immune responses by

enhancing the recruitment and functionality of antigen-presenting cells leading to enhanced T cell priming and activation [29–31]. Moreover, specific chemotherapeutic agents have immunomodulatory properties that influence the proportion and phenotype of myeloid and adaptive immune cells that can result in a shift in the delicate balance between pro- and anti-tumor immunity [28,32]. The current challenge is to find the most optimal combination strategies that induce effective T cell responses that eradicate (disseminated) cancer.

In this study we aim to determine how *de novo* mammary tumors fail to induce effective anti-tumor T cell responses using a conditional mouse model for invasive breast cancer; *i.e. K14Cre;Cdh1$^{F/F}$;Trp53$^{F/F}$* (KEP) mice [33]. We investigate whether immune checkpoint blockade can unleash anti-tumor T cell responses in mammary tumor-bearing KEP mice, and whether combination treatment with conventional chemotherapy can enhance responsiveness to immune checkpoint blockade.

Results

KEP mammary tumor-infiltrating lymphocytes are functionally impaired

Previously, we showed that genetic elimination of the adaptive immune system does not alter the onset or growth kinetics of mammary tumors in a conditional mouse model of invasive breast cancer; *i.e. K14Cre;Cdh1$^{F/F}$;Trp53$^{F/F}$* (KEP) mice [27,34], indicating that *de novo* mammary tumorigenesis does not spontaneously elicit effective anti-tumor immune responses. To investigate whether the T cell compartment is influenced by a spontaneously developing mammary tumor, we analyzed the T lymphocyte influx at different stages during breast cancer progression in KEP mice. While epithelial ducts in normal mammary glands from wild-type mice are almost completely devoid of infiltrating lymphocytes, early neoplastic lesions and established mammary tumors in KEP mice are infiltrated with T lymphocytes (Fig. 1a). While the total leukocyte influx was strongly increased in KEP mammary tumors compared to wild-type mammary glands, the relative proportions of CD8$^+$ and CD4$^+$ T cells of total immune cells were significantly reduced (Fig. 1b). Within the CD4$^+$ T cell population, FOXP3$^+$ regulatory T cells (T_{regs}) were increased in KEP mammary tumors compared to wild-type mammary glands (Fig. 1b), and the CD8/FOXP3 ratio was significantly lower in mammary tumor-bearing KEP mice as compared to wild-type mammary glands (Fig. 1b).

We next set out to assess the phenotype and function of intratumoral and systemic T cells. We found that expression of the negative regulator of T cell activation CTLA-4 was mainly present on FOXP3$^+$ regulatory T cells, as is the case in non-tumor bearing wild-type mice (Fig. 2a, b and Supplementary Fig. 1b). In contrast to CTLA-4, PD-1 levels were strongly induced in all T cell subsets in mammary tumors, blood and lymphoid organs of KEP mice as compared to wild-type mice (Fig. 2c, d and Supplementary Fig. 1b). PD-1 is usually expressed on antigen-experienced T cells, and some studies suggest that PD-1, rather than being a marker of T cell activation, identifies functionally exhausted T cells [35]. We therefore tested whether KEP tumors affect the functional state of T cells by assessing

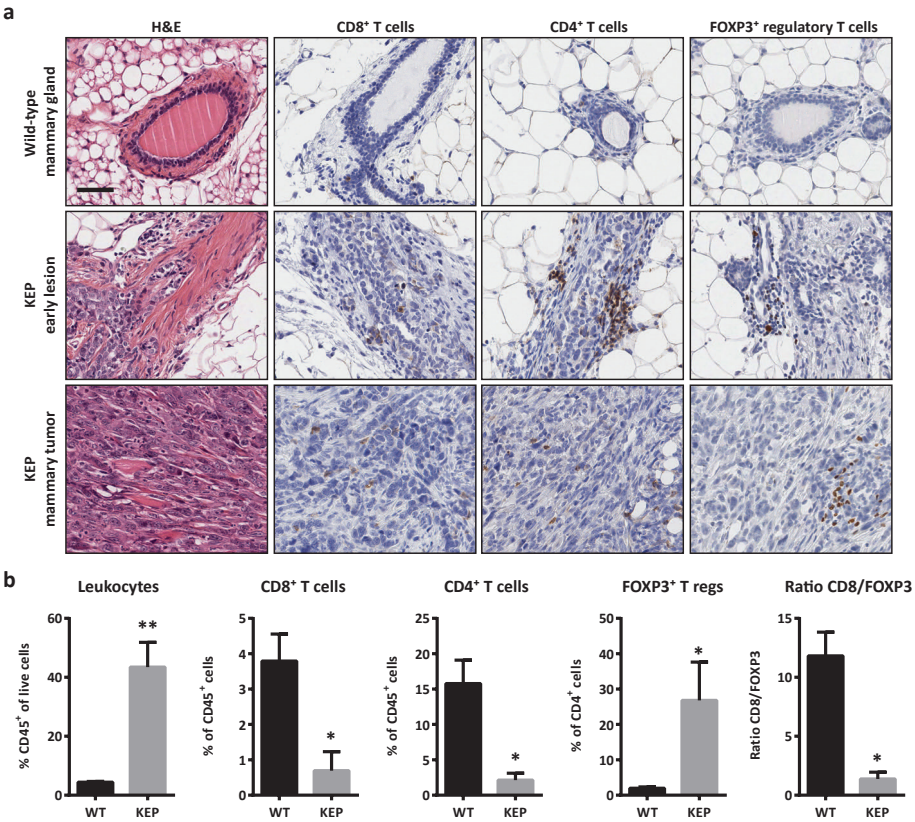

Figure 1. Altered T cell balance in *de novo* mammary tumors in *K14cre;Cdh1$^{F/F}$;Trp53$^{F/F}$* mice. a) Analysis of different populations of T lymphocytes in mammary glands of wild-type mice and early neoplastic lesions and established mammary tumors of *K14cre:Cdh1$^{F/F}$;Trp53$^{F/F}$* mice by immunohistochemistry. Representative images of H&E, CD8$^+$, CD4$^+$ and FOXP3$^+$ stainings are shown. Scale bar 50 µm. b) Quantification of different T cell populations in established mammary tumors in *K14cre;Cdh1$^{F/F}$;Trp53$^{F/F}$* mice (n = 8) and age-matched wild-type mammary glands (n = 7) as determined by flow cytometry. (*p<0.05, **p<0.01, Mann-Whitney U test). All data are ± s.e.m.

their ability to produce IFNγ upon brief *ex vivo* stimulation with PMA and ionomycin in the presence of Golgiplug. Intracellular flow cytometric analysis revealed that ~15% of all CD8$^+$ T cells present in various organs of wild-type mice produce the effector cytokine IFNγ upon *ex vivo* stimulation (Fig. 2e). CD8$^+$ T cells from mammary tumor-bearing KEP mice were severely impaired in their IFNγ production in blood, lymph nodes and tumors when compared to wild-type mice (Fig. 2e). In both wild-type and mammary tumor-bearing KEP mice, IFNγ production by CD4$^+$ T cells was markedly lower than CD8$^+$ T cells, and only showed a modest impairment in KEP tumors (Fig. 2f). In contrast to wild-type mice, the majority of CD8$^+$ and CD4$^+$ T cells in lymphoid organs of KEP mice expressed the activation marker CD44 upon *ex vivo* stimulation (Fig. 2g, h). Interestingly, this activated phenotype was reversed in tumor-infiltrating CD8$^+$ T lymphocytes as compared to wild-

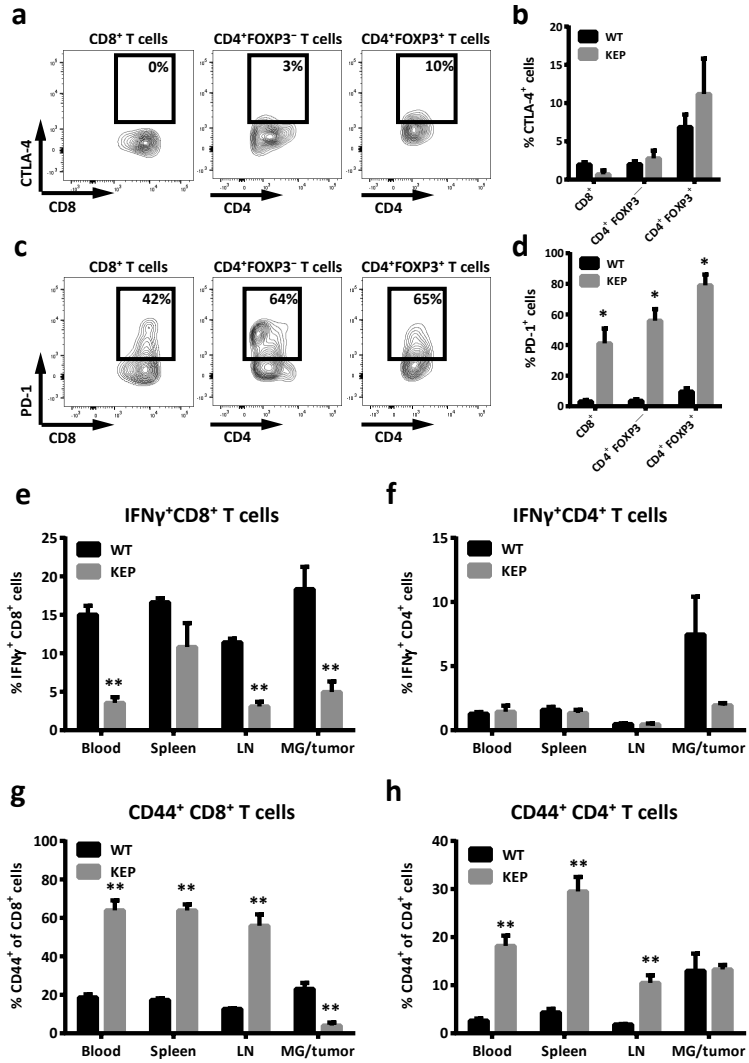

Figure 2. KEP T lymphocytes express immune checkpoint molecules and are functionally impaired. a) Representative flow cytometry contour plots of CTLA-4 expression gated on tumor-infiltrating $CD8^+$, $CD4^+FOXP3^-$ and $CD4^+FOXP3^+$ T cells. b) Quantification of the percentage of CTLA-4 positive cells within the $CD8^+$, $CD4^+FOXP3^-$ and $CD4^+FOXP3^+$ T cell populations infiltrating KEP mammary tumors (n = 3) or wild-type mammary glands (n = 7) based on flow cytometry as shown in (a). c) Representative contour plots of PD-1 expression on tumor-infiltrating $CD8^+$, $CD4^+FOXP3^-$ and $CD4^+FOXP3^+$ T cell populations. d) Quantification of the percentage PD-1 positive cells within the $CD8^+$, $CD4^+FOXP3^-$ and $CD4^+FOXP3^+$ T cell populations infiltrating KEP mammary tumors (n = 3) and wild-type mammary glands (n = 7). e-h) Single cell suspensions generated from blood, spleen, lymph nodes and mammary gland or tumor from wild-type (n = 7) or KEP mice (n = 5) were stimulated *ex vivo* for 3 hrs with PMA and ionomycin in the presence of Golgiplug and analyzed by (intracellular) flow cytometry for IFNγ or CD44 expression. The percentages $IFN\gamma^+$ cells gated on $CD8^+$ (e) and gated on $CD4^+$ T cells (f) are shown. g-h) Quantification of the percentages $CD44^+$ cells gated on $CD8^+$ (g) and $CD4^+$ cells (h) are shown. (*p<0.05, **p<0.01, Mann-Whitney U test). All data are ± s.e.m.

type mice (Fig. 2g). Together, these results suggest that *de novo* mammary tumors induces an antigen-experienced or exhaustive T cell phenotype and renders these cells functionally impaired, even after *ex vivo* stimulation with a strong TCR-independent trigger.

Immune checkpoint blockade in KEP mice does not prolong survival as a single treatment modality, but synergizes with chemotherapy treatment in a drug-dependent manner

Since tumor-infiltrating T cells in KEP mammary tumors express high levels of inhibitory receptors PD-1 and CTLA-4 and display an impaired functionality, we hypothesized that blockade of these immune checkpoints would enhance anti-tumor T cell responses and restrain growth of established tumors. To this end, we treated KEP mice bearing established mammary tumors with dual immune checkpoint blockade (anti-CTLA-4 and anti-PD-1) (Fig. 3a). However, dual checkpoint blockade did not inhibit tumor growth or prolong tumor-specific survival (Fig. 3b).

We next tested whether dual checkpoint blockade could improve the anti-cancer efficacy of clinically relevant chemotherapeutic drugs in mammary tumor-bearing KEP mice. Chemotherapeutic agents influence both tumor-intrinsic and –extrinsic stromal processes, some of which have been reported to be beneficial for anti-tumor immunity, including enhanced antigen-release through cancer cell death [29–31,36], increased permissive state of the tumor microenvironment for anti-tumor immunity [37], and enhanced tumor susceptibility to T cell-mediated killing [38,39] (reviewed in [28]). To investigate whether immunotherapy improves chemotherapy-mediated anti-tumor responses, mammary tumor-bearing KEP mice were treated with the platinum drug cisplatin as a monotherapy or in combination with anti-PD-1 and anti-CTLA-4. Combined treatment of cisplatin with dual immune checkpoint blockade significantly prolonged tumor-specific survival compared to cisplatin alone (Fig. 3b) by delaying tumor growth (Fig. 3c). These results suggest that cisplatin enhances the responsiveness of KEP mammary tumors to immune checkpoint blockade.

Because cisplatin synergized with dual immune checkpoint blockade, we wondered whether both anti-CTLA-4 and anti-PD-1 were required for this effect, or whether the same beneficial effect could be achieved with one of these immunotherapeutic agents. To test this, KEP mice were treated with cisplatin and anti-CTLA-4 or anti-PD-1. Cisplatin with neither immune checkpoint inhibitor prolonged survival compared to cisplatin alone (Fig. 3d), demonstrating that both immune checkpoint inhibitors are required for the synergy with cisplatin.

Next we investigated whether other chemotherapeutic drugs also synergize with anti-CTLA-4 and anti-PD-1. To this end, we turned to the mitotic spindle poison, docetaxel, which is commonly used in breast cancer patients. Like cisplatin, treatment of KEP mice bearing established mammary tumors with docetaxel significantly prolonged tumor-specific survival, albeit to a lesser extent (Fig 3e). However, the combination of docetaxel with dual immune checkpoint blockade did not have a beneficial effect compared to docetaxel alone (Fig. 3e). Together these results demonstrate that chemotherapy synergizes with immune checkpoint blockade in a drug-dependent manner.

Therapeutic synergy between cisplatin and dual immune checkpoint blockade is dependent on CD8⁺ T cells

We next monitored the quantitative and qualitative changes in T cell presence and behavior that may explain the synergy between cisplatin and dual checkpoint blockade, but not with docetaxel. We observed that chemotherapy (either cisplatin or docetaxel) modestly reduced the numbers of tumor-infiltrating CD3⁺ T cells as compared to controls (Fig. 4a). While the addition of immune checkpoint blockade to the cisplatin treatment regimen caused a significant increase in the number of tumor-infiltrating CD3⁺ T cells, the

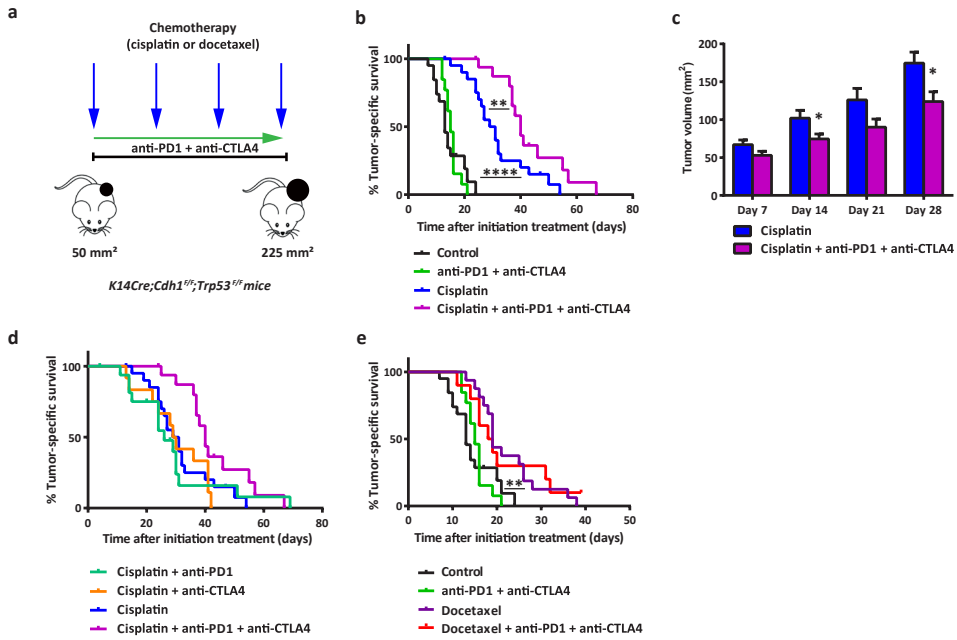

Figure 3. Chemotherapy synergizes with dual immune checkpoint blockade in a drug-dependent manner in KEP mice bearing established spontaneous mammary tumors. a) Experimental design of chemoimmunotherapy treatment. Mammary tumor-bearing KEP mice (25 mm²) are treated with anti-PD-1 and anti-CTLA-4 twice weekly, either alone or combined with cisplatin or docetaxel (4 cycles at MTD dosing). Animals were sacrificed when tumors reached 225 mm². b) Kaplan-Meier survival curves of untreated (n = 20, of which 4 censored), anti-PD-1 and anti-CTLA-4-treated (n = 13), cisplatin-treated (n = 21, of which 2 censored) and cisplatin + anti-PD-1 + anti-CTLA-4-treated KEP mice (n = 17, of which 4 censored). Untreated ≠ cisplatin p<0.0001; cisplatin ≠ cisplatin + anti-PD-1 + anti-CTLA-4 p=0.0091. c) Tumor volume of animals treated with cisplatin and cisplatin + anti-PD-1 + anti-CTLA-4 on day 7, 14, 21 and 28 after initiation treatment. Statistical analysis was conducted using Mann-Whitney U test. All data are ± s.e.m. d) Kaplan-Meier survival curve of cisplatin-treated (n = 21, of which 2 censored), cisplatin + anti-PD-1 + anti-CTLA-4-treated (n = 17, of which 4 censored) (same curves as shown in (b)), cisplatin + anti-PD-1-treated (n = 17, of which 3 censored), and cisplatin + anti-CTLA-4-treated KEP mice (n = 12, of which 1 censored). e) Kaplan-Meier survival curve of untreated (n = 20, of which 4 censored), anti-PD-1 and anti-CTLA-4-treated (n = 13) (same curves as shown in (b)), docetaxel-treated (n = 16) and docetaxel + anti-PD-1 and anti-CTLA-4-treated KEP mice (n = 10, of which 1 censored). Untreated ≠ docetaxel p=0.0016; docetaxel ≠ docetaxel + anti-PD-1 and anti-CTLA-4 p=0.9015. Statistical analysis of curve comparison was conducted using Log-rank test. (*p<0.05, **p<0.01, ***p<0.001, ****p<0.0001).

combination of docetaxel with immune checkpoint blockade did not affect CD3$^+$ T cell numbers when compared to docetaxel monotherapy (Fig. 4a). Next, we set out to assess the absolute numbers of the different T cell subsets infiltrating KEP mammary tumors following the different treatment regimens. CD8$^+$ T cells were not affected by cisplatin treatment, while docetaxel treatment modestly reduced CD8$^+$ T cells (Fig. 4b). In line with the enhanced anti-cancer efficacy of cisplatin and dual checkpoint blockade (Fig. 3b), this combination caused a 3-fold increase in the number of CD8$^+$ T cells infiltrating the tumors as compared to chemotherapy or immunotherapy alone (Fig. 4b). Moreover, the addition of dual checkpoint blockade to docetaxel failed to induce this CD8$^+$ T cell influx (Fig. 4b), consistent with the absence of a synergistic effect of this therapy combination (Fig. 3e). Moreover, the population of CD4$^+$ T cells was strongly increased upon immune checkpoint blockade irrespective of the addition of chemotherapy (Fig. 4c). The majority of the CD4$^+$ T cell population consisted of FOXP3$^+$ T_{regs} (Fig. 4d). The ratio of CD8$^+$/FOXP3$^+$ T cells was more favorable in cisplatin-treated mice compared to docetaxel (Fig. 4e),

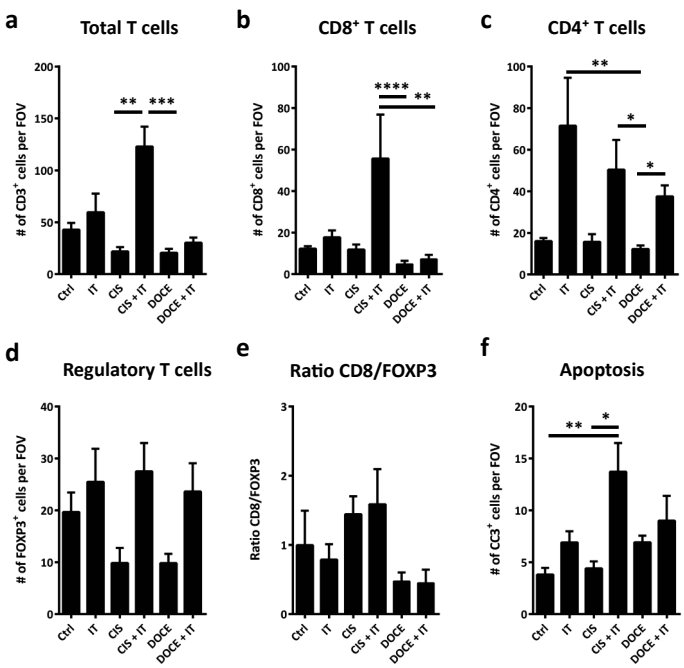

Figure 4. Analysis of intratumoral T cell populations upon chemoimmunotherapy in KEP mice. a-f) Quantification of immunohistochemical stainings of CD3$^+$ T cells (a), CD8$^+$ T cells (b), CD4$^+$ T cells (c), FOXP3$^+$ regulatory T cells (d) and cleaved caspase-3$^+$ cells (f) in end-stage mammary tumors treated with the indicated therapeutic strategies. e) Ratio of CD8$^+$ T cells over FOXP3$^+$ regulatory T cells as determined based on the data in (b) and (d). For all analyses the number of positive cells in 5 microscopic fields of view (FOV) on 40X magnification were counted blindly and the average cell number per FOV is represented. Ctrl = untreated (n = 7), IT = anti-PD-1 and anti-CTLA-4 (n = 6), CIS = cisplatin (n = 10), CIS + IT = cisplatin + anti-PD-1 + anti-CTLA-4 (n = 9), DOCE = docetaxel (n = 10), DOCE + IT = docetaxel + anti-PD-1 + anti-CTLA-4 (n = 8). (*p<0.05, **p<0.01, ***p<0.001, ****p<0.0001, Kruskal-Wallis followed by post-hoc Dunn's test). All data are ± s.e.m.

which was maintained by addition of immunotherapy. Moreover, tumors treated with cisplatin and immune checkpoint blockade showed a significant increase in cleaved caspase-3$^+$ apoptotic cells compared to cisplatin alone (Fig. 4f). These data indicate that the combination of cisplatin and immunotherapy enhances the influx of potential anti-tumor T cell subsets.

We next investigated whether the combination treatment of cisplatin and immune checkpoint blockade affects the functionality of CD8$^+$ T cells as effector cells. We analyzed the activation state of CD8$^+$ and CD4$^+$ T cells in tumor-bearing mice at the therapy-responsive phase, *i.e*. after two cycles of cisplatin, or when tumors reached 100 mm^2 (for the non-cisplatin-treated groups) (Fig. 5a). To determine whether the functionality of T cells is affected by different treatment regimens, we analyzed the potential of CD8$^+$ and CD4$^+$ T cells to produce the effector cytokine IFNγ by intracellular flow cytometry. We found that the proportion of IFNγ-producing tumor-infiltrating CD8$^+$ T cells was not affected by cisplatin treatment, but was enhanced when cisplatin was combined with immune checkpoint blockade, albeit not significant (Fig. 5b, c). The proportion of IFNγ-producing CD4$^+$ T cells was modestly increased in cisplatin treated tumors compared to controls (Fig. 5d), but this was not further enhanced by the addition of immunotherapy.

Since PD-1 is expressed on antigen-experienced T cells, we investigated whether PD-1 expression was effected by the different treatment regimens. PD-1 expression on tumor-infiltrating CD8$^+$ and CD4$^+$ T cells was not influenced by the different therapy conditions (Fig. 5e). Interestingly, the proportion of PD-1-expressing CD4$^+$ and CD8$^+$ T cells was strongly increased in in lymph nodes (Fig. 5f), and spleen (data not shown) upon cisplatin and immunotherapy treatment, perhaps suggesting that these cells might play a role in the survival benefit observed with this combination treatment.

To determine whether the synergistic therapeutic effect of cisplatin and dual checkpoint blockade is dependent on CD8$^+$ T cells, we depleted CD8$^+$ T cells from mammary tumor-bearing KEP mice during treatment with cisplatin and dual checkpoint blockade. We have previously reported that the anti-cancer efficacy of cisplatin alone is independent of CD8$^+$ T cells [27]. Here we show that CD8-depletion abrogated the synergistic effect between cisplatin and dual checkpoint blockade (Fig. 5g), demonstrating that CD8$^+$ T cells are required for the therapeutic benefit of dual checkpoint blockade in combination with cisplatin.

In summary, these results show that cisplatin and docetaxel have a differential effect on the recruitment of different subsets of tumor-infiltrating T cells. Cisplatin treatment combined with dual immune checkpoint blockade results in higher numbers and enhanced IFNγ production by CD8$^+$ T cells, which are required for the synergistic effect of these therapies.

Immunomodulatory properties of cisplatin

We further explored the potential mechanisms underlying the synergy between cisplatin and immune checkpoint blockade in the KEP model. First, we hypothesized that cisplatin, which induces DNA damage by crosslinking the DNA, might cause an increase in somatic

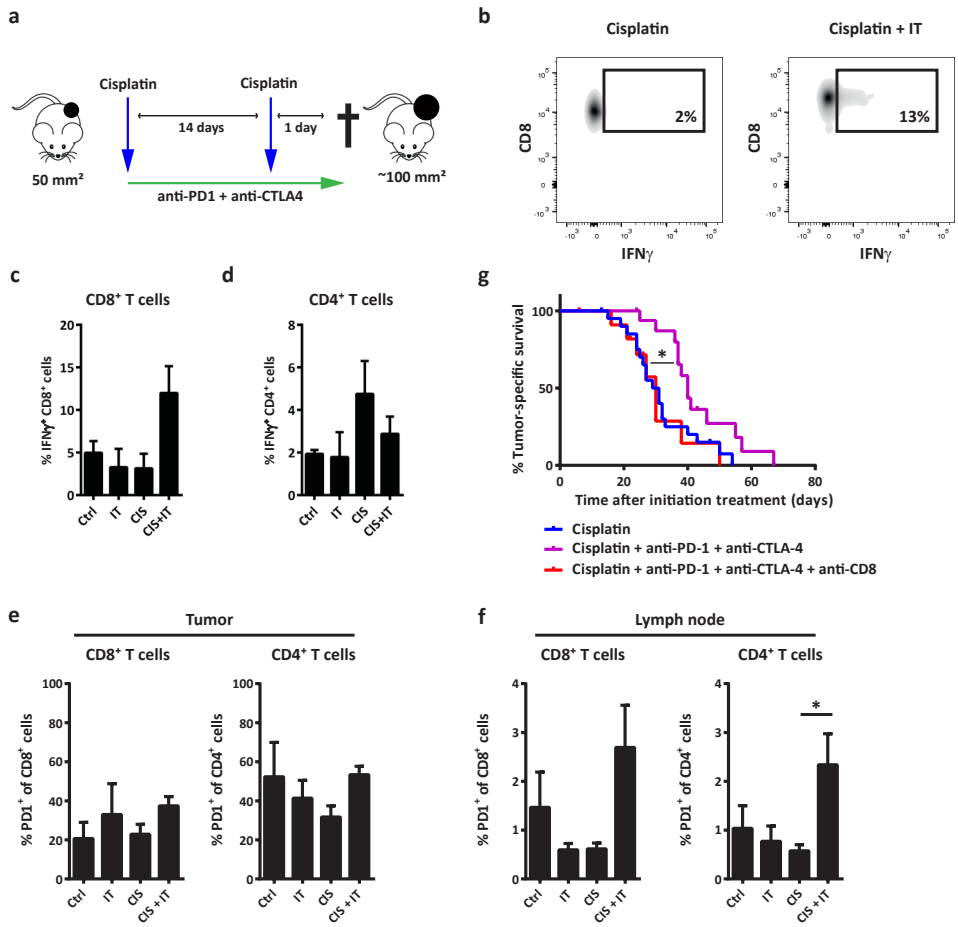

Figure 5. Synergy between cisplatin and dual immune checkpoint blockade in KEP mice is dependent on CD8⁺ T cells. a) Experimental design. Mammary tumor-bearing KEP mice (25 mm^2) were left untreated (Ctrl) or treated with anti-PD-1 + anti-CTLA-4 (IT), 2 cycles of cisplatin alone (CIS) or in combination with anti-PD-1 and anti-CTLA-4 (CIS + IT). Animals were sacrificed one day after 2nd cisplatin treatment and anti-PD-1 + anti-CTLA-4 treatment (for CIS and CIS + IT groups), or when tumors reached 100 mm^2 (for Ctrl and IT groups). b) Representative density plots of IFNγ-producing CD8⁺ T cells in tumors treated as indicated as determined by intracellular flow cytometry. c-d) Quantification of IFNγ⁺ cells gated on CD8⁺ T cells (c) and CD4⁺ T cells (d) in KEP tumors treated as indicated. Ctrl (n = 6), IT (n = 3), CIS (n = 5) and CIS + IT (n = 5). e) Quantification of PD-1⁺ cells gated on CD8⁺ (left) and CD4⁺ T cells (right) by flow cytometry in KEP tumors treated as indicated. Ctrl (n = 6), IT (n = 3), CIS (n = 5) and CIS + IT (n = 5). f) Quantification of PD-1⁺ cells gated on CD8⁺ (left) and CD4⁺ T cells (right) in lymph nodes of tumor-bearing KEP mice treated as indicated. Ctrl (n = 6), IT (n = 3), CIS (n = 5) and CIS + IT (n = 5). (*p<0.05, Kruskal-Wallis followed by Dunn's multiple comparisons test). All data are ± s.e.m. g) Kaplan-Meier survival curve of cisplatin-treated (n = 21, of which 2 censored), cisplatin + anti-PD-1 + anti-CTLA-4-treated (n = 17, of which 4 censored), and cisplatin + anti-PD-1 + anti-CTLA-4 + anti-CD8-treated KEP mice (n = 12, of which 4 censored). The curves of cisplatin- and cisplatin + anti-PD-1 + anti-CTLA-4-treated KEP mice are the same as in Fig. 3b. Statistical analysis of curve comparison was conducted using Log-rank test. (p=0.0159 by Log-rank test).

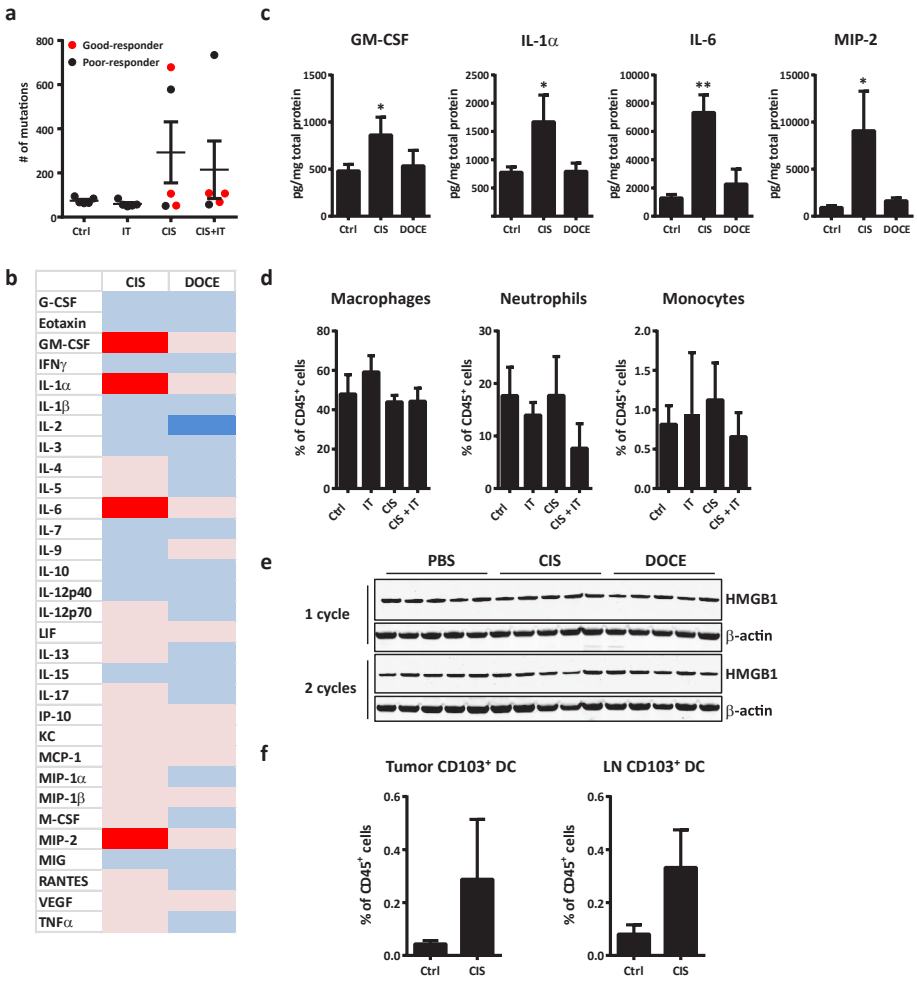

Figure 6. Immunomodulatory properties of cisplatin. a) Number of non-synonymous mutations in the genome (with a somatic score >29) as determined by whole exome sequencing of KEP mammary tumors treated as indicated (n = 5 per group). See Material and Methods section for details on sequencing. Red circles indicate individual mice that lived longer, and black circled indicate mice that lived shorter than the median of the total treatment group. b) Protein expression of cytokines in KEP mammary tumors treated with one cycle of cisplatin (n = 5) or docetaxel (n = 5) determined by a premixed Luminex-based cytokine expression array. Values are normalized to untreated tumors (n = 5) and $\log_2$ transformed. Light blue and red indicates non-significant reduction and increase, respectively, as compared to untreated tumors. Bright blue and red indicate significant reduction and increase, respectively, as compared to untreated tumors. c) Raw data of the expression of GM-CSF, IL1α, IL6 and MIP-2 represented in the heat-map in (b). (*p<0.05, Mann-Whitney U test) All data are ± s.e.m. d) Flow cytometric analysis of the proportion of $CD11b^+F4/80^+$ macrophages, $CD11b^+Ly6G^+$ neutrophils and $CD11b^+Ly6C^+$ monocytes gated of $CD45^+$ cells in KEP mammary tumors treated as indicated. Ctrl (n = 6), IT (n = 3), CIS (n = 5), CIS + IT (n = 5). e) Western Blot analysis of HMGB1 expression in protein lysates from KEP mammary tumors treated with 1 or 2 cycles of chemotherapy (according to experimental design in Fig. 5a) as indicated. β-actin was used as a loading control. f) Flow cytometric analysis of $CD11b^-CD11c^+MHCII^+CD103^+$ dendritic cells as gated of total $CD45^+$ cells in mammary tumors and lymph nodes (LN) of KEP mice untreated (n = 5) or treated with cisplatin (n = 5). (*p<0.05, Mann-Whitney U test). All data are ± s.e.m.

mutations that could serve as neo-antigens for $CD8^+$ T cells, thus increasing the 'foreignness' of mammary tumors for the immune system. To test this hypothesis, we performed whole exome sequencing on genomic DNA isolated from untreated KEP tumors and tumors treated with immunotherapy alone, cisplatin alone or cisplatin and immunotherapy, and determined the number of tumor-specific non-synonymous genetic variants per sample. Although 2/5 cisplatin-treated tumors, and 1/5 cisplatin and immunotherapy-treated tumors showed increased numbers of mutations as compared to untreated tumors, the number of mutations did not correspond to the response to treatment of individual mice (Fig. 6a), which makes it unlikely that the induction of additional mutations is the underlying reason for the synergy of cisplatin with immune checkpoint blockade.

It has been hypothesized that a T cell-inflamed tumor microenvironment contributes to clinical response to immune checkpoint blockade [40]. Because previous studies report an immunomodulatory role for cisplatin in vaccination approaches [41–43], we wondered whether cisplatin reprograms the tumor microenvironment of KEP mammary tumors to be more permissive for tumor-reactive T cells. To this end we took an unbiased approach and determined the expression pattern of a large panel of inflammatory cytokines in KEP tumors treated with cisplatin or docetaxel, as compared to untreated controls. Unlike docetaxel-treated tumors, cisplatin-treated tumors showed a statistically significant increase in the expression of GM-CSF, IL1α, IL6 and MIP-2 compared to controls (Fig. 6b, c). Since these cytokines and chemokines have an important role in regulating myeloid immune cells, we wondered whether this differential cytokine expression affected the composition of tumor-infiltrating myeloid cells upon cisplatin monotherapy or in combination with immunotherapy as compared to controls. Flow cytometric analysis of different myeloid populations in KEP tumors treated with cisplatin with or without the addition of immunotherapy revealed no significant changes in the proportions of macrophages, neutrophils and monocytes upon treatment (Fig. 6d).

Besides being an important factor for the development of macrophages, neutrophils and monocytes, GM-CSF is also required for differentiation of dendritic cells (DCs) [44]. Therefore we assessed whether the activation of $CD8^+$ T cells upon chemoimmunotherapy was a result of enhanced activation of DCs and T cell priming. Previous studies imply that specific types of chemotherapy induce the release of danger signals from cancer cells, resulting in improved function and maturation of DC to enhance anti-tumor T cell responses [45,46]. One of the key danger signals from tumors undergoing this so-called immunogenic cell death is the release of high mobility group protein B1 (HMGB1) in the extracellular space where it can bind to and trigger Toll-like receptors (TLRs) on antigen-presenting cells enhancing their functionality [45]. To investigate whether cisplatin and docetaxel induce the release of HMGB1 in KEP tumors, we performed Western Blot analysis on whole tumor lysates from KEP mice treated with 1 or 2 cycles of these chemotherapeutics. We did not detect changes in HMGB1 levels in spontaneous mammary tumors treated with chemotherapy as compared to untreated controls (Fig. 6e), suggesting that the beneficial effect of cisplatin as a combination partner for immune checkpoint inhibition does not depend on increased exposure to the danger signal HMGB1.

To further explore the potential role of dendritic cells in chemotherapy response, we analyzed the presence of different DC populations in tumors and lymph nodes of mammary tumor-bearing mice upon cisplatin treatment as compared to untreated controls. Preliminary data show that the presence of $CD11b^{+}CD11c^{+}MHCII^{+}$ conventional DC and $CD11b^{-}CD11c^{+}MHCII^{+}B220^{+}$ plasmacytoid DC are unaltered by cisplatin treatment (data not shown). However, the presence of $CD103^{+}$ DC is modestly increased in mammary tumors and lymph nodes of mice treated with cisplatin compared to untreated controls (Fig. 6f). Previous studies demonstrate that these $CD103^{+}$ dendritic cells are important and potent activators of anti-tumor T cells [47,48]. These results, although preliminary, suggest that these cells may be involved in enhanced priming of $CD8^{+}$ T cells upon cisplatin and immunotherapy treatment. Further studies are required to determine the exact role of $CD103^{+}$ DCs in cisplatin-induced priming of anti-tumor T cell responses in the KEP model.

Discussion

Cancer immunotherapy has initiated a turning point in the treatment of cancer patients. A growing amount of clinical and experimental data show that therapeutic strategies aimed at enhancing anti-tumor immunity can successfully fight cancer [49]. However, a substantial proportion of patients do not respond to immunotherapy approaches, indicating that there is room for improvement. To obtain more insights into the potential mechanisms of immune evasion, we need to get a better understanding of the qualitative and quantitative impact of *de novo* tumors on T cell biology. Breast cancer is not considered a highly immunogenic type of cancer. The mutational load of human breast cancers is relatively low as compared to melanoma and lung cancer [11], although this varies per breast cancer subtype [50]. Moreover, the incidence of breast cancer is not increased in immunocompromised patients [9,10]. In line with this, we and others have shown in experimental mouse models for *de novo* mammary tumorigenesis, that mammary tumors do not spontaneously elicit effective anti-tumor immune responses [24,26,27,51]. How these *de novo* tumors fail to induce potent anti-tumor T cell responses remains largely unknown.

Our work presented here, using a spontaneous mouse model of invasive breast cancer, *i.e. K14cre;Cdh1$^{F/F}$;Trp53$^{F/F}$* (KEP) mice [33], reports that *de novo* mammary tumors are immune evasive. Compelling evidence indicates that genetic instability and the number of somatic mutations in tumors increases the foreignness and thereby the potential of T lymphocytes to recognize their targets [52–55]. Whole exome sequencing analysis of *de novo* tumors in the KEP model revealed that these tumors have a relatively low mutational load. Additional reported mechanisms of T cell evasion are impaired T cell trafficking, preventing these cells from entering the tumor [21], and downregulation of MHC class I expression on cancer cells rendering them invisible for T cells [56]. Although the levels of MHC expression were not assessed in this study, T cells are able to infiltrate KEP tumors. The decreased CD8/FOXP3 ratio suggests that KEP mammary tumors induce a T cell

suppressive environment as compared to wild-type mammary glands. Further analyses of these T cells revealed that they are functionally impaired. T cells in lymphoid organs and tumors of KEP mice highly expressed the negative regulators of T cell activation CTLA-4 and PD-1, and displayed a poor capacity to produce the effector cytokine IFNγ, as compared to wild-type mice. Thus *de novo* mammary tumors negatively influence the T cell compartment. Since the tumor antigens on KEP tumors are unknown, we cannot discriminate between tumor-specific T cells and T cells with other specificities. However, the observation that *ex vivo* TCR-independent triggering with PMA and ionomycin failed to induce IFNγ production from KEP-derived $CD8^+$ T cells may suggest that KEP tumor induce a general state of immunosuppression. At the same time, the expression of PD-1 and CD44 on a subset of $CD8^+$ and $CD4^+$ T cells in lymphoid organs of KEP mice may suggest that these cells have encountered tumor-antigen. Interestingly, the expression of CD44 on $CD8^+$ T cells in the tumor was strongly reversed, indicating that these T cells are impaired possibly by a local network of immunosuppression. Together these data demonstrate that T cells are able to successfully infiltrate *de novo* KEP mammary tumors, but become functionally impaired and fail to control tumor growth.

One way to overcome the functional impairment of T cells is the use of immune checkpoint inhibitors. Based on the promising response rates in clinical trials for treatment of advanced melanoma and lung cancer that show long-term durable responses in a fraction of patients [5–8], blockade of T cell checkpoints is now being extended to other cancer types with varying results [16–19,57–59]. We hypothesized that the functional impairment of T cells in the KEP mammary tumor model could be reversed by blocking CTLA-4 and PD-1 with immune checkpoint inhibitors, which may enhance anti-tumor T cell responses against KEP mammary tumors. However, this was not the case when immunotherapy was administered as a monotherapy treatment modality. Pre-existing $CD8^+$ T cells are present in *de novo* KEP tumors – which correlates with improved response to immunotherapy in melanoma patients [60–63]–, but treatment with immune checkpoint blockade fails to unleash effective anti-tumor T cell responses. These results suggest that additional (tumor-induced) mechanisms are at work that could potentially dampen anti-tumor immunity or protect tumors from destruction by the immune system.

Tumors often induce an inflammatory and immunosuppressive microenvironment that is unfavorable for T cells to perform their effector function [21,64]. For example, tumor-associated macrophages and neutrophils are notorious for their T cell suppressive properties [65,66]. Using the *MMTV-PyMT* breast cancer mouse model it was shown that macrophages counteract the anti-cancer efficacy of $CD8^+$ T cells in response to chemotherapy [51,67]. Moreover, preliminary results of a clinical trial targeting macrophages in patients with various types of solid malignancies showed an increased intratumoral CD8/CD4 ratio [68], suggesting that macrophages blunt anti-tumor immune responses. In addition, we have previously reported that KEP mammary tumors elicit a systemic immunosuppressive state, characterized by the expansion of neutrophils that dampen anti-tumor T cell responses, which facilitates metastasis formation [34]. Depletion of

neutrophils was sufficient to unleash anti-tumor T cell responses that inhibited the formation metastasis in distant organs [34]. In the study reported here, we did not observe significant changes in macrophage or neutrophil proportions upon treatment with dual immune checkpoint blockade, although it remains to be established whether immune checkpoint blockade influences the polarization state of these cells. It would be interesting to see whether the lack of response to dual immune checkpoint blockade in the KEP model could be rescued by targeting neutrophils. Interestingly, elevated numbers of neutrophils expressing PD-L1 correlate with poor response to anti-CTLA-4 treatment in melanoma patients [69], suggesting that targeting neutrophils would enhance the response to immune checkpoint inhibitors. Indeed, recent experimental studies show that CXCR2-mediated targeting of neutrophils synergizes with PD-1 blockade [70,71].

Another potential roadblock in generating effective anti-tumor T cell responses is caused by defective T cell priming by dendritic cells. Tumors often show dysfunctional recruitment and activation of dendritic cells affecting tumor-antigen capture and cross-presentation, which causes a failure in T cell priming to kick start the anti-tumor immune response [72]. Several strategies can be employed to overcome this obstacle and to potentially enhance anti-tumor immunity, for example by chemotherapy.

Current studies are focused on combining immunotherapy with conventional anti-cancer drugs like targeted therapy, chemotherapy and radiation to obtain the best of both worlds: rapid induction of cell death and activation of durable anti-tumor T cell responses. Here we report that combining immune checkpoint blockade with chemotherapy enhances tumor-specific survival in a breast cancer mouse model, albeit in a drug-dependent manner. Our results raise the question why cisplatin, and not docetaxel, synergizes with immunotherapy. Several studies in experimental mouse models have suggested that certain chemotherapeutic agents, including doxorubicin, oxaliplatin and cyclophosphamide, induce so-called 'immunogenic cell death' characterized by the release of HMGB1, that activates dendritic cells resulting in enhanced anti-tumor immune responses [29–31,36]. Cisplatin – which provides synergy with dual immune checkpoint blockade in the KEP model – is not considered an inducer of immunogenic cell death [46], and did not affect HMGB1 release in KEP tumors. These results suggest another role for cisplatin in modulating anti-tumor immune responses in the KEP model. We show that cisplatin – although it is a DNA damaging agent – increases the mutational load of only 3 out of 10 KEP tumors, but did not correlate with the response to therapy. Thus it is unlikely that increased foreignness is the reason for the synergistic effect between cisplatin and dual immune checkpoint blockade, and not with the mitotic spindle-poison docetaxel.

An alternative hypothesis is that cisplatin induces a microenvironment that is more permissive to anti-tumor immunity. In line with this, preclinical studies using vaccination strategies against HPV-induced cervical cancer show enhanced anti-tumor responses in mice treated with cisplatin by sensitizing cancer cells to CTL-mediated killing [41–43]. Our data show that cisplatin-treated KEP tumors express a distinct pattern of pro-inflammatory cytokines including GM-CSF, IL1α, IL6 and MIP-2, as compared to docetaxel-

treated tumors. These factors have been described to regulate myeloid cells, however their increased expression did not change the proportion of macrophages, neutrophils and monocytes upon cisplatin treatment alone or in combination with dual checkpoint blockade. Interestingly, in cancer cell inoculation models it has been shown that cisplatin induces the accumulation of intratumoral CD11c$^+$ DC [37]. In line with this, our preliminary data show that cisplatin increases the proportions of CD103$^+$ DCs in KEP tumors and lymph nodes. Recent studies show that CD103$^+$ DCs, although their presence is scarce, are very potent activators of anti-tumor T cells in various experimental models [47,48,67]. Moreover, their presence is required for successful responses to immune checkpoint blockade [73].

Future studies are required to reveal the exact mechanisms underlying cisplatin-mediated activation of anti-tumor T cell responses in the KEP model, potentially via the activation of CD103$^+$ DCs. Transplantation of GFP-tagged KEP tumors in recipient mice would allow us to determine whether chemotherapy affects the ability of DC subsets to phagocytose tumor-derived debris and their ability to traffic to the tumor-draining LN to present these potential antigens to T cells. If cisplatin indeed enhances the functionality of CD103$^+$ DC in these experiments, it will be important to validate these findings: (1) by boosting this DC population with FLT3L or poly I:C [47,48,73], or (2) to use CD103-deficient *Batf3*$^{-/-}$ mice as recipients for transplantation studies to confirm the necessity of these cells for therapeutic response to cisplatin and dual immune checkpoint blockade. Moreover, it would be interesting to explore the potential role of CD4$^+$ T cells in the therapeutic synergy between cisplatin and dual immune checkpoint blockade. *In vivo* CD4-depletion studies in the KEP model will reveal whether CD4$^+$ T cells are needed for the synergy between cisplatin and dual immune checkpoint blockade, for example via direct cytotoxicity against cancer cells, or by providing 'help' in CD8$^+$ T cell priming [74].

Altogether our data show that immune evasive cancers, like breast cancer, could benefit from immune checkpoint blockade when combined with the proper chemotherapy. Across different breast cancer subtypes the vast majority of immunological studies is performed in triple-negative breast cancer (TNBC) because this subtype shows increased genetic instability – in part caused by mutations in BRCA1/2 genes – and therefore it is hypothesized to have a higher mutational load as compared to other subtypes [50]. Moreover, the lymphocytic infiltrate in TNBC is more prominent then in hormone receptor-positive breast cancers [75]. However, this does not necessarily mean that the functional significance of immune cells in hormone receptor-positive breast cancer, such as lobular cancers, is negligible. Strikingly, a CD103-associated gene signature provided strong prognostic value in breast cancer patients across all subtypes; patients with a 'high CD103-signature' had improved survival compared to patients with a 'low CD103-signature' [47]. More specifically, a recent study showed that CD103$^+$ and CD8$^+$ cells are enriched and correlate with improved survival in basal-like breast cancer [76]. It will be interesting to see whether patients with high CD103 expression have superior response to immune checkpoint blockade. Moreover, does treatment with certain chemotherapeutic agents affect the presence or function of CD103$^+$ DC, and how does this correlate with

tumor-reactive $CD8^+$ T cells and the response of breast cancer patients to immune checkpoint blockade? Our results presented here, obtained in a mouse model for *de novo* immune evasive breast cancer, shed more light on the therapeutic combination strategies that might unleash anti-tumor immunity. Ongoing clinical trials testing the clinical efficacy of immune checkpoint inhibitors in combination with different types of chemotherapeutic agents should confirm these preclinical results.

Materials and methods

Animal studies

The generation of *K14cre;Cdh1$^{F/F}$;Trp53$^{F/F}$* (KEP) mice has been described in detail [33]. KEP mice were backcrossed to the FVB/N background. Mammary tumor formation was monitored twice weekly by palpation and caliper measurements. Animals were kept in individually ventilated cages and food and water were provided *ad libitum*. Animal experimental procedures were approved by the Animal Ethics Committee of the Netherlands Cancer Institute and performed in accordance with national and institutional guidelines for Animal Care and Use.

In vivo immune checkpoint blockade and chemotherapy treatment

Mammary tumor-bearing KEP animals were treated twice weekly with 100 µg anti-CTLA-4 (clone 9D9; BioXcell) and 100 µg anti-PD-1 (clone RMP1-14;BioXcell) by intraperitoneal injection. Cisplatin was administered intravenously dosed at 6mg/kg per dose for 4 cycles with 14 day intervals. Docetaxel was administered intravenously dosed at 15 mg/kg (diluted in NaCl) per dose for 4 cycles with 7 day intervals. Chemotherapy and immunotherapy treatment was initiated simultaneously when mammary tumors reached a size of 50 mm^2 and was continued until animals were sacrificed once their primary tumor reached 225 mm^2. For time point experiments chemotherapy and immunotherapy treatment was initiated simultaneously when mammary tumors reached a size of 50 mm^2 and was continued for 2 chemotherapy cycles. Animals were sacrificed one day after their 2nd chemotherapy cycle and administration of checkpoint inhibitors, or when (non-chemotherapy-treated) tumor reached ~100 mm^2. Animals were randomized before initiating treatment. Animals that were sacrificed due to chemotherapy-related toxicity (weight loss or lethargy),or ulcerated tumors were censored in tumor-specific survival graphs.

Surface and intracellular staining for flow cytometry

Tissue preparation for flow cytometry was performed as described previously [34]. Briefly, tissues were collected in ice-cold PBS. Blood samples were collected in tubes containing heparin (Leo Pharma, USA) and treated with NH_4 lysis buffer. Tumors and mammary glands were mechanically chopped using a McIlwain Tissue Chopper (Mickle Laboratory Engineering Co. Ltd, Guildford, UK) and digested for 1 hour at 37°C in a digestion mix of 3 mg/ml collagenase type A (Roche) and 25 µg/ml DNAse (Sigma), in serum-free DMEM

(Invitrogen). Reactions were terminated by addition of DMEM containing 8% FCS. Cell suspensions were dispersed through a 70 µm cell strainer (BD Falcon). All single cell suspensions were treated with NH_4 lysis buffer to remove red blood cells.

For *ex vivo* cytokine stimulation, single cells were collected at 1500 rpm for 5 min in a round bottom 96-wells tissue culture plate (Thermo Scientific) in IMDM containing 8% FCS, 100 IU/ml penicillin, 100 µg/ml streptomycin (Invitrogen) and 0.5% β-mercaptoethanol. Cells were stimulated with phorbol 12-myristate 13-acetate (PMA; 50 ng/ml) and ionomycin (1 µM) in the presence of Golgi-Plug™(BD) for 3 h at 37°C.

For flow cytometric staining, either stimulated or unstimulated single cells were collected at 1500 rpm for 5 min and resuspended in PBS containing 1% BSA (Sigma-Aldrich, USA). Single cell suspensions were plated in round bottom 96-wells plates (Thermo Scientific) and incubated for 30 min in the dark at 4°C with different combinations of fluorescently labelled monoclonal antibodies. For intracellular staining cells were washed twice with PBS containing 1% BSA and fixed and permeabilised using the Cytofix/Cytoperm™ kit (BD) according to manufacturer's instructions. Cells were subsequently incubated for 30 min in the dark at 4°C with antibodies against IFNγ and FOXP3. Fixable Viability Dye APC eFluor780 (eBioscience) or 7AAD viability staining solution (eBioscience) was added in order to exclude dead cells. Flow cytometric analysis was performed on a BD LSRII using Diva Software (BD Biosciences, USA). Data analyses were performed using FlowJo Software version 10.0 (Tree Star, Ashland, OR, USA).

The following antibody panels were used:
Myeloid – CD45-eFluor605NC (1:100; clone 30-F11), CD11b-BV650 (1:400; clone M1/70; Biolegend), Ly6G-AlexaFluor700 (1:400; clone 1A8; BD Pharmingen), Ly6C-eFluor450 (1:400; clone HK1.4), F4/80-APC-eFluor780 (1:200; clone BM8), CD49b-APC (1:400; clone DX5), PD-1-FITC (CD279; 1:100; clone J43), CTLA-4-PE (CD152; 1:50; clone UC10-4F10-11), CD3-PerCp- Cy5.5 (1:100; clone 145-2c11; BD Bioscience), 7AAD.

Lymphoid I - CD45-eFluor605NC (1:100; clone 30-F11), CD11b-BV650 (1:400; clone M1/70; Biolegend), CD19-APC-eFluor780 (1:200; clone eBio1D3), CD3-PE-Cy7 (1:200; clone 145-2C11), CD8-PerCP-eFluor710 (1:400; clone 53-6.7), CD4-eFluor450 (1:200; clone GK1.5), CTLA-4-PE (CD152; 1:50; clone UC10-4F10-11), PD-1-FITC (CD279; 1:100; clone J43), FOXP3-APC (1:50; clone FJK-16s), CD62L-AlexaFluor700 (1:400; clone MEL-14), Fixable Viability Dye eFluor® 780.

Lymphoid II - CD45-eFluor605NC (1:100; clone 30-F11), CD11b- APC-eFluor780 (1:200; clone M1/70), CD19-APC-eFluor780 (1:200; clone eBio1D3), CD3-PE-Cy7 (1:200; clone 145-2C11), CD8-PerCP-eFluor710 (1:400; clone 53-6.7), IFNγ-eFluor450 (1:100; clone xmg1.2), CD4-PE (1:200; clone GK1.5), CD44-FITC (1:200; clone IM7), FOXP3-APC (1:50; clone FJK-16s), CD62L-AlexaFluor700 (1:400; clone MEL-14), Fixable Viability Dye eFluor® 780. All antibodies were obtained from eBiosciences, unless indicated otherwise.

Immunohistochemistry
Formalin-fixed tissues were processed by routine procedures. The following antibodies were used: CD3; clone SP7; cat #RM-9107, Thermo Scientific. CD4; cat # 14-9766-80, eBioscience. CD8, cat # 14-0808, eBioscience. FOXP3, cat # 14-5773, eBioscience. Cleaved caspase-3 (Asp175), cat # 9661, Cell Signaling. Antigen retrieval was performed by Tris/EDTA PH 9.0, except for FOXP3 were citrate buffer was used. The number of positive cells was quantified by blind scoring of 5 fields of view (FOV) at 40X magnification by at least two researchers. Stained slides were digitally processed using the Aperio ScanScope (Aperio, Vista, CA, USA) and captured using ImageScope software version 11.0.2 (Aperio, Vista, CA, USA). Brightness and contrast for representative images were adjusted equally among groups.

Luminex-based cytokine array
Multiplex quantification of inflammatory cytokines and chemokines was performed using the premixed 32-plex Mouse Immunology Multiplex assay (Milliplex-Map, MCYTMAG-70K-PX32, Millipore). Assays and tissue preparations were performed according to manufacturer's recommendations. 100 µg of total protein from lysed tissues was used for measurements. Fluorescence was measured on a Luminex FlexMap3D System using xPonent 4.0 software (Luminex Corporation).

Whole exome sequencing
DNA of 20 KEP mammary tumors with strain-matching reference (toe tip DNA of female wild-type littermates) was isolated using the DNA Easy Blood & Tissue Kit (Qiagen) according to manufacturer's protocol and was dissolved in 1x TE buffer. DNA in samples was sheared to get mainly fragments of 300bp which were enriched for exome sequences using the Agilent SureSelect Mouse Exome Enrichment capture set (Agilent, 5190-4641). DNA content and quality were measured using a Qubit Bioanalyzer (2100) before sequencing 100 basepairs paired-end on an Illumina HiSeq 2500. Overlapping paired-end reads were joined using ea-utils fastq-join [77], and adapter sequences removed using cutadapt [78], version 1.8.1. Joined overlapping reads were aligned single end, others paired-end, both with BWA [79], version 0.7.10 using the mem algorithm against the ensembl mouse genome, GRCm38 [80]. Aligned reads were sorted on genomic coordinates and stored in bam format using SAMtools [81], version 0.1.19, after which potential PCR duplicates were tagged using Picardtools [82] MarkDuplicates, version 1.128. Single end and paired end aligned bam files for identical samples were recombined using SAMtools merge. Indels were realigned and base qualities recalibrated using GATK [83], version 3.3-0. To detect somatic variants, matched samples were compared using strelka [84] version 1.0.14. Resulting indels and somatic variants were remerged with bcftools merge. Variants were annotated using snpeff [85] and snpsift [85] using the dbSNP database [86] version 142 resulting in annotated variant call format (vcf) files. Using in-house tools, variants known in FVB mice were marked and vcf files were converted to tables.

Western Blot

Tissue lysates that were used for Luminex-based cytokine array were used for Western Blot procedures. Protein lysates were clarified by centrifugation at 14.000 rpm for 5 min at 4°C and protein content was measured using Bradford Protein Assay (Bio-rad) according to manufacturer's instructions. Protein lysates diluted in 4x LDS Sample buffer (Invitrogen) and supplemented with 100mM dithiothreitol (DTT) were incubated at 95°C for 5 min. Equal amounts of protein (30µg) were separated by SDS-PAGE electrophoresis using NuPAGE 4-12% Bis-Tris midi gels (Invitrogen) and transferred onto Whatman Protran nitrocellulose membranes (Sigma-Aldrich) using the Trans-Blot Turbo system (Bio-Rad) according to the manufacturer's instructions. Membranes were blocked in 10% Western blocking solution (Roche) in TBS, washed and incubated overnight at 4°C with primary antibodies against HMGB1 (1:1000; cat # 3935; Cell Signaling) and β-actin (1:5000; cat # A1978; Sigma Aldrich) diluted in 5% Western blocking solution (Roche) in TBST. After washing, membranes were probed with the appropriate IRdye-conjugated secondary antibodies Donkey-α-rabbit IgG, IRdye800CW (1:10000; cat # 32212; Li-cor) and Donkey-α-mouse IgG, IRdye680RD (1:10000; cat # 68072; Licor) in 5% Western blocking solution (Roche) in TBST. Infrared signals were visualized using the Odyssey Imaging System (LI-COR) and images were captured using Image Studio version 2.0 (LICOR).

Statistical analysis

Data analyses were performed using GraphPad Prism version 6.01 (GraphPad Software Inc, La Jolla, CA, USA). Applied analyses are indicated in the corresponding legends. Sample sizes were based on previous experience with the models [34,27]. Differences with a $p<0.05$ were considered statistically significant.

Author contributions

K.K., K.V. and K.E.dV. conceived the ideas and designed the experiments. K.K., K.V., C.S., M.D.W., S.B.C. and C-S.H. performed the experiments. K.K., K.V., C.S., M.D.W., S.B.C. and C-S.H. and K.E.dV. analyzed the data. K.K. and K.E.dV. wrote the paper.

Acknowledgements

We wish to acknowledge the Netherlands Cancer Institute Laboratory Animal Facility, Animal Pathology Facility, Flow Cytometry Facility, and Genomics Core Facility for technical assistance. We thank Roel Kluin, Arno Velds and Ron Kerkhoven for their assistance, expertise and analysis of whole exome sequencing data. This study was supported by a European Research Council Consolidator award (INFLAMET 615300), the European Union (FP7 MCA-ITN 317445 TIMCC) and the Beug Foundation for Metastasis Research to K.E.d.V. K.E.d.V. is an EMBO Young Investigator.

References

1. Bindea, G. *et al.* Spatiotemporal Dynamics of Intratumoral Immune Cells Reveal the Immune Landscape in Human Cancer. *Immunity* **39,** 782–795 (2013).
2. Gentles, A. J. *et al.* The prognostic landscape of genes and infiltrating immune cells across human cancers. *Nat. Med.* **21,** 938–945 (2015).
3. Galon, J. *et al.* Type, density, and location of immune cells within human colorectal tumors predict clinical outcome. *Science* **313,** 1960–1964 (2006).
4. Mlecnik, B. *et al.* Integrative Analyses of Colorectal Cancer Show Immunoscore Is a Stronger Predictor of Patient Survival Than Microsatellite Instability. *Immunity* **44,** 698–711 (2016).
5. Hodi, F. S. *et al.* Improved survival with ipilimumab in patients with metastatic melanoma. *N. Engl. J. Med.* **363,** 711–723 (2010).
6. Topalian, S. L. *et al.* Safety, activity, and immune correlates of anti-PD-1 antibody in cancer. *N. Engl. J. Med.* **366,** 2443–2454 (2012).
7. Brahmer, J. R. *et al.* Safety and activity of anti-PD-L1 antibody in patients with advanced cancer. *N. Engl. J. Med.* **366,** 2455–2465 (2012).
8. Wolchok, J. D. *et al.* Nivolumab plus ipilimumab in advanced melanoma. *N. Engl. J. Med.* **369,** 122–133 (2013).
9. Stewart, T., Tsai, S. C., Grayson, H., Henderson, R. & Opelz, G. Incidence of de-novo breast cancer in women chronically immunosuppressed after organ transplantation. *Lancet* **346,** 796–798 (1995).
10. Frisch, M., Biggar, R. J., Engels, E. A., Goedert, J. J. & AIDS-Cancer Match Registry Study Group. Association of cancer with AIDS-related immunosuppression in adults. *JAMA* **285,** 1736–1745 (2001).
11. Alexandrov, L. B. *et al.* Signatures of mutational processes in human cancer. *Nature* **500,** 415–421 (2013).
12. Mittendorf, E. A. *et al.* PD-L1 expression in triple-negative breast cancer. *Cancer Immunol. Res.* **2,** 361–370 (2014).
13. Ibrahim, E. M., Al-Foheidi, M. E., Al-Mansour, M. M. & Kazkaz, G. A. The prognostic value of tumor-infiltrating lymphocytes in triple-negative breast cancer: a meta-analysis. *Breast Cancer Res. Treat.* **148,** 467–476 (2014).
14. Wimberly, H. *et al.* PD-L1 Expression Correlates with Tumor-Infiltrating Lymphocytes and Response to Neoadjuvant Chemotherapy in Breast Cancer. *Cancer Immunol. Res.* **3,** 326–332 (2015).
15. Cimino-Mathews, A. *et al.* PD-L1 (B7-H1) expression and the immune tumor microenvironment in primary and metastatic breast carcinomas. *Hum. Pathol.* **47,** 52–63 (2016).
16. Emens, L. A. *et al.* Abstract PD1-6: Inhibition of PD-L1 by MPDL3280A leads to clinical activity in patients with metastatic triple-negative breast cancer [abstract]. In: Proceedings of the Thirty-Seventh Annual CTRC-AACR San Antonio Breast Cancer Symposium: 2014 Dec 9-13; San Antonio, TX. Philadelphia (PA): AACR; *Cancer Res.* **75,** Abstract nr PD1-6 (2015).
17. Dirix, L. Y. *et al.* Abstract S1-04: Avelumab (MSB0010718C), an anti-PD-L1 antibody, in patients with locally advanced or metastatic breast cancer: A phase Ib JAVELIN solid tumor trial [abstract]. In: Proceedings of the Thirty-Eighth Annual CTRC-AACR San Antonio Breast Cancer Symposium: 2015 Dec 8-12; San Antonio, TX. Philadelphia (PA): AACR; *Cancer Res.* **76,** Abstract nr S1-04 (2016).
18. Rugo, H. S. *et al.* Preliminary efficacy and safety of pembrolizumab (MK-3475) in patients with PD-L1–positive, estrogen receptor-positive (ER+)/HER2-negative advanced breast cancer enrolled in KEYNOTE-028. [abstract]. In: Proceedings of the Thirty-Eighth Annual CTRC-AACR San Antonio Breast Cancer Symposium: 2015 Dec 8-12; San Antonio, TX. Philadelphia (PA): AACR; *Cancer Res.* **76,** Abstract nr S5-07 (2016).
19. Nanda, R. *et al.* Pembrolizumab in Patients With Advanced Triple-Negative Breast Cancer: Phase Ib KEYNOTE-012 Study. *J. Clin. Oncol.* (2016). doi:10.1200/JCO.2015.64.8931
20. Chen, D. S. & Mellman, I. Oncology meets immunology: the cancer-immunity cycle. *Immunity* **39,** 1–10 (2013).
21. Joyce, J. A. & Fearon, D. T. T cell exclusion, immune privilege, and the tumor microenvironment. *Science* **348,** 74–80 (2015).
22. Willimsky, G. & Blankenstein, T. Sporadic immunogenic tumours avoid destruction by inducing T-cell tolerance. *Nature* **437,** 141–146 (2005).
23. Garbe, A. I. *et al.* Genetically induced pancreatic adenocarcinoma is highly immunogenic and causes spontaneous tumor-specific immune responses. *Cancer Res.* **66,** 508–516 (2006).
24. DeNardo, D. G. *et al.* CD4(+) T cells regulate pulmonary metastasis of mammary carcinomas by enhancing protumor properties of macrophages. *Cancer Cell* **16,** 91–102 (2009).
25. DuPage, M. *et al.* Endogenous T cell responses to antigens expressed in lung adenocarcinomas delay malignant tumor progression. *Cancer Cell* **19,** 72–85 (2011).

26. Ciampricotti, M. *et al.* Development of metastatic HER2(+) breast cancer is independent of the adaptive immune system. *J. Pathol.* **224,** 56–66 (2011).
27. Ciampricotti, M., Hau, C.-S., Doornebal, C. W., Jonkers, J. & de Visser, K. E. Chemotherapy response of spontaneous mammary tumors is independent of the adaptive immune system. *Nat. Med.* **18,** 344–346 (2012).
28. Kersten, K., Salvagno, C. & de Visser, K. E. Exploiting the Immunomodulatory Properties of Chemotherapeutic Drugs to Improve the Success of Cancer Immunotherapy. *Front. Immunol.* **6,** 516 (2015).
29. Obeid, M. *et al.* Calreticulin exposure dictates the immunogenicity of cancer cell death. *Nat. Med.* **13,** 54–61 (2007).
30. Apetoh, L. *et al.* Toll-like receptor 4-dependent contribution of the immune system to anticancer chemotherapy and radiotherapy. *Nat. Med.* **13,** 1050–1059 (2007).
31. Ma, Y. *et al.* Anticancer chemotherapy-induced intratumoral recruitment and differentiation of antigen-presenting cells. *Immunity* **38,** 729–741 (2013).
32. Coffelt, S. B. & de Visser, K. E. Immune-mediated mechanisms influencing the efficacy of anticancer therapies. *Trends Immunol.* **36,** 198–216 (2015).
33. Derksen, P. W. B. *et al.* Somatic inactivation of E-cadherin and p53 in mice leads to metastatic lobular mammary carcinoma through induction of anoikis resistance and angiogenesis. *Cancer Cell* **10,** 437–449 (2006).
34. Coffelt, S. B. *et al.* IL-17-producing γδ T cells and neutrophils conspire to promote breast cancer metastasis. *Nature* **522,** 345–348 (2015).
35. Barber, D. L. *et al.* Restoring function in exhausted CD8 T cells during chronic viral infection. *Nature* **439,** 682–687 (2006).
36. Ghiringhelli, F. *et al.* Activation of the NLRP3 inflammasome in dendritic cells induces IL-1beta-dependent adaptive immunity against tumors. *Nat. Med.* **15,** 1170–1178 (2009).
37. Kang, T. H. *et al.* Chemotherapy Acts as an Adjuvant to Convert the Tumor Microenvironment into a Highly Permissive State for Vaccination-Induced Antitumor Immunity. *Cancer Res.* **73,** 2493–2504 (2013).
38. Sin, J.-I. *et al.* Adoptive Transfer of Human Papillomavirus E7-specific CTL Enhances Tumor Chemoresponse Through the Perforin/Granzyme-mediated Pathway. *Mol. Ther.* **17,** 906–913 (2009).
39. Ramakrishnan, R. *et al.* Chemotherapy enhances tumor cell susceptibility to CTL-mediated killing during cancer immunotherapy in mice. *J. Clin. Invest.* **120,** 1111–1124 (2010).
40. Gajewski, T. F. The Next Hurdle in Cancer Immunotherapy: Overcoming the Non-T-Cell-Inflamed Tumor Microenvironment. *Semin. Oncol.* **42,** 663–671 (2015).
41. Tseng, C.-W. *et al.* Pretreatment with cisplatin enhances E7-specific CD8+ T-Cell-mediated antitumor immunity induced by DNA vaccination. *Clin. Cancer Res.* **14,** 3185–3192 (2008).
42. Lee, S. Y. *et al.* Intratumoral injection of therapeutic HPV vaccinia vaccine following cisplatin enhances HPV-specific antitumor effects. *Cancer Immunol. Immunother.* **62,** 1175–1185 (2013).
43. van der Sluis, T. C. *et al.* Vaccine-induced tumor necrosis factor-producing T cells synergize with cisplatin to promote tumor cell death. *Clin. Cancer Res.* **21,** 781–794 (2015).
44. Hamilton, J. A. & Achuthan, A. Colony stimulating factors and myeloid cell biology in health and disease. *Trends Immunol.* **34,** 81–89 (2013).
45. Krysko, D. V. *et al.* Immunogenic cell death and DAMPs in cancer therapy. *Nat. Rev. Cancer* **12,** 860–875 (2012).
46. Bezu, L. *et al.* Combinatorial Strategies for the Induction of Immunogenic Cell Death. *Front. Immunol.* **6,** (2015).
47. Broz, M. L. *et al.* Dissecting the Tumor Myeloid Compartment Reveals Rare Activating Antigen-Presenting Cells Critical for T Cell Immunity. *Cancer Cell* **26,** 638–652 (2014).
48. Salmon, H. *et al.* Expansion and Activation of CD103+ Dendritic Cell Progenitors at the Tumor Site Enhances Tumor Responses to Therapeutic PD-L1 and BRAF Inhibition. *Immunity* **44,** 924–938 (2016).
49. Sharma, P. & Allison, J. P. The future of immune checkpoint therapy. *Science* **348,** 56–61 (2015).
50. Budczies, J. *et al.* Classical pathology and mutational load of breast cancer – integration of two worlds. *J. Pathol.* **1,** 225–238 (2015).
51. DeNardo, D. G. *et al.* Leukocyte Complexity Predicts Breast Cancer Survival and Functionally Regulates Response to Chemotherapy. *Cancer Discov.* **1,** 54–67 (2011).
52. Snyder, A. *et al.* Genetic basis for clinical response to CTLA-4 blockade in melanoma. *N. Engl. J. Med.* **371,** 2189–2199 (2014).
53. Rizvi, N. A. *et al.* Cancer immunology. Mutational landscape determines sensitivity to PD-1 blockade in non-small cell lung cancer. *Science* **348,** 124–128 (2015).
54. Le, D. T. *et al.* PD-1 Blockade in Tumors with Mismatch-Repair Deficiency. *N. Engl. J. Med.* **372,** 2509–2520 (2015).
55. Schumacher, T. N. & Schreiber, R. D. Neoantigens in cancer immunotherapy. *Science* **348,** 69–74 (2015).

56. Pardoll, D. M. The blockade of immune checkpoints in cancer immunotherapy. *Nat. Rev. Cancer* **12,** 252–264 (2012).
57. Powles, T. *et al.* MPDL3280A (anti-PD-L1) treatment leads to clinical activity in metastatic bladder cancer. *Nature* **515,** 558–562 (2014).
58. Motzer, R. J. *et al.* Nivolumab for Metastatic Renal Cell Carcinoma: Results of a Randomized Phase II Trial. *J. Clin. Oncol.* **33,** 1430–1437 (2015).
59. Ansell, S. M. *et al.* PD-1 blockade with nivolumab in relapsed or refractory Hodgkin's lymphoma. *N. Engl. J. Med.* **372,** 311–319 (2015).
60. Taube, J. M. *et al.* Association of PD-1, PD-1 ligands, and other features of the tumor immune microenvironment with response to anti-PD-1 therapy. *Clin. Cancer Res.* **20,** 5064–5074 (2014).
61. Herbst, R. S. *et al.* Predictive correlates of response to the anti-PD-L1 antibody MPDL3280A in cancer patients. *Nature* **515,** 563–567 (2014).
62. Tumeh, P. C. *et al.* PD-1 blockade induces responses by inhibiting adaptive immune resistance. *Nature* **515,** 568–571 (2014).
63. Rooney, M. S., Shukla, S. A., Wu, C. J., Getz, G. & Hacohen, N. Molecular and genetic properties of tumors associated with local immune cytolytic activity. *Cell* **160,** 48–61 (2015).
64. Palucka, A. K. & Coussens, L. M. The Basis of Oncoimmunology. *Cell* **164,** 1233–1247 (2016).
65. Ruffell, B. & Coussens, L. M. Macrophages and Therapeutic Resistance in Cancer. *Cancer Cell* **27,** 462–472 (2015).
66. Coffelt, S. B., Wellenstein, M. D. & de Visser, K. E. Neutrophils in cancer: neutral no more. *Nat. Rev. Cancer* **16,** 431–446 (2016).
67. Ruffell, B. *et al.* Macrophage IL-10 blocks CD8+ T cell-dependent responses to chemotherapy by suppressing IL-12 expression in intratumoral dendritic cells. *Cancer Cell* **26,** 623–637 (2014).
68. Ries, C. H. *et al.* Targeting tumor-associated macrophages with anti-CSF-1R antibody reveals a strategy for cancer therapy. *Cancer Cell* **25,** 846–859 (2014).
69. Gebhardt, C. *et al.* Myeloid Cells and Related Chronic Inflammatory Factors as Novel Predictive Markers in Melanoma Treatment with Ipilimumab. *Clin. Cancer Res.* **21,** 5453–5459 (2015).
70. Highfill, S. L. *et al.* Disruption of CXCR2-mediated MDSC tumor trafficking enhances anti-PD1 efficacy. *Sci. Transl. Med.* **6,** 237ra67 (2014).
71. Steele, C. W. *et al.* CXCR2 Inhibition Profoundly Suppresses Metastases and Augments Immunotherapy in Pancreatic Ductal Adenocarcinoma. *Cancer Cell* **29,** 832–845 (2016).
72. Melief, C. J. M. Cancer Immunotherapy by Dendritic Cells. *Immunity* **29,** 372–383 (2008).
73. Sánchez-Paulete, A. R. *et al.* Cancer Immunotherapy with Immunomodulatory Anti-CD137 and Anti-PD-1 Monoclonal Antibodies Requires BATF3-Dependent Dendritic Cells. *Cancer Discov.* **6,** 71–79 (2016).
74. Bevan, M. J. Helping the CD8+ T-cell response. *Nat. Rev. Immunol.* **4,** 595–602 (2004).
75. Stanton, S. E., Adams, S. & Disis, M. L. Variation in the Incidence and Magnitude of Tumor-Infiltrating Lymphocytes in Breast Cancer Subtypes: A Systematic Review. *JAMA Oncol.* (2016). doi:10.1001/jamaoncol.2016.1061
76. Wang, Z.-Q. *et al.* CD103 and Intratumoral Immune Response in Breast Cancer. *Clin. Cancer Res.* (2016). doi:10.1158/1078-0432.CCR-16-0732
77. Aronesty, E. Comparison of sequencing utility programs. *Open Bioinforma. J.* **7,**
78. Martin, M. Cutadapt removes adapter sequences from high-throughput sequencing reads. *EMBnet. journal* **17,** 10–12 (2011).
79. Heng, Li. Aligning sequence reads, clone sequences and assembly contigs with BWA-MEM. *ArXiv13033997v2 Q-BioGN Httpbio-Bwasourceforgenet*
80. Mouse Genome Sequencing Consortium *et al.* Initial sequencing and comparative analysis of the mouse genome. *Nature* **420,** 520–562 (2002).
81. Li, H. *et al.* The Sequence Alignment/Map format and SAMtools. *Bioinformatics* **25,** 2078–2079 (2009).
82. picardtools: http://broadinstitute.github.io/picard.
83. DePristo, M. A. *et al.* A framework for variation discovery and genotyping using next-generation DNA sequencing data. *Nat. Genet.* **43,** 491–498 (2011).
84. Saunders, C. T. *et al.* Strelka: accurate somatic small-variant calling from sequenced tumor-normal sample pairs. *Bioinformatics* **28,** 1811–1817 (2012).
85. Cingolani, P. *et al.* A program for annotating and predicting the effects of single nucleotide polymorphisms, SnpEff: SNPs in the genome of Drosophila melanogaster strain w1118; iso-2; iso-3. *Fly (Austin)* **6,** 80–92 (2012).
86. Database of Single Nucleotide Polymorphisms (dbSNP). Bethesda (MD): National Center for Biotechnology Information, National Library of Medicine. (dbSNP mouse 142). Available from: http://www.ncbi.nlm.nih.gov/SNP/.

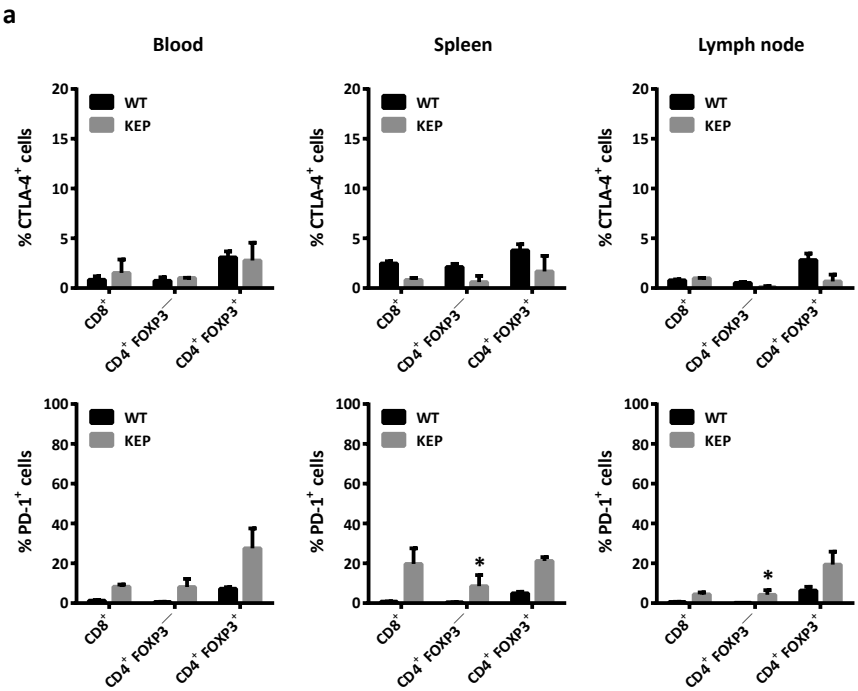

Supplementary Figure 1. Phenotypic analysis of systemic subsets of T lymphocytes in wild-type and mammary tumor-bearing KEP mice. a) Flow cytometric analysis of the expression of CTLA-4 and PD-1 on different subsets of T lymphocytes in blood, spleen and lymph node of wild-type (n = 7) and mammary tumor-bearing KEP mice (n = 3). (*p<0.05, Mann-Whitney U test) All data are ± s.e.m.

-7-

General discussion

Metastasis is a multistep process by which cancer cells disseminate from the primary tumor and spread throughout the body, emphasizing the notion that cancer is a systemic disease. Every step in the metastatic cascade is tightly regulated by the reciprocal interactions between stromal cells and cancer cells modulating both cancer cell-intrinsic and -extrinsic processes. Over the past decades, several studies have demonstrated that immune cells play an important role in cancer progression and metastasis [1,2]. Many solid cancers are characterized by chronic inflammation – one of the hallmarks of cancer [3]. Via the secretion of chemokines, cytokines and growth factors tumors elicit a systemic inflammatory response and mobilize a plethora of immune cell types that not only affect the primary tumor, but also distant organs and potential (pre-) metastatic niches. Depending on the external cues, immune cells can exert anti-tumor or pro-tumor functions. For example, macrophages are notorious for their tumor-promoting properties [4]. In contrast, $CD8^+$ T cells can kill cancer cells when activated properly [5].

Despite the recent clinical successes of cancer immunotherapy by means of immune checkpoint blockade (anti-CTLA-4 and anti-PD-1) in patients with advanced melanoma and lung cancer, the majority of patients does not respond [6–9]. Compelling evidence demonstrates that a combination of both cancer cell-intrinsic as well as cancer cell-extrinsic parameters determines the likelihood of clinical response to cancer immunotherapy. This growing knowledge will lead to the discovery of biomarkers to optimize patient stratification and, ultimately, will lead to the design of improved cancer immunotherapy strategies.

In this thesis I describe how mammary tumors in a genetically engineered mouse model for spontaneous breast cancer metastasis, induce an inflammatory cascade that results in systemic immunosuppression to facilitate spontaneous metastasis formation in distant organs. This cascade is characterized by the expansion and polarization of pro-metastatic neutrophils. We demonstrate that different tumor-derived factors dictate neutrophils to actively suppress anti-tumor T cells to prevent destruction of disseminated cancer cells. Interfering with these factors resulted in relief of immunosuppression and decreased multi-organ metastasis in mice. Because the clinical availability of drugs interfering with immunosuppressive networks is limited, we sought for other options to enhance anti-tumor immune responses, like immune checkpoint blockade. We show that immune checkpoint blockade is not sufficient to enhance anti-tumor T cell responses in KEP mice. However, combination treatment with conventional chemotherapeutics synergizes with immune checkpoint blockade in a drug-dependent manner. Together these studies suggest that direct targeting of immunosuppressive factors or the use of immunomodulatory chemotherapeutics might be an attractive strategy to improve the efficacy of immunotherapy to target metastatic breast cancer.

Immune-mediated mechanisms of metastasis

The controversial role of neutrophils in metastasis

Among circulating leukocytes, neutrophils are most abundant. Neutrophils play an essential role in fighting infections and wound healing. However, their role in cancer progression and metastasis is poorly understood and controversial [10,11]. In cancer patients, high neutrophil abundance in the circulation correlates with an increased risk of metastasis [12–14]. Moreover, based on computational analysis of gene expression data of more than 39 subtypes of cancer, a neutrophil-associated gene signature emerged as a significant predictor of poor survival [15]. But what is the functional significance of these cells during metastasis?

Similar as in patients, several preclinical mouse cancer models show elevated neutrophil proportions in the circulation and accumulation in peripheral organs during tumor progression [16–18]. However, their role in metastasis remains controversial. While some studies report anti-metastatic functions of neutrophils [19,20], others demonstrate their pro-metastatic properties [17,18,21,22]. Using the 4T1 breast cancer inoculation model it was reported that tumor-entrained neutrophils inhibit metastatic seeding in the lung via direct cytotoxicity towards disseminated cancer cells [19]. Moreover, a recent study showed that a subpopulation of neutrophils expressing the MET proto-oncogene protects against the formation of metastasis [20]. In contrast, using the *MMTV-PyMT* mammary tumor model it was shown that neutrophils facilitate metastasis to the lung by propagating the number of metastasis-initiating cancer cells via the secretion of leukotrienes [18]. In addition, using the conditional KEP mammary tumor model we reported that neutrophils promote metastasis by dampening anti-tumor immunity (chapter 3) [17]. Depletion of $Ly6G^+$ neutrophils resulted in enhanced activity of $CD8^+$ T cells and reduced metastatic burden. Co-depletion of neutrophils and $CD8^+$ T cells reversed the metastatic phenotype. Gene expression analysis revealed the differential expression of several immunosuppressive factors in tumor-entrained neutrophils compared to wild-type neutrophils, among which *Nos2* (encoding the enzyme iNOS) was dramatically increased. Functional studies confirmed that KEP neutrophils actively suppress the anti-tumor reactivity of $CD8^+$ T cells via iNOS, and therefore these cells could be classified as myeloid-derived suppressor cells, although this nomenclature is far from accurate [11,23]. The findings described in the previous studies raise the question of how neutrophils are instructed to perform these opposing functions in different preclinical models of cancer.

Inflammatory cues dictate neutrophil expansion and phenotype

Neutrophils display a remarkable plasticity. Previous studies demonstrate that the polarization of neutrophils is context-dependent, and that external cues dictate their phenotypic diversity and opposing functions. Many of the molecules involved in homeostatic regulation of neutrophils are upregulated by tumors [16,17,21,24], allowing cancer cells to hijack the functional properties of these cells to their benefit. For example, a study

using mice bearing subcutaneous mesotheliomas showed that TGFβ was responsible for shifting the phenotype of tumor-associated neutrophils from an anti-tumor state to a pro-tumor and immunosuppressive state [25]. Moreover, we and others have shown that the expansion and polarization of neutrophils is dependent on G-CSF which promotes granulopoiesis in the bone marrow [16,17,21,24]. Phenotypic analyses of pro-metastatic neutrophils in the KEP model revealed that these neutrophils have an immature nuclear morphology and express the hematopoietic stem cell marker cKIT [17], suggesting that these cells might have left the bone marrow early before they are fully differentiated. In homeostatic conditions, once outside the bone marrow, the population of neutrophils is maintained by tight regulation of G-CSF-dependent granulopoiesis via IL23 and IL17 signaling. When neutrophils have migrated to distant tissues and have performed their function, they undergo apoptosis and are phagocytosed by macrophages and dendritic cells. These phagocytes then secrete IL23 which stimulates the production of IL17 by γδ T cells, αβ T cells and other lymphoid cells [26,27]. Lower levels of IL17 resulted in reduced G-CSF levels and reduced neutrophil abundance in the circulation [26], illustrating the importance of this homeostatic regulator. In the KEP model we found that G-CSF-dependent expansion and polarization of neutrophils is tightly regulated by tumor-induced IL17-producing γδ T cells [17]. Similarly, in human colorectal cancer, IL-17 producing γδ T cells induce intratumoral accumulation of polymorphonuclear-myeloid-derived suppressor cells (PMN-MDSC) [28], which share many features with neutrophils.

Taken together, experimental findings that demonstrate a pro-metastatic role for neutrophils, and data demonstrating that tumors hijack neutrophil regulatory pathways support the notion that targeting neutrophil expansion, recruitment or function would be an interesting therapeutic strategy to relieve immunosuppression and prevent metastasis formation.

The pro-inflammatory tumor microenvironment induces immune evasion

At present, one of the most important questions is: how do tumors initiate an inflammatory microenvironment causing downstream systemic effects that promote metastasis formation? Cancer-associated inflammation is characterized by the mobilization and recruitment of a variety of immune cells of which macrophages are most abundant. Using the KEP breast cancer mouse model we found that mammary tumors secrete a variety of inflammatory cytokines among which the chemokine CCL2 was most abundantly expressed (chapter 4 and [17]). CCL2 is a cytokine largely known for its involvement in the recruitment of $CCR2^{+}$ monocytes from the bone marrow to other sites in the body where they differentiate into macrophages [29]. Clinical studies have reported that increased expression of CCL2 correlates with the presence of macrophages, tumor invasiveness and poor prognosis in patients with invasive breast cancer [30–32]. However, preclinical studies in experimental mouse models suggests that the role of CCL2 in cancer progression and metastasis is dual [33,34]. While some studies report a protective role for CCL2 during cancer progression [19,34,35], others demonstrate its tumor-promoting abilities [36–39].

Like neutrophils, macrophages are highly plastic cells and their role in tumorigenesis is dictated by a plethora of environmental stimuli. Generally, tumor-associated macrophages (TAMs) are considered pro-tumorigenic in nature since they are able to promote angiogenesis, stimulate matrix remodeling and enhance tumor cell invasion and motility [4]. In line with this, compelling evidence in experimental mouse models suggest the pro-tumorigenic role of macrophages [40–42], and their role in metastasis formation [40,43,44]. Moreover, several studies have shown that macrophages suppress anti-tumor T cell responses to protect cancer cells from attack by the adaptive immune system [41,44,45]. The polarization of macrophages has been studied extensively both *in vitro* and *in vivo* and led to the nomenclature of tumoricidal (M1) and pro-tumorigenic (M2) macrophages [46], but recently it has become clear that these polarization states represent two extremes and might not recapitulate the situation as occurs *in vivo* [47].

In the KEP breast cancer model we show that tumor-derived CCL2 promotes breast cancer metastasis via activation of a systemic inflammatory cascade that suppresses anti-tumor immune responses. We demonstrate that CCL2 regulates the expression of IL1β by CCR2-expressing TAMs in the primary tumor. IL1β activates systemic IL17-producing γδ T cells which triggers G-CSF-dependent neutrophil expansion and polarization. Blockade of CCL2 in KEP mice resulted in reduced IL17-producing γδ T cells, reduced proportions of cKIT$^+$ neutrophils and enhanced activity of CD8$^+$ T cells. To determine whether these observations would translate to human breast cancer patients, we analyzed gene expression data of different breast cancer subtypes. We found that expression of *CCL2* and *IL1B* is enriched in human breast cancers of the basal subtype, and their expression is highly correlated across all breast cancer subtypes. In line with our findings in the KEP model, *CCL2* and *IL1B* gene expression correlates with macrophage-marker CD68, suggesting that macrophage-rich tumors express high levels of CCL2 and IL1β. Indeed, computational analysis of the intratumoral immune composition by Cibersort [15,48] revealed that basal tumors have significantly more macrophages compared to HER2$^+$ and luminal tumors. Our experimental data provide novel insight into the underlying mechanisms of how CCL2 — via different immunological steps — induces systemic immunosuppression to facilitate breast cancer metastasis. Additional studies in metastatic breast cancer patients are required to investigate whether there is a correlation between intratumoral levels of *CCL2* and *IL1B* and (the phenotype of) circulating neutrophils and tumor-reactivity of T cells. Moreover, it would be interesting to explore how different tumor characteristics (genetic drivers, hormone-receptor and HER2 status and morphology) affect the different steps of this inflammatory cascade.

Together these clinical and preclinical findings suggest that tumor-associated macrophages could be an interesting therapeutic target to block tumor-induced immunosuppression and unleash anti-tumor immune responses to fight disseminated cancer.

Targeting tumor-induced immunosuppression to unleash anti-tumor immunity

Extrinsic determinants of anti-cancer immunity

Besides the presence of tumor-associated antigens, an obvious requirement for kick-starting a successful anti-tumor T cell response is proper T cell priming. Tumors often show dysfunctional recruitment and activation of dendritic cells (DCs), which are the most potent APCs for initiating T cell responses. Tumor-infiltrating DCs frequently display an immature phenotype, fail to migrate to the tumor-draining lymph node and provide the proper co-stimulatory molecules to successfully activate T cells [49]. A thorough analysis of the antigen-presenting myeloid immune cell compartment in the *MMTV-PyMT* mammary tumor model showed that intratumoral DCs are able to ingest and present tumor antigens to T cells, but they fail to activate them [50]. Nevertheless, even in these immunoevasive tumors, a rare population of $CD103^+$ DCs is able to prime tumor antigen-specific T cells [51].

An additional requirement for successful response to immunotherapy is the ability of T cells to migrate into the tumor and to kill cancer cells. Indeed, the presence of pre-existing $CD8^+$ T cells in tumor margins is associated with positive outcome to anti-PD-1 therapy in advanced melanoma patients [52]. Failure to enter the tumor can be due to the lack of T cell-recruiting inflammatory cytokines, aberrant vasculature or the dense fibrotic structure of tumors [53]. But even when T cells are able to infiltrate the tumor they usually face a local immunosuppressive microenvironment that impairs their functionality. This can be induced by PD-L1 expression on cancer cells and/or immune cells, or via other mediators like neutrophils and macrophages that secrete factors that counteract T cell functionality. Besides local immunosuppression, several studies including our work, indicate that tumors induce systemic immunosuppression that could render T cells inactive. A recent study has shown that patients that do not respond to anti-CTLA-4 therapy have elevated systemic levels of neutrophils and monocytes compared to baseline levels and patients that do respond. Moreover, these cells expressed high levels of nitric oxide and PD-L1 suggesting their immunosuppressive properties [54]. These observations indicate that therapeutic enhancement of T cell priming or targeting of immunosuppressive cells might boost the functionality of tumor-reactive T cells to enhance anti-cancer immunity.

Targeting neutrophil-induced immunosuppression

The clinical and experimental findings described above support the notion that targeting neutrophil expansion, recruitment or function would be an interesting therapeutic strategy to relieve immunosuppression in cancer patients. Because the inflammatory pathways regulating neutrophil biology show striking similarities with inflammatory diseases, like psoriasis and rheumatoid arthritis, drugs targeting these pathways in inflammatory disorders might also be applied to treat metastasized cancer. For example, drugs targeting CXCR2 signaling reduced neutrophil numbers and the secretion of pro-inflammatory mediators in patients with chronic obstructive pulmonary disease, resulting

in symptom relief [55]. Moreover, drugs targeting the IL23-IL17 signaling pathway are available for the treatment of psoriasis, providing several options to target neutrophils in cancer patients.

Although neutrophils seem an interesting therapeutic target, there is a risk of developing severe neutropenia when blocking these cells, which could lead to fatal opportunistic infections. However, in early-stage breast cancer patients, chemotherapy-induced neutropenia is an independent predictor of increased survival [56]. Of consideration, patients with severe neutropenia are often administered with doses of recombinant G-CSF to stimulate the generation of neutrophils and other myeloid cells to prevent opportunistic infections [57]. Based on the previously described preclinical work, one could raise the question whether the administration of G-CSF to patients favors the expansion of a population of pro-metastatic neutrophils thereby promoting the spread of tumors.

An additional approach to enhance anti-tumor immunity is to target immunosuppressive neutrophils in combination with T cell-boosting immune checkpoint blockade. Indeed, several experimental studies support this hypothesis. Recently it was demonstrated that blockade of CXCR2-mediated trafficking of immunosuppressive neutrophils greatly enhanced the anti-tumor efficacy of anti-PD-1 resulting in delayed tumor growth in a model of rhabdomyosarcoma and reduced metastasis in a model of metastatic pancreatic cancer [58,59]. Future studies should focus on determining the efficacy of different combinatorial strategies combining T cell-boosting immunotherapy and neutrophil-targeting compounds to enhance anti-tumor immunity to fight disseminated cancer.

Targeting tumor-associated chronic inflammation

Since many tumors are characterized by the infiltration of immunosuppressive macrophages, these cells might be an integral part of combinatorial treatment strategies. In a preclinical setting, targeting macrophages is usually performed by the use of monoclonal antibodies or small molecule inhibitors targeting CSF-1/CSF-1R signaling, strategies that are also under clinical investigation [60]. In a glioblastoma mouse model interference of CSF-1 signaling did not affect macrophage numbers, but instead, resulted in reprogramming of these cells in an anti-tumor phenotype [42]. In contrast, in the *MMTV-PyMT* breast cancer model, interference of CSF-1/CSF-1R signaling resulted in specific depletion of tumor-associated macrophages without altering TAM maturation and differentiation [61]. Macrophage depletion resulted in enhanced responsiveness of breast and pancreatic tumors to chemotherapy at least in part due to relief of macrophage-induced immunosuppression [41,44,45,61]. Moreover, ablation of macrophages improves the response to immune checkpoint blockade in a mouse model of pancreatic cancer [44]. In line with experimental data showing enhanced anti-tumor T cell responses after macrophage inhibition in different types of cancer [44,45], a recent clinical trial reports objective responses in patients with diffuse-type giant cell tumors treated with anti-CSF-1R antibodies, which was associated with increased $CD8^+/CD4^+$ T cell ratios [62].

Based on many studies including the work described in this thesis, also the CCL2/CCR2 signaling pathway is of interest for therapeutic targeting of macrophages. In contrast to our observations, several preclinical studies in breast cancer models show that CCL2 blockade reduces the influx of macrophages in primary tumors and at the metastatic site [36]. In prostate cancer, CCL2 protects cancer cells from chemotherapy-induced cell death [63]. Clinical trials are ongoing to test the efficacy in patients with different types of cancer, although the initial effects are modest. Phase I/II studies in patients with solid tumors showed that treatment was well-tolerated with carlumab (a monoclonal antibody against CCL2) alone or in combination with conventional chemotherapy, but showed little anti-tumor efficacy. Moreover, systemic CCL2 levels were only transiently suppressed by carlumab and continued administration lead to increasing levels of free CCL2 [64,65], likely caused by a compensatory feedback loop. Similar results were obtained in patients with metastatic prostate cancer [66]. Interestingly, results from a recent phase 1b clinical trial in patients with pancreatic cancer revealed that therapeutic targeting of CCL2/CCR2 signaling in combination with a chemotherapy regimen has clinical activity and resulted in reduced immunosuppression and an increase in the number of tumor-infiltrating lymphocytes [67]. Based on our findings that CCL2 blockade relieves suppression of $CD8^+$ T cells, it would be interesting to see how the proportions of circulating neutrophils relate to CCL2 levels and $CD8^+$ T cell activation in cancer patients. Moreover, it remains to be seen whether CCL2 blockade can also unleash anti-tumor immune responses to attack metastatic disease.

Tumor-intrinsic drivers of immune evasion

For successful activation of a T cell-mediated anti-tumor immune response, T cells need to "see" the cancer cells with their TCR. Recent studies demonstrate that the number of somatic mutations in tumors is associated with response to immunotherapy; tumors with a high mutational load are more likely to respond to immune checkpoint blockade in melanoma and lung cancer patients [68,69]. Moreover, genetically instable cancers tend to respond better to anti-PD-1 therapy than their stable counterparts [70]. Breast cancer is generally not considered an immunogenic type of cancer and usually has a relatively limited number of mutations [71]. Whole-exome sequencing analyses of somatic mutation landscapes in breast cancer patients revealed distinct mutational signatures corresponding to tumors with homologues recombination-defective DNA repair characterized by loss of BRCA1/2 [72,73]. The presence of tumor-infiltrating lymphocytes and expression of PD-L1 seems to provide prognostic value, mostly in triple negative breast cancers [74–77]. $HER2^+$ breast cancers show a similar incidence of immune cell influx as TNBC irrespective of their hormone receptor status, while hormone receptor-positive breast cancers display the lowest numbers of tumor-infiltrating lymphocytes [78]. Is the magnitude of tumor-infiltrating lymphocytes a consequence of the 'foreignness' of different breast cancer subtypes? As a result of genetic instability in TNBC the mutational load in these tumors is higher compared to $HER2^+$ and hormone receptor-positive cancers [79], which could make cancer cells more visible for T cells. If in breast

cancer, like in melanoma and lung cancer, the mutational load is a dominant factor in the clinical efficacy of immune checkpoint blockade one would expect that patients with BRCA-deficient tumors are expected to respond better to immunotherapy than patients with BRCA-proficient tumors. But does that mean that 'genetically stable' breast cancer subtypes will not benefit from immunotherapy? Our data show that also breast cancers with a relatively low mutational load can benefit from immunotherapy when combined with certain chemotherapeutics, like cisplatin.

In addition, compelling data demonstrate that activation of certain oncogenes or loss of tumor suppressor genes is associated with the immune composition of tumors. For example, in a mouse model of hepatocellular carcinoma induced by chronic liver damage, p53-proficient senescent cancer cells released factors that skewed macrophage polarization into an anti-tumor phenotype, while proliferating p53-deficient cells secreted factors promoting a pro-tumor macrophage phenotype [80]. Moreover, recent studies highlight that activation of oncogenic pathways can mediate immune evasion. In melanoma, activation of the oncogenic β-catenin and PI3K-AKT signaling pathways have been associated with reduced chemokine secretion, immunosuppression and low T cell infiltrate resulting in poor responses to immunotherapy [81,82]. Similarly, MYC-driven T cell acute lymphoblastic leukemia cells upregulate PD-L1 and CD47 to evade recognition by the immune system [83]. Intriguingly, *TP53, MYC* and *PIK3CA* are among the 10 most frequently altered genes in breast cancer patients [72,73], which could negatively affect responses to immunotherapy. But for now, it remains unclear whether alterations in these genes have an effect on immune evasion in breast cancer patients.

Enhancing anti-tumor immunity by immunomodulatory chemotherapy

We and others have shown in experimental mouse models for *de novo* mammary tumorigenesis, that mammary tumors do not spontaneously elicit effective anti-tumor immune responses [17,43,84,85]. We demonstrate here that tumor-infiltrating T cells in KEP mammary tumors are functionally impaired and express immune checkpoint molecules CTLA-4 and PD-1. Since clinical data on immune checkpoint inhibition in breast cancer are still preliminary or lacking, we set out to test whether immune checkpoint blockade would be a feasible approach to overcome the functional impairment of T cells in a mouse model for *de novo* breast cancer (KEP mice). We found that dual immune checkpoint blockade by anti-CTLA-4 and anti-PD-1 did not affect primary tumor growth in KEP mice. Thus these data suggest that neutralizing the inhibitory effects of CTLA-4 and PD-1 on T cells is not sufficient to induce potent anti-tumor T cell responses, and that KEP tumors elicit additional mechanisms of immune evasion.

In the past years it has become apparent that therapeutic strategies that combine the debulking properties of conventional anti-cancer drugs with immunotherapy might lead to long-lasting responses in cancer patients. The use of chemotherapeutic agents is of particular interest because several studies report a therapy-induced reprogramming of the tumor microenvironment towards a more permissive state for anti-tumor immunity to occur. Depending on the different modes of action, certain types of chemotherapeutic

agents including doxorubicin, oxaliplatin and cyclophosphamide, have been suggested to induce so-called 'immunogenic cell death' characterized by the release of HMGB1, that activates dendritic cells resulting in enhanced anti-tumor immune responses [86–89]. In the KEP model, when chemotherapy was added to the treatment regimen of dual immune checkpoint blockade we observed synergy with dual immune checkpoint blockade in a drug-dependent manner. Interestingly, cisplatin – which provides synergy with dual immune checkpoint blockade in the KEP model – is not considered an inducer of 'immunogenic cell death' and we did not find any changes in HMGB1 release in KEP tumors upon cisplatin treatment. These results suggest that in the KEP model, cisplatin promotes anti-tumor immune responses in a different manner.

Previous studies using vaccination approaches against HPV-induced cervical cancer show enhanced anti-tumor responses in mice treated with cisplatin (and not other types of chemotherapeutic agents) by sensitizing cancer cells to CTL-mediated killing [90–92]. In line with this, uur results demonstrate that different chemotherapeutic agents have different effects on the inflammatory microenvironment: while cisplatin induces the expression of various pro-inflammatory cytokines, docetaxel dampens these factors. Cisplatin-induced expression of these cytokines did not result in proportional changes of macrophages, neutrophils and monocytes, although — due to their plasticity — the polarization state might be affected. Future studies will shed more light on how chemotherapy affects the polarization state of immune cell populations.

Interestingly, our preliminary data show that cisplatin increases the proportions of $CD103^+$ DCs in KEP tumors and lymph nodes. Recent studies show that a rare population of $CD103^+$ DCs are very potent activators of anti-tumor T cells in various experimental models [45,51,93]. Moreover, their presence is required for successful responses to immune checkpoint blockade [94]. In breast cancer patients, a CD103-associated gene signature provided strong prognostic value; patients with a 'high CD103-signature' had improved survival compared to patients with a 'low CD103-signature' [51], suggesting that these cells are important for tumor control. Our results have important implications for the clinic because it shows that the choice of chemotherapeutic agent can influence the anti-cancer efficacy of immunotherapy. More importantly, our results suggest that – even in cancer types that have a limited number of somatic mutations – combination therapy regimens are able to unleash anti-tumor immunity to fight cancer.

Conclusions and future perspectives

Due to the clinical success of cancer immunotherapy, the realization that the patient's own immune system can be manipulated to fight cancer has gained a lot of attention. Clinical and experimental studies emphasize the efficacy of immune checkpoint blockade to unleash anti-tumor T cell responses in different cancer types, however, cancers elicit several mechanisms to prevent destruction by the immune system. To address and ultimately overcome these hurdles, we have to gain a better understanding of tumor-induced mechanisms of immune evasion, which can be either cancer cell-intrinsic or cancer cell-extrinsic. The research described in this thesis supports the notion that interference with tumor-induced immunosuppression can unleash anti-tumor immunity to fight disseminated cancer. Moreover, we show that certain chemotherapeutic agents in combination with T cell-boosting immune checkpoint blockade can overcome T cell dysfunction resulting in improved anti-tumor responses, even in tumors with a relatively low number of mutations like breast cancer. Future studies are required that provide more insight into the extent to which the cancer subtype, genetic make-up of the tumors, disease stage and treatment history will affect natural and therapy-induced anti-cancer immunity. Studying these different cancer-immune parameters will provide an integrative approach to provide personalized treatment options and will ultimately improve cancer patient care.

References

1. McAllister, S. S. & Weinberg, R. A. The tumour-induced systemic environment as a critical regulator of cancer progression and metastasis. *Nat. Cell Biol.* **16,** 717–727 (2014).
2. Kitamura, T., Qian, B.-Z. & Pollard, J. W. Immune cell promotion of metastasis. *Nat. Rev. Immunol.* **15,** 73–86 (2015).
3. Hanahan, D. & Weinberg, R. A. Hallmarks of cancer: the next generation. *Cell* **144,** 646–674 (2011).
4. Noy, R. & Pollard, J. W. Tumor-Associated Macrophages: From Mechanisms to Therapy. *Immunity* **41,** 49–61 (2014).
5. Wolchok, J. D. & Chan, T. A. Cancer: Antitumour immunity gets a boost. *Nature* **515,** 496–498 (2014).
6. Hodi, F. S. *et al.* Improved survival with ipilimumab in patients with metastatic melanoma. *N. Engl. J. Med.* **363,** 711–723 (2010).
7. Brahmer, J. R. *et al.* Safety and activity of anti-PD-L1 antibody in patients with advanced cancer. *N. Engl. J. Med.* **366,** 2455–2465 (2012).
8. Topalian, S. L. *et al.* Safety, activity, and immune correlates of anti-PD-1 antibody in cancer. *N. Engl. J. Med.* **366,** 2443–2454 (2012).
9. Wolchok, J. D. *et al.* Nivolumab plus ipilimumab in advanced melanoma. *N. Engl. J. Med.* **369,** 122–133 (2013).
10. Tüting, T. & Visser, K. E. de. How neutrophils promote metastasis. *Science* **352,** 145–146 (2016).
11. Coffelt, S. B., Wellenstein, M. D. & de Visser, K. E. Neutrophils in cancer: neutral no more. *Nat. Rev. Cancer* **16,** 431–446 (2016).
12. Azab, B. *et al.* Usefulness of the neutrophil-to-lymphocyte ratio in predicting short- and long-term mortality in breast cancer patients. *Ann. Surg. Oncol.* **19,** 217–224 (2012).
13. Noh, H., Eomm, M. & Han, A. Usefulness of pretreatment neutrophil to lymphocyte ratio in predicting disease-specific survival in breast cancer patients. *J. Breast Cancer* **16,** 55–59 (2013).
14. Templeton, A. J. *et al.* Prognostic role of neutrophil-to-lymphocyte ratio in solid tumors: a systematic review and meta-analysis. *J. Natl. Cancer Inst.* **106,** dju124 (2014).
15. Gentles, A. J. *et al.* The prognostic landscape of genes and infiltrating immune cells across human cancers. *Nat. Med.* **21,** 938–945 (2015).
16. Casbon, A.-J. *et al.* Invasive breast cancer reprograms early myeloid differentiation in the bone marrow to generate immunosuppressive neutrophils. *Proc. Natl. Acad. Sci. U. S. A.* **112,** E566-575 (2015).
17. Coffelt, S. B. *et al.* IL-17-producing γδ T cells and neutrophils conspire to promote breast cancer metastasis. *Nature* **522,** 345–348 (2015).
18. Wculek, S. K. & Malanchi, I. Neutrophils support lung colonization of metastasis-initiating breast cancer cells. *Nature* **528,** 413–417 (2015).
19. Granot, Z. *et al.* Tumor entrained neutrophils inhibit seeding in the premetastatic lung. *Cancer Cell* **20,** 300–314 (2011).
20. Finisguerra, V. *et al.* MET is required for the recruitment of anti-tumoural neutrophils. *Nature* **522,** 349–353 (2015).
21. Kowanetz, M. *et al.* Granulocyte-colony stimulating factor promotes lung metastasis through mobilization of Ly6G+Ly6C+ granulocytes. *Proc. Natl. Acad. Sci. U. S. A.* **107,** 21248–21255 (2010).
22. Bald, T. *et al.* Ultraviolet-radiation-induced inflammation promotes angiotropism and metastasis in melanoma. *Nature* **507,** 109–113 (2014).
23. Gabrilovich, D. I. *et al.* The terminology issue for myeloid-derived suppressor cells. *Cancer Res.* **67,** 425; author reply 426 (2007).
24. Waight, J. D., Hu, Q., Miller, A., Liu, S. & Abrams, S. I. Tumor-derived G-CSF facilitates neoplastic growth through a granulocytic myeloid-derived suppressor cell-dependent mechanism. *PloS One* **6,** e27690 (2011).
25. Fridlender, Z. G. *et al.* Polarization of tumor-associated neutrophil phenotype by TGF-beta: 'N1' versus 'N2' TAN. *Cancer Cell* **16,** 183–194 (2009).
26. Stark, M. A. *et al.* Phagocytosis of apoptotic neutrophils regulates granulopoiesis via IL-23 and IL-17. *Immunity* **22,** 285–294 (2005).
27. Gaffen, S. L., Jain, R., Garg, A. V. & Cua, D. J. The IL-23-IL-17 immune axis: from mechanisms to therapeutic testing. *Nat. Rev. Immunol.* **14,** 585–600 (2014).
28. Wu, P. *et al.* γδT17 cells promote the accumulation and expansion of myeloid-derived suppressor cells in human colorectal cancer. *Immunity* **40,** 785–800 (2014).
29. Fuentes, M. E. *et al.* Controlled recruitment of monocytes and macrophages to specific organs through

transgenic expression of monocyte chemoattractant protein-1. *J. Immunol.* **155,** 5769–5776 (1995).
30. Leek, R. D. *et al.* Association of macrophage infiltration with angiogenesis and prognosis in invasive breast carcinoma. *Cancer Res.* **56,** 4625–4629 (1996).
31. Ueno, T. *et al.* Significance of macrophage chemoattractant protein-1 in macrophage recruitment, angiogenesis, and survival in human breast cancer. *Clin. Cancer Res.* **6,** 3282–3289 (2000).
32. Saji, H. *et al.* Significant correlation of monocyte chemoattractant protein-1 expression with neovascularization and progression of breast carcinoma. *Cancer* **92,** 1085–1091 (2001).
33. Mitchem, J. B. & DeNardo, D. G. Battle over CCL2 for control of the metastatic niche: neutrophils versus monocytes. *Breast Cancer Res.* **14,** 315 (2012).
34. Li, M., Knight, D. A., Snyder, L. A. & Stewart, M. J. S. and T. J. A role for CCL2 in both tumor progression and immunosurveillance. *OncoImmunology* **2,** e25474 (2013).
35. Lança, T. *et al.* Protective role of the inflammatory CCR2/CCL2 chemokine pathway through recruitment of type 1 cytotoxic γδ T lymphocytes to tumor beds. *J. Immunol.* **190,** 6673–6680 (2013).
36. Qian, B.-Z. *et al.* CCL2 recruits inflammatory monocytes to facilitate breast-tumour metastasis. *Nature* **475,** 222–225 (2011).
37. Kudo-Saito, C., Shirako, H., Ohike, M., Tsukamoto, N. & Kawakami, Y. CCL2 is critical for immunosuppression to promote cancer metastasis. *Clin. Exp. Metastasis* **30,** 393–405 (2013).
38. Yoshimura, T. *et al.* Monocyte Chemoattractant Protein-1/CCL2 produced by stromal cells promotes lung metastasis of 4T1 murine breast cancer cells. *PLoS ONE* **8,** e58791 (2013).
39. Kitamura, T. *et al.* CCL2-induced chemokine cascade promotes breast cancer metastasis by enhancing retention of metastasis-associated macrophages. *J. Exp. Med.* **212,** 1043–1059 (2015).
40. Lin, E. Y., Nguyen, A. V., Russell, R. G. & Pollard, J. W. Colony-stimulating factor 1 promotes progression of mammary tumors to malignancy. *J. Exp. Med.* **193,** 727–740 (2001).
41. Mitchem, J. B. *et al.* Targeting Tumor-Infiltrating Macrophages Decreases Tumor-Initiating Cells, Relieves Immunosuppression, and Improves Chemotherapeutic Responses. *Cancer Res.* **73,** 1128–1141 (2013).
42. Pyonteck, S. M. *et al.* CSF-1R inhibition alters macrophage polarization and blocks glioma progression. *Nat. Med.* **19,** 1264–1272 (2013).
43. DeNardo, D. G. *et al.* CD4(+) T cells regulate pulmonary metastasis of mammary carcinomas by enhancing protumor properties of macrophages. *Cancer Cell* **16,** 91–102 (2009).
44. Zhu, Y. *et al.* CSF1/CSF1R Blockade Reprograms Tumor-Infiltrating Macrophages and Improves Response to T-cell Checkpoint Immunotherapy in Pancreatic Cancer Models. *Cancer Res.* **74,** 5057–5069 (2014).
45. Ruffell, B. *et al.* Macrophage IL-10 blocks CD8+ T cell-dependent responses to chemotherapy by suppressing IL-12 expression in intratumoral dendritic cells. *Cancer Cell* **26,** 623–637 (2014).
46. Mantovani, A. *et al.* The chemokine system in diverse forms of macrophage activation and polarization. *Trends Immunol.* **25,** 677–686 (2004).
47. Murray, P. J. *et al.* Macrophage Activation and Polarization: Nomenclature and Experimental Guidelines. *Immunity* **41,** 14–20 (2014).
48. Newman, A. M. *et al.* Robust enumeration of cell subsets from tissue expression profiles. *Nat. Methods* **12,** 453–457 (2015).
49. Pinzon-Charry, A., Maxwell, T. & López, J. A. Dendritic cell dysfunction in cancer: a mechanism for immunosuppression. *Immunol. Cell Biol.* **83,** 451–461 (2005).
50. Engelhardt, J. J. *et al.* Marginating dendritic cells of the tumor microenvironment cross-present tumor antigens and stably engage tumor-specific T cells. *Cancer Cell* **21,** 402–417 (2012).
51. Broz, M. L. *et al.* Dissecting the Tumor Myeloid Compartment Reveals Rare Activating Antigen-Presenting Cells Critical for T Cell Immunity. *Cancer Cell* **26,** 638–652 (2014).
52. Tumeh, P. C. *et al.* PD-1 blockade induces responses by inhibiting adaptive immune resistance. *Nature* **515,** 568–571 (2014).
53. Joyce, J. A. & Fearon, D. T. T cell exclusion, immune privilege, and the tumor microenvironment. *Science* **348,** 74–80 (2015).
54. Gebhardt, C. *et al.* Myeloid Cells and Related Chronic Inflammatory Factors as Novel Predictive Markers in Melanoma Treatment with Ipilimumab. *Clin. Cancer Res.* **21,** 5453–5459 (2015).
55. Rennard, S. I. *et al.* CXCR2 Antagonist MK-7123. A Phase 2 Proof-of-Concept Trial for Chronic Obstructive Pulmonary Disease. *Am. J. Respir. Crit. Care Med.* **191,** 1001–1011 (2015).
56. Han, Y. *et al.* Prognostic value of chemotherapy-induced neutropenia in early-stage breast cancer. *Breast Cancer Res. Treat.* **131,** 483–490 (2012).
57. Tan, H. *et al.* Comparative effectiveness of colony-stimulating factors for febrile neutropenia: a retrospective study. *Curr. Med. Res. Opin.* **27,** 79–86 (2011).

58. Highfill, S. L. *et al.* Disruption of CXCR2-mediated MDSC tumor trafficking enhances anti-PD1 efficacy. *Sci. Transl. Med.* **6,** 237ra67 (2014).
59. Steele, C. W. *et al.* CXCR2 Inhibition Profoundly Suppresses Metastases and Augments Immunotherapy in Pancreatic Ductal Adenocarcinoma. *Cancer Cell* **29,** 832–845 (2016).
60. Coussens, L. M., Zitvogel, L. & Palucka, A. K. Neutralizing tumor-promoting chronic inflammation: a magic bullet? *Science* **339,** 286–291 (2013).
61. DeNardo, D. G. *et al.* Leukocyte Complexity Predicts Breast Cancer Survival and Functionally Regulates Response to Chemotherapy. *Cancer Discov.* **1,** 54–67 (2011).
62. Ries, C. H. *et al.* Targeting tumor-associated macrophages with anti-CSF-1R antibody reveals a strategy for cancer therapy. *Cancer Cell* **25,** 846–859 (2014).
63. Qian, D. Z. *et al.* CCL2 is induced by chemotherapy and protects prostate cancer cells from docetaxel-induced cytotoxicity. *The Prostate* **70,** 433–442 (2010).
64. Sandhu, S. K. *et al.* A first-in-human, first-in-class, phase I study of carlumab (CNTO 888), a human monoclonal antibody against CC-chemokine ligand 2 in patients with solid tumors. *Cancer Chemother. Pharmacol.* (2013). doi:10.1007/s00280-013-2099-8
65. Brana, I. *et al.* Carlumab, an anti-C-C chemokine ligand 2 monoclonal antibody, in combination with four chemotherapy regimens for the treatment of patients with solid tumors: an open-label, multicenter phase 1b study. *Target. Oncol.* (2014). doi:10.1007/s11523-014-0320-2
66. Pienta, K. J. *et al.* Phase 2 study of carlumab (cnto 888), a human monoclonal antibody against cc-chemokine ligand 2 (ccl2), in metastatic castration-resistant prostate cancer. *Invest. New Drugs* **31,** 760–768 (2012).
67. Nywening, T. M. *et al.* Targeting tumour-associated macrophages with CCR2 inhibition in combination with FOLFIRINOX in patients with borderline resectable and locally advanced pancreatic cancer: a single-centre, open-label, dose-finding, non-randomised, phase 1b trial. *Lancet Oncol.* **17,** 651–662 (2016).
68. Snyder, A. *et al.* Genetic basis for clinical response to CTLA-4 blockade in melanoma. *N. Engl. J. Med.* **371,** 2189–2199 (2014).
69. Rizvi, N. A. *et al.* Cancer immunology. Mutational landscape determines sensitivity to PD-1 blockade in non-small cell lung cancer. *Science* **348,** 124–128 (2015).
70. Le, D. T. *et al.* PD-1 Blockade in Tumors with Mismatch-Repair Deficiency. *N. Engl. J. Med.* **372,** 2509–2520 (2015).
71. Alexandrov, L. B. *et al.* Signatures of mutational processes in human cancer. *Nature* **500,** 415–421 (2013).
72. Nik-Zainal, S. *et al.* Landscape of somatic mutations in 560 breast cancer whole-genome sequences. *Nature* (2016). doi:10.1038/nature17676
73. Morganella, S. *et al.* The topography of mutational processes in breast cancer genomes. *Nat. Commun.* **7,** 11383 (2016).
74. Mittendorf, E. A. *et al.* PD-L1 expression in triple-negative breast cancer. *Cancer Immunol. Res.* **2,** 361–370 (2014).
75. Ibrahim, E. M., Al-Foheidi, M. E., Al-Mansour, M. M. & Kazkaz, G. A. The prognostic value of tumor-infiltrating lymphocytes in triple-negative breast cancer: a meta-analysis. *Breast Cancer Res. Treat.* **148,** 467–476 (2014).
76. Wimberly, H. *et al.* PD-L1 Expression Correlates with Tumor-Infiltrating Lymphocytes and Response to Neoadjuvant Chemotherapy in Breast Cancer. *Cancer Immunol. Res.* **3,** 326–332 (2015).
77. Cimino-Mathews, A. *et al.* PD-L1 (B7-H1) expression and the immune tumor microenvironment in primary and metastatic breast carcinomas. *Hum. Pathol.* **47,** 52–63 (2016).
78. Stanton, S. E., Adams, S. & Disis, M. L. Variation in the Incidence and Magnitude of Tumor-Infiltrating Lymphocytes in Breast Cancer Subtypes: A Systematic Review. *JAMA Oncol.* (2016). doi:10.1001/jamaoncol.2016.1061
79. Budczies, J. *et al.* Classical pathology and mutational load of breast cancer – integration of two worlds. *J. Pathol.* **1,** 225–238 (2015).
80. Lujambio, A. *et al.* Non-Cell-Autonomous Tumor Suppression by p53. *Cell* **153,** 449–460 (2013).
81. Spranger, S., Bao, R. & Gajewski, T. F. Melanoma-intrinsic β-catenin signalling prevents anti-tumour immunity. *Nature* **523,** 231–235 (2015).
82. Peng, W. *et al.* Loss of PTEN Promotes Resistance to T Cell-Mediated Immunotherapy. *Cancer Discov.* **6,** 202–216 (2016).
83. Casey, S. C. *et al.* MYC regulates the antitumor immune response through CD47 and PD-L1. *Science* **352,** 227–231 (2016).
84. Ciampricotti, M. *et al.* Development of metastatic HER2(+) breast cancer is independent of the adaptive

immune system. *J. Pathol.* **224,** 56–66 (2011).
85. Ciampricotti, M., Hau, C.-S., Doornebal, C. W., Jonkers, J. & de Visser, K. E. Chemotherapy response of spontaneous mammary tumors is independent of the adaptive immune system. *Nat. Med.* **18,** 344–346 (2012).
86. Obeid, M. *et al.* Calreticulin exposure dictates the immunogenicity of cancer cell death. *Nat. Med.* **13,** 54–61 (2007).
87. Apetoh, L. *et al.* Toll-like receptor 4-dependent contribution of the immune system to anticancer chemotherapy and radiotherapy. *Nat. Med.* **13,** 1050–1059 (2007).
88. Ma, Y. *et al.* Anticancer chemotherapy-induced intratumoral recruitment and differentiation of antigen-presenting cells. *Immunity* **38,** 729–741 (2013).
89. Ghiringhelli, F. *et al.* Activation of the NLRP3 inflammasome in dendritic cells induces IL-1beta-dependent adaptive immunity against tumors. *Nat. Med.* **15,** 1170–1178 (2009).
90. Tseng, C.-W. *et al.* Pretreatment with cisplatin enhances E7-specific CD8+ T-Cell-mediated antitumor immunity induced by DNA vaccination. *Clin. Cancer Res.* **14,** 3185–3192 (2008).
91. Lee, S. Y. *et al.* Intratumoral injection of therapeutic HPV vaccinia vaccine following cisplatin enhances HPV-specific antitumor effects. *Cancer Immunol. Immunother.* **62,** 1175–1185 (2013).
92. van der Sluis, T. C. *et al.* Vaccine-induced tumor necrosis factor-producing T cells synergize with cisplatin to promote tumor cell death. *Clin. Cancer Res.* **21,** 781–794 (2015).
93. Salmon, H. *et al.* Expansion and Activation of CD103+ Dendritic Cell Progenitors at the Tumor Site Enhances Tumor Responses to Therapeutic PD-L1 and BRAF Inhibition. *Immunity* **44,** 924–938 (2016).
94. Sánchez-Paulete, A. R. *et al.* Cancer Immunotherapy with Immunomodulatory Anti-CD137 and Anti-PD-1 Monoclonal Antibodies Requires BATF3-Dependent Dendritic Cells. *Cancer Discov.* **6,** 71–79 (2016).

-&-

Appendices

English summary

Nederlandse samenvatting

Curriculum Vitae

List of publications

English summary

Despite recent clinical advances, breast cancer still remains one of the main causes of cancer-related death in women. The majority of these deaths are caused by metastatic disease, which is still poorly understood and incurable. Thus, there is an urgent need for novel therapeutic strategies that successfully target metastatic cancer.

In the past decades it has become clear that tumors do not merely consist of cancer cells, but also endothelial cells, fibroblasts and immune cells, which collectively form the tumor microenvironment (TME). The TME is a critical determinant of cancer development, progression and metastasis. Recent clinical studies have shown that the immune system is able to attack and kill disseminated cancer cells when activated by immunotherapeutic strategies such as immune checkpoint inhibition. However, a substantial proportion of patients fail to respond. This might be explained by the paradoxical nature of different immune cell populations in cancer progression and therapy responsiveness. While some immune cells, including $CD4^+$ and $CD8^+$ T cells and NK cells, are able to attack and kill cancer cells, other populations, like macrophages and neutrophils, counteract anti-tumor immune responses and promote cancer progression. To provide optimal treatment options for patients with disseminated cancer, we need to gain a better understanding of the delicate balance between pro- and anti-tumor immunity. Through the use of novel immunomodulatory drugs, we will be able to push this balance towards anti-tumor immunity to attack disseminated cancer. This thesis describes the complex interactions between innate and adaptive cells that facilitate metastasis in a mouse model of spontaneous invasive breast cancer. Moreover, this thesis describes that the use of chemo-immunotherapy as a therapeutic strategy can enhance anti-tumor immunity to fight breast cancer.

Despite successful validation of novel anti-cancer therapies in preclinical mouse models, the majority of the phase 3 clinical trials fail. The poor translation from animal models to the clinic illustrates the poor predictive power of currently used preclinical models. In **chapter 2** we propose the use of genetically engineered mouse models (GEMMs) of cancer for preclinical studies, because these models closely resemble both cancer cell-intrinsic and –extrinsic properties of human cancer. Especially the development of novel immunomodulatory compounds and combinatorial treatment strategies will benefit from preclinical studies in GEMMs because these models develop *de novo* cancer in an immunoproficient environment. With the recent advances in genome editing, GEMMs can be generated that faithfully recapitulate specific patient cohorts, which will greatly improve our understanding of the complex role of the immune system in cancer development, metastasis formation and drug resistance.

In **chapter 3** we use a GEMM of invasive breast cancer, i.e. *K14cre;Cdh1$^{F/F}$;Trp53$^{F/F}$* (KEP) mice, to demonstrate that *de novo* mammary tumors induce a systemic inflammatory and immunosuppressive state that facilitates the formation of metastasis in distant organs. We show that this inflammatory cascade is characterized by the expansion of immunosuppressive neutrophils via IL17-producing γδ T cells. These

neutrophils actively suppress the activation of anti-tumor $CD8^+$ T cells via iNOS allowing the formation of metastases in distant organs. We found that activation of γδ T cells was dependent on IL1β derived from tumor-associated macrophages (TAMs). In **chapter 4** we demonstrate that the pro-inflammatory cytokine CCL2 is a key player in initiating this cascade by regulating the secretion of IL1β from TAMs. In line with these findings, we found that gene expression of *CCL2* and *IL1B* is highly correlated across human breast cancers, and is most pronounced in macrophage-rich tumors. Blockade of CCL2 in KEP mice resulted in reduced IL1β secretion by TAMs, decreased IL17-producing γδ T cells, reduced proportions of $cKIT^+$ neutrophils and enhanced activity of $CD8^+$ T cells. Together these data suggest that therapeutic targeting of different steps of this systemic immunosuppressive cascade could unleash anti-tumor immune responses to target metastatic breast cancer.

Since the clinical availability of drugs specifically targeting immunosuppressive networks is limited, an alternative approach is to use conventional anti-cancer drugs that have immunomodulatory properties. Based on review of the current literature, we propose in **chapter 5** to use chemotherapeutics to relieve immunosuppression to enhance anti-tumor immunity. Therapeutic strategies combining carefully selected chemotherapy drugs with T cell-boosting immunotherapy will unleash anti-tumor reactivity and extend the success of cancer immunotherapy.

In **chapter 6** we show that *de novo* mammary tumors in the KEP mouse model are infiltrated by different populations of T lymphocytes, but the lack of tumor control suggests that these cells are dysfunctional. We found that tumor-infiltrating T cells express high levels of immune checkpoint molecules CTLA-4 and PD-1 that act as negative regulators of T cell activation. We demonstrate that dual immune checkpoint blockade does not affect tumor growth, but synergizes with conventional chemotherapy in a drug-dependent manner. The therapeutic benefit of chemo-immunotherapy was dependent on the activation of $CD8^+$ T cells. Preliminary data imply that the drug cisplatin might enhance the functionality of $CD103^+$ dendritic cells resulting in enhanced T cell priming and tumor-reactive T cells. These results might have important implications for clinical practice, because they show that also cancer types with limited number of mutations can benefit from immunotherapy when combined with the proper chemotherapeutic drug.

Chapter 7 contains a brief summary of the research described in this thesis. The general discussion puts our research in the context of the current literature and proposes clinical implications based on our findings.

Nederlandse samenvatting

Ondanks de recente vooruitgang in de behandeling van kanker blijft borstkanker nog altijd een van de meest voorkomende kanker-gerelateerde doodsoorzaken bij vrouwen. Het merendeel hiervan is te wijten aan de uitzaaiing van borstkanker, een proces dat nog altijd grotendeels onduidelijk is en daardoor ongeneeslijk. Daarom is het van groot belang om nieuwe therapieën te ontwikkelen die uitgezaaide borstkanker kunnen bestrijden. Tumoren bestaan niet alleen uit kankercellen. Naast deze cellen zijn ook stromale cellen zoals endotheelcellen – welke bloed- en lymfevaten vormen –, fibroblasten en immuuncellen aanwezig welke samen de tumor microenvironment (TME) vormen.

Dit proefschrift beschrijft mijn onderzoek naar de rol van verschillende populaties immuuncellen in de ontwikkeling, groei en uitzaaiing van kanker. Recente klinische studies laten zien dat het immuunsysteem – wanneer het geactiveerd wordt met immunotherapie, bijvoorbeeld met zogenaamde 'immuun checkpoint inhibitors' – uitgezaaide kanker kan herkennen, aanvallen en doden. Echter, de meerderheid van de kankerpatiënten die behandeld wordt met immunotherapie reageert niet op deze behandeling. Deze observatie kan verklaard worden door de tegengestelde functies van verschillende immuuncelpopulaties in kankerprogressie en de respons op anti-kanker behandelingen. Sommige typen immuuncellen, zoals $CD4^+$ en $CD8^+$ T cellen en NK cellen, zijn in staat zijn om kankercellen aan te vallen en op te ruimen. Maar andere populaties, zoals macrofagen en neutrofielen, kunnen anti-kanker immuunreacties tegenwerken en de progressie van kanker bevorderen. Om de meest optimale behandeling te ontwikkelen voor patiënten met uitgezaaide kanker, moeten we meer inzicht krijgen in de processen die de delicate balans tussen pro- en anti-kanker immuunresponsen bepalen. Met de ontwikkeling van nieuwe immuunmodulerende therapieën kunnen we deze balans zodanig beïnvloeden dat het in het voordeel werkt van de anti-kanker immuniteit. Dit proefschrift beschrijft de complexe interacties tussen cellen van het aangeboren en adaptieve immuunsysteem in een muismodel voor uitgezaaide borstkanker. Daarnaast beschrijft dit proefschrift hoe we gebruik kunnen maken van conventionele chemotherapie om anti-kanker immuunresponsen te versterken in de behandeling van borstkanker.

Ondanks dat de werking van veel nieuwe anti-kanker therapieën succesvol gevalideerd wordt in preklinische muismodellen, faalt de meerderheid van de fase 3 klinische studies. Deze observatie onderstreept het feit dat preklinische muismodellen slecht kunnen voorspellen hoe patiënten zullen reageren op anti-kanker therapieën. In **hoofdstuk 2** stellen wij voor om genetische gemodificeerde muismodellen (GEMMs) te gebruiken in preklinische studies, omdat deze modellen veel gelijkenis vertonen met humane kanker, zowel op het niveau van kanker-intrinsieke als kanker-extrinsieke aspecten. In het bijzonder de ontwikkeling van immuunmodulerende medicijnen en combinatie therapieën zal gebaat zijn bij GEMMs, omdat deze modellen spontaan kanker ontwikkelen in de aanwezigheid van een functionerend immuunsysteem. Met behulp van de recente ontwikkelingen in ‘genoom editing’ kunnen bij GEMMs genetische

veranderingen in het DNA worden geïntroduceerd die kenmerkend zijn voor specifieke groepen patiënten. Met behulp van deze ontwikkelingen zullen we een beter inzicht krijgen in de complexe rol van het immuunsysteem in kankerontwikkeling, uitzaaiing en de respons op anti-kanker therapieën.

In **hoofdstuk 3** gebruiken we een GEMM voor invasieve borstkanker, de zogenaamde *K14cre;Cdh1$^{F/F}$;Trp53$^{F/F}$* (KEP) muis, waarin we laten zien dat spontane borsttumoren een systemische ontstekingsreactie opwekken die de uitzaaiing van borstkanker bevordert. Deze ontstekingsreactie wordt gekenmerkt door de toename van immuunsuppressieve neutrofielen die de anti-kanker activiteit van CD8$^+$ T cellen remmen, waardoor uitzaaiingen zich kunnen nestelen in verschillende organen. Deze neutrofielen worden gereguleerd door een domino-effect van immuunreacties, geactiveerd door de primaire borsttumor. Allereerst, macrofagen die aanwezig zijn in de primaire tumor produceren IL1β, een cytokine die op zijn beurt een kleine populatie γδ T cellen aanstuurt om IL17 te produceren. IL17 induceert vervolgens, via G-CSF, de toename van immunosuppressieve neutrofielen. In **hoofdstuk 4** beschrijven we een aanvullende factor in dit complexe geheel. We laten zien dat het pro-inflammatoire cytokine CCL2 een belangrijke rol speelt in het starten van de hierboven beschreven ontstekingsreactie, door IL1β secretie door tumor-geassocieerde macrofagen te reguleren. Om te onderzoeken of deze bevindingen ook van toepassingen zijn in humane patiënten, hebben we een analyse gedaan van genexpressie in tumoren van borstkankerpatiënten. Vergelijkbaar met de resultaten uit het KEP muismodel, vonden we dat genexpressie van *CCL2* en *IL1B* sterk gecorreleerd is in verschillende subtypen borstkanker, met de hoogste correlatie in macrofaag-rijke tumoren. Remming van CCL2 in KEP muizen resulteerde in verlaagde IL1β secretie door tumor-geassocieerde macrofagen, verminderde IL17 productie door γδ T cellen, verlaagde proporties neutrofielen en een verhoogde anti-kanker activiteit van CD8$^+$ T cellen. Deze resultaten suggereren dat het remmen van neutrofielen of andere componenten van deze immuunsuppressieve ontstekingsreactie, anti-tumor immuunresponsen zal ontketenen tegen uitgezaaide borstkanker.

De beschikbaarheid van middelen die specifiek deze immuunsuppressieve netwerken remmen is momenteel zeer beperkt. Een alternatief is om gebruik te maken van conventionele anti-kanker therapieën die immuunmodulerende eigenschappen hebben, zoals chemotherapie. In **hoofdstuk 5** doen we het voorstel, gebaseerd op de recente literatuur, om chemotherapie te gebruiken om immuunsuppressie tegen te gaan en anti-kanker immuunreacties te bevorderen. We verwachten dat de combinatie van nauwkeurig geselecteerde chemotherapeutica en T cel-activerende immunotherapie zal leiden tot optimale anti-kanker immuunreacties en daarmee verbeterde responsen op kanker immunotherapie.

In **hoofdstuk 6** laten we zien dat spontane borsttumoren in het KEP muismodel geïnfiltreerd zijn met verschillende populaties T cellen, maar deze zijn niet functioneel. Deze T cellen brengen immuun checkpoint moleculen tot expressie, CTLA-4 en PD-1, die T cel activatie remmen. Het blokkeren van deze remmende signalen met ‘immune checkpoint inhibitors’ had geen effect op tumorgroei, maar er was synergie

wanneer 'immune checkpoint inhibitors' werden gecombineerd met een specifieke chemotherapie, cisplatin. Het anti-tumor effect van deze combinatietherapie was afhankelijk van de aanwezigheid van $CD8^+$ T cellen. Preliminaire data doet vermoeden dat cisplatin de functionaliteit van $CD103^+$ dendritische cellen verhoogt, waardoor T cellen beter geactiveerd worden. Maar meer onderzoek is nodig om deze resultaten te bevestigen. Onze resultaten hebben belangrijke consequenties voor klinische studies, want ze laten zien dat ook niet-immunogene typen kanker, zoals borstkanker, succesvol behandeld kunnen worden met immunotherapie wanneer deze gecombineerd wordt met de juiste chemotherapeutica. **Hoofdstuk 7** bevat een algemene discussie van het onderzoek beschreven in dit proefschrift en plaatst het in de context van de huidige literatuur. Daarnaast worden, op basis van dit onderzoek, voorstellen gedaan voor nieuwe anti-kanker behandelingen in de kliniek.

Curriculum Vitae

Kelly Kersten was born on April 16th, 1987 in Ede, the Netherlands. In 1999 she attended VWO at the Pallas Athene College in Ede, from which she graduated in 2005. In the same year she enrolled into the Biology Bachelor program at Utrecht University. Due to her interest in medical biology, she participated in several courses organized by the Biomedical Sciences program. Triggered by her interest in oncology she wrote her bachelor thesis about hypoxia and breast cancer, and she graduated as a Bachelor of Science in 2008. Later that year, she started the Master program Cancer Genomics and Developmental Biology at Utrecht University. She performed her first internship in the lab of Prof. Marc Vooijs at the University Medical Centre Utrecht (UMCU), working on the role of Hypoxia Inducible Factor-1 (HIF-1) in breast cancer. In 2010, she performed her second internship in the lab of Prof. Zena Werb at the University of California San Francisco (UCSF). Under direct supervision of Dr. Vicki Plaks, she studied the role of antigen-presenting cells in mammary branching morphogenesis and breast cancer. After completing her Master's thesis on the formation of the pre-metastatic niche under supervision of Prof. Jacco van Rheenen, she obtained her Master of Science degree in February 2011. On May 1, 2011, Kelly joined the lab of Dr. Karin de Visser at the Netherlands Cancer Institute – Antoni van Leeuwenhoek Hospital, where she conducted the research that is described in this thesis. In October 2016, Kelly moved back to San Francisco to continue her research on tumor immunology as a postdoctoral fellow in the lab of Prof. Matthew Krummel at UCSF.

List of publications

Dual immune checkpoint blockade synergizes with chemotherapy in a drug-dependent manner in a mouse model for *de novo* mammary tumorigenesis.
Kelly Kersten, Kim Vrijland, Camilla Salvagno, Max D. Wellenstein, Seth B. Coffelt, Cheei-Sing Hau and Karin E. de Visser

In preparation.

Mammary tumor-derived CCL2 enhances pro-metastatic systemic inflammation through upregulation of macrophage-derived IL1β.
Kelly Kersten, Seth B. Coffelt, Marlous Hoogstraat, Niels J.M. Verstegen, Kim Vrijland, Metamia Ciampricotti, Chris W. Doornebal, Cheei-Sing Hau, Parul Doshi, Esther H. Lips, Lodewyk F.A. Wessels and Karin E. de Visser

In revision.

Genetically engineered mouse models in oncology and cancer medicine.
Kelly Kersten, Karin E. de Visser, Martine H. van Miltenburg, Jos Jonkers.

EMBO Molecular Medicine, in revision.

IL17-producing γδT cells and neutrophils conspire to promote breast cancer metastasis.
Seth B. Coffelt, Kelly Kersten*, Chris W. Doornebal*, Jorieke Weiden, Cheei-Sing Hau, Kim Vrijland, Metamia Ciampricotti, Jos Jonkers and Karin E. de Visser.

Nature. 2015. 522:345-348 * equal contribution

Next generation immunotherapy; exploiting the immunomodulatory properties of chemotherapeutic drugs to improve immunotherapy response.
Kelly Kersten*, Camilla Salvagno*, Karin E. de Visser.

Frontiers in Immunology. 2015, 6:516 * equal contribution

Adaptive immune regulation of mammary postnatal organogenesis.
Vicki Plaks, Bijan Boldajipour, Jelena R. Linnemann, Nguyen H. Nguyen, Kelly Kersten, Yochai Wolf, Amy-Jo Casbon, Niwen Kong, Renske J.E. van den Bijgaart, Dean Sheppard, Andrew C. Melton, Matthew F. Krummel and Zena Werb.

Developmental Cell. 2015. 34(5):493-504.